Assessing the Efficacy of Bicycle Helmets in Reducing Risk of Head Injury

Megan L. Bland

Dissertation submitted to the faculty of the Virginia Polytechnic Institute and State University in partial fulfillment of the requirements for the degree of:

Doctor of Philosophy

In

Biomedical Engineering

Steven Rowson, Chair

Stefan M. Duma

H. Clay Gabler

Joel D. Stitzel

Bethany M. Rowson

March 28, 2019

Blacksburg, Virginia

Keywords: cycling, brain injury, biomechanics, impact kinematics, concussion

Assessing the Efficacy of Bicycle Helmets in Reducing Risk of Head Injury

Megan L. Bland

ABSTRACT

Although cycling offers many health and environmental benefits, it is not an activity free of injury risk. Increases in cycling popularity in the United States over the past 15 years have been paralleled by a 120% growth in cycling-related hospital admissions, with injuries to the head among the most common and debilitating injuries. Bicycle helmets can reduce head injury risk and are presently required to meet safety standard certification criteria specifying a minimal level of acceptable impact protection. However, the conditions surrounding cyclist head impacts are thought to be much more complex than the test conditions prescribed in standards and have important implications related to mechanisms of injury. The overarching aim of this dissertation was thus to investigate the protective capabilities of bicycle helmets in the context of real-world impact conditions and relevant head injury mechanisms. This aim was achieved through a series of studies, the objectives of which were to: compare helmet impact performance across standards impact testing and more realistic, oblique impact testing; to probe how changing boundary conditions of oblique impact testing may influence helmet test outcomes; to use this knowledge to inform the development of an objective helmet evaluation protocol reflective of realistic impact conditions and related head injury risks; and finally, to enhance the body of knowledge pertaining to cyclist head impact conditions via advanced helmet damage reconstruction techniques. The compilation of results across these studies serves to enhance cyclist safety by stimulating improved helmet evaluation and design while simultaneously providing objective, biomechanical data to consumers, enabling them to make safety-based purchasing decisions.

Assessing the Efficacy of Bicycle Helmets in Reducing Risk of Head Injury

Megan L. Bland

GENERAL AUDIENCE ABSTRACT

Although cycling offers many health and environmental benefits and is increasing in popularity in the United States, it is not always a perfectly safe activity. The number of cycling-related hospital admissions in the US has been increasing over the past 15 years. Cyclists often sustain head injuries from crashes, which can be particularly debilitating. Fortunately, wearing a helmet can protect against head injuries during a crash. Bicycle helmets are presently designed around safety standards that drop a helmeted dummy head onto a horizontal anvil and require the helmet to limit the force on the head to acceptable levels. However, standards tests overly simplify how cyclists actually hit their head during a crash and are consequently unable to assess how well helmets protect against common brain injuries like concussion. The overarching goal of this research was to evaluate how effectively bicycle helmets protect cyclists from concussion in realistic impact scenarios. Several studies were conducted to achieve this goal. Their individual objectives were to: compare how bicycle helmets reduce impact forces associated with standards tests versus more realistic, angled impact tests; to understand how changing constraints of an angled impact setup influences helmet effectiveness; to develop an unbiased evaluation protocol for bicycle helmets based on realistic cyclist crash scenarios and concussion risk assessment; and finally, to further explore how cyclists impact their head in real-world crashes using advanced techniques for reconstructing bicycle helmet damage from actual accidents. All of these studies lead to improved cyclist safety by stimulating improved helmet evaluation and design, while also providing consumers with information on how protective their helmets are.

ACKNOWLEDGMENTS

I would first and foremost like to thank my advisor and committee chair, Dr. Steven Rowson, for his invaluable guidance pertaining to the work presented in this dissertation. He fostered a positive and enjoyable laboratory work environment throughout my years in graduate school and has provided exemplary mentorship and support that have considerably enriched my professional development. I would also like to thank my other committee members, Dr. Bethany Rowson, Dr. Clay Gabler, Dr. Stefan Duma, and Dr. Joel Stitzel for offering up their time and insight in order to enhance the quality and scope of this work.

The friends I have made during graduate school as well as from previous phases of life have been a constant source of encouragement. I cannot thank them enough for their friendship, and especially for ensuring that my graduate school experience was largely well-balanced and fun. Aside from being wonderful friends, my fellow lab coworkers throughout the years have greatly enhanced my educational experience as well. They deserve additional thanks for always being willing to drop everything to be a sounding board for helping me think through complex issues as they arose.

Lastly, I am so extremely grateful to my family for their unending love and support. Their listening ears and encouraging words in times of triumph as well as times of frustration have meant more than I can express. They have always challenged me to be the best possible version of myself and believed in me especially when I did not, and I owe all of my accomplishments to them. I certainly could not have pursued my many aspirations to the extent that I have been able to without them to support me.

TABLE OF CONTENTS

LIST OF FIGURES

LIST OF TABLES

CHAPTER 1

INTRODUCTION

INJURIES IN CYCLING

Cycling is a popular activity for recreation, sport, and transportation in many countries around the world. In the United States, cycling has become increasingly popular in recent years, with many embracing the health and environmental benefits it can afford [1-3]. It is estimated that 103.7 million Americans ages 3 and older rode a bicycle in 2015 [1]. However, cycling is not a risk-free activity. Its increase in popularity has been paralleled by an increase in injuries, with the number of bicycle-related hospital admissions growing 120% over the past 15 years [4] and the number of fatalities increasing by 12% from 2014 to 2015 [1]. Associated US health care costs for these injuries were estimated at $24.4 billion in 2013 [5].

The head is among the most frequently injured body parts from cycling accidents, with concussion presenting in a large majority of head injury cases [6-9]. Injury surveillance systems have shown that over 81,000 head injuries related to cycling were treated in US emergency rooms in 2015, making cycling a leading cause of head injury out of all sports and recreational activity [10,11]. The incidence rate is likely even higher still, as many less-severe injuries are assessed at home or by a primary care provider rather than in emergency rooms. Associated US health care costs specific to head injuries alone is estimated to exceed $2 billion annually [12], suggesting there is considerable economic and societal burden from cycling-related head injuries.

HEAD INJURY MECHANISMS

Head impact events are typically characterized in terms of linear and rotational motion (kinematics) of the skull. During an impact, the brain experiences an inertial lagging effect as the

skull is accelerated, producing relative movement at the brain-skull interface that creates pressures and strains in the brain tissue [13,14]. The severity of these effects are generally related to skull kinematic motion. Linear and rotational kinematics, in conjunction with the duration of impact, are thought to be associated with unique injury mechanisms [15,16]. Skull fracture generally occurs when linear accelerations exceed a tolerable threshold [17-21]. Linear accelerations are also linked to the development of transient intracranial pressure gradients in the brain that can result in focal injuries such as hematoma or contusion [22,23]. In contrast, rotational kinematics (often described in terms of velocity or acceleration) have been correlated to the development of shear strains within the brain tissue that can result in concussion or other forms of diffuse axonal injury [22,23]. Almost all head injuries involve both linear and rotational motions [24]. The nature of injury that may result from a given head impact is therefore related to the combination of these kinematics and their respective severities.

SAFETY STANDARDS FOR BICYCLE HELMETS

Bicycle helmets have been shown to be effective in reducing head injury risk [6,7,25-29]. In the US, helmets must be certified based on the Consumer Product Safety Commission (CPSC) standard, which mandates that a helmet limit peak linear acceleration (PLA) to less than 300 g in prescribed guided drop tests of a helmeted headform [30]. Although standards ensure energy input to the head is reduced, they have limited representation of real-world cyclist head impacts. Only impacts normal to the impact surface are assessed, while real-world cyclist head impacts are thought to occur oblique to the surface [8]. Oblique impacts generate considerable rotational motion of the head as well as linear, the interplay of which is known to be an important factor in producing brain injury [22,23,31,32]. Standards measure only linear acceleration, limiting their ability to evaluate helmet effectiveness in reducing brain injury risk. The prescribed impact normal velocities are also thought to be generally more severe than those commonly seen in cycling

accidents [33-39]. Further, standards utilize a headform and neck joint that are not biofidelic and thus likely exhibit different impact characteristics than a human might.

Because safety standards certify helmets based on a pass-fail threshold, they do not provide relative performance data indicating which helmets offer superior protection to others. Although most helmets are comprised of a crushable expanded polystyrene (EPS) liner and plastic outer shell, design varies considerably across helmet style. It is likely that the various helmet styles produce markedly different impact performance characteristics. With little available biomechanical data available to the public differentiating helmet performance, consumers presently have limited resources enabling them to choose a helmet based on the relative safety it affords. There is a need for an objective helmet evaluation system to be established in order to disseminate bicycle helmet impact performance data.

LABORATORY REPLICATION OF CYCLIST HEAD IMPACTS

Recent research has suggested that evaluating bicycle helmets under more realistic impact conditions may provide an avenue for improving helmet design to increase cyclist safety [26,40-42]. A number of impact systems capable of generating oblique impacts have been developed for bicycle helmet impact testing [40-46]. However, there is presently no universally-accepted method for this type of testing, and the boundary conditions across impact system vary considerably. Head impact angle, choice of anthropomorphic test device (ATD) headform, and the use of an ATD neck and effective torso mass are just a few of the factors that differ across systems. Understanding the effects of these varied boundary conditions on helmet performance is necessary for interpreting differences across published bicycle helmet oblique impact studies and for assessment of injury risk.

Laboratory evaluation of helmet performance is most effective when common impact scenarios from real-world crashes are well understood. While it is thought that cyclists head impacts are generally oblique [8,35-39], limited data are available regarding exact impact conditions and resulting head impact kinematics. Traditionally, these factors have been estimated through computational simulation studies of cyclist crashes and through laboratory reconstructions of damage to bicycle helmets from real-world accidents [33-39,47]. Simulation data provide insight into trends surrounding these impacts; however, results are influenced by the validity of the computational framework used, and there are minimal cyclist head impact data available for validation purposes. Damage reconstructions provide an alternative avenue for estimating cyclist head impact conditions. The bicycle helmet damage reconstruction studies that have been conducted to-date have been limited by use of standards test equipment and visual-observation based damage quantification [33,34,47]. Recent motorcycle helmet damage reconstruction studies have begun to employ more advance techniques, conducting oblique impact tests or quantifying damage using computed tomography (CT) [48-50]. Reconstructing helmet damage using oblique impacts and CT-based quantification may enhance knowledge of real-world cyclist head impact conditions, which can be used to inform laboratory evaluation of helmets. Additionally, resulting head impact kinematics can be linked to injury outcomes in order to improve assessment of cycling-specific injury scenarios.

RESEARCH OBJECTIVES

The following chapters center around investigation of bicycle helmet impact performance. A variety of impact systems are employed and a number of helmet models consisting of varied designs are evaluated. Comparison of impact characteristics across system allows for interpretation of published bicycle helmet impact data and assessment of related injury risks, while comparative testing of helmet performance across varied helmet styles enables consumers to

make informed purchasing decisions and encourages design of safer helmets. Common cyclist head impact conditions are also investigated to enable laboratory evaluation of helmets in the most realist conditions possible. Specifically, the overall objectives of the following chapters are:

1. To investigate how impact performance of bicycle helmets varies across models using standards equipment and an oblique impact rig.
2. To determine the effects of varied oblique impact rig boundary conditions on helmet performance.
3. To establish a methodology for objective evaluation of bicycle helmets that is informed by real-world cyclist accident conditions and relevant brain injury mechanisms.
4. To enhance knowledge of cyclist head impact exposure and associated kinematics through oblique impact bicycle helmet damage reconstructions.

REFERENCES

1. Fischer, P. A Right to the Road: Understanding and Addressing Bicyclist Safety, G.H.S. Association, Editor. 2017, Governors Highway Safety Association.
2. Wen, L.M. and Rissel, C. Inverse associations between cycling to work, public transport, and overweight and obesity: findings from a population based study in Australia. *Prev. Med.*, 2008. 46(1): p. 29-32
3. Hamer, M. and Chida, Y. Active commuting and cardiovascular risk: a meta-analytic review. *Preventive medicine*, 2008. 46(1): p. 9-13
4. Sanford, T., McCulloch, C.E., and Callcut, R.A. Bicycle trauma injuries and hospital admissions in the United States, 1998-2013. *Jama*, 2015. 314(9): p. 947-949
5. Gaither, T.W., Sanford, T.A., et al. Estimated total costs from non-fatal and fatal bicycle crashes in the USA: 1997-2013. *Inj. Prev.*, 2018. 24(2): p. 135-141
6. Thompson, D.C., Rivara, F.P., and Thompson, R.S. Effectiveness of bicycle safety helmets in preventing head injuries. A case-control study. *The Journal of the American Medical Association*, 1996. 276(24): p. 1968-73
7. Sacks, J.J., Holmgreen, P., Smith, S.M., and Sosin, D.M. Bicycle-associated head injuries and deaths in the United States from 1984 through 1988: How many are preventable? *The Journal of the American Medical Association*, 1991. 266: p. 3016-3018
8. Otte, D. Injury Mechanism and crash kinematics of cyclists in accidents - An analysis of real accidents. *Proceedings of 33rd Stapp Car Crash Conference*, 1989. Warrendale, PA
9. Haileyesus, T., Annest, J.L., and Dellinger, A.M. Cyclists injured while sharing the road with motor vehicles. *Injury prevention : journal of the International Society for Child and Adolescent Injury Prevention*, 2007. 13(3): p. 202-6
10. CPSC. "National Electronic Injury Surveillance System Database" Internet www.cpsc.gov/en/Research--Statistics/NEISS-Injury-Data/. July 26, 2016].
11. Coronado, V.G., Haileyesus, T., et al. Trends in Sports- and Recreation-Related Traumatic Brain Injuries Treated in US Emergency Departments: The National Electronic Injury Surveillance System-All Injury Program (NEISS-AIP) 2001-2012. *J. Head Trauma Rehabil.*, 2015. 30(3): p. 185-197
12. Schulman, J., Sacks, J., and Provenzano, G. State level estimates of the incidence and economic burden of head injuries stemming from non-universal use of bicycle helmets. *Injury Prevention*, 2002. 8(1): p. 47-52
13. Hardy, W.N., Mason, M.J., et al. A study of the response of the human cadaver head to impact. *Stapp car crash journal*, 2007. 51: p. 17-80
14. Hardy, W.N., Foster, C.D., et al. Investigation of Head Injury Mechanisms Using Neutral Density Technology and High-Speed Biplanar X-ray. *Stapp car crash journal*, 2001. 45: p. 337-68
15. Unterharnscheidt, F.J. Translational versus rotational acceleration: animal experiements with measured inputs. *Proceedings of the 15th Stapp Car Crash Conference*, 1971. SAE 710880
16. King, A.I., Yang, K.H., Zhang, L., Hardy, W., and Viano, D.C. Is Head Injury Caused by Linear or Angular Acceleration? *Proceedings of Proceedings of the International Research Conference on the Biomechanics of Impact (IRCOBI)*, 2003. Lisbon, Portugal
17. Versace, J. A Review of the Severity Index. *SAE Technical Paper Series*, 1971. SAE 710881
18. Gadd, C.W. Use of a weighted-impulse criterion for estimating injury hazard. *Proceedings of the 10th Stapp Car Crash Conference*, 1966. SAE 660793
19. Lissner, H.R., Lebow, M., and Evans, F.G. Experimental Studies on the Relation between Acceleration and Intracranial Pressure Changes in Man. *Surgery, gynecology & obstetrics*, 1960. 111: p. 329-338

20. Gurdjian, E., Lissner, H., Evans, F., Patrick, L., and Hardy, W. Intracranial pressure and acceleration accompanying head impacts in human cadavers. *Surgery, gynecology & obstetrics*, 1961. 113: p. 185
21. Mertz, H.J., Irwin, A.L., and Prasad, P. Biomechanical and scaling bases for frontal and side impact injury assessment reference values. *Stapp car crash journal*, 2003. 47: p. 155-88
22. Gennarelli, T., Ommaya, A., and Thibault, L. Comparison of translational and rotational head motions in experimental cerebral concussion. *Proceedings of 15th Stapp Car Crash Conference*, 1971.
23. Gennarelli, T.A., Thibault, L.E., and Ommaya, A.K. Pathophysiologic responses to rotational and translational accelerations of the head. *SAE Technical Paper Series*, 1972. 720970: p. 296-308
24. Rowson, S., Brolinson, G., Goforth, M., Dietter, D., and Duma, S.M. Linear and angular head acceleration measurements in collegiate football. *Journal of biomechanical engineering*, 2009. 131(6): p. 061016
25. Olivier, J. and Creighton, P. Bicycle injuries and helmet use: a systematic review and meta-analysis. *Int. J. Epidemiol.*, 2017. 46(1): p. 278-292
26. McIntosh, A.S., Lai, A., and Schilter, E. Bicycle helmets: head impact dynamics in helmeted and unhelmeted oblique impact tests. *Traffic Inj. Prev.*, 2013. 14(5): p. 501-8
27. Amoros, E., Chiron, M., Martin, J.L., Thelot, B., and Laumon, B. Bicycle helmet wearing and the risk of head, face, and neck injury: a French case--control study based on a road trauma registry. *Injury prevention : journal of the International Society for Child and Adolescent Injury Prevention*, 2012. 18(1): p. 27-32
28. Elvik, R. Corrigendum to: "Publication bias and time-trend bias in meta-analysis of bicycle helmet efficacy: a re-analysis of Attewell, Glase and McFadden, 2001" [Accid. Anal. Prev. 43 (2011) 1245-1251]. *Accident Analysis & Prevention*, 2013. 60: p. 245-53
29. Cripton, P.A., Dressler, D.M., Stuart, C.A., Dennison, C.R., and Richards, D. Bicycle helmets are highly effective at preventing head injury during head impact: head-form accelerations and injury criteria for helmeted and unhelmeted impacts. *Accident Analysis & Prevention*, 2014. 70: p. 1-7
30. CPSC. Safety Standard for Bicycle Helmets Final Rule (16 CFR Part 1203). 1998, United States Consumer Product Safety Commission. p. 11711-11747.
31. Ommaya, A.K., Hirsch, A.E., and Martinez, J.L. The role of whiplash in cerebral concussion. *Proceedings of Proc. 10th Stapp Car Crash Conference*, 1966.
32. Ommaya, A. and Hirsch, A. Tolerances for cerebral concussion from head impact and whiplash in primates. *Journal of biomechanics*, 1971. 4(1): p. 13-21
33. Williams, M. The protective performance of bicyclists' helmets in accidents. *Accid. Anal. Prev.*, 1991. 23(2-3): p. 119-131
34. Smith, T.A., Tees, D., Thom, D.R., and Hurt, H.H. Evaluation and replication of impact damage to bicycle helmets. *Accid. Anal. Prev.*, 1994. 26(6): p. 795-802
35. Verschueren, P. Biomechanical analysis of head injuries related to bicycle accidents and a new bicycle helmet concept, in *Faculteit Ingenieurswetenschappen Departement Werktuigkunde Afdeling Biomechanica en Grafisch Ontwerpen*. 2009, Katholieke Universiteit Leuven: Leuven, Belgium.
36. Bourdet, N., Deck, C., et al. In-depth real-world bicycle accident reconstructions. *Int. J. Crashworthiness*, 2014. 19(3): p. 222-232
37. Bourdet, N., Deck, C., Carreira, R.P., and Willinger, R. Head impact conditions in the case of cyclist falls. *Proc. Inst. Mech. Eng. P*, 2012. 226(3-4): p. 282-289
38. Peng, Y., Chen, Y., Yang, J., Otte, D., and Willinger, R. A study of pedestrian and bicyclist exposure to head injury in passenger car collisions based on accident data and simulations. *Safety Science*, 2012. 50(9): p. 1749-1759

39. Fahlstedt, M., Baeck, K., et al. Influence of Impact Velocity and Angle in a Detailed Reconstruction of a Bicycle Accident. *IRCOBI Conference*, 2012. 12(84): p. 787-799
40. Milne, G., Deck, C., et al. Bicycle helmet modelling and validation under linear and tangential impacts. *Int. J. Crashworthiness*, 2014. 19(4): p. 323-333
41. Mills, N.J. and Gilchrist, A. Oblique impact testing of bicycle helmets. *Int. J. Impact Eng.*, 2008. 35(9): p. 1075-1086
42. Aare, M. and Halldin, P. A new laboratory rig for evaluating helmets subject to oblique impacts. *Traffic injury prevention*, 2003. 4(3): p. 240-8
43. Hansen, K., Dau, N., et al. Angular Impact Mitigation system for bicycle helmets to reduce head acceleration and risk of traumatic brain injury. *Accident Analysis & Prevention*, 2013. 59: p. 109-17
44. Klug, C., Feist, F., and Tomasch, E. Testing of bicycle helmets for preadolescents. *Proceedings of IRCOBI Conference*, 2015. Lyon, France
45. Pang, T.Y., Thai, K.T., et al. Head and neck responses in oblique motorcycle helmet impacts: a novel laboratory test method. *International Journal of Crashworthiness*, 2011. 16(3): p. 297-307
46. Stigson, H., Rizzi, M., Ydenius, A., Egnstrom, E., and Kullgren, A. Consumer Testing of Bicycle Helmets, in *IRCOBI Conference*. 2017, IRCOBI Conference: Antwerp, Belgium. p. 173-181.
47. McIntosh, A.S. and Patton, D.A. Impact reconstruction from damage to pedal and motorcycle helmets. *Proceedings of the Institution of Mechanical Engineers, Part P: Journal of Sports Engineering and Technology*, 2012. 226(3-4): p. 274-281
48. Chinn, B., Canaple, B., et al. COST 327: Motorcycle Safety Helmets, B. Chinn, Editor. 2001, European Commission, Directorate General for Energy and Transport: Belgium.
49. Bonin, S.J., Luck, J.F., et al. Dynamic Response and Residual Helmet Liner Crush Using Cadaver Heads and Standard Headforms. *Ann Biomed Eng*, 2017. 45(3): p. 656-667
50. Loftis, K.L., Moreno, D.P., Tan, J., Gabler, H.C., and Stitzel, J.D. Utilizing computed tomography scans for analysis of motorcycle helmets in real-world crashes. *Proceedings of 48th Rocky Mountain Bioengineering Symposium & 48th International ISA Biomedical Sciences Instrumentation Symposium*, 2011. Denver, Colorado

CHAPTER 2

DIFFERENCES IN THE PROTECTIVE CAPABILITIES OF BICYCLE HELMETS IN REAL-WORLD AND STANDARD-SPECIFIED IMPACT SCENARIOS

ABSTRACT

Cycling is the leading cause of recreation-related head injuries in the U.S. each year. While bicycle helmets are required by standards to limit peak linear acceleration (PLA) of the head to <300 g, limited data are available differentiating performance among helmets on the market. Further, standards represent more severe impacts than those common in real-world cycling accidents and do not allow for impacts at the helmet rim, a commonly-impacted location in cyclist accidents. The purpose of this study was to investigate relative differences in impact attenuation capabilities of bicycle helmets under real-world impact conditions and safety standard-specified conditions. Ten helmet models were tested using standards equipment at a frontal rim and a temporal location at velocities of 3.4 m/s (common in cycling accidents) and 6.2 m/s (standard-specified). PLA and AIS ≥ 4 brain injury risk were evaluated as well as other impact attenuation characteristics. Helmet performance varied significantly between models. PLA ranging from 78-169 g at 3.4 m/s (0-2% AIS ≥ 4 brain injury risk) and 165-432 g (10-100% risk) at 6.2 m/s. Temporal impacts generally produced higher PLA than frontal, likely due to higher effective stiffness, although two helmets exceeded 300 g at the frontal rim location (>70% risk). Force-displacement curves suggest that bottoming out occurred in these impacts. As this is a commonly impacted location in cyclist accidents, there may be benefit to expanding the testable area in standards to include the rim. Aside from bottoming out cases, helmets that performed worse in one impact configuration tended to perform worse in others, with non-road style helmets among the worst. These results demonstrate the value in testing non-standard conditions, and will ideally inform future standards testing and helmet manufacturers, aiding the development of improved bicycle helmet safety.

INTRODUCTION

Cycling is a popular sport, recreational activity, and mode of transportation worldwide. Although a generally safe activity, it is not without risks, as bicycle accidents result in a large number of hospitalizations and deaths each year. In 2014 alone, there were 720 cyclists killed in motor vehicle crashes in the United States [1]. Most of the severe injuries seen in cycling accidents are to the head [2, 3]. According to the National Electronic Injury Surveillance System (NEISS) published by the U.S. Consumer Product Safety Commission (CPSC), cycling was the number one activity responsible for sports-related head injuries treated in U.S. emergency rooms in 2009, accounting for over 19% of the total that year [4]. The actual incidence is likely much higher, as many less-severe head injuries are treated in a physician's office or are self-treated. Resulting economic and societal costs of cycling-related head injuries are substantial, with estimated associated U.S. healthcare costs totaling over $2 billion annually [5]. Fortunately, many studies, both epidemiological [3, 6, 7] and biomechanical [8, 9], have shown that risk of head injury can be effectively reduced through bicycle helmet use.

To sell a bicycle helmet on US markets, manufacturers must document that their helmet passes a series of tests specified by the CPSC Safety Standard for Bicycle Helmets [10]. The impact attenuation portion of this standard evaluates helmets through a series of drop tests on a twin-wire or monorail drop rig. Helmets are fitted onto a magnesium ISO headform that is mounted to the drop carriage via a ball joint, which is outfitted with a single-axis accelerometer at the center of gravity. The entire drop carriage has a mass of 5 kg. For each helmet model evaluated, multiple samples are subjected to varying environmental conditions and are dropped onto either a flat anvil at 6.2 m/s or a hemispherical or curbstone anvil at 4.8 m/s. The standard also specifies that helmets be impacted above a superimposed test line, with centers of successive impacts kept to a minimum of 120 mm apart. According to CPSC, this separation distance is sufficient to prevent

overlap of damage profiles from prior impacts, which would affect subsequent accelerations of impacts to the same helmet [10]. Order of testing conditions is determined by the tester, whose aim is to pose the most difficult series of impacts for the given sample. Linear acceleration of the headform is measured for every impact, and peak linear acceleration (PLA) must not exceed 300 g (>50% risk of skull fracture or severe brain injury [11]) for the helmet to pass.

While the CPSC standard and many similar standards require bicycle helmet design to minimize risk of severe head injury, none require testing at lower impact energies, which helmet damage replication studies have shown are more common in real-world cyclist accidents [12, 13]. These studies collect helmets from riders involved in an accident and match the damage through drop tests onto a flat anvil. Average impact PLAs in these studies are usually around 100 g, a magnitude of head impact PLA that has been associated with concussion in football players [14, 15]. Additionally, helmet damage replication studies, along with data from computational analyses of bicycle crash kinematics, have shown that a majority of real-world impacts are to the front and sides of the helmet and often around the rim [13, 16-18], which is inferior to the impact test line specified by the CPSC standard. Helmets are not currently required to be tested at these common energies or at the rim in order to be sold on the market.

Bicycle helmet standards also do not differentiate performance among helmets that pass impact testing. Although conventional bicycle helmets are generally comprised of the same basic components – a polycarbonate (PC) outer shell, an expanded polystyrene (EPS) liner (which crushes and absorbs energy upon impact), and comfort padding – design varies widely across helmet styles. Motivation for varying designs typically stems from the manufacturer's aim to balance aesthetics, ventilation and aerodynamics, and impact attenuation. Many helmets deviate from normal shell and liner materials, and design also varies in overall shape, vent configuration,

thickness of shell and liner, density of liner, and a number of additional parameters. All of these design considerations affect impact performance, but with little available data comparing model types, it is difficult for consumers to choose a helmet based on the relative safety it offers.

The objective of this study was to investigate differences in bicycle helmet impact attenuation on a CPSC test rig under head impact conditions commonly seen in bicycle accidents and those specified by the present CPSC standard.

METHODS

Helmet Models

Ten commercially-available helmet models of varied design were selected for comparative testing (Table 2.1). Most were categorized as road helmets based on their elongated shape and vents, while the non-road helmets (BMIPS, GMIPS, and N) had a more rounded shape, smaller or fewer vents, and greater head coverage. The exception was the CW helmet, which was classified as a road helmet but characterized by a more irregular shape due to its unique vent structure. Helmet mass, excluding any included attachments, ranged from 250 to 465 grams, with the non-road helmets being the heaviest. The materials comprising a majority of these helmets were the standard PC shell and EPS liner, although the N helmet had an acrylonitrile butadiene styrene (ABS) shell and the SOO helmet incorporated a patented, plastic honeycomb-structure called Koroyd® into its liner. The non-road helmet shells were thicker and generally stiffer than the road helmet shells (average thickness of 1.2 ± 0.7 mm for non-road versus 0.5 ± 0.1 mm for road). Two locations on each helmet were selected for impact testing: a frontal location at the rim and a temporal location above standard test lines. At these locations, liner thickness was similar between all helmet models, averaging 2.6 ± 0.4 cm. The thickness of the frontal location of the GS helmet was substantially lower, as a vent overlapped this location.

Table 2.1. Helmet model design parameters. MIPS: multidirectional impact protection system, PC: polycarbonate, ABS: acrylonitrile butadiene styrene, EPS: expanded polystyrene, F: frontal, T: temporal.

Helmet	Style	Mass [gm]	Vents	Shell Material	Shell Thickness [mm]	Liner Material	Liner Thickness [cm]		Radius of Curvature [cm]	
							F	T	F	T
Bell Solar Flare (BSF)	Road	312	23	PC	0.5	EPS	2.6	3.2	20.6	19.7
Bell Star Pro (BSP)	Road	296	15	PC	0.4	EPS	2.9	2.6	13.2	22.3
Bell Super 2 MIPS (BMIPS)	Mountain	360	23	PC	0.7	EPS	2.4	2.6	5.6	22.9
Catlike Whisper (CW)	Road	283	39	PC	0.5	EPS	2.9	2.1	5.7	4.7
Giro Sutton MIPS (GMIPS)	Urban/ street	370	8	PC	0.7	EPS	2.7	2.9	5.8	9.5
Giro Synthe (GS)	Road	250	26	PC	0.3	EPS	1.6	2.9	4.8	12.0
Nutcase Watermelon (N)	Urban/ street	465	11	ABS	2.2	EPS	2.8	2.7	16.1	12.2
Smith Optics Overtake (SOO)	Road	250	21	PC	0.3	EPS/ Koroyd	3.1	2.9	7.4	18.2
Schwinn Thrasher (ST)	Road	340	20	PC	0.4	EPS	2.5	2.3	6.9	9.6
S-Works Evade (SWE)	Road	317	15	PC	0.6	EPS	2.5	2.7	16.3	17.8

Radius of curvature in the transverse plane was also approximated at each location for all models. A photo was taken of each helmet perpendicular to the transverse plane such that the impact location fell on the horizon of the helmet. Slopes between the impact center and points along the helmet edge ~0.4 cm to either side of the center were determined and used to calculate equations of perpendicular lines at these points, then the intersection of these perpendicular lines was determined. The radius was computed as the distance between the helmet edge and the intersection point. Radii were generally larger at the temporal location of each helmet compared to frontal, reflecting the overall shape of the human head in the transverse plane, although local grooves or vents created variations in this trend.

Drop Tests

A twin-wire drop rig with a magnesium ISO headform (size J, Cadex, Richmond, BC, Canada) and a total drop carriage mass of 5.0 kg was used to replicate the CPSC standard test setup. All helmets sizes were selected such that the ISO J headform circumference fell within the center of the manufacturer-provided circumference range for the given helmet size. Although it is important for the standard to conduct tests under a spectrum of preconditioning environments and anvil types, impacts in this study were under ambient temperatures and against a flat anvil.

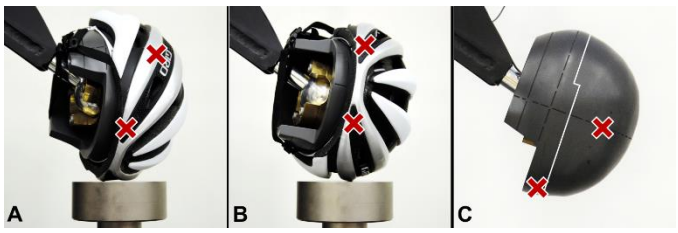

Figure 2.1 Headform orientation for (A) frontal and (B) temporal (above standard test lines) impact locations, and both locations on midsagittal view of ISO headform showing the impact test line in white (C). Locations were mirrored on the helmet and were a minimum of 120 mm apart, with the

frontal location falling below the test line. Visible impact centers are denoted with X's. Drop tests were performed at both locations at 3.4 and 6.2 m/s.

A total of 160 drop tests were conducted using four samples of each of the ten models with four impact configurations per sample. These impact configurations included two velocities: 3.4 and 6.2 m/s, and two locations: frontal at the rim and temporal above standard test lines (Fig. 2.1). The 3.4 m/s velocity and rim location are not in accordance with typical bicycle helmet standards, but were chosen to reflect common impact velocities (normal component) and locations found in literature [12, 13, 16-18]. Specifically, 3.4 m/s was determined through digitization of data from helmet damage replication studies [12, 13]; a normal impact velocity of 3.4 m/s and resulting head PLA of 100 g represent median values of the distribution of these data (Fig. 2.2). Conversely, the 6.2 m/s impact velocity was chosen to match the CPSC standard, which evaluates more severe head impact conditions. This velocity corresponds with the 96^{th} percentile of damage replication tests, while the 300 g pass-fail CPSC threshold corresponds with the 99^{th} percentile. Exact drop heights necessary to achieve these desired velocities on the CPSC rig were determined through preliminary testing (0.78 m yielded 3.4 ± 0.01 m/s and 2.22 m yielded 6.2 ± 0.02 m/s).

Impact locations were mirrored on the left and right sides of helmets, resulting in four impact centers per helmet sample. These impact centers were made to be a minimum of 120 mm apart to avoid overlap of crush profiles from prior impacts, as specified by the CPSC standard. Consistency in impacting these precise locations for all tests, which was made complicated by the lack of position indexing on the ball joint, was ensured through the use of a custom laser-positioning system. A polypropylene block was machined on one side to hold three lasers aligned in a triangle, while the opposing side was machined to press-fit onto the flat CPSC anvil. The block was rotated to a predetermined orientation and the headform was lowered to a set distance

from the anvil for each position change. At each impact location, points on the headform marked by the lasers were measured from the reference, coronal, and median planes to precisely mirror locations on both sides of the headform. Laser points were then permanently marked on the headform for each location, ensuring repeatability and reducing time spent in position changes.

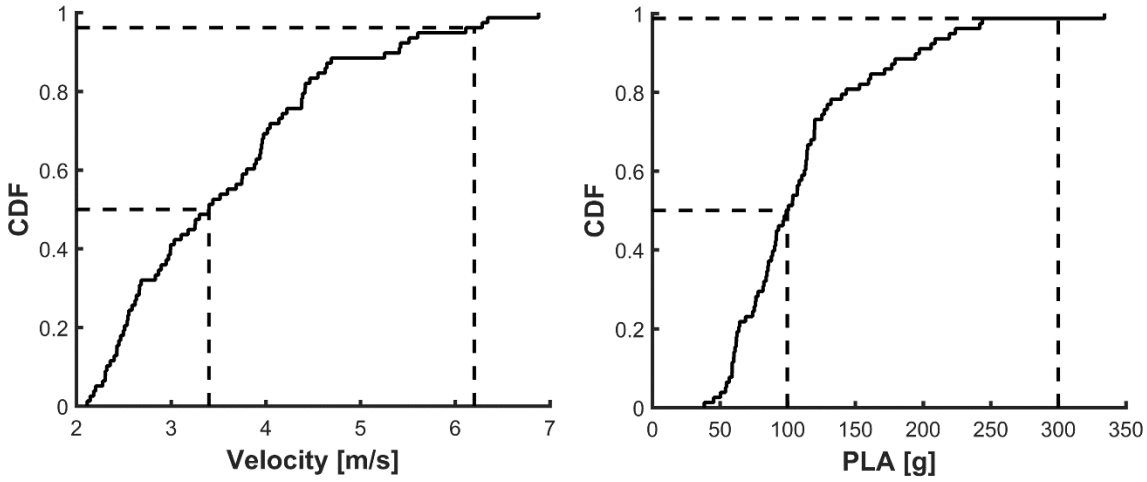

Figure 2.2. Cumulative distribution functions (CDFs) of normal velocity (left) and PLA (right) based on digitization of helmet damage replication data [12, 13]. Inner dashed lines indicate the 50th-percentile, and were found to correspond with 3.4 m/s (A) and 100 g (B). Outer dashed lines align with 6.2 m/s (A) and 300 g (B) to reflect common standards test levels, and correspond with the 96th and 99th percentiles, respectively.

Each helmet sample was subjected to each of the four impact configurations once (frontal-3.4 m/s, frontal-6.2 m/s, temporal-3.4 m/s, temporal-6.2 m/s), with the left and right sides of the helmet subjected to each velocity once. As an extra measure of precaution beyond the 120 mm-minimum spacing, order of impact configuration was randomized between samples to avoid introduction of bias from test configuration order. Finally, any included helmet attachments (i.e., visors) were removed prior to testing, as preliminary tests showed that visor effects on impact attenuation were

insignificant. Helmets were positioned with the rim 1.80 cm above the headform reference plane (along the midsagittal plane) for each test with retention straps and fit adjustment dials tightened maximally.

Data Collection and Analysis

For each impact, linear acceleration data were collected from a single-axis accelerometer (353B18, PCB, Depew, NY) at the center of gravity of the drop carriage using a TDAS PRO SIM data acquisition system (DTS, Seal Beach, CA), and were filtered in compliance with the CPSC standard (SAE J211 CFC 1000). Average PLA was calculated for each helmet per impact configuration, as well as 15 ms Head Impact Criterion (HIC). Risk of severe brain injury (Abbreviated Injury Scale (AIS) ≥ 4) was also calculated from HIC values using a previously published risk curve [11]. AIS ≥ 4 brain injuries include epidural and subdural hematomas, severe diffuse axonal injury, and other injuries of similar severity or even death. All results were compared within impact configurations using ANOVA and Tukey HSD post hoc tests ($\alpha = 0.05$). Correlation in helmet rank order between configurations was also evaluated using Kendall's coefficient of concordance within the framework of a Friedman test, as well as Spearman rank correlation coefficients.

Helmet impact attenuation characteristics were further investigated by determining impact duration, change in velocity (delta V), effective stiffness, and energy dissipated for every test. Duration was measured as the time when the linear acceleration pulse exceeded 5 g to the time when it first returned below 5 g again. This 5 g threshold was selected to provide consistency in determining the end point of an impact, and was found in preliminary testing to reliably quantify impact duration. Change in velocity was defined as the difference between the peak rebound velocity and the initial impact velocity, and was obtained through integration of linear acceleration

data. Headform displacement was then calculated through integration of velocity data. Headform displacement was assumed to reflect helmet deformation upon impact since the headform center of gravity in the CPSC rig is constrained to travel along a single degree of freedom, and any helmet rotation on the headform was found to occur after the initial impact. Others have used this same assumption for similar single-degree of freedom systems [19]. Effective stiffness of each helmet was then estimated from the loading slope to the point of peak displacement on the force-displacement curves, which were fairly linear during the loading segment unless bottoming out was apparent. In such cases, effective stiffness was estimated using the linear portion of the slope prior to the sharp peak in force coinciding with the deformation limit. Lastly, energy dissipated in each test was found by determining the area between the loading and unloading force-displacement curves. Correlations between each of these variables, as well as PLA and HIC, were investigated using coefficients of determination from simple linear regression models for each relationship.

All data processing and analyses were performed using MATLAB (R2014b, Mathworks Inc, Natick, MA) and JMP Pro 11 statistical software (SAS Institute Inc, Cary, NC).

RESULTS

The four impact configurations produced distinct distributions of head PLAs (Fig. 2.3). Overall, this sample of ten helmet models yielded average PLAs of 105.0 ± 22.4 g at 3.4 m/s and 226.8 ± 45.5 g at 6.2 m/s. The frontal location generally resulted in lower PLAs, averaging 87.8 ± 7.4 g at 3.4 m/s and 219.1 ± 57.8 g at 6.2 m/s compared to the temporal averages of 122.3 ± 18.7 g at 3.4 m/s and 234.4 ± 27.2 g at 6.2 m/s. However, the highest head accelerations were seen with two helmet models in the frontal-6.2 m/s configuration.

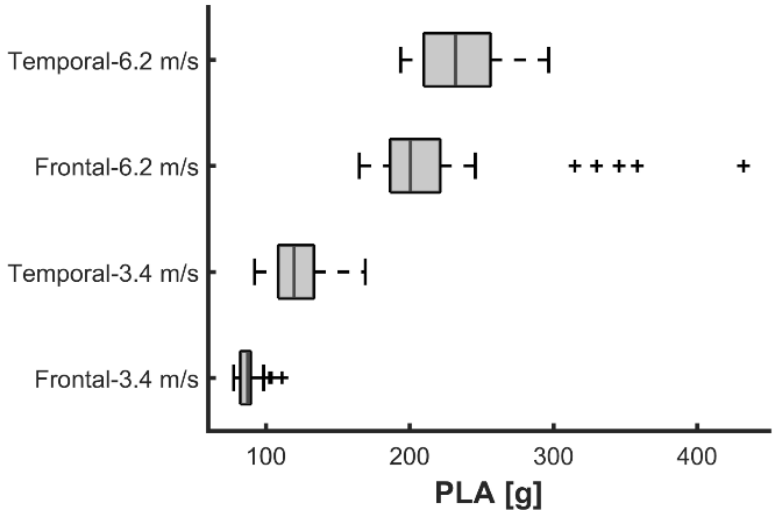

Figure 2.3. Distribution of PLA by impact configuration. Lower and upper bounds of boxes correspond with 25th and 75th percentiles, respectively, and whiskers extend to ±2.7σ. The frontal location generally resulted in lower PLAs than the temporal location when comparing across the same velocity, with the exception of several outliers at the frontal-6.2 m/s configuration.

Within each impact configuration, PLA also varied by helmet model (Fig. 2.4). Most helmets at the frontal location yielded similar PLAs to each other (not significantly different) with the exception of several outliers (Table 2.2). At the frontal-6.2 m/s configuration, all GS impacts and one GMIPS impact qualified as outliers, exceeding 300 g (GS: 362.9 ± 49.8 g, GMIPS: 255.0 ± 51.5 g). Conversely, the temporal location produced a greater number of helmets that were significantly different from a majority of other helmets. The temporal location also generally resulted in higher PLAs than the frontal location, with all helmets at 3.4 m/s and seven of the ten helmets at 6.2 m/s having higher PLAs at the temporal location as compared to their frontal counterpart. Relative helmet rank order was significantly correlated between the two velocities at the temporal location ($\rho = 0.84$, $p = 0.002$, Table 2.3), indicating that helmets that better reduced PLA at one velocity also better reduced PLA at the other for this location. This was dissimilar to the frontal location ($\rho = 0.27$, $p = 0.45$), where rank order varied more drastically between the two

velocities. Rank order also was not significantly correlated between the frontal and temporal locations at each velocity ($\rho < 0.50$, $p > 0.1$), as the lowest and highest ranked helmets varied between locations. Despite this variance, significant association was found to exist in rank order between all impact configurations ($W = 0.50$, $p < 0.001$), indicating that a helmet that performed better in one impact configuration was likely to also perform better in other configurations.

PLAs were well below those associated with AIS ≥ 4 brain injury at 3.4 m/s, making AIS ≥ 4 injury risk essentially zero for this velocity (0.2-2%). At 6.2 m/s, risks at the temporal location varied considerably and reflected relative PLA trends (Fig. 2.5). BMIPS, N, and ST had significantly higher risks than a majority of other helmets (88-97%), while BSF, GS, and SOO had significantly lower risks (51-54%) (Table 2.4). AIS ≥ 4 brain injury risks also showed large differences between helmets at the frontal location. Several of the helmets had relatively low risks (< 30%), while the GMIPS and GS helmets had significantly higher risks at 49% and 90%, respectively.

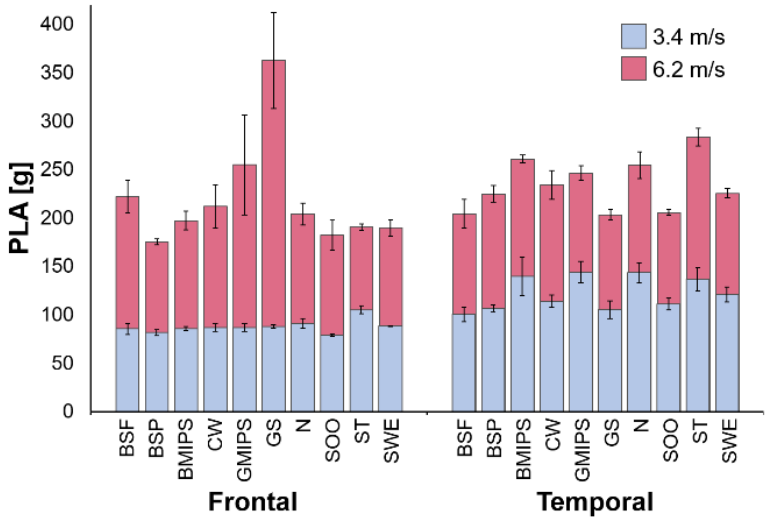

Figure 2.4. PLA per helmet type and location for 3.4 and 6.2 m/s (standard deviations error bars).

Table 2.2. Significance groupings between helmet types based on PLA. Helmets in the same column that are not connected by a common letter are significantly different (α = 0.05). PLA is organized in ascending order for each impact configuration, indicating relative performance rank order (best to worst performing). Helmets groupings that performed significantly better or worse than at least five other helmets are outlined in bold.

Frontal								Temporal							
3.4 m/s					6.2 m/s			3.4 m/s					6.2 m/s		
Helmet				PLA [g]	Helmet		PLA [g]	Helmet			PLA [g]		Helmet		PLA [g]
SOO	A			79.2	BSP	A	175.2	BSF	A		100.4		GS	A	203.4
BSP	A	B		81.6	SOO	A	182.3	GS	A		105.4		BSF	A	204.5
BSF	A	B	C	85.4	SWE	A	189.8	BSP	A		106.8		SOO	A	205.6
BMIPS	A	B	C	85.5	ST	A	190.5	SOO	A		111.0		BSP	A B	224.9
CW	A	B	C	86.7	BMIPS	A B	197.4	CW	A	B	114.0		SWE	A B	225.4
GMIPS	A	B	C	86.7	N	A B	204.1	SWE	A	B C	121.0		CW	B C	234.1
GS		B	C	88.0	CW	A B	212.0	ST		B C	136.8		GMIPS	B C D	246.5
SWE		B	C	88.2	BSF	A B	222.3	BMIPS		C	139.6		N	C D	254.9
N			C	91.3	GMIPS	B	255.0	N		C	143.5		BMIPS	D E	260.8
ST			D	105.2	GS	C	362.9	GMIPS		C	144.1		ST	E	283.7

Table 2.3. Relative performance rank order per helmet across all impact configurations. Helmets that produced lower summed ranks are listed first, with subsequent helmets having increasingly higher summed ranks. This provides an approximate indication of overall performance.

	Rank			
	Frontal		Temporal	
Helmet	3.4 m/s	6.2 m/s	3.4 m/s	6.2 m/s
BSP	2	1	3	4
SOO	1	2	4	3
BSF	3	8	1	2
GS	7	10	2	1
SWE	8	3	6	5
CW	5	7	5	6
BMIPS	4	5	8	9
ST	10	4	7	10
GMIPS	6	9	10	7
N	9	6	9	8

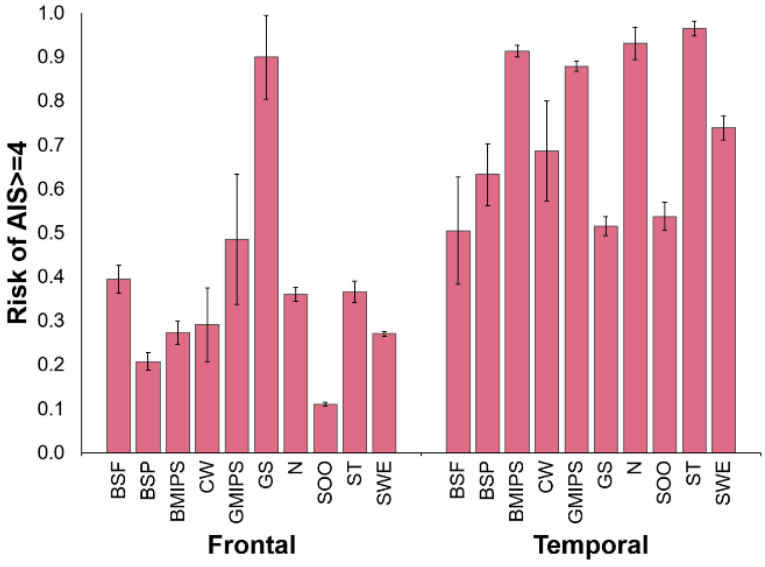

Figure 2.5. Risk of AIS ≥ 4 brain injury at 6.2 m/s per helmet and location (standard deviation error bars).

Table 2.4. Significance groupings between helmet types based on risk of AIS≥4 brain injury risk. Helmets in the same column that are not connected by a common letter are significantly different (α = 0.05). Risks are organized in ascending order for each impact configuration, indicating relative performance order (best performing to worst performing). Helmets groupings that performed significantly better or worse than at least five other helmets are outlined in bold.

Frontal						Temporal					
6.2 m/s						6.2 m/s					
Helmet					**Risk**	**Helmet**					**Risk**
SOO	A				0.11	BSF	A				0.51
BSP	A	B			0.21	GS	A				0.52
SWE		B	C		0.27	SOO	A				0.54
BMIPS		B	C		0.27	BSP	A	B			0.63
CW		B	C		0.29	CW		B			0.69
N		B	C	D	0.36	SWE		B	C		0.74
ST			C	D	0.37	GMIPS			C	D	0.88
BSF			C	D	0.39	BMIPS				D	0.91
GMIPS				D	0.49	N				D	0.93
GS					E 0.90	ST				D	0.97

Assessment of other impact attenuation variables showed that PLA, HIC, duration, and effective stiffness were well-correlated with each other at 3.4 m/s but not with delta V or energy dissipated, which were only well-correlated with each other (Fig. 2.6). Correlations were similar but generally weaker at 6.2 m/s (Fig. 2.7) than at 3.4 m/s due to the influence of several outliers. Duration ranged from 5-11 ms for both impact velocities and decreased with increasing PLA, HIC, and effective stiffness. Delta V revealed rebound velocities of approximately 1.5-2.5 m/s, and increasing delta V was associated with decreasing energy dissipated by the helmet.

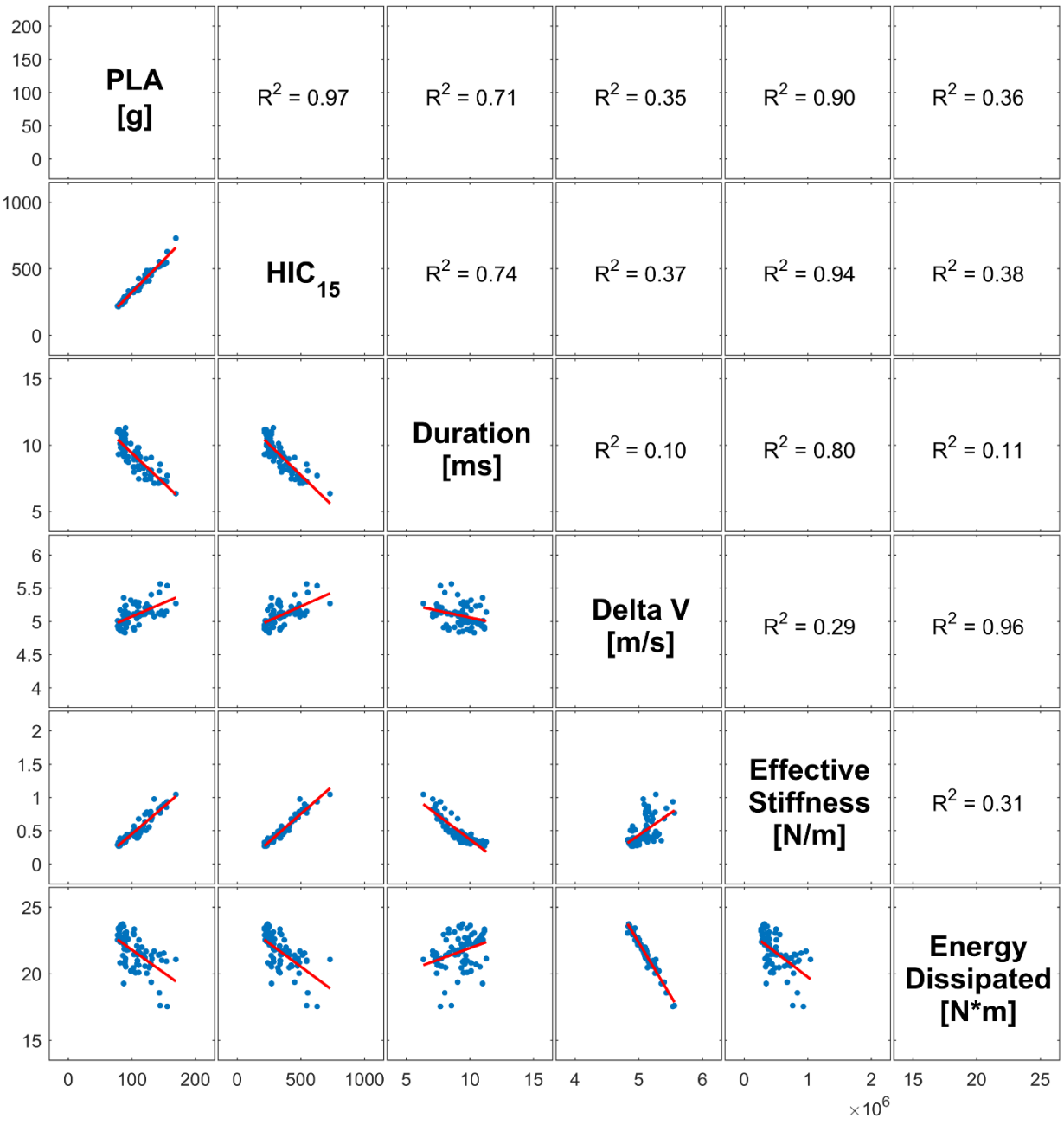

Figure 2.6. Impact attenuation variable scatter matrix at 3.4 m/s. Coefficients of determination correspond with the scatter plot in the transpose cell location. Strong correlations were found between PLA, HIC, duration, and effective stiffness ($R^2 > 0.7$), and between delta V and energy dissipated ($R^2 = 0.96$).

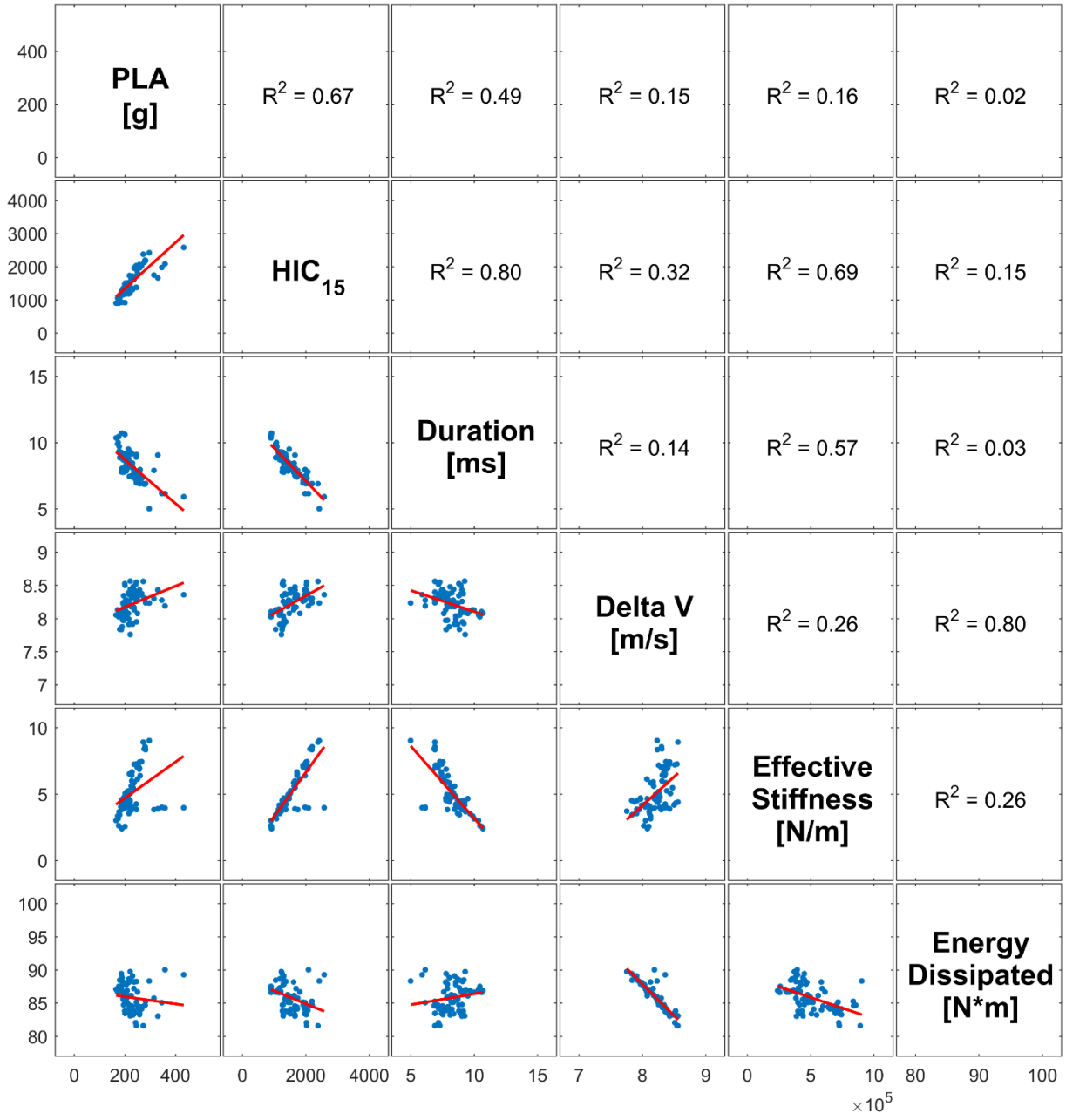

Figure 2.7. Impact attenuation variable scatter matrix at 6.2 m/s. Coefficients of determination correspond with the scatter plot in the transpose cell location. Stronger correlations were found between PLA, HIC, and duration ($R^2 \geq 0.49$), between effective stiffness, HIC, and duration ($R2 \geq 0.57$), and between delta V and energy dissipated ($R^2 = 0.80$). Several outliers appeared to affect PLA correlations.

DISCUSSION

Substantial differences in helmet impact attenuation capabilities under both real-world and standard-specified impact conditions were identified using the CPSC rig. These differences were more pronounced at the temporal location, with several of the helmets producing significantly higher or lower PLAs than a majority of other helmets at both velocities. Temporal PLAs and risks were also generally higher than those of frontal impacts, likely due to varying helmet geometry. Helmets typically exhibit a larger radius of curvature in the transverse plane at the temporal location compared to the frontal location, leading to a larger contact area upon impact. Although this was not the case for three of the helmets based on the radii given in Table 2.1, these radii are greatly influenced by small local geometrical variations, and the overall shape of all helmets did appear to reflect a larger radius at the temporal location. The impact force would thereby be distributed over a larger surface at the temporal location, leading to a lower pressure and increased effective stiffness, which reduce liner crush and cause higher PLAs [20]. The temporal location is also further from the edge of the helmet shell, so the more continuous shell often present at this location may increase force distribution for thicker shells, also contributing to a higher effective stiffness. This is supported by trends in effective stiffnesses between the frontal and temporal locations (Fig. 2.8). Data from several other studies that impacted bicycle helmets at multiple locations exhibit similar trends between frontal and side impacts as well [19, 21].

At the frontal location, helmet performance relative to other helmets was not significantly correlated between the two velocities ($p = 0.45$), as different helmets ranked worse at 3.4 m/s than those that ranked worse at 6.2 m/s. The GS helmet in particular produced extremely high PLAs and AIS ≥ 4 brain injury risk at 6.2 m/s, while having low-to-moderate PLAs and risks at 3.4 m/s. This helmet, as well as the GMIPS helmet, yielded PLAs exceeding the 300 g CPSC pass-fail threshold at the frontal-6.2 m/s impact configuration, corresponding to 90% risk for GS. These

extreme PLAs likely point to local weak points in helmet design, which would have been exacerbated at the higher impact velocity. For instance, the GS frontal impact location was over a vent and was thus associated with an exceptionally thin underlying liner (Table 2.1), indicating that the liner may have been insufficient to effectively modulate this higher impact energy, causing the helmet to bottom out. Bottoming out was confirmed by evaluation of force-displacement curves; these helmets exhibited a sharp increase in force coinciding with a deformation limit and resulting in a sharp linear acceleration peak (Fig. 2.9). It is important to note, however, that because the frontal location is at the rim and below the CPSC test line, helmet performance at this location is unregulated. Many bicycle helmet damage replication and accident reconstruction studies have shown that this is one of the most commonly impacted helmet locations [13, 16-18], suggesting that lowering the test line in current standards to include testing at the helmet rim may be necessary to ensure adequate cyclist safety.

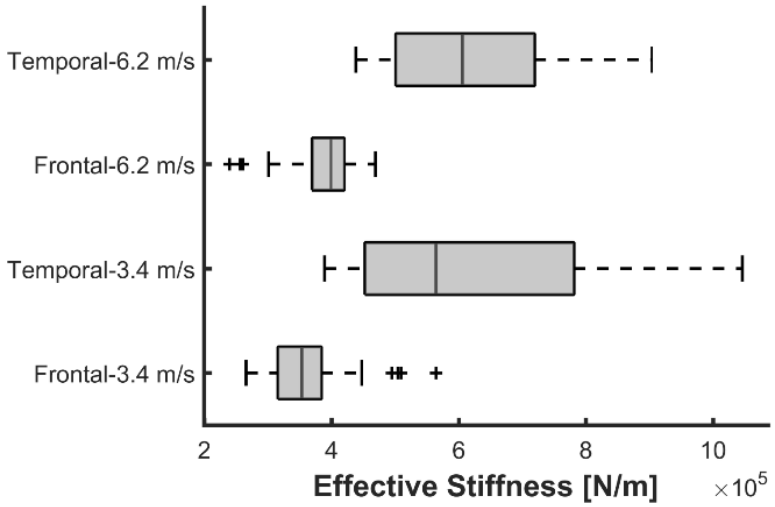

Figure 2.8. Distribution of effective helmet stiffnesses between impact configurations. The frontal location resulted in lower stiffnesses than the frontal location, averaging 374.0 ± 62.8 kN/m versus 622.7 ± 162.9 N/m, respectively.

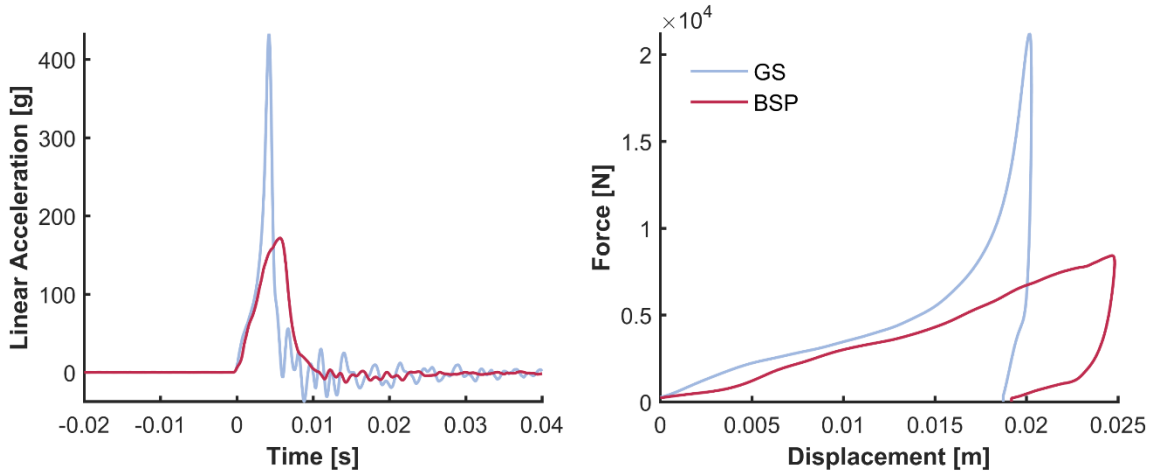

Figure 2.9. Linear acceleration (left) and force-displacement (right) curves for a representative bottoming-out case and non-bottoming out case. Both impacts were in the frontal-6.2 m/s configuration. The GS helmet experienced a large increase in force at a particular deformation limit (bottomed out), corresponding with a sharp acceleration pulse. Conversely, the BSP helmet had a nearly linear loading profile and a wider acceleration pulse.

The temporal location showed more correlation in relative helmet performance between the two velocities ($p = 0.002$). BMIPS, GMIPS, N, and ST yielded higher accelerations at both velocities, while GS, SOO, BSF, and BSP yielded lower accelerations. As current helmet design is based around passing standards testing and thereby aimed at reducing severe injury risk, investigation of any tradeoff in performance at lower impact energies, such as those commonly seen in cyclist accidents, was of particular interest. Since helmet performance was well-correlated between impact velocities at the temporal location, and since trends at the frontal location likely varied as a function of local geometry effects, no tradeoff is apparent within this sample of helmets. Significant association was found between rank orders from all impact configurations ($p < 0.001$), meaning that helmets that performed worse overall at the higher velocity were more likely to also perform worse at the lower velocity, and vice versa. Although each helmet tested was standard-certified and produced minimal risk of severe brain injury at the lower impact energy, impacts at

this velocity yielded PLAs that fall within a distribution of impact PLAs resulting in concussion in football players [14, 22-24]. This suggests that impacts at this energy, such as those common in real-world conditions, may pose considerable risk of mild brain injury, and demonstrates that there is room for improvement of helmet design in order to minimize likelihood of sustaining mild traumatic brain injuries as well as severe.

The helmets that performed worse in overall rank between impact configurations include BMIPS, GMIPS, N, and ST. Interestingly, this subset includes all three non-road helmets, which produced significantly greater PLAs at the temporal location versus the non-road helmets ($p < 0.001$ at 3.4 m/s and $p = 0.002$ at 6.2 m/s). This suggests that these styles of helmets may offer inferior impact protection compared to traditional road helmets. The non-road helmets in the present study were characterized as being heavier (398 ± 58.0 grams for non-road versus 293 ± 34.0 grams for road) with thicker shells (1.22 ± 0.73 mm for non-road versus 0.45 ± 0.11 mm for road), and having a rounded shape with less venting. Several of these parameters may contribute to reduced impact attenuation; the thicker shell may distribute impact forces over a larger area, decreasing the pressure upon impact and thus increasing effective liner stiffness, while the decreased venting may also lead to a larger contact area upon impact, again increasing effective liner stiffness (Mills 1990). Effective stiffness values were indeed significantly greater for the non-road helmets and ST versus all other helmets ($p < 0.004$ for all configurations). However, a larger sample of helmet models would be required in order to establish any definitive correlation between non-road helmet design parameters and impact performance. The only road helmet that consistently performed poorly was ST. This was the heaviest and stiffest road helmet, making the four heaviest and stiffest helmets the worse-performing helmets. This helmet was also the only road helmet that did not contain vents at the temporal location, further suggesting that interrupting the continuity of the helmet with venting may be beneficial to impact attenuation by reducing effective stiffness.

Helmets that consistently ranked best in all impact configurations include BSP, SOO, and BSF. Trends between design parameters of these helmets were less notable, other than that they were all road helmets. However, force-displacement curves and stiffness-PLA correlations indicate that helmet designs facilitating greater liner crush through lower effective stiffness (without reaching a deformation limit) will generally be more effective in reducing injury risks. Many design parameters may affect liner crush, such as liner material and density, vent placement, shell geometry, initial liner thickness, etc. It is interesting to note that the SOO helmet, which had a liner primarily comprised of a honeycomb structure, yielded generally greater displacements for all impact configurations and consistently had among the lowest risk values. Thus, it appears that this alternative liner material may attenuate impact accelerations as well as, if not more than, traditional EPS liners. Other helmets incorporated a technology called multidirectional impact protection system (MIPS), which is intended to reduce rotational accelerations experienced by the head during impact. These helmets were both among the worse-performing helmets at the temporal location, but rotational acceleration was not assessed in this testing due to the constrained CPSC setup, and therefore the effectiveness of MIPS cannot be assessed herein.

Analysis of additional helmet impact attenuation characteristics revealed strong correlations between PLA, HIC, impact duration, and effective stiffness. HIC and stiffness increased with increasing PLA, while duration decreased with increasing PLA. Correlations were not as strong at 6.2 m/s due to the influence of several outliers. Further investigation showed that these outliers were entirely comprised of the high PLA, bottoming-out cases for the GS and GMIPS helmets at the frontal-6.2 m/s configuration. Due to the sharp increase in force at the deformation limit that is characteristic of bottoming out, effective stiffness was estimated using only the linear loading portion, resulting in relatively low stiffness estimates corresponding with high accelerations and

reducing the strength of the PLA-stiffness correlation. These same outliers were evident in the PLA-HIC relationship; the bottoming out cases generally had very narrow acceleration pulses and thus shorter durations (Fig. 2.9), causing HIC values to be relatively low for high PLA values. Because of this, HIC was unable to identify when bottoming-out occurred, whereas PLA clearly differentiated these cases. Although there is a paucity of definitive data demonstrating whether HIC or PLA is a better predictor of head injury for such short duration impacts, bottoming out is a phenomenon that intuitively would appear better if detected and avoided.

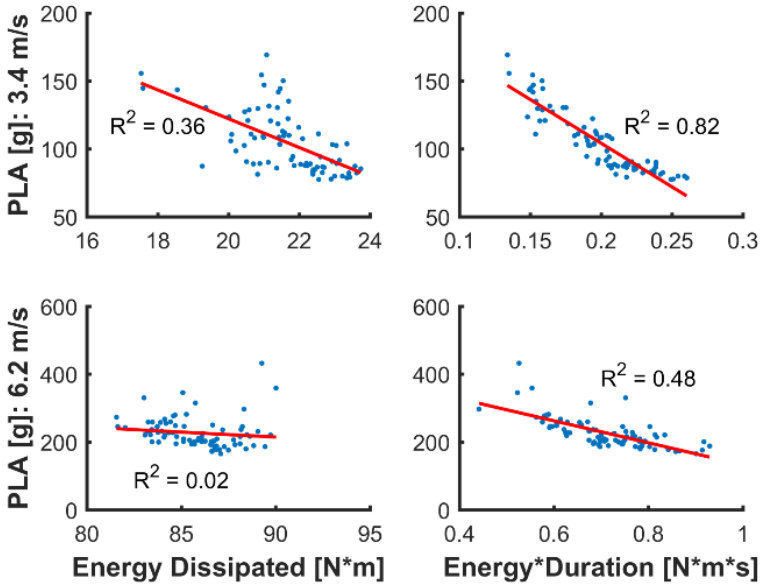

Figure 2.10. Energy dissipation versus PLA at 3.4 and 6.2 m/s. Energy alone correlated poorly with PLA (left), while incorporating duration in a linear fashion (right) improved correlations.

Impact attenuation variable analyses also indicated that PLA, HIC, duration, and stiffness were poorly correlated with delta V and energy dissipated, which were well-correlated with each other. The strong correlation between these two variables was expected since delta V is also indicative of energy dissipated. The lack of correlation between PLA and energy dissipated was more surprising, however, as a helmet that dissipates more energy could be expected to also reduce

acceleration more effectively. This ostensible contradiction can be explained by the lack of duration accounted for in the energy dissipation parameter. If duration is accounted for in a linear fashion by multiplying by energy dissipated, correlations with PLA are much improved (Fig. 2.10).

This study, although able to identify differences in the ability of helmets to mitigate head impacts and thereby reduce risk of injury, was limited in several ways. The first of these is that only a small sample of helmets was evaluated, restricting possible inferences on correlations between design parameters and helmet performance. It appears evident that several helmet characteristics, such as larger radii of curvature, thicker shells, and less venting, may contribute to increased effective stiffness and thereby greater PLAs and risks, but testing a larger variety of helmets is needed to provide a more definitive assessment of these correlations. Second, non-road helmets may be exposed to a wider variety of impact conditions differing from the conditions imposed herein. However, due to lack of data characterizing these types of impacts, as well as the fact that many people wear urban/street helmets in day-to-day recreational activity or commutes, ensuring effectiveness of these helmets under common impact conditions is valuable. Third, the test setup in the present study only considers two impact locations (mirrored on both sides of the helmet), and results were likely greatly influenced by local geometries of the helmet. While it is important that manufacturers design helmets to offer sufficient protection in all impact scenarios, testing helmets at more locations could provide a more holistic indication of overall performance. And lastly, because this study used standards test equipment, only linear accelerations from idealized, normal impacts were evaluated. Oblique impacts (involving normal and tangential velocity components) are far more common in cyclist crashes than normal impacts [2]. Oblique impacts also involve both linear and rotational accelerations of the head, the combination of which can cause diffuse brain injury such as concussion [25-27]. Testing a variety of helmets on oblique impact rigs, such as those already developed by a number of researchers [9, 19, 21, 28-30], may

better discriminate the ability of different helmets to reduce risk of concussion and other diffuse brain injuries. Should standards testing be modified to include oblique impacts, the test rig would likely need to incorporate a more realistic headform and possibly a surrogate neck to provide realistic rotational motion. Other injury metrics that consider both linear and rotational kinematics would need to be evaluated to better assess performance, as both contribute to injury risk.

As large differences in helmet performance were identified in the present study, it would be valuable for manufacturers or standards agencies to incorporate additional testing in order to compare relative performance and evaluate impact protection capabilities in scenarios reflecting real-world accidents. This should not replace current standards testing, which is vitally important for ensuring protection against severe impact energies at virtually any location (above the impact test line). However, the addition of such a battery of tests would provide insight to consumers on the level of safety afforded by different helmets and would ultimately stimulate improved design for common impact locations and lower impact energies.

CONCLUSIONS

This study identified considerable variation in the impact attenuation capabilities of different helmets on a standards test rig, even within the small sample of commercially-available helmets that were tested. These differences were detected at both standard-specified impact conditions and non-standard impact conditions, which were imposed based on common impact conditions reported in literature. The results suggest that there is value in considering these non-standard conditions, as helmets generally yielded concussive-level accelerations at the lower impact velocity, and impacting below the test line revealed hazardous brain injury risks at the high velocity, with PLAs even exceeding the CPSC-specified pass-fail threshold for several bottoming-out cases. Lowering the impact test line in current standards is recommended in order to improve impact protection at this commonly impacted location. Aside from bottoming-out cases, helmets

that performed worse in one configuration tended to also perform worse in others. The temporal location of most helmets produced higher PLAs and risks than the frontal location, likely due to increased effective stiffness. Additionally, non-road helmets tended to be ranked worse across all impact configurations, also due to increased effective stiffness. Developing strategies to reduce effective helmet stiffness and facilitate improved liner crush within deformation limits would lead to improved impact attenuation. Ideally, these data will be used to inform future standards testing and helmet manufacturers, aiding the development of improved of bicycle helmet safety.

REFERENCES

1. IIHS. Pedestrians and Bicyclists. *Fatality Facts* [Web]. 2016; www.iihs.org/iihs/topics/t/pedestrians-and-bicyclists/fatalityfacts/bicycles#cite-text-0-0. Accessed February 18, 2016, 2016.
2. Otte D. Injury Mechanism and crash kinematics of cyclists in accidents. Paper presented at: 33rd Stapp Car Crash Conference 1989; Warrendale, PA.
3. Sacks JJ, Holmgreen P, Smith SM, Sosin DM. Bicycle-associated head injuries and deaths in the United States from 1984 through 1988: How many are preventable? *JAMA.* 1991;266:3016-3018.
4. AANS. Sports-Related Head Injury. *Patient Information* [Web]. 2014; www.aans.org/patient%20information/conditions%20and%20treatments/sports-related%20head%20injury.aspx. Accessed February 18, 2016, 2015.
5. Schulman J, Sacks J, Provenzano G. State level estimates of the incidence and economic burden of head injuries stemming from non-universal use of bicycle helmets. *Inj Prev.* 2002;8(1):47-52.
6. Elvik R. Corrigendum to: "Publication bias and time-trend bias in meta-analysis of bicycle helmet efficacy: a re-analysis of Attewell, Glase and McFadden, 2001" [Accid. Anal. Prev. 43 (2011) 1245-1251]. *Accid Anal Prev.* 2013;60:245-253.
7. Thompson DC, Nunn ME, Thompson RS, Rivara FP. Effectiveness of bicycle safety helmets in preventing serious facial injury. *JAMA.* 1996;276(24):1974-1975.
8. Cripton PA, Dressler DM, Stuart CA, Dennison CR, Richards D. Bicycle helmets are highly effective at preventing head injury during head impact: head-form accelerations and injury criteria for helmeted and unhelmeted impacts. *Accid Anal Prev.* 2014;70:1-7.
9. McIntosh AS, Lai A, Schilter E. Bicycle helmets: head impact dynamics in helmeted and unhelmeted oblique impact tests. *Traffic Inj Prev.* 2013;14(5):501-508.
10. CPSC. Safety Standard for Bicycle Helmets Final Rule (16 CFR Part 1203). In. Vol 63: United States Consumer Product Safety Commission; 1998:11711-11747.
11. Mertz HJ, Irwin AL, Prasad P. Biomechanical and scaling bases for frontal and side impact injury assessment reference values. *Stapp Car Crash J.* 2003;47:155-188.
12. Smith TA, Tees D, Thom DR, Hurt HH. Evaluation and replication of impact damage to bicycle helmets. *Accid Anal Prev.* 1994;26(6):795-802.
13. Williams M. The protective performance of bicyclists' helmets in accidents. *Accid Anal Prev.* 1991;23(2-3):119-131.

14. Pellman EJ, Viano DC, Tucker AM, Casson IR, Waeckerle JF. Concussion in professional football: reconstruction of game impacts and injuries. *Neurosurgery.* 2003;53(4):799-812.
15. Rowson S, Duma SM. Brain injury prediction: assessing the combined probability of concussion using linear and rotational head acceleration. *Ann Biomed Eng.* 2013;41(5):873-882.
16. Bourdet N, Deck C, Carreira RP, Willinger R. Head impact conditions in the case of cyclist falls. *Proc IMechE Part P: J Sports Engineering and Technology.* 2012;226(3-4):282-289.
17. Ching RP, Thompson DC, Thompson RS, Thomas DJ, Chilcott WC, Rivara FP. Damage to bicycle helmets involved with crashes. *Accid Anal Prev.* 1997;29(5):555-562.
18. McIntosh A, Dowdell B, Svensson N. Pedal cycle helmet effectiveness: A field study of pedal cycle accidents. *Accid Anal Prev.* 1998;30:161-168.
19. Mills NJ, Gilchrist A. Oblique impact testing of bicycle helmets. *Int Journal Impact Eng.* 2008;35(9):1075-1086.
20. Mills NJ. Protective capability of bicycle helmets. *Br J Sports Med.* 1990;24(1):55-60.
21. Milne G, Deck C, Bourdet N, Carreira RP, Allinne Q, Gallego A, Willinger R. Bicycle helmet modelling and validation under linear and tangential impacts. *Int J Crashworthiness.* 2013;19(4):323-333.
22. Broglio SP, Schnebel B, Sosnoff JJ, Shin S, Fend X, He X, Zimmerman J. Biomechanical properties of concussions in high school football. *Med Sci Sports Exerc.* 2010;42(11):2064-2071.
23. Guskiewicz KM, Mihalik JP, Shankar V, Marshall SW, Crowell DH, Oliaro SM, Ciocca MF, Hooker DN. Measurement of head impacts in collegiate football players: relationship between head impact biomechanics and acute clinical outcome after concussion. *Neurosurgery.* 2007;61(6):1244-1253.
24. Rowson S, Duma SM, Beckwith JG, Chu JJ, Greenwald RM, Crisco JJ, Brolinson PG, Duhaime AC, McAllister TW, Maerlender AC. Rotational head kinematics in football impacts: an injury risk function for concussion. *Ann Biomed Eng.* 2012;40(1):1-13.
25. Gennarelli T, Ommaya A, Thibault L. Comparison of translational and rotational head motions in experimental cerebral concussion. Paper presented at: 15th Stapp Car Crash Conference 1971.
26. Gennarelli TA, Thibault LE, Ommaya AK. Pathophysiologic responses to rotational and translational accelerations of the head. *SAE Technical Paper Series.* 1972;720970:296-308.
27. Ommaya AK. Biomechanics of head injuries: experimental aspects. In: Nahum AM, Melvin J, editors. Biomechanics of trauma. Eat Norwalk, CT: Appleton-Century-Crofts 1985.
28. Aare M, Halldin P. A new laboratory rig for evaluating helmets subject to oblique impacts. *Traffic Inj Prev.* 2003;4(3):240-248.
29. Hansen K, Dau N, Feist F, Deck C, Willinger R, Madey SM, Bottlang M. Angular Impact Mitigation system for bicycle helmets to reduce head acceleration and risk of traumatic brain injury. *Accid Anal Prev.* 2013;59:109-117.
30. Klug C, Feist F, Tomasch E. Testing of bicycle helmets for preadolescents. Paper presented at: IRCOBI Conference 2015; Lyon, France.

CHAPTER 3

DIFFERENCES IN IMPACT PERFORMANCE OF BICYCLE HELMETS DURING OBLIQUE IMPACTS

ABSTRACT

Cycling is a leading cause of sport-related head injuries in the U.S. Although bicycle helmets must comply with standards limiting head acceleration in severe impacts, helmets are not evaluated under more common, concussive-level impacts, and limited data are available indicating which helmets offer superior protection. Further, standards evaluate normal impacts, while real-world cyclist head impacts are oblique – involving normal and tangential velocities. The objective of this study was to investigate differences in protective capabilities of ten helmet models under common real-world accident conditions. Oblique impacts were evaluated through drop tests onto an angled anvil at common cyclist head impact velocities and locations. Linear and rotational accelerations were evaluated and related to concussion risk, which was then correlated with design parameters. Significant differences were observed in linear and rotational accelerations between models, producing concussion risks spanning >50% within single impact configurations. Risk differences were more attributable to linear acceleration, as rotational varied less between models. At the temporal location, shell thickness, vent configuration, and radius of curvature were found to influence helmet effective stiffness. This should be optimized to reduce impact kinematics. At the frontal, helmet rim location, liner thickness tapered off for some helmets, likely due to lack of standards testing at this location. This is a frequently impacted location for cyclists, suggesting that the standards testable area should be expanded to include the rim. These results can inform manufacturers, standards bodies, and consumers alike, aiding the development of improved bicycle helmet safety.

INTRODUCTION

Copious media attention and research efforts have been directed towards head injury in football due to the high incidence of injury and the popularity of the sport. Although football-induced head injury is a pressing issue, injury surveillance systems have shown that cycling is actually the leading cause of sport-related head injuries treated in U.S. emergency rooms [1], accounting for an estimated 81,000 cases in 2015 [2]. The incidence rate is likely even higher than this, as many less-severe head injuries are assessed at home or by a primary care provider rather than in emergency rooms. The resulting economic and societal burden is substantial, with associated U.S. healthcare costs for cycling-related head injuries estimated to exceed $2 billion annually [3]. Moreover, cycling is a popular activity for sport, transport, and leisure across a variety of ages and in numerous countries, making head injury from cycling accidents a concern worldwide.

The risk of sustaining a head injury from cycling is mitigated through bicycle helmet use. This has been demonstrated by both epidemiological studies [4-7], showing that helmets can reduce head injury risk by up to 69%, as well as biomechanical studies of helmeted versus unhelmeted impacts [8, 9]. Helmets in the U.S. are presently subject to the Consumer Product Safety Commission (CPSC) Safety Standard for Bicycle Helmets [10]. In the impact attenuation portion of this standard, helmets are fitted onto an International Organization for Standardization (ISO) half headform and subjected to a series of normal impacts through guided drop tests. Multiple samples of each helmet are exposed to a variety of environmental conditions and are dropped onto either a flat anvil at 6.2 m/s or a hemispherical or curbstone anvil at 4.8 m/s. All impact centers must be superior to a specified test line. Centers of successive impacts to the same helmet must be >120 mm apart to avoid overlap of damage profiles, which would influence subsequent accelerations. Helmets that reduce peak linear acceleration (PLA) of the headform to less than 300 g (a level associated with >50% risk of severe brain injury or skull fracture [11]) in all tests pass the standard.

Standards are limited in their representation of real-world cyclist accidents in several ways. Because testing is based around PLA thresholds associated with severe head injury, performance at lower impact energies is not considered, which helmet damage replication studies have shown are more common in cyclist accidents [12, 13]. Damage replication studies collect helmets from accidents and recreate the damage on new helmets through standard drop tests onto a flat anvil, generating approximations of real-world impact velocities and resulting linear accelerations. PLA in these studies averages around 100 g – a level generally associated with risk of concussion in athletes [14, 15]. Additionally, these studies have suggested that cyclist head impacts most commonly occur at the front and sides of the head, and often around the helmet rim region. This finding is further supported by accident case reviews and computational simulation studies of cyclist accidents [16-21]. The rim of the helmet falls inferior to the testable region defined by current standards, meaning design is not regulated at this commonly-impacted location.

Standards also present limited representation of real-world cyclist head impacts by testing only normal-velocity impacts and assessing only linear acceleration. Normal impacts produce forces through the center of gravity (CG) of the headform, while studies have shown substantial tangential forces on the helmet in addition to normal forces [16, 20-23]. This occurs due to the cyclist typically approaching the ground at an angle during impact with both normal and tangential incident velocities [24]. Resultant incident angles have been estimated via simulation studies to commonly vary between 30° and 60° [16, 20-23]. These angled impacts are often termed *oblique*, and produce a moment about the head CG, inducing rotational acceleration as well as linear [9, 25, 26]. Standards drop rigs contain a rigid connection between the headform and drop carriage rather than allowing for movement of the headform upon impact (i.e. through a surrogate neck), so these systems are not well-equipped to provide a realistic assessment of rotation.

The addition of rotation is an important factor in injury risk evaluation. Kinematic parameters of head impact are frequently related to brain injury risk, as they are thought to represent the inertial response of the brain inside the skull [27-32]. Rotational kinematics has been shown to correlate well with relative brain motion and strain that occurs upon head impact, associated with diffuse tissue injury. Linear acceleration, on the other hand, has been shown to be correlated with transient intracranial pressure gradients that associated with more focal injury. There is likely an interplay of these two types of motions in producing brain injury, as real-world head impacts involve both linear and rotational accelerations [31-33].

Given the prevalence of oblique head impacts in cyclist accidents and the injurious nature of the resulting linear and rotational impact kinematics, it has been suggested that bicycle helmets be evaluated for their performance under oblique impacts [9, 25, 26, 34, 35]. Several research groups have developed test rigs capable of impacting helmets with both normal and tangential incident velocity components through use of either an angled anvil [25, 36, 37] or a horizontally-moving striker plate [9, 26, 34]. One rig, which subjects a free-falling Hybrid III headform to impacts against an angled anvil coated with abrasive paper, has been proposed by CEN/TC 158 Working Group 11 for implementation into European standards and represents the first potential incorporation of oblique impact testing into bicycle helmet regulations [35].

While bicycle helmet safety standards ensure that commercially-available helmets reduce risk of severe injury, their purpose does not include differentiating performance among helmets that pass the testing process. It is probable that bicycle helmets show a wide range in impact attenuation capabilities, as design varies considerably from helmet to helmet. These variations generally stem from a balance between helmet aesthetics, aerodynamics, and impact protection. Conventional helmets contain a plastic outer shell (typically polycarbonate (PC)) and an expanded polystyrene

(EPS) liner, which crushes upon impact to dissipate a portion of the energy transferred to the head. However, designs may contain other liner and shell materials, and often present variations in liner densities and thicknesses, shell thicknesses, vent configuration, and overall shape, as well as in many other parameters. Several studies testing small subsets of helmet models have indeed demonstrated differences in performance [34, 36, 38], highlighting the need for investigation of which design parameters are most conducive to impact protection. This data may then equip manufacturers to implement safety-oriented design changes.

Additionally, in light of the importance of rotation in producing brain injury, new technologies have been incorporated into helmets meant to reduce the rotational kinematics of head impact. One common technology in bicycle helmets is the multi-directional impact protection system (MIPS AB, Täby, Sweden), which uses a slip-plane concept wherein a thin, low-friction layer interfacing with the wearer's head is attached by elastomeric suspension to the outer shell. Upon impact, this layer is meant to facilitate sliding of the head relative to the rest of the helmet, mitigating the rotational kinematics experienced by the head. A few studies have demonstrated the superiority of this technology [36, 38], although additional testing is needed to further investigate its effectiveness in a vast array of helmet models. Ultimately, providing objective impact attenuation data comparing helmet models to consumers will allow them to make informed safety-based decisions when purchasing a helmet. The objective of the present study was to investigate differences in the ability of ten bicycle helmet models of varied designs to attenuate impact accelerations when subjected to oblique impacts under common cyclist accident conditions.

METHODS

Helmet Models

Ten helmet models were selected for impact testing based on their varied design parameters

(Table 3.1). Seven of the helmets were classified as road helmets, which generally contain an elongated shape with aerodynamic venting, while non-road helmets have a more rounded shape with smaller or fewer vents. The non-road helmets were also the heaviest helmets and had thicker shells. All shells were comprised of PC except for the N helmet, which had a thicker acrylonitrile butadiene styrene (ABS) shell, and all liners were comprised of EPS, although the SOO helmet also incorporated a honeycomb structure called Koroyd® for a majority of its liner with EPS limited to smaller areas. Liner thickness was measured at a frontal and a temporal location that were selected for impact testing. One sample of each model was set aside for thickness measurements, wherein a section of liner surrounding the predefined impact center was cut radially and removed from the surrounding liner, allowing radial thickness at the impact center to be measured with calipers. Thickness was found to be similar between all helmet models except for GS, which was thinner at the frontal location due to a coinciding vent. Helmet price was defined as the manufacturer's suggested retail price (MSRP) at the time of the study, and ranged from $23 to $250, reflecting a range in aerodynamics and aesthetics. Additionally, two of the selected helmets contained MIPS technology (BMIPS, GMIPS).

Radii of curvature of the transverse plane at these locations were also approximated via image analysis. Each helmet was photographed in an orientation perpendicular to the transverse plane of the head with the exact impact center on the horizon of the helmet (Fig. 3.1). The slopes between the impact center and points 0.5 cm to either side along the helmet edge were calculated and used to determine equations of perpendicular lines at these points. The radius was then computed as the distance between the intersection of the perpendicular lines and the impact center. Radii were typically larger at the temporal location ($p = 0.048$, one-tailed t-test), reflecting the general shape of the human head in the transverse plane, although local variations in helmet geometry caused inconsistencies in this trend.

Table 3.1. Helmet models used in testing. Price indicates the MSRP at the time of the study. Frontal and temporal locations are denoted by F and T, respectively, where each helmet was impacted. Two of the helmets contained multi-directional impact protection system (MIPS) technology. ABS is acrylonitrile butadiene styrene.

Helmet	Style	Price [$]	Mass [grams]	Vents	Shell Material	Shell Thickness [mm]	Liner Material	Liner Thickness [cm]		Radius of Curvature [cm]	
								F	T	F	T
Bell Solar Flare (BSF)	Road	40	312	23	PC	0.5	EPS	2.60	3.23	20.6	19.7
Bell Star Pro (BSP)	Road	240	296	15	PC	0.4	EPS	2.94	2.55	13.2	22.3
Bell Super 2 MIPS (BMIPS)	Mountain	155	360	23	PC	0.7	EPS	2.37	2.64	5.6	22.9
Catlike Whisper (CW)	Road	235	283	39	PC	0.5	EPS	2.86	2.06	5.7	4.7
Giro Sutton MIPS (GMIPS)	Urban/ street	100	370	8	PC	0.7	EPS	2.67	2.93	5.8	9.5
Giro Synthe (GS)	Road	250	250	26	PC	0.3	EPS	1.62	2.92	4.8	12.0
Nutcase Watermelon (N)	Urban/ street	70	465	11	ABS	2.2	EPS	2.84	2.65	16.1	12.2
Smith Optics Overtake (SOO)	Road	250	250	21	PC	0.3	EPS/ Koroyd	3.08	2.92	7.4	18.2
Schwinn Thrasher (ST)	Road	23	340	20	PC	0.4	EPS	2.54	2.26	6.9	9.6
S-Works Evade (SWE)	Road	225	317	15	PC	0.6	EPS	2.47	2.71	16.3	17.8

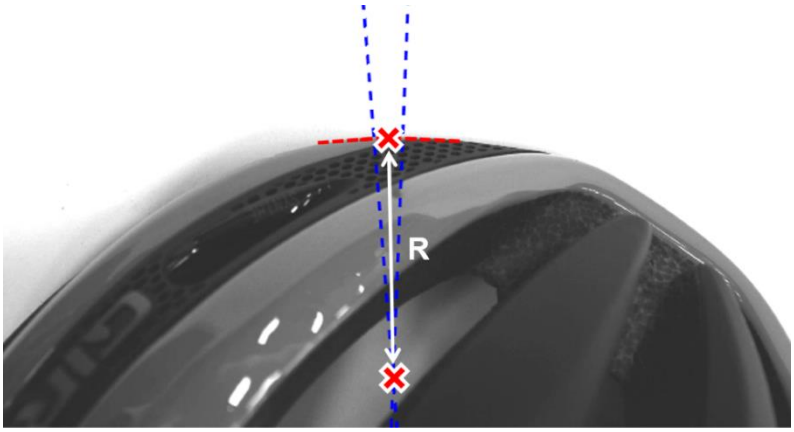

Figure 3.1. Example radius of curvature determination process for a frontal impact location. The impact center was specified (indicated by the upper X), then tangential lines were calculated using points 0.5 cm along the helmet edge to either side of the center. Radial lines were then calculated, and the intersection of these lines determined (lower X). Radius, R was computed as the distance between the intersection and impact center.

Impact Tests

A custom linear drop tower was developed for the purpose of subjecting bicycle helmets to oblique impacts. The drop mass consisted of a National Operating Committee on Standards for Athletic Equipment (NOCSAE) headform, a Hybrid III 50th-percentile male neck, and a steel plate intended to simulate effective torso mass (16 kg, [39]). A custom adaptor plate was used to mount the headform on the neck [40, 41]. The head-neck assembly was able to rotate in fixed increments about two axes, providing consistency in specifying impact location. Impacts were against a 30° anvil – a common impact angle in cyclist accident computational analyses [16, 20-23]), which created an oblique impact by generating normal and tangential incident velocities and impact forces similar to what a cyclist may experience. The anvil was coated with adhesive-backed 80-grit sandpaper for all tests to simulate road surfaces (0.5 coefficient of friction, in accordance with ECE R-22.05 standard for motorcycle helmet testing [42]), and was replaced between tests. In

order to avoid excessive loading of the neck, the drop mass was stopped by a spring located on the base of the drop tower at approximately 13 ms into the impact. This occurred subsequent to the linear acceleration trace returning to 0, and was thus determined to be sufficient time to be considered separate from the initial head impact pulse.

Impact configurations were chosen to replicate conditions commonly seen in cyclist accidents. Helmet damage reconstruction and cyclist accident investigation studies have shown that helmets are most frequently impacted at the front and sides [12, 13, 16-21]; therefore, a front and a side location were selected for testing (Fig. 3.2). The front location was set in the frontal-temporal region at the helmet rim (below testable region in standards), while the side location was set in the temporal region (within testable region). These locations were then mirrored across the midsagittal plane of the helmet to produce four impact centers per helmet (each tested once per helmet sample), which were predetermined to maintain a minimum distance of 120 mm between all centers in accordance with the CPSC standard [10]. As helmets are symmetrical across this plane, impacts on the left and right sides were considered to be identical, and results were averaged into frontal and temporal locations.

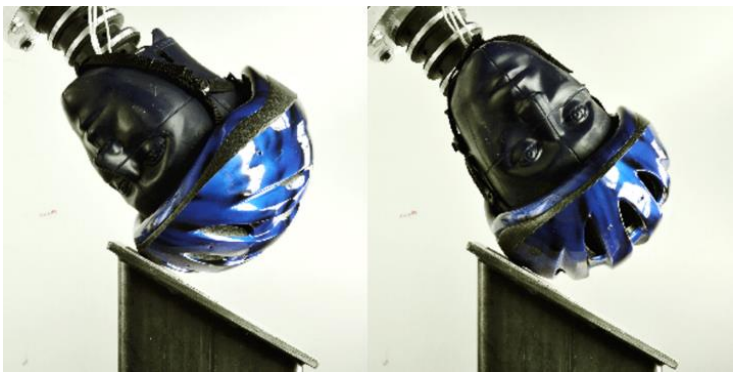

Figure 3.2. Headform orientation for a frontal impact (left) and a temporal impact (right). The anvil was sloped 30° from the horizontal to generate appropriate normal and tangential incident

velocities. The offset angle between the neck and anvil was 15°. Impact centers were mirrored across the midsagittal plane of the helmet and were a minimum of 120 mm apart.

Impact velocities were also determined based on real-world cyclist accidents. Preliminary testing showed that a resultant impact velocity of 5.1 m/s produced linear head accelerations of ~100 g, which is the median of data from helmet damage replication studies [12, 13] and poses a considerable risk of concussion [14, 15]. An additional resultant velocity of 6.6 m/s was also chosen to assess helmet effectiveness at a higher severity. These resultant velocities and their associated normal velocities fall within a range identified in damage replication studies as well as computational simulation studies [12, 13, 16, 20-23]. Drop heights required to attain the desired velocities were determined using a velocity light gate sensor (Velocity Timer Model 1204, KME Company, Troy, MI), which determines speed by recording the time for a flag on the falling mass to trip two lasers of a set distance apart. Repeatability in velocities between impacts was ensured by measuring height through a laser-positioning system (IL-2000, Keyence, Osaka, Japan). Using this setup, velocities were within ± 0.01 m/s for all tests.

The specified locations and velocities yielded a total of four possible impact configurations (frontal-5.1 m/s, temporal-5.1 m/s, frontal-6.6 m/s, temporal-6.6 m/s). While it is important for standards to test under a variety of environmental conditions, helmets in this study were only subject to ambient conditions. Four samples for testing were purchased per helmet model, and all samples were impacted at each configuration once (one impact per the four impact centers). This resulted in 16 impacts for each model with four trials per impact configuration and 160 impact tests in total. As an extra measure of precaution beyond the 120 mm minimum distance between impact locations, the impact configuration order was randomized between samples of the same model to avoid potential bias from testing order. Prior to testing, extraneous helmet attachments

(i.e. visors) were removed, as preliminary tests showed these did not significantly affect impact performance. Helmets were positioned with the rim 6 cm above the headform basic plane as measured along the midsagittal plane (~2.5 cm above brow line), then fit dials and retention straps were tightened in accordance with manufacturer recommendation.

Data Collection and Analysis

For each test, impact kinematics were measured using three linear accelerometers (Endevco 7264B-2000, Meggitt Sensing Systems, Irvine, CA) and three angular rate sensors (ARS, ARS3 PRO-18K, DTS, Seal Beach, CA) at the headform CG. The ARS package was selected over other conventional rotational kinematic measurement systems (i.e. 9-accelerometer array, 9AA) for its relative compactness, which is better suited to the limited space within the NOCSAE headform instrumentation channel. Data were collected at 20,000 Hz using a TDAS SLICE PRO SIM data acquisition system (DTS, Seal Beach, CA) and filtered using a 4-pole phaseless Butterworth low-pass filter with a cutoff frequency of 1650 Hz for linear accelerations (in accordance with the CPSC standard), and 255.8 Hz for angular rates. Rotational acceleration was calculated by differentiating angular rate data. The angular rate filter specification is not defined in current standards, but has been optimized in previous studies to produce matching rotational accelerations as the conventional 9AA system in helmeted impact loading scenarios [41, 44]. Using resultant acceleration traces, peak linear and rotational values were determined and used to calculate average peak accelerations per impact configuration for each helmet.

To evaluate acceleration results in a clinically meaningful context, risk of concussion was calculated for every test using a bivariate risk function for concussion that incorporates both linear (a) and rotational (α) head accelerations (Eq. 3.1, [15]).

$$R(a,\alpha) = 1/[1 + e\text{^} - (-10.2 + 0.0433a + 0.000873\alpha - 0.000000920a\alpha)] \quad (3.1)$$

This risk function was generated using head impact data collected from high school and college football players, and accounts for under-reporting of concussion [45, 46]. Average risks were calculated for each helmet per impact configuration. Differences in risk and peak acceleration between helmet models and impact configurations were assessed using one-way ANOVA (Tukey HSD post hoc tests, $\alpha = 0.05$). Nonparametric correlations in helmet rank order were evaluated using Spearman rank correlation coefficients and Kendall's coefficient of concordance within the framework of a Friedman test. MATLAB (R2014b, Mathworks Inc, Natick, MA) and JMP Pro 11 statistical software (SAS Institute Inc, Cary, NC) were used for data processing and analysis.

A weighted cumulative risk (WCR) metric was generated to summarize helmet performance at each impact location. Risks were weighted based on how frequently each impact configuration may occur in real-world cycling accidents according to existing helmet damage replication studies. These studies evaluate PLA, providing an indication of how frequently cyclists experience head impacts of a relative severity. To relate results from the present study to this data, average PLA results across all helmet models ± one standard deviation was computed for each configuration. This was then mapped to a cumulative distribution function of helmet damage replication PLA data [12, 13] (Fig. 3.3), and the percentile corresponding with the lower bound of the standard deviation range was subtracted from the percentile corresponding with the upper bound to give an associated probability that an impact would occur in that range. Assuming a total of 100 head impacts, the weighting represents how many of those head impacts might occur at the given configuration. The resulting weighted WCR equations for the frontal and temporal locations are given in Equations 3.2 and 3.3, respectively.

$$WCR_{frontal} = 20.5\left(risk_{frontal,5.1}\right) + 9.0(risk_{frontal,6.6}) \tag{3.2}$$

$$WCR_{temporal} = 21.8\left(risk_{temporal,5.1}\right) + 9.0(risk_{temporal,6.6}) \tag{3.3}$$

WCR was calculated per location for each helmet. Values represent an estimated number of

concussions one might sustain while wearing a particular helmet from 100 impacts at that location.

In order to relate helmet design characteristics to impact protection, regression analysis was conducted between WCR at each location and several helmet design parameters. These included mass, number of vents, shell thickness, local liner thickness, and local radius of curvature, as well as price. The individual parameter best correlated to WCR was determined per location. Additionally, multiple linear regression analysis was conducted to determine the combination of parameters most predictive of WCR for each location, referred to as helmet linear models (HLMs). These models were then assessed to evaluate how the interplay of various design aspects influenced protective capabilities, providing a basis for recommending avenues of helmet improvement to manufacturers. RStudio (V 1.0.136, RStudio, Inc., Boston, MA) was used to compute all correlations.

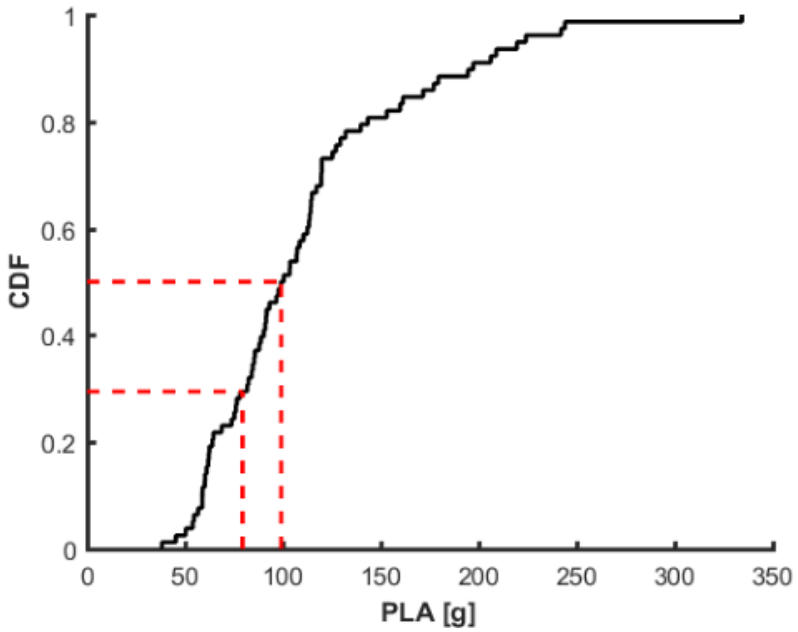

Figure 3.3. Empirical cumulative distribution function (CDF) of helmet damage replication data [12, 13]. Average PLA ± one standard deviation ranges were mapped to CDF percentiles, which

were then used to determine weightings for each impact configuration based on an assumed total of 100 impacts. The dashed lines show an example of this range for the frontal-5.1 m/s results, which corresponded with a weighting of 20.5.

RESULTS

The ten helmet models produced a wide distribution of peak accelerations across all impact configurations (Fig. 3.4), with PLA ranging from 66-234 g and PRA ranging from 3348-11682 rad/s^2. PLA was typically higher at the temporal location compared to the frontal at each velocity. The temporal location averaged 129±17 g and 170±25 g at 5.1 and 6.6 m/s, respectively, compared to 89±10 g and 139±19 g at the frontal location. PRA was less location-dependent, averaging 4889±744 rad/s^2 and 6381±1315 rad/s^2 at the temporal location at 5.1 and 6.6 m/s, and 4403±541 rad/s^2 and 5983±703 rad/s^2 at the frontal location. Both PLA and PRA were higher on average at 6.6 m/s than at 5.1 m/s, as expected.

Peak accelerations also varied by helmet model within each impact configuration (Fig. 3.5, Tables 3.2-3.3). The temporal location produced higher PLAs on average and more significant differences in PLA between helmet models compared to the frontal location. PRA varied less between helmet models at both locations, with the exception of the GMIPS helmet at the temporal location. This helmet yielded significantly higher PRAs at both velocities. Assigning each helmet a 1-10 rank for each impact configuration for both PLA and PRA revealed significant correlations in rank order. Each impact configuration showed significant correlation between PLA and PRA ranking except temporal-5.1 m/s (frontal-5.1 m/s: $r_s = 0.89$, $p < 0.01$, temporal-5.1 m/s: $r_s = 0.26$, $p = 0.47$, frontal-6.6 m/s: $r_s = 0.79$, $p = 0.01$, temporal-6.6 m/s: $r_s = 0.64$, $p = 0.05$). This indicates that a helmet that reduced PLA better was likely to also reduce PRA better, and vice versa. Additionally, significant association was found in PLA and PRA rank order across all impact

configurations (W = 0.52, p = <0.01), suggesting that a helmet that reduced accelerations better in one configuration was likely to also reduce them better in another.

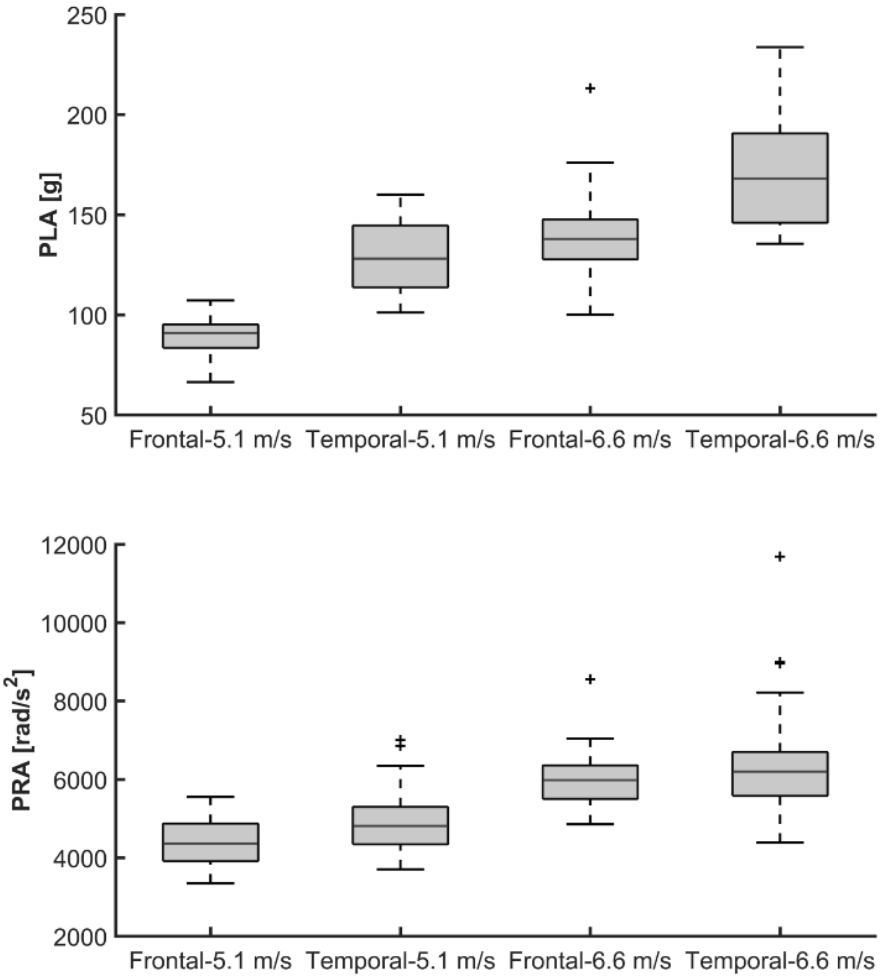

Figure 3.4. Distributions of PLA (top) and PRA (bottom) by impact configuration. Lower and upper bounds of boxes correspond with 25th and 75th percentiles, respectively, and whiskers extend to ±2.7σ. At each velocity, the frontal location tended to produce lower PLAs than the temporal location. PRA varied less across impact location.

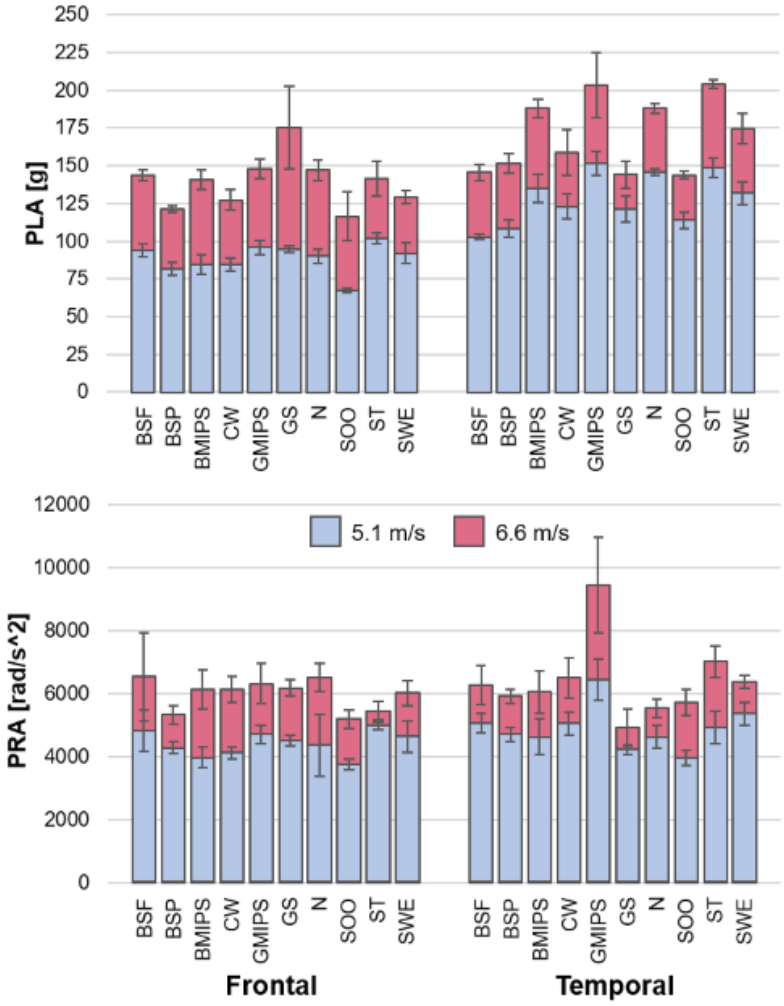

Figure 3.5. PLA (top) and PRA (bottom) per helmet model and location at each velocity. Error bars are standard deviations. Significance groupings are shown in Tables 3.2-3.3. The temporal location generally produced more significant differences in PLA between models. PRA showed fewer differences, with the exception of GMIPS at the temporal location.

Table 3.2. Significance groupings between helmet models based on PLA. For each configuration, helmets not connected by a common letter are significantly different (α = 0.05). Accelerations are organized in ascending order for each configuration, indicating relative performance rank.

Frontal								Temporal							
5.1 m/s					6.6 m/s			5.1 m/s					6.6 m/s		
Helmet				PLA [g]	Helmet		PLA [g]	Helmet				PLA [g]	Helmet		PLA [g]
SOO	A			68.2	SOO	A	116.6	BSF	A			103.3	SOO	A	143.9
BSP		B		82.2	BSP	A B	121.5	BSP	A	B		109.1	GS	A	144.1
CW		B	C	85.2	CW	A B	127.3	SOO	A	B		114.6	BSF	A	145.5
BMIPS		B	C	85.3	SWE	A B	129.2	GS		B	C	121.7	BSP	A B	151.6
N		B	C	D 90.6	BMIPS	A B	140.8	CW		B	C	123.5	CW	A B	159.0
SWE		B	C	D E 92.6	ST	A B	141.5	SWE			C	D 132.6	SWE	B C	174.6
BSF			C	D E 94.3	BSF	A B	143.7	BMIPS			C	D E 135.3	N	C D	188.1
GS			C	D E 95.2	N	B	146.9	N				D E F 146.5	BMIPS	C D	188.1
GMIPS				D E 96.5	GMIPS	B C	147.8	ST				E F 149.3	GMIPS	D	203.2
ST				E 102.3	GS	C	175.3	GMIPS				F 152.3	ST	D	204.2

Table 3.3. Significance groupings between helmet models based on PRA. For each configuration, helmets not connected by a common letter are significantly different (α = 0.05). Accelerations are organized in ascending order for each configuration, indicating relative performance rank.

Frontal								Temporal							
5.1 m/s					6.6 m/s			5.1 m/s					6.6 m/s		
Helmet				PRA [rad/s^2]	Helmet		PRA [rad/s^2]	Helmet				PRA [rad/s^2]	Helmet		PRA [rad/s^2]
SOO	A			3740	SOO	A	5188	SOO	A			3949	GS	A	4922
BMIPS	A	B		3958	BSP	A	5335	GS	A	B		4213	N	A B	5544
CW	A	B		4111	ST	A	5460	N	A	B	C	4611	SOO	A B	5719
BSP	A	B		4271	SWE	A	6020	BMIPS	A	B	C	4616	BSP	A B	5925
N	A	B		4346	CW	A	6140	BSP	A	B	C	4695	BMIPS	A B	6059
GS	A	B		4507	BMIPS	A	6141	ST	A	B	C	4916	BSF	A B	6282
SWE	A	B		4628	GS	A	6184	CW		B	C	5038	SWE	A B	6376
GMIPS	A	B		4694	GMIPS	A	6315	BSF		B	C	5060	CW	A B	6498
BSF		B		4811	N	A	6512	SWE			C	5353	ST	B	7021
ST		B		4969	BSF	A	6535	GMIPS				D 6435	GMIPS	C	9461

Concussion risk based on peak accelerations indicated a range in performance for the different impact configurations and reflected general kinematic trends (Fig. 3.6, Table 3.4). The frontal-5.1 m/s impacts yielded low risks (<13%) and fewer significant differences between helmets, with most falling at the asymptotic low end of the risk curve. The other three configurations produced higher risks and more variance between helmet models, with average risks spanning over 50% between helmets within each configuration. At the temporal-6.6 m/s configuration, concussion risk was nearly saturated at 100% for the ST and GMIPS helmets. Helmet rank order was found to be significantly correlated between the two velocities at the temporal location ($r_s = 0.89$, $p < 0.01$), suggesting that the same helmets were likely to reduce risk at either velocity at this location. The frontal location did not exhibit this same correlation between velocities ($r_s = 0.43$, $p = 0.21$), nor were locations significantly correlated at either velocity (frontal/temporal-5.1 m/s: $r_s = 0.59$, $p = 0.07$; frontal/ temporal-6.6 m/s: $r_s = 0.14$, $p = 0.70$). However, significant association was still found in overall helmet rank across all impact configurations ($W = 0.61$, $p < 0.01$).

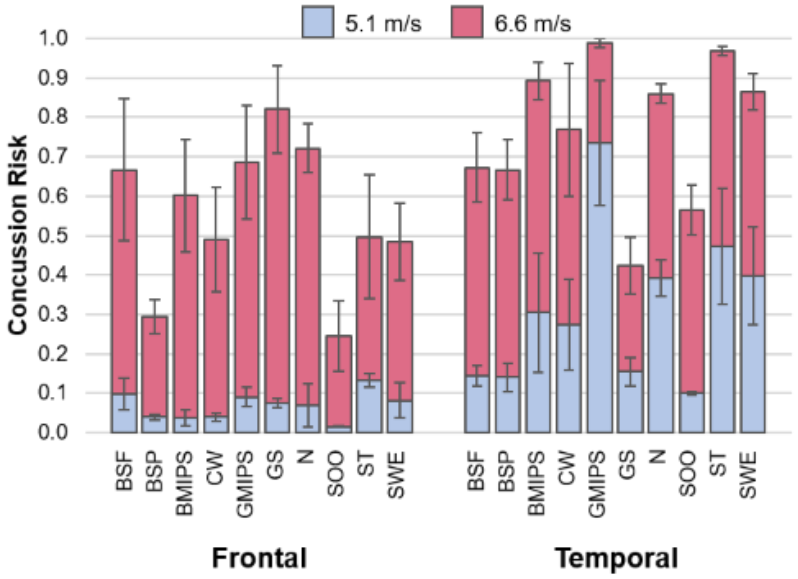

Figure 3.6. Concussion risk per helmet model and location at both velocities (standard deviation error bars). Significance groupings are shown in Table 3.4. Risk varied widely between models.

Table 3.4. Significance groupings between helmet models based on concussion risk. For each impact configuration, helmets that are not connected by a common letter are significantly different (α = 0.05). Accelerations are organized in ascending order for each impact configuration, indicating relative performance rank.

Frontal						Temporal					
5.1 m/s			6.6 m/s			5.1 m/s			6.6 m/s		
Helmet		Risk	Helmet		Risk	Helmet		Risk	Helmet		Risk
SOO	A	0.02	SOO	A	0.25	SOO	A	0.10	GS	A	0.42
BMIPS	A B	0.04	BSP	A	0.30	BSP	A	0.14	SOO	A	0.56
BSP	A B	0.04	SWE	A B	0.49	BSF	A B	0.15	BSP	A B	0.67
CW	A B	0.04	CW	A B	0.49	GS	A B C	0.16	BSF	A B C	0.67
N	A B C	0.07	ST	A B	0.50	CW	A B C D	0.27	CW	A B C D	0.77
GS	A B C	0.07	BMIPS	B C	0.60	BMIPS	A B C D	0.30	N	A B C D	0.86
SWE	A B C	0.08	BSF	B C	0.67	N	B C D	0.39	SWE	B C D	0.87
GMIPS	B C	0.09	GMIPS	B C	0.69	SWE	C D	0.40	BMIPS	C D	0.89
BSF	B C	0.10	N	B C	0.72	ST	D	0.47	ST	D	0.97
ST	C	0.13	GS	C	0.82	GMIPS	E	0.73	GMIPS	E	0.99

Computed WCR values ranged from 2.5 for SOO at the frontal location to 24.8 for GMIPS at the temporal location. Regression analysis between individual helmet design parameters/price and WCR revealed a range in correlations at each location (Fig. 3.7). At the frontal location, WCR was only significantly correlated with liner thickness ($r = -0.66$, $p = 0.04$). WCR and price showed the next strongest correlation, although not significant ($r = -0.57$, $p = 0.08$), while all other parameters showed weaker correlations ($|r| \leq 0.42$, $p \geq 0.23$). At the temporal location, WCR was only significantly correlated with mass ($r = 0.65$, $p = 0.04$). WCR and price again showed the next strongest correlation, although not significant ($r = -0.53$, $p = 0.12$), while all other parameters again showed weaker correlations ($|r| \leq 0.49$, $p \geq 0.15$). Combining the design parameters into location-specific HLMs much improved predictive capabilities. All parameters were incorporated into the

original HLM for each location, then least significant parameters were sequentially removed in successive iterations until the model predictions were significantly correlated with WCR. Price, mass, shell thickness, and liner thickness remained in the frontal HLM, while price, mass, vent number, shell thickness, and radius of curvature remained in the temporal HLM (Table 3.5).

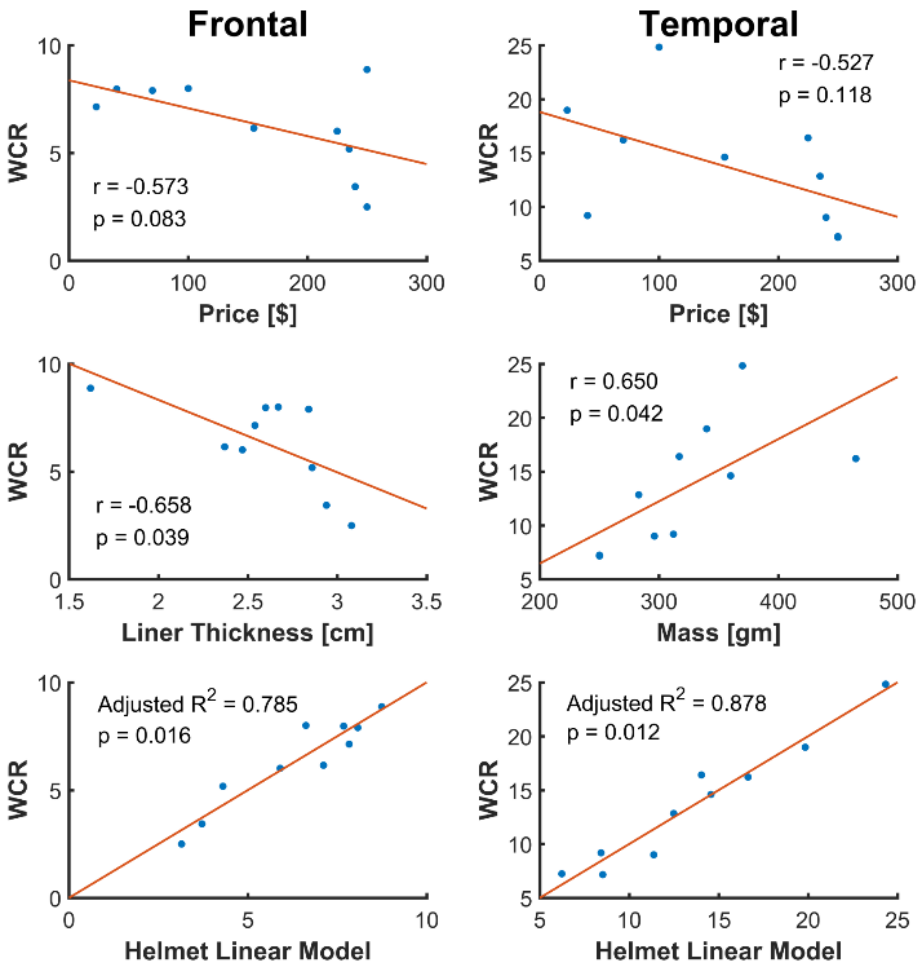

Figure 3.7. Correlations between WCR and helmet price (top), liner thickness or mass (middle), and predictive helmet linear model results from MLR (bottom) for each location. Price and liner thickness were the most significantly correlated with WCR at the frontal location, while price and mass were the most significantly correlated with WCR at the temporal location.

Table 3.5. Frontal and temporal HLM terms. Liner thickness and price were the most significant design parameters in the frontal model, while mass, shell thickness, and radius of curvature were the most significant parameters in the temporal model.

Frontal			Temporal		
Term	**Coefficient**	**p-value**	**Term**	**Coefficient**	**p-value**
Price	-0.013	0.063	Price	0.021	0.140
Mass	-0.005	0.745	Mass	0.170	0.008
Shell thickness	1.476	0.351	Vent number	-0.166	0.182
Liner Thickness	-3.835	0.005	Shell thickness	-14.272	0.010
			Radius of curvature	-0.502	0.014
Intercept	19.065	0.014	Intercept	-24.759	0.113
	HLM adjusted R^2: 0.785	HLM p-value: 0.016		HLM adjusted R^2: 0.878	HLM p-value: 0.012

DISCUSSION

The present study demonstrates substantial differences in the ability of bicycle helmets to attenuate impact kinematics when subjected to common, oblique impact configurations. Differences between models were generally more significant for PLA than PRA and were more pronounced at the temporal location. PLA was also higher on average at the temporal location. This may be attributable to varying helmet geometry at these locations; the transverse plane of most helmets has a larger radius of curvature at the sides compared to the front (mirroring the shape of the head), resulting in a larger contact area upon impact. The larger contact area produces a lower pressure for a given impact force, thus increasing the effective liner stiffness and reducing liner crush [47]. All but three helmets in this study indeed exhibited larger radii at the temporal location (Table 3.1). The radii measured herein were influenced by local geometrical variations that may have masked the overall curvature of the helmet, possibly contributing to the

lack of larger radii at the temporal location for these three helmets. Additionally, the temporal location tested in this study is further removed from the edge of the helmet, meaning that the shell is more continuous at this location (barring vents) and may lead to increased force distribution for thicker shells. This would also contribute to increased stiffness and reduced liner crush. Several other studies investigating both front and side locations of helmets have similarly shown higher PLA at the side [25, 34, 48, 49].

PRA results did not produce as many significant differences or show location-dependency, with the frontal and temporal locations yielding more comparable results. This may suggest that rotational acceleration is more influenced by other design aspects aside from liner crush. Nonetheless, helmet rank was largely correlated between PLA and PRA results, suggesting that design parameters affecting linear and rotational accelerations are not entirely independent in the helmet models tested. To determine the clinical meaningfulness of linear and rotational results, PLA and PRA were used to calculate concussion risk. Trends in PLA and PRA were thus reflected in the computed risks, which spanned over 50% within single impact configurations. PLA contributed more to the observed differences in risk, as PRA varied less between models. Computed risks also reflect the combined error of both kinematic variables. The 5.1 m/s condition, which was selected to represent a median cyclist head impact severity, demonstrated a considerable range in risk (2-73%). This large range is partly attributable to the accelerations produced at this impact velocity in conjunction with the nonlinear weighting of the underlying risk curve; the tolerance of the human brain to concussive injury is thought to vary widely within this acceleration range, so small differences in acceleration from model to model are manifested as large differences in risk [15]. Other impact velocities producing accelerations outside of this critical range would produce lesser differences in concussion risk. Nonetheless, while still vital for helmets to account for risk of severe head injury, this suggests that there is room for design

improvements to minimize concussion risk at this common impact severity as well.

In order to relate design to overall performance, trends were evaluated between various design parameters and impact protection at each location. At the temporal location, helmet rankings based on concussion risk were well-correlated between velocities. BMIPS, GMIPS, N, ST, and SWE models comprised the five worst-performing helmets. These helmets produced the highest PLAs but relatively average PRAs, with the exception of GMIPS, which produced significantly greater PRAs as well. All three non-road helmets are included in this grouping, suggesting that some design aspects specific to this style are not as conducive to impact attenuation. These helmets had thicker shells, larger masses, and smaller or fewer vents than the road helmets. Correlations between design parameters and WCR confirm these trends; the individual design parameter best correlated to WCR at this location was mass, and the HLM consisted of price, mass, vent number, shell thickness, and radius of curvature. Mass is likely reflective of other parameters in the HLM, as it is a general characteristic indicative of other factors such as vent number, shell thickness, and overall shape. It is possible that thicker shells deform less upon impact and distribute forces more across the liner, increasing effective stiffness and reducing crush. The decreased venting may increase contact area upon impact, also increasing effective stiffness. It was observed that the five worse-performing helmets indeed lacked venting at the temporal impact location. Strategies to optimize effective stiffness through variation of vent configuration, radius of curvature, and shell thickness may provide improved impact protection at this location. Price was also reasonably indicative of performance at this location, although the correlation was not significant.

The frontal location showed differing trends between design parameters and performance. Helmet rankings based on concussion risk were not well-correlated between velocities at this location,

owing partly to fewer significant differences between models and partly to several individual models that showed inconsistent results across velocities. Variance in risk at this location was predominantly due to PLA results, as PRA did not vary considerably. The GS helmet in particular produced significantly higher PLAs at 6.6 m/s, in turn yielding the highest concussion risk, while generating a more average PLA and risk at 5.1 m/s. These inconsistencies across velocity are likely due to local geometry effects, which may be exacerbated at higher impact energies. The frontal location on the GS helmet coincided with a vent, suggesting there may have been insufficient liner material to modulate the impact energy effectively. Liner thickness was found to be the individual parameter most significantly correlated with WCR. The frontal HLM consisted of price, mass, shell thickness, and liner thickness, with liner thickness being the most significant term even if GS results were removed. The frontal location was set at the helmet rim and fell outside the testable area defined in most standards, so design at this location is not regulated. Liner thickness may taper off as a result, making it a significant predictor of performance at this location and not at the temporal location. Since this frontal rim location is known to be among the most commonly impacted locations in cyclist accidents [12, 13, 16-19, 21], there may be value in expanding the testable area in standards to ensure adequate protection. This recommendation has previously been made by various other groups as well [13, 16-19, 21].

Several of the helmets assessed herein contain technologies less traditional in helmet design. The SOO helmet performed better across most configurations, and was the only helmet to incorporate a largely honeycomb-structure liner, suggesting that this alternative material may attenuate impacts as well as or better than traditional EPS. Additionally, the two helmet models containing MIPS did not appear to provide superior protection compared to the non-MIPS helmets. GMIPS produced significantly higher PRAs at the temporal location, while BMIPS produced relatively average PRAs across all configurations. No direct comparisons were made

between the same helmet with and without MIPS, however, and it is possible that MIPS does reduce PRA within the same helmet. If such is the case, it is likely that other design aspects specific to the MIPS helmets tested in this study were more indicative of relative performance (i.e. liner and shell properties, vent configuration). Aside from the GMIPS helmet results, PRA generally did not vary substantially within the helmets tested herein, demonstrating that there is room for advancements in helmet technologies that specifically address rotation.

The authors previously conducted comparative impact testing of the same ten helmet models using a CPSC standard test rig [50]. Results from the standards tests were compared to results from the current oblique tests by assessing correlations in performance rank, where helmets are assigned a 1-10 rank per impact configuration based on PLA results for standards tests and risk results for oblique tests. It was found that helmet performance order was generally well-correlated when comparing similar impact configurations. This was not unexpected, as oblique impacts also involve a considerable normal velocity component, which is a primary determinant of PLA results. However, the addition of PRA results from the oblique impact tests did appear to enhance discrimination of helmet performance. For instance, GMIPS and SOO were much more definitively identifiable as the worst- and best- performing helmets in the present study, respectively, owing largely to the PRAs they produced. Because of the importance of rotational impact kinematics in relation to injury risk, it is recommended that helmet performance be evaluated using oblique impacts that enable assessment of realistic rotational motion.

While this study was able to effectively identify differences in the ability of helmets to reduce impact kinematics and risk of concussion, its scope was limited in several ways. One limitation is that only ten helmet models were evaluated, so possible inferences on correlations between design characteristics and helmet performance were limited. The parameters identified in the

present HLMs as most predictive of performance are specific to the models tested, and may not fully encompass impact attenuation capacities of all available helmets on the market. Testing a larger sampling of helmets would enhance the generalizability of these trends. The present study also only impacted two locations, so results were likely heavily influenced by local geometries of the helmet. While manufacturers are responsible for producing helmets that offer sufficient protection in all impact scenarios and should consider effects of local geometries during the design process, evaluating helmets at more locations could provide a more holistic indication of overall helmet performance.

Other limitations relate to the concussion risk function, which was developed using football head impact data. Head impacts in football are not directly representative of those in cycling, and football players likely exhibit differing tolerance to head impact than the general population [15]. Collection of cycling-specific head impact kinematics and injury data would enhance the ability to predict brain injury risk for cyclists. Additionally, the underlying data for the risk function lacks the resolution to evaluate directionality dependence, but it is generally accepted that brain injury tolerance to impact differs as a function of direction [51]. The function also relies on estimates for rotational acceleration, which, although not directly captured by the sensors used to measure football head impacts, were validated through six degree-of-freedom and laboratory studies [52-53]. Nonetheless, this risk function is based in one of the most comprehensive databases of injurious versus non-injurious head impacts, and can be assumed to at least estimate a population response to head impact [15]. It has also been shown to be more predictive of head/brain injuries than other common risk curves in additional loading scenarios, such as automotive crashes [54], demonstrating its applicability in other fields.

The process of weighting risks to compute WCR also has associated limitations. The damage

replication data used to determine the weightings are PLA values based on impact tests onto a flat anvil using a standard drop rig, and also do not differentiate frontal and temporal impact locations. However, these data represent the best approximation of relative impact acceleration levels, as there are presently no helmet damage replication studies using oblique impacts, and there is very little computational simulation data providing cyclist head impact accelerations in helmeted scenarios.

A final consideration to account for in this study is the impact rig setup relative to other oblique impact studies. Other studies have utilized varied boundary conditions, including different headforms, no neck, impacts against a horizontally sliding table or a different anvil angle, sandpaper of a different specification, etc. [9, 25, 26, 34-37]. The NOSCAE headform used in the present study was selected for its more biofidelic shape compared to other headforms common in impact testing (i.e. ISO, Hybrid III), which may affect helmet fit and behavior during impact [55]. Additionally, the Hybrid III neck used in this study was originally validated in flexion and extension from frontal sled impact tests, and has been shown to be overly stiff in other loading directions [56]. However, the Hybrid III neck is the most widely-used human neck surrogate, and it has been suggested that a neck could improve impact boundary conditions since it may affect the kinematic response of the head [9, 26, 42, 57]. Future work is needed to evaluate the effects of these varying test rig configurations on bicycle helmet performance.

CONCLUSIONS

The present study identified a considerable range in the ability of bicycle helmets of varied designs to mitigate head impacts. Testing was conducted using an oblique impact rig, allowing for realistic representation of cyclist head impacts and evaluation of rotational acceleration as well as linear (a known key factor in brain injury). Impact locations and velocities were selected to mimic those

common in cyclist accidents. Significant differences in peak linear and rotational accelerations were observed between helmets, producing concussion risks spanning over 50% within single impact configurations.

Various design parameters were correlated to concussion risk results to investigate which were most predictive of performance. At the temporal location, shell thickness, vent configuration, and radius of curvature likely all affect helmet effective stiffness, which should be optimized to reduce impact kinematics. At the frontal location, special attention should be given to liner thickness, which may taper off due to lack of standards testing at this location. Because of the relative frequency at which cyclists impact their head at this location, lowering the test line to include testing at the helmet rim is recommended. Additionally, PRA results revealed fewer significant differences between models, suggesting there is room for improvement of current helmet technologies to reduce rotational impact kinematics. These results can inform manufacturers, standards bodies, and consumers alike, aiding the development of improved bicycle helmet safety.

REFERENCES

1. AANS, 2014, "Sports-Related Head Injury," Web, www.aans.org/patient %20information/ conditions%20and%20treatments/sports-related%20head%20injury.aspx.
2. CPSC, 2015, "National Electronic Injury Surveillance System Database," Web, www.cpsc.gov/en/Research--Statistics/NEISS-Injury-Data/.
3. Schulman, J., Sacks, J., and Provenzano, G., 2002, "State level estimates of the incidence and economic burden of head injuries stemming from non-universal use of bicycle helmets," Injury Prevention, 8(1), pp. 47-52. DOI: 10.1136/ip.8.1.47
4. Sacks, J. J., Holmgreen, P., Smith, S. M., and Sosin, D. M., 1991, "Bicycle-associated head injuries and deaths in the United States from 1984 through 1988: How many are preventable?," The Journal of the American Medical Association, 266, pp. 3016-3018.
5. Thompson, D. C., Rivara, F. P., and Thompson, R. S., 1996, "Effectiveness of bicycle safety helmets in preventing head injuries. A case-control study," The Journal of the American Medical Association, 276(24), pp. 1968-1973.
6. Elvik, R., 2013, "Corrigendum to: "Publication bias and time-trend bias in meta-analysis of bicycle helmet efficacy: a re-analysis of Attewell, Glase and McFadden, 2001" [Accid. Anal. Prev. 43 (2011) 1245-1251]," Accident Analysis & Prevention, 60, pp. 245-253.

7. Amoros, E., Chiron, M., Martin, J. L., Thelot, B., and Laumon, B., 2012, "Bicycle helmet wearing and the risk of head, face, and neck injury: a French case--control study based on a road trauma registry," Injury prevention : journal of the International Society for Child and Adolescent Injury Prevention, 18(1), pp. 27-32. DOI: 10.1136/ip.2011.031815
8. Cripton, P. A., Dressler, D. M., Stuart, C. A., Dennison, C. R., and Richards, D., 2014, "Bicycle helmets are highly effective at preventing head injury during head impact: head-form accelerations and injury criteria for helmeted and unhelmeted impacts," Accident Analysis & Prevention, 70, pp. 1-7. DOI: 10.1016/j.aap.2014.02.016
9. McIntosh, A. S., Lai, A., and Schilter, E., 2013, "Bicycle helmets: head impact dynamics in helmeted and unhelmeted oblique impact tests," Traffic injury prevention, 14(5), pp. 501-508. DOI: 10.1080/15389588.2012.727217
10. CPSC, 1998, "Safety Standard for Bicycle Helmets Final Rule (16 CFR Part 1203)," United States Consumer Product Safety Commission, pp. 11711-11747.
11. Mertz, H. J., Irwin, A. L., and Prasad, P., 2003, "Biomechanical and scaling bases for frontal and side impact injury assessment reference values," Stapp car crash journal, 47, pp. 155-188.
12. Smith, T. A., Tees, D., Thom, D. R., and Hurt, H. H., 1994, "Evaluation and replication of impact damage to bicycle helmets," Accident Analysis & Prevention, 26(6), pp. 795-802.
13. Williams, M., 1991, "The protective performance of bicyclists' helmets in accidents," Accident Analysis & Prevention, 23(2-3), pp. 119-131.
14. Pellman, E. J., Viano, D. C., Tucker, A. M., Casson, I. R., and Waeckerle, J. F., 2003, "Concussion in professional football: reconstruction of game impacts and injuries," Neurosurgery, 53(4), pp. 799-812. DOI: 10.1227/01.NEU.0000083559.68424.3F
15. Rowson, S., and Duma, S. M., 2013, "Brain injury prediction: assessing the combined probability of concussion using linear and rotational head acceleration," Annals of Biomedical Engineering, 41(5), pp. 873-882. DOI: 10.1007/s10439-012-0731-0
16. Bourdet, N., Deck, C., Carreira, R. P., and Willinger, R., 2012, "Head impact conditions in the case of cyclist falls," Proceedings of the Institution of Mechanical Engineers, Part P: Journal of Sports Engineering and Technology, 226(3-4), pp. 282-289. DOI: 10.1177/1754337112442326
17. Ching, R. P., Thompson, D. C., Thompson, R. S., Thomas, D. J., Chilcott, W. C., and Rivara, F. P., 1997, "Damage to bicycle helmets involved with crashes," Accident Analysis & Prevention, 29(5), pp. 555-562.
18. McIntosh, A., Dowdell, B., and Svensson, N., 1998, "Pedal cycle helmet effectiveness: A field study of pedal cycle accidents," Accident Analysis & Prevention, 30(2), pp. 161-168.
19. Depreitere, B., Van Lierde, C., Maene, S., Plets, C., Vander Sloten, J., Van Audekercke, R., Van der Perre, G., and Goffin, J., 2004, “Bicycle-related head injury: a study of 86 cases,” Accident Analysis & Prevention, **36**(4), pp. 561-567.
20. Bourdet, N., Deck, C., Serre, T., Perrin, C., Llari, M., and Willinger, R., 2014, "In-depth real-world bicycle accident reconstructions," International Journal of Crashworthiness, 19(3), pp. 222-232. DOI: 10.1080/13588265.2013.805293
21. Verschueren, P., 2009, "Biomechanical analysis of head injuries related to bicycle accidents and a new bicycle helmet concept," Katholieke Universiteit Leuven, Leuven.
22. Fahlstedt, M., Baeck, K., Halldin, P., Vander Sloten, J., Goffin, J., Deprietere, B., and Kleiven, S., 2012, "Influence of Impact Velocity and Angle in a Detailed Reconstruction of a Bicycle Accident," IRCOBI Conference, 12(84), pp. 787-799.
23. Peng, Y., Chen, Y., Yang, J., Otte, D., and Willinger, R., 2012, "A study of pedestrian and bicyclist exposure to head injury in passenger car collisions based on accident data and simulations," Safety Science, 50(9), pp. 1749-1759. DOI: 10.1016/j.ssci.2012.03.005

24. Otte, D., 1989, “Injury mechanism and crash kinematics of cyclists in accidents,” Proc. 33rd Stapp Car Crash Conference, SAE 892425.
25. Milne, G., Deck, C., Bourdet, N., Carreira, R. P., Allinne, Q., Gallego, A., and Willinger, R., 2014, "Bicycle helmet modelling and validation under linear and tangential impacts," International Journal of Crashworthiness, 19(4), pp. 323-333. DOI: 10.1080/13588265.2013.859470
26. Aare, M., and Halldin, P., 2003, "A new laboratory rig for evaluating helmets subject to oblique impacts," Traffic injury prevention, 4(3), pp. 240-248. DOI: 10.1080/15389580309879
27. King, A. I., Yang, K. H., Zhang, L., Hardy, W., and Viano, D. C., 2003, "Is Head Injury Caused by Linear or Angular Acceleration?," Proceedings of the International Research Conference on the Biomechanics of Impact (IRCOBI)Lisbon, Portugal.
28. Unterharnscheidt, F. J., 1971, "Translational versus rotational acceleration: animal experiements with measured inputs," Proceedings of the 15th Stapp Car Crash Conference, SAE 710880.
29. Gennarelli, T., Ommaya, A., and Thibault, L., 1971, "Comparison of translational and rotational head motions in experimental cerebral concussion," 15th Stapp Car Crash Conference, pp. 797-803.
30. Gennarelli, T. A., Thibault, L. E., and Ommaya, A. K., 1972, "Pathophysiologic responses to rotational and translational accelerations of the head," SAE Technical Paper Series, 720970, pp. 296-308.
31. Ommaya, A., and Hirsch, A., 1971, "Tolerances for cerebral concussion from head impact and whiplash in primates," Journal of biomechanics, 4(1), pp. 13-21.
32. Ommaya, A. K., Hirsch, A. E., and Martinez, J. L., 1966, "The role of whiplash in cerebral concussion," Proc. 10th Stapp Car Crash Conference, pp. 314-324.
33. Rowson, S., G. Brolinson, M. Goforth, D. Dietter, and S. M. Duma. Linear and angular head acceleration measurements in collegiate football. J. Biomech. Eng. 131(6):061016, 2009.
34. Mills, N. J., and Gilchrist, A., 2008, "Oblique impact testing of bicycle helmets," International Journal of Impact Engineering, 35(9), pp. 1075-1086. DOI: 10.1016/j.ijimpeng.2007.05.005
35. Halldin, P., and Kleiven, S., 2013, "The development of next generation test standards for helmets," Helmet Performance and Design, P. Childs, A. Bull, and M. Ghajari, eds., DEG Imperial College London, Imperial College London.
36. Klug, C., Feist, F., and Tomasch, E., 2015, "Testing of bicycle helmets for preadolescents," IRCOBI ConferenceLyon, France, pp. 136-155.
37. Hansen, K., Dau, N., Feist, F., Deck, C., Willinger, R., Madey, S. M., and Bottlang, M., 2013, "Angular Impact Mitigation system for bicycle helmets to reduce head acceleration and risk of traumatic brain injury," Accident Analysis & Prevention, 59, pp. 109-117. DOI: 10.1016/j.aap.2013.05.019
38. Folksam, 2015, "Bicycle helmet test."
39. Nightingale, R. W., McElhaney, J. H., Richardson, W. J., and Myers, B. S., 1996, “Dynamic responses of the head and cervical spine to axial impact loading,” Journal of Biomechanics, 29(3), pp. 307-318.
40. Rowson, B., Rowson, S., and Duma, S. M., 2015, "Hockey STAR: A Methodology for Assessing the Biomechanical Performance of Hockey Helmets," Annals of biomedical engineering, 43(10), pp. 2429-2443. DOI: 10.1007/s10439-015-1278-7
41. Cobb, B. R., Zadnik, A. M., and Rowson, S., 2015, "Comparative analysis of helmeted impact response of Hybrid III and National Operating Committee on Standards for Athletic Equipment headforms," Proceedings of the Institution of Mechanical Engineers, Part P: Journal of Sports Engineering and Technology, 230(1), pp. 50-60. DOI: 10.1177/1754337115599133

42. Hering, A. M., and Derler, S., 2000, "Motorcycle helmet drop tests using a Hybrid III dummy," the International IRCOBI Conference on the Biomechanics of Impact, International Research Council on the Biomechanics of Impacts, Zurich, Switzerland.
43. ECE, 1999, "R-22.05: Uniform Provisions Concerning the Approval of Protective Helmets for Drivers and Passengers of Motorcycles and Mopeds," United Nations Economic Commission for Europe.
44. Cobb, B. R., Tyson, A. M., and Rowson, S., 2017, "Head acceleration measurement techniques: Reliability of angular rate sensor data in helmeted impact testing," Proceedings of the Institution of Mechanical Engineers, Part P: Journal of Sports Engineering and Technology, p. 1-6. DOI: 10.1177/1754337117708092
45. Langburt, W., Cohen, B., Akhthar, N., O'Neill, K., and Lee, J. C., 2001, "Incidence of concussion in high school football players of Ohio and Pennsylvania," J Child Neurol, 16(2), pp. 83-85.
46. McCrea, M., Hammeke, T., Olsen, G., Leo, P., and Guskiewicz, K., 2004, "Unreported concussion in high school football players: implications for prevention," Clin J Sport Med, 14(1), pp. 13-17.
47. Mills, N. J., 1990, "Protective capability of bicycle helmets," British journal of sports medicine, 24(1), pp. 55-60.
48. Mills, N. J., and Gilchrist, A., 1996, "Response of helmets in direct and oblique impacts," International Journal of Crashworthiness, 2(1), pp. 7-24. DOI: 10.1533/cras.1997.0032
49. Mills, N. J., and Gilchrist, A., 2008, "Finite-element analysis of bicycle helmet oblique impacts," International Journal of Impact Engineering, 25, pp. 1087-1101.
50. Bland, M. L., Zuby, D. S., Mueller, B. C., and Rowson, S., 2018, “Differences in the protective capabilities of bicycle helmets in real-world and standard-specified impact scenarios,” Traffic Injury Prevention, 19(sup1), pp. S158-S163.
51. Newman, J. A., Shewchenko, N., and Welbourne, E., 2000, “A proposed new biomechanical head injury assessment function—the maximum power index”, Stapp Car Crash Journal, 44, pp. 215-247.
52. Rowson, S., Duma, S. M., Beckwith, J. G., Chu, J. J., Greenwald, R. M., Crisco, J. J., Brolinson, P. G., Duhaime, A. C., McAllister, T. W., and Maerlender, A. C., 2012, “Rotational head kinematics in football impacts: an injury risk function for concussion,” Annals of Biomedical Engineering, 40(1), pp. 1-13. DOI: 10.1007/s10439-011-0392-4
53. Rowson, S., Beckwith, J. G., Chu, J. J., Leonard, D. S., Greenwald, R. M., and Duma, S. M., 2011, “A six degree of freedom head acceleration measurement device for use in football,” Journal of Applied Biomechanics, 27(1), pp. 8-14.
54. Laituri, T. R., El-Jawahri, R. E., Henry, S., and Sullivan, K., 2015, “Field-Based Assessments of Various AIS2+ Head Risk Curves for Frontal Impact,” SAE Technical Paper Series, 2015-01-1437. DOI: 10.4271/2015-01-1437
55. Cobb, B. R., MacAlister, A., Young, T. J., Kemper, A. R., Rowson, S., and Duma, S. M., 2014, "Quantitative comparison of Hybrid III and National Operating Committee on Standards for Athletic Equipment headform shape characteristics and implications on football helmet fit," Proceedings of the Institution of Mechanical Engineers, Part P: Journal of Sports Engineering and Technology, 229(1), pp. 39-46. DOI: 10.1177/1754337114548245
56. Sances, A., Carlin, F., Kumaresan, S., 2002, “Biomechanical analysis of head-neck force in Hybrid III dummy during inverted vertical drops,” Biomedical Sciences Instrumentation 38, pp. 459–464.
57. Ghajari, M., Peldschus, S., Galvanetto, U., and Iannucci, L., 2013, “Effects of the presence of the body in helmet oblique impacts,” Accident Analysis & Prevention, 50, pp. 263-271. DOI: 10.1016/j.aap.2012.04.016

CHAPTER 4

EFFECT OF ANVIL ANGLE ON IMPACT KINEMATICS IN LABORATORY EVALUATION OF BICYCLE HELMETS

ABSTRACT

Cycling is the leading cause of sport-related head injuries in the US. Bicycle helmets are subject to standards limiting peak linear acceleration (PLA) in normal impacts. However, real-world cycling accidents occur at a variety of impact angles and involve both normal and tangential incident velocities. Real-world head impacts also induce rotational acceleration, a major contributor to brain injury. The objective of this study was to assess performance differences of bicycle helmets across impact angles under real-world cyclist impact conditions. Ten helmet models were impacted on a custom drop tower using biofidelic headform and neck surrogates. Impacts were against a 0° or 30° anvil and at two impact locations and velocities common in cyclist accidents. PLA was not significantly different across anvil ($p>0.40$) while peak rotational acceleration (PRA) was higher at 0° ($p<0.01$), reflecting differences in resultant force proximity to the assembly center of gravity. Kinematic results produced a considerable range in concussion risk, with risks differing up to 50% across anvil angle in matched impact configurations. These data suggest that evaluating helmet performance under a variety of impact angles may aid in the development of bicycle helmet technologies equipped to mitigate injury risk under a wider variety of loading scenarios.

INTRODUCTION

Cycling is a popular recreational activity, sport, and mode of transportation in the U.S. and throughout the world. Despite its popularity, it is not a risk-free activity; cycling caused the most head injuries treated in U.S. emergency rooms in 2015 out of any sport or recreational activity, accounting for over 81,000 cases [1]. The societal and economic burden from these injuries is considerable, with associated annual healthcare costs estimated to exceed $2 billion [2]. Fortunately, risk of sustaining a head injury has been shown to be significantly reduced by wearing a bicycle helmet [3, 4].

Bicycle helmets are presently subject to standards limiting peak linear acceleration (PLA) in specified impact tests [5]. While standards ensure that helmets lower head injury risk, the prescribed impact testing has limited representation of real-world cyclist accidents. The metal half-headform and the rigid neck joint are not biofidelic and preclude assessment of relative head-neck motion during impact. Further, all impacts are normal to the impact surface, while real-world cyclist head impacts frequently involve both normal and tangential incident velocities (termed “oblique”) [6]. Real-world head impacts also induce rotational acceleration, a major contributor to diffuse brain injury such as concussion [7].

Given the limitations of standards impact testing, several research groups have developed oblique impact rigs with more biofidelic test setups [4, 8-11]. These rigs differ in boundary conditions. For instance, many groups drop helmets onto an angled anvil to simulate oblique impacts, but the choice of anvil angle is not consistent [8, 10, 11]. This is attributable to the range of head impact angles relative to the ground that a cyclist may experience, which spans from close to normal to more commonly between 30° and 60° [12, 13]. Linear and rotational impact accelerations likely vary as a function of angle; however, to-date this possible range is relatively unexplored. The

several studies that have subjected helmets to both normal and oblique impacts have used different test rigs for the two impact types, have evaluated different velocities across impact type, or have assessed only linear accelerations for normal impacts, limiting direct comparisons in helmet performance across impact angle [8, 10, 14].

The objective of this study was to assess differences in protective capabilities of commercially-available bicycle helmets across impact angles using matched conditions reflective of real-world cyclist accidents.

METHODS

Impact tests were conducted using a custom, linear drop tower. The drop mass consisted of a National Operating Committee on Standards for Athletic Equipment (NOCSAE) headform connected to a Hybrid III (HIII) 50th-percentile male neck via a custom adaptor plate [15], which was then connected to a steel plate simulating effective torso mass (16 kg [16]). The NOCSAE headform and HIII neck are common in impact testing [15] and possess greater biofidelity than standards equipment. The bicycle-helmeted headform was impacted against one of two anvil angles (relative to horizontal): 0°, simulating a normal impact, and 30°, simulating normal and tangential incident velocities associated with oblique impacts (Fig. 4.1). The latter angle falls within a range of head impact angles common in computational simulations of cyclist accidents [12, 13]. Anvils were coated with 80-grit sandpaper to simulate road surface conditions (0.5 friction coefficient, as specified by motorcycle helmet standards [17]). Sandpaper was replaced between tests. The drop mass steel plate was caught by a spring on the base of the drop tower subsequent to the head impact pulse (at ~13 ms) in order to avoid excessive loading of the neck.

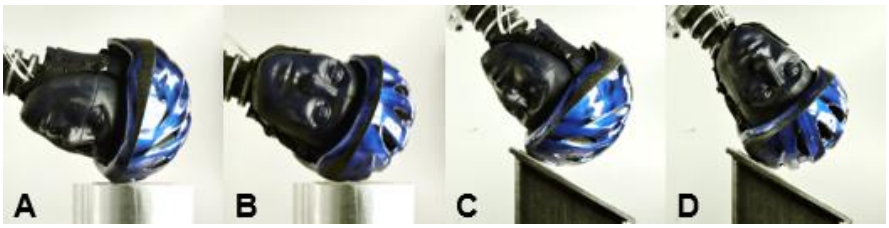

Figure 4.1. Frontal (A,C) and temporal (B,D) impact locations for the 0° (A,B) and 30° (C,D) anvils.

Impact locations were selected to represent common cyclist head impact scenarios. Helmet damage replication studies, which take helmets damaged in real-world accidents and recreate the damage on a standards impact rig, have shown that the front and sides of helmets are most commonly impacted, frequently around the rim [18, 19]. This is further supported by computational simulation studies [12, 13]. A frontal and temporal location were selected for impact testing, with the frontal location at the helmet rim and the temporal location higher on the helmet (Fig. 4.1). An offset of 15° between the anvil and an axis running axially through the neck was used to impact both locations. Locations were mirrored across the midsagittal plane of the helmet, producing four impact centers per helmet. These impact centers were predetermined to maintain a minimum distance of 120 mm apart in order to avoid overlap of damage profiles (as specified by present standards [5]), and each helmet sample was tested once per impact center. As helmets are symmetrical across the midsagittal plane, results from both sides of the helmet were averaged into frontal and temporal locations.

Impact velocities were also selected to represent common cyclist head impacts. These were determined using helmet damage reconstruction data, which suggest a median PLA of ~100 g [18, 19]. A velocity of 4.4 m/s on the 0° anvil was found in preliminary testing to produce PLAs at this level. This velocity was thus selected for impact testing, as well as a velocity of 5.7 m/s to assess more severe impacts that still fall within a range of helmet damage replication study PLAs.

For the 30° anvil, impact velocities were chosen so that normal impact velocities matched that of the 0° anvil tests, as it has been suggested that normal impact velocity is directly related to PLA in bicycle helmet testing [20]. Normal and resultant velocity components for each anvil are detailed in Table 4.1. Necessary drop heights to attain these resultant impact velocities were determined using a velocity light-gate sensor (IL-2000, Keyence, Osaka, Japan). Velocity was also monitored per test, and was found to remain within ± 0.01 m/s for all tests.

Table 4.1. Normal (V_N) and resultant (V_R) components of the two impact velocities for the 0° and 30° anvils. Normal velocities were matched across anvil. For all helmet models, both impact locations were tested at each velocity on each anvil.

Anvil	V_N [m/s]	V_R [m/s]
0°	4.4	4.4
	5.7	5.7
30°	4.4	5.1
	5.7	6.6

The two anvil angles, two impact locations, and two impact velocities produced a total of eight possible test conditions. Ten helmet models of varied design were selected for testing to represent a full spectrum of commercially-available products. Eight samples were purchased per model; four were impacted on the 0° anvil only and four were impacted on the 30° anvil only. Each was subjected to every velocity-location combination once. This produced 32 tests per helmet model with 4 trials per configuration, and 320 tests in total. Order of velocity-location combination was randomized between helmet samples to avoid introduction of test order bias. Prior to testing, any extraneous helmet attachments were removed and helmets were positioned 2.5 cm above the brow line, then fitted by tightening the fit adjustment dials and retention straps in accordance with manufacturer recommendations.

Impact kinematics for all tests were collected at 20,000 Hz using three linear accelerometers (Endevco 7264B-2000, Meggitt Sensing Systems, Irvine, CA) and three angular rate sensors (ARS, ARS3 PRO-18K, DTS, Seal Beach, CA) located at the headform center of gravity (CG). Data were filtered using a 4-pole phaseless Butterworth low-pass filter with cutoff frequencies of 1650 Hz for linear accelerations (standard-specified) and 255.8 Hz for angular rates (optimized in previous studies [15, 21]). Rotational accelerations were then computed by differentiation of angular rate data. Peak resultant linear accelerations (PLA) and rotational accelerations (PRA) were determined for each test. These were also used to estimate risk of concussion through a bivariate concussion risk function that incorporates both PLA (*a*) and PRA (*α*) (Eq. 4.1, [22]). This function was developed using head impact data from high school and collegiate football players, and accounts for underreporting of concussion [23]. Differences in results across anvil angles were compared using matched Student's t-tests (significance level of 0.05).

$$R(a,\alpha) = 1/(1+\exp-(-10.2+0.0433a+0.000873\alpha-0.00000920a\alpha)) \quad (4.1)$$

RESULTS

Wide ranges in accelerations were observed across the ten helmet models; PLA spanned 66-234 g across all impact configurations, while PRA spanned 3348-12520 rad/s^2. There were significant correlations between PRA and PLA for both anvils (Fig. 4.2), with regression slopes of 25.6 at 30° (R^2=0.55, p<0.001) and 44.5 at 0° (R^2=0.73, p<0.001). The large range in kinematics produced a considerable range in concussion risk as well, which spanned 2-99% across all impact configurations. PLA was not significantly affected by anvil angle, with average differences of <3% at either velocity. Conversely, PRA was significantly greater at 0°, with average differences of 23-25% across both velocities (Table 4.2).

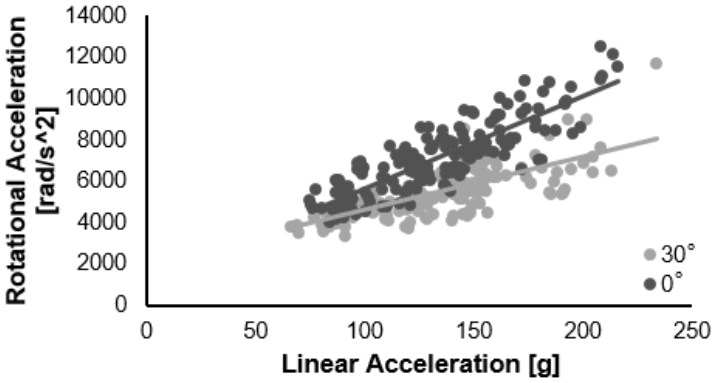

Figure 4.2. Rotational versus linear accelerations (PRA vs PLA) for all tests. PLA was similar across anvil angles, while PRA was greater for 0° impacts.

Table 4.2. Average acceleration results (± standard deviation) per velocity for both anvil angles. Differences between averages are given, along with their significance level. Anvil angle produced significant differences in PRA, but not PLA.

	PLA [g]			PRA [rad/s^2]		
Velocity [m/s]	**0° Anvil**	**30° Anvil**	**Avg Difference [%]**	**0° Anvil**	**30° Anvil**	**Avg Difference [%]**
4.4	112 ± 23	109 ± 24	2.7 (p = 0.49)	6168 ± 1408	4646 ± 687	24.7 (p < 0.01)
5.7	154 ± 29	155 ± 27	0.6 (p = 0.96)	8036 ± 1573	6182 ± 1060	23.1 (p < 0.01)

Further analyzing PLA and PRA revealed distinct distributions for each velocity-location configuration (Fig. 4.3). The temporal location generally produced greater PLAs than the frontal location at each velocity for both anvils ($p<0.001$). PRA was also significantly greater at the temporal location for the 0° anvil at each velocity ($p<0.001$), while the 30° anvil produced smaller differences in PRA across impact location (4.4 m/s: $p=0.001$, 5.7 m/s: $p=0.096$). The 0° anvil also produced greater PRAs per configuration than the 30° anvil ($p<0.001$).

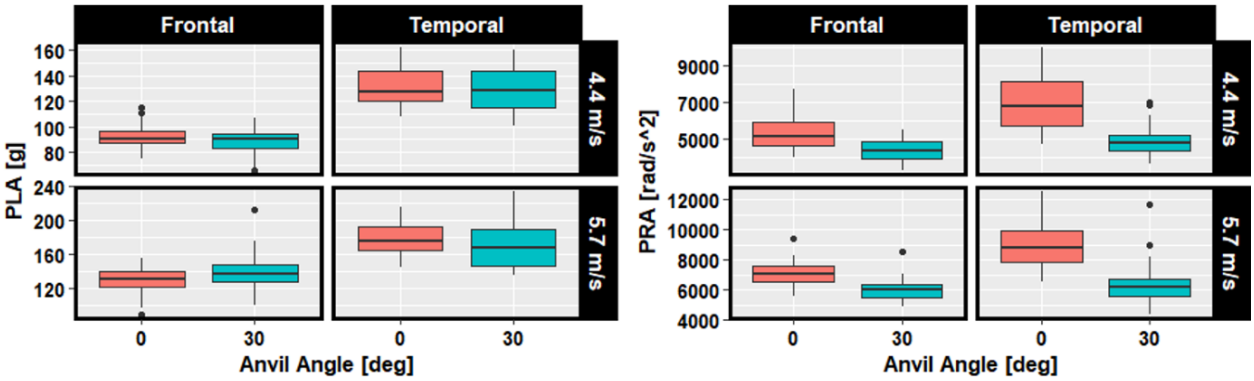

Figure 4.3. Distributions of PLA and PRA per impact configuration across both anvils. Lower and upper box bounds represent first and third quartiles (25th and 75th percentiles), and whiskers extend to the largest value or 1.5x the interquartile range.

For each helmet model, differences in average PLA, PRA, and concussion risk across anvil angle were determined per configuration. Distributions of these differences demonstrate the overall effect of anvil angle on kinematics for each configuration (Fig. 4.4). At 4.4 m/s, differences in PLA across anvil were insignificant (frontal: p=0.083, temporal, p=0.192). This was dissimilar to trends at 5.7 m/s, where 30° anvil PLAs were significantly greater than 0° PLAs at the frontal location (p=0.049) and significantly less than 0° PLAs at the temporal location (p=0.041). Despite this, PLA differences were generally small for all configurations (≤6.2%). Paired differences in PRA across anvil were considerably larger (>15.2%, p<0.009 for all configurations), with 0° PRAs greater than 30° PRAs and differences more pronounced at the temporal location. Resulting differences in concussion risk across anvil angle reflected these differences in PLA and PRA; 0° risks were significantly greater than 30° risks for all configurations except frontal-5.7 m/s impacts (frontal-5.7 m/s: p=0.114, other configurations: p<0.038). At the temporal location, differences in risk were as high as 50.5%.

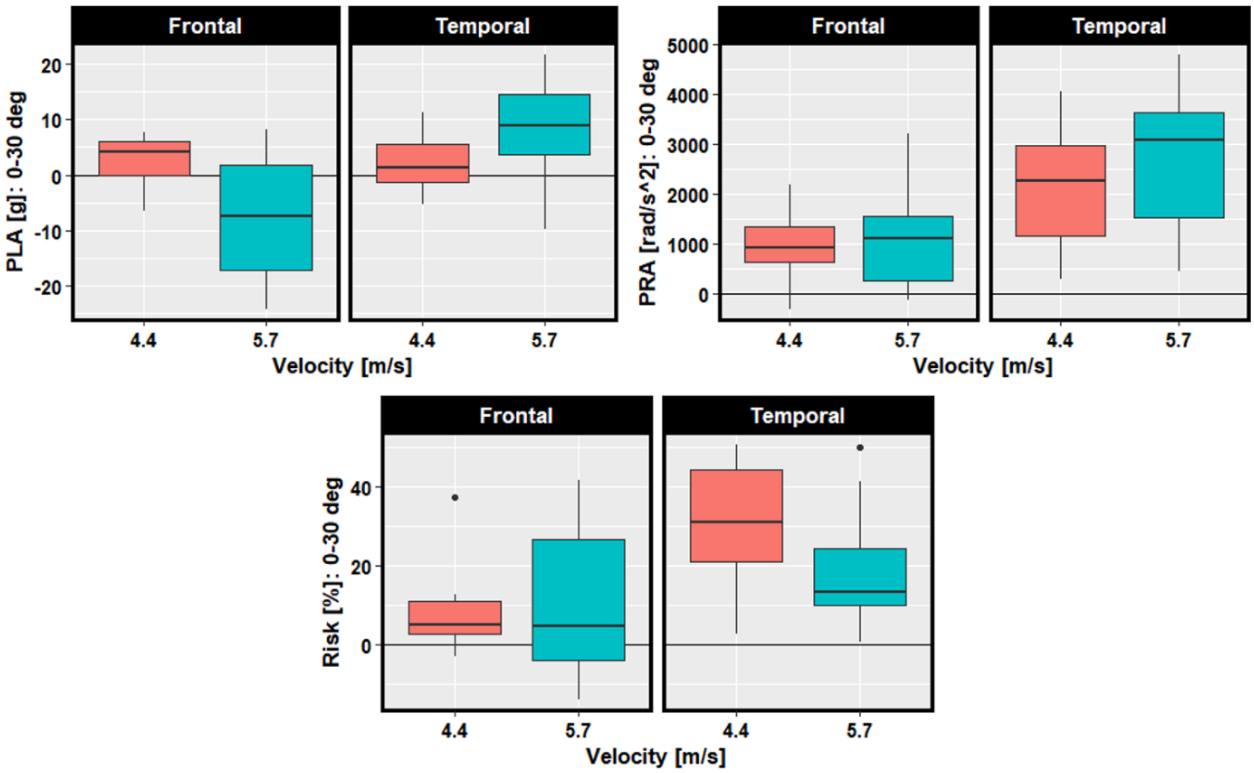

Figure 4.4. Difference distributions in PLA, PRA, and concussion risk, calculated as 30° anvil results subtracted from 0° anvil results per helmet model for each impact configuration. Lower and upper box bounds represent first and third quartiles (25th and 75th percentiles), and whiskers extend to the largest value or 1.5x the interquartile range.

DISCUSSION

The ten bicycle helmets tested herein revealed considerable differences in impact attenuation characteristics across anvil angle with a biofidelic test rig. Anvil effects were larger for PRA than PLA, with PLA varying minimally across anvil and PRA being greater for the 0° anvil. As normal impact velocities were matched across anvil angle, these similarities in PLA were expected. Conventional helmets are composed of a foam liner that crushes upon impact to absorb energy, and it has previously been observed that PLA is well-modeled as a function of normal velocity, with liner crushing distance thought to increase approximately linearly with normal force [20].

Differences in PRA across anvil angle are thus likely attributable primarily to the differing tangential forces involved. The tangential force resulting from the 30° impacts causes the resultant force to be directed closer to the CG of the head/neck system (assumed to fall slightly superior to the occipital condyles), producing a smaller moment arm (Fig. 4. 5). This would effectively reduce rotational kinematics experienced by the head. Tangential forces for the 0° anvil can be considered negligible in comparison, as the incident velocity was normal to the surface.

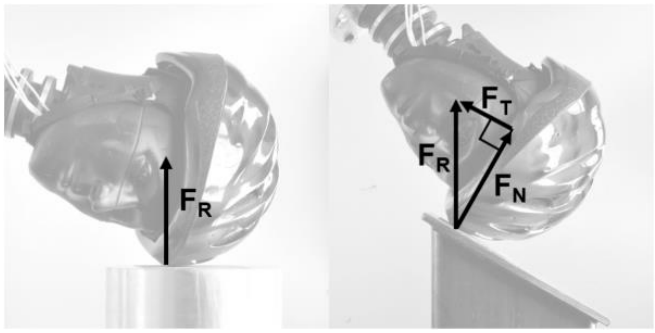

Figure 4.5. Reaction force components for the 0° (left) and 30° (right) anvils. The 30° anvil involves a considerable tangential force, which counteracts the moment produced by the normal force to produce a smaller net moment and lower PRA.

Impact accelerations varied across location for both anvils. The temporal location generated greater PLAs than the frontal location, possibly due to varying helmet geometry. The radius of curvature of bicycle helmets in the transverse plane is typically larger at the sides than at the front; this results in a larger contact area upon impact, which reduces pressure for a given impact force and decreases liner crush [24]. Similar trends were reflected in PRA across location for the 0° anvil. These impacts were primarily normal, so it is likely that the same mechanisms reducing PLA in normal impacts would also reduce PRA. Conversely, differences in PRA across location were less substantial for the 30° anvil. The tangential forces involved in these impacts have considerable effects on rotation, suggesting that location differences in PRA for oblique impacts

may be effectively evened out by the addition of tangential forces. Further, differences across location may be partly attributed to varying properties of the HIII neck in different loading directions [25]. At 5.7 m/s, helmets generally produced greater differences in accelerations across anvil, potentially due to exacerbated effects of the neck at this higher impact energy.

The range of differences in PLA and PRA across anvil angles produced large differences in concussion risk as well. Risks resulting from 0° impacts were up to 50% greater than risks from 30° impacts, owing primarily to the large PRA differences across each anvil. This suggests that conventional helmets present markedly different capabilities in reducing injury risk at different impact angles. The large differences in risk are also partly a result of the impact velocities prescribed herein, which produced accelerations falling within a range where tolerance of the human brain to concussive injury is thought to vary considerably [22]. As these accelerations have been suggested to be especially common in cyclist accidents [18, 19], however, there is added clinical relevance to evaluating helmet performance at the present impact energies. Standards currently test helmets at much higher energies and utilize a 300 g pass-fail threshold, associated with >50% risk of severe brain injury or skull fracture [26]. Although imperative to ensure helmets protect against these more severe injuries, it would be particularly valuable to assess helmet performance at the most common impact severities as well, especially given that these severities also pose high injury risk.

As standards impact testing evaluates normal impacts and resulting PLA, conventional bicycle helmets are based around mitigating linear impacts and generally lack specific mechanisms for reducing rotational accelerations. However, recent attention given to the importance of rotational kinematics in brain injury has led to the development of the multi-directional impact protection system (MIPS, AB, Täby, Sweden). This technology is intended to reduce rotational accelerations

through a slip-plane interfacing with the wearer's head, allowing the head to slide independently of the outer shell upon impact. Two of the helmets evaluated in the present study contained MIPS. These helmets often demonstrated smaller differences in PRA across anvil angles compared to other models (notably at the frontal location), which may suggest some effectiveness of MIPS. Despite this, the MIPS helmets produced average or greater PRAs than many other models, especially for 30° impacts and at the temporal location. This may be due to MIPS counteracting the reduction in applied moment achieved by tangential forces for the 30° anvil. However, possible inferences on the effectiveness of this technology are limited by the fact that matched helmet models with and without MIPS were not evaluated in this study.

There are several limitations to the current study that should be considered when evaluating results. The first is that the HIII neck was originally designed for frontal impacts and is thought to be overly stiff in other loading scenarios [25]. Nonetheless, the HIII is the most widely-used dummy neck, and the use of a neck in impact testing may improve biofidelity compared to a rigid joint [4, 27]. Second, the sandpaper-coated metal anvil reflects road conditions as specified by current standards [17], but is more rigid than asphalt and likely produces higher severity impacts. Additionally, the concussion risk function used was developed from head impact data from football players, and may not be representative of the general population [22]. Another limitation pertains to the impact velocities selected herein; these were chosen based on PLAs from helmet damage replication studies, which used standards rigs and normal impacts. Presently, this data represents the best approximation of impact kinematics from real-world accidents, as there are no oblique-impact damage reconstruction studies. The final limitation is that only two anvil angles were assessed. These were selected to represent a broad range in possible impact scenarios. However, oblique impacts are thought to be more common in cyclist accidents than normal impacts [6].

CONCLUSIONS

The present study demonstrates the importance of anvil angle on impact kinematics and subsequent injury risks during laboratory testing of bicycle helmets. With matched incident normal velocities, PLA was similar across anvil angle. Conversely, PRA was greater for normal impacts, likely owing to a smaller net moment arm produced by tangential reaction forces associated with the 30° anvil. Differences in performance also varied as a function of impact location, and could be attributed to differences in helmet geometry and neck interactions across location. The considerable concussion risks observed suggest that there is value in assessing helmet performance at common impact severities and with more biofidelic test rigs. Additionally, results suggest there is value in evaluating helmet performance under multiple impact angles, as impact attenuation characteristics varied with angle. Knowledge of these characteristics may aid in the development of helmet technologies equipped to address a wider variety of loading scenarios.

REFERENCES

1. CPSC. (2015, July 26, 2016). *National Electronic Injury Surveillance System Database* [Web]. Available: www.cpsc.gov/en/Research--Statistics/NEISS-Injury-Data/
2. J. Schulman, J. Sacks, and G. Provenzano, "State level estimates of the incidence and economic burden of head injuries stemming from non-universal use of bicycle helmets," *Injury Prevention,* vol. 8, pp. 47-52, Mar 2002.
3. E. Amoros, M. Chiron, J. L. Martin, B. Thelot, and B. Laumon, "Bicycle helmet wearing and the risk of head, face, and neck injury: a French case--control study based on a road trauma registry," *Inj Prev,* vol. 18, pp. 27-32, Feb 2012.

A. S. McIntosh, A. Lai, and E. Schilter, "Bicycle helmets: head impact dynamics in helmeted and unhelmeted oblique impact tests," *Traffic Injury Prevention,* vol. 14, pp. 501-8, 2013.

4. CPSC, "Safety Standard for Bicycle Helmets Final Rule (16 CFR Part 1203)," vol. 63, ed: United States Consumer Product Safety Commission, 1998, pp. 11711-11747.
5. D. Otte, "Injury Mechanism and crash kinematics of cyclists in accidents," in *33rd Stapp Car Crash Conference*, Warrendale, PA, 1989.
6. T. A. Gennarelli, L. E. Thibault, and A. K. Ommaya, "Pathophysiologic responses to rotational and translational accelerations of the head," *SAE Technical Paper Series,* vol. 720970, pp. 296-308, 1972.
7. G. Milne, C. Deck, N. Bourdet, R. P. Carreira, Q. Allinne, A. Gallego*, et al.*, "Bicycle helmet modelling and validation under linear and tangential impacts," *International Journal of Crashworthiness,* vol. 19, pp. 323-333, 2014.
8. N. J. Mills and A. Gilchrist, "Oblique impact testing of bicycle helmets," *International Journal of Impact Engineering,* vol. 35, pp. 1075-1086, 2008.

9. K. Hansen, N. Dau, F. Feist, C. Deck, R. Willinger, S. M. Madey*, et al.*, "Angular Impact Mitigation system for bicycle helmets to reduce head acceleration and risk of traumatic brain injury," *Accident Analysis & Prevention,* vol. 59, pp. 109-17, Oct 2013.
10. C. Klug, F. Feist, and E. Tomasch, "Testing of bicycle helmets for preadolescents," in *IRCOBI Conference*, Lyon, France, 2015, pp. 136-155.
11. P. Verschueren, "Biomechanical analysis of head injuries related to bicycle accidents and a new bicycle helmet concept," PhD, Faculteit Ingenieurswetenschappen Departement Werktuigkunde Afdeling Biomechanica en Grafisch Ontwerpen, Katholieke Universiteit Leuven, Leuven, 2009.
12. N. Bourdet, C. Deck, R. P. Carreira, and R. Willinger, "Head impact conditions in the case of cyclist falls," *Proceedings of the Institution of Mechanical Engineers, Part P: Journal of Sports Engineering and Technology,* vol. 226, pp. 282-289, 2012.
13. M. Aare and P. Halldin, "A new laboratory rig for evaluating helmets subject to oblique impacts," *Traffic Injury Prevention,* vol. 4, pp. 240-8, Sep 2003.
14. B. R. Cobb, A. M. Zadnik, and S. Rowson, "Comparative analysis of helmeted impact response of Hybrid III and National Operating Committee on Standards for Athletic Equipment headforms," *Proceedings of the Institution of Mechanical Engineers, Part P: Journal of Sports Engineering and Technology,* vol. 230, pp. 50-60, 2015.
15. R. W. Nightingale, J. H. McElhaney, W. J. Richardson, and B. S. Myers, "Dynamic responses of the head and cervical spine to axial impact loading," *J Biomech,* vol. 29, pp. 307-318, 1996.

A. M. Hering and S. Derler, "Motorcycle helmet drop tests using a Hybrid III dummy," in *the International IRCOBI Conference on the Biomechanics of Impact*, Zurich, Switzerland, 2000.

16. M. Williams, "The protective performance of bicyclists' helmets in accidents," *Accident Analysis & Prevention,* vol. 23, pp. 119-31, Apr-Jun 1991.
17. T. A. Smith, D. Tees, D. R. Thom, and H. H. Hurt, "Evaluation and replication of impact damage to bicycle helmets," *Accident Analysis & Prevention,* vol. 26, pp. 795-802, 1994.
18. N. J. Mills, "Critical evaluation of the SHARP motorcycle helmet rating," *International Journal of Crashworthiness,* vol. 15, pp. 331-342, 2010.
19. B. R. Cobb, A. M. Tyson, and S. Rowson, "Head acceleration measurement techniques: Reliability of angular rate sensor data in helmeted impact testing," *Proceedings of the Institution of Mechanical Engineers, Part P: Journal of Sports Engineering and Technology,* pp. 1-6, 2017.
20. S. Rowson and S. M. Duma, "Brain injury prediction: assessing the combined probability of concussion using linear and rotational head acceleration," *Annals of Biomedical Engineering,* vol. 41, pp. 873-82, May 2013.
21. M. McCrea, T. Hammeke, G. Olsen, P. Leo, and K. Guskiewicz, "Unreported concussion in high school football players: implications for prevention," *Clin J Sport Med,* vol. 14, pp. 13-7, Jan 2004.
22. N. J. Mills, "Protective capability of bicycle helmets," *British Journal of Sports Medicine,* vol. 24, pp. 55-60, Mar 1990.

A. J. Sances, F. Carlin, and S. Kumaresan, "Biomechanical analysis of head-neck force in Hybrid III dummy during inverted vertical drops," *Biomed Sci Instrum,* vol. 38, pp. 459-464, 2002.

23. H. J. Mertz, A. L. Irwin, and P. Prasad, "Biomechanical and scaling bases for frontal and side impact injury assessment reference values," *Stapp Car Crash Journal,* vol. 47, pp. 155-88, Oct 2003.
24. M. Ghajari, S. Peldschus, U. Galvanetto, and L. Iannucci, "Effects of the presence of the body in helmet oblique impacts," *Accid Anal Prev,* vol. 50, pp. 263-71, Jan 2013.

CHAPTER 5

HEADFORM AND NECK EFFECTS ON DYNAMIC RESPONSE IN BICYCLE HELMET OBLIQUE IMPACT TESTING

ABSTRACT

The incidence of cycling-related injuries in the US has increased in recent years, with the head being among the most commonly and seriously injury body parts. Current bicycle helmet standards present limited representation of real-world cyclist accidents. Researchers generally agree that evaluating helmets using oblique impacts, which are common in cyclist impacts, could enhance helmet design. However, the boundary conditions across various oblique impact rigs vary widely. The purpose of this study was to evaluate effects of the anthropomorphic test device (ATD) headform and neck on dynamic response in bicycle-helmeted, oblique impacts. A Hybrid III (HIII) and National Operating Committee on Standards for Athletic Equipment (NOCSAE) headform were impacted in drop tests onto an angled anvil with or without a HIII neck. Both headforms produced similar linear response (0.4% average difference in peaks, $p=0.76$), while rotational velocity and acceleration peak responses were ~22 and 31% greater for the HIII ($p<0.01$). The headform-only tests produced 17-35% greater peak linear and rotational values than the tests with a neck, although impact location influenced neck effects. Trends in these results can be used to interpret differences across published bicycle helmet oblique impact studies and have important implications for injury risk.

INTRODUCTION

Cycling is a common activity and form of transit worldwide and is becoming increasingly popular in the United States, with many embracing the health and environmental benefits it affords [1-3]. However, its increase in popularity is paralleled by increasing injury rates from cycling as well. The number of bicycle-related hospital admissions has grown 120% over the past 15 years [4], and in 2015 alone there were 818 cyclist fatalities – a 12% increase from the previous year [1]. The associated costs are considerable, with adult cycling-related injuries accounting for an estimated $24.4 billion in the US in 2013 [5]. The head is the among the most commonly injured body parts from these accidents, especially for more severe or fatal injuries [6-8].

Helmet use has been repeatedly demonstrated to reduce head injury risk in cycling [6,7,9-13]. During an impact, the expanded polystyrene (EPS) liner of a typical helmet permanently crushes, dissipating the energy that would otherwise be transferred to the head. Helmet impact performance is regulated by safety standards that impose a limit on peak linear acceleration (PLA) of an anthropomorphic test device (ATD) headform during prescribed impact testing [14,15]. This testing involves guided drop tests of the headform onto an anvil at an impact angle normal to the anvil surface. In the US standard, the magnesium International Organization for Standardization (ISO) half-headform is rigidly attached to the drop mass so that rotation of the head is constrained upon impact [14].

Standards impact testing, although effective in limiting energy input into the head, is not completely representative of real-world cyclist accidents. In contrast to the solely normal impacts conducted in standards testing, it has been shown that cyclist head impacts involve both normal and tangential incident velocities (termed “oblique”) [8]. This occurs because cyclists typically approach the ground at an angle upon falling, often between 30 and 60° from the horizontal [16-

20]. Standards also only assess PLA, while oblique impacts generate considerable rotational motion of the head in addition to linear. This has significant implications for injury risk, as the brain is known to be especially susceptible to diffuse injury from the relative motion and tissue strain that are associated with rotational impact [21-24]. Peak rotational velocity (PRV) and acceleration (PRA), often in conjunction with PLA, have been correlated with occurrence of traumatic brain injury [23-28]. Lastly, the metal half-headform and rigid connection to the drop mass in standards testing are not reflective of human properties and preclude realistic assessment of headform motion upon impact.

Due to the limitations of standards testing in replicating real-world cyclist head impacts, more recent research has suggested evaluating bicycle helmets in oblique impacts as an avenue for further improvement of helmet design [12,29-31]. A variety of oblique impact test rigs have been developed for such testing. Several rigs involve a horizontally-moving plate to generate the normal and tangential inbound velocities characteristic of oblique impacts [30-32], while others make use of an angled anvil [29,33,34]. Choice of headform and use of an ATD neck also vary across these studies, as do prescribed impact velocities and locations. However, there is currently no universally accepted method for oblique impact testing, and the effects of varying several of these boundary conditions on resulting helmet performance are not well understood.

The incorporation of a neck is a particularly debated boundary condition for oblique impact rigs. The Hybrid III (HIII) 50th percentile male neck is one of the most commonly-used surrogate necks for impact testing. Originally developed for use in the automotive industry and validated based on post mortem human subject (PMHS) flexion/extension response in frontal sled tests [35], it has also been used extensively in athletic equipment testing in recent years [12,32,33,36-40]. Despite its wide usage, the HIII neck has been shown to be less biofidelic in other loading scenarios and

directions [41-46]. This has produced disagreement as to whether it is suitable to incorporate the neck (and effective torso mass) in sports ATD head impact testing and what the effects of testing with and without it may be. Some researchers have suggested that the neck does not play a role in the initial impact response of the head in humans, and therefore it is better to forego it due to its lacking biofidelity [31,47]. Others advocate for its use, stating that the neck in fact plays a key role in the impact response of the head [12,48,49]. Among those opining that the neck does affect impact response, various theories on its exact effects on kinematic outcomes have been presented [34,42,47,48,50,51].

The choice of headform is another debated boundary condition for head impact testing. For sports helmet testing, the 50th percentile male HIII and National Operating Committee on Standards for Athletic Equipment (NOCSAE) are two of the most commonly used headforms [29,32,36,37,39,40,49,52,53]. The HIII headform was developed in tandem with the HIII neck for automotive testing [54], and contains a large central cavity allowing for placement of a nine-accelerometer array (9AA) that enables calculation of linear and angular head acceleration [55]. The NOCSAE headform, conversely, was developed for helmet testing specifically [56]. It has a more biofidelic shape compared to the HIII [57] and is thought to be more humanlike in its construction, with a gel-filled cavity meant to simulate the brain [56]. While the NOCSAE was not designed to be coupled to a neck and contains a smaller instrumentation channel, past studies have modified the headform to allow coupling of a HIII neck and have used tri-axial angular rate sensors (ARS) and linear accelerometers to measure linear and rotational kinematics [36,58]. Both the HIII and NOCSAE headforms were validated based on PMHS linear acceleration curves in drop tests [54,56]; however, differences in overall geometry, material construction, instrumentation, and inertial properties between the two headforms likely affect dynamic response. To-date, two studies have investigated these differences in matched impact conditions,

but none have utilized oblique impacts such as those characteristic of cyclist head impacts [36,53].

The purpose of this study was therefore to investigate the effects of choice of ATD headform and neck use on dynamic response in bicycle-helmeted, oblique impacts.

METHODS

Impact testing was conducted using a linear drop tower with a sandpaper-coated 45° anvil (80 grit to mimic road surfaces [59]). A blue, medium NOCSAE headform and a 50th percentile male HIII headform were used in testing, and were connected to a 50th percentile male HIII neck for half the tests (Fig. 5.1). The neck was also attached to an effective torso mass (16 kg [60]) that was constrained to the drop tower. The drop mass was stopped just after impact to limit the load on the neck. For the No Neck tests, the headform was positioned in hoop of a larger diameter than the anvil such that it passed outside the anvil upon impact, separating it from the headform. The headform was secured in place using a lever arm that released just prior to impact, and was then free to rotate off the anvil upon impact. For the Neck tests, the NOCSAE headform required modification to render it compatible with the HIII neck. This modification has been outlined in previous studies, and resulted in a similar mass between headforms and a center of gravity (CG) location relative to the occipital condyle (OC) pin 22 mm superior for the NOCSAE headform compared to the HIII [36,58].

Each headform-neck configuration was tested at 6 m/s at both frontal and parietal impact locations (commonly impacted velocity and locations in cyclist accidents [16,19,20]). Consistent headform positioning between tests for the Neck impacts was ensured using defined Y and Z axis rotation increments on the drop mass (SAE J211 standard coordinate system). For the No Neck tests,

matching impact locations were defined using a dual-axis inclinometer (DMI600, Omni Instruments, Dundee, UK). Five trials were conducted for each of the eight headform-neck-location configurations, totaling 40 tests in all. Prior to testing, headforms were fitted with a bicycle helmet, with a new helmet used per test.

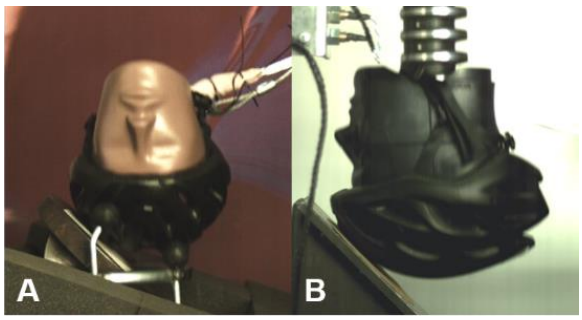

Figure 5.1. Representative configurations for oblique impact testing. A HIII, No Neck, parietal impact is shown in (A), while a NOCSAE, Neck, frontal impact is depicted in (B).

Linear acceleration and rotational velocity data were collected at 20 kHz for all tests using three linear accelerometers (Endevco 7264B-2000, Meggitt Sensing Systems, Irvine, CA) and a tri-axis ARS (ARS3 PRO-18K, DTS, Seal Beach, CA) located at the CG of both headforms. The ARS was selected as it is more readily compatible with the NOCSAE headform than the traditional 9AA system [36,61]. Rotational accelerations were calculated as the derivative of rotational velocity traces. Linear acceleration was filtered in accordance with SAE J211 using a channel frequency class (CFC) of 1000, while rotational velocity was filtered at a CFC of 175. The latter CFC was optimized in previous studies to minimize the error between ARS-calculated PRA and 9AA-calculated PRA in pendulum impacts to a football-helmeted HIII headform [61]. This filter choice was also validated in the present study by instrumenting the HIII with a 9AA as well as the ARS; the average difference in PRA between the two systems was 0.23%, so the ARS-calculated PRA was used in analysis.

Resultant PLA, PRV, and PRA were determined per test, as well as duration, time to PLA, and time to PRA. Duration was defined as the time between the resultant linear acceleration curve first exceeding 5 g and first falling below 5 g after the peak (5 g threshold determined to reliably detect endpoint of impact pulse). All metrics were compared across headform-neck-location configurations using 3-way ANOVA with Tukey's HSD post hoc tests.

RESULTS

Distinct kinematic properties were observed for each of the headform and neck configurations. Average parameter values per headform and neck configuration are given in Table 5.1, while more detailed results for each impact configuration and all significant comparisons are provided in the Appendix (Tables 5.A1 and 5.A2). Both headforms produced similar time-based metrics and PLA, with average differences less than 6.5%. PLA was within 0.4% on average ($p=0.76$), and resultant linear acceleration curves for the HIII and NOCSAE were very similar across the entire time series (Fig. 5.2). This was contrasted by the resultant rotational velocity and acceleration curves (Fig. 5.3-5.4), which were markedly different across headform and produced peak values for the NOCSAE that were 20-30% less than those for the HIII ($p<0.01$). The Neck curves showed a secondary peak corresponding with the drop mass being caught following impact. This peak was ignored, and only the first peaks were used in analysis. All trends in headform differences were generalizable across impact location, with the exception of PRV for the parietal Neck impacts; PRV was not significantly different across headform for this configuration ($p=0.39$), while the HIII produced greater PRVs for all other configurations. Variance was low for both headforms, with coefficients of variance (CV) averaging 5.3% and 6.3% for the HIII and NOCSAE, respectively.

Table 5.1. Parameter averages ± standard deviations per headform and neck condition. The NOCSAE and No Neck columns give the percent difference and significance levels from the preceding column.

	HIII	NOCSAE	Neck	No Neck
Duration (ms)	10.0 ± 0.7	9.8 ± 1.2 -2.1% (p=0.23)	10.3 ± 1.0	9.5 ± 0.7 -7.6% (p<0.01)
Time to PLA (ms)	4.4 ± 0.6	4.2 ± 0.4 -4.5% (p=0.06)	4.3 ± 0.6	4.4 ± 0.4 0.1% (p=0.96)
Time to PRA (ms)	3.7 ± 1.1	4.0 ± 1.3 6.4% (p=0.35)	3.7 ± 1.6	4.0 ± 0.5 10.7% (p=0.46)
PLA (g)	134.7 ± 20.6	135.2 ± 24.2 0.4% (p=0.76)	114.8 ± 10.2	155.1 ± 7.4 35.1% (p<0.01)
PRV (rad/s)	32.0 ± 6.0	25.0 ± 3.5 -21.9% (p<0.01)	26.3 ± 6.1	30.7 ± 5.1 16.9% (p<0.01)
PRA (rad/s^2)	7699 ± 1164	5316 ± 1430 -30.9% (p<0.01)	5901 ± 2121	7114 ± 1057 20.5% (p<0.01)

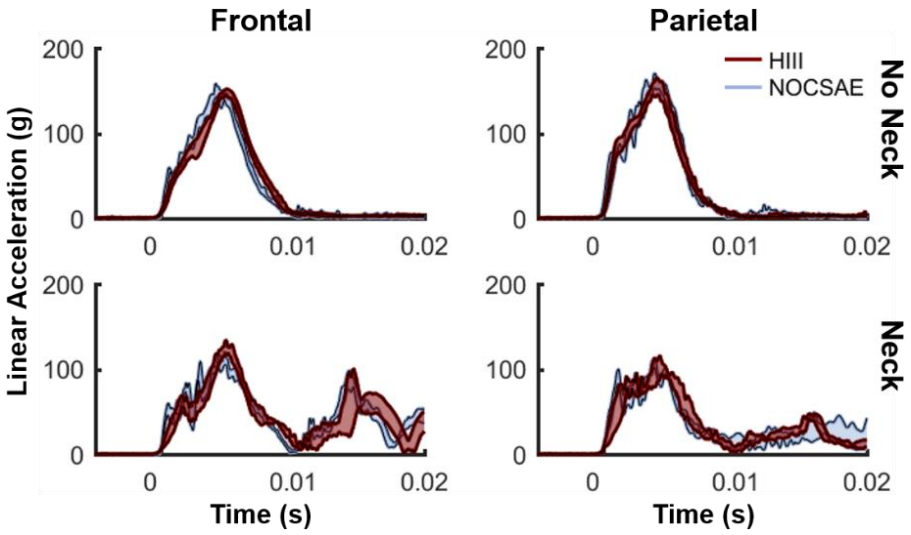

Figure 5.2. Time series linear acceleration corridors (min/max) across headform. No Neck (top), Neck (bottom), frontal (left), and parietal (right) conditions are shown. Curves were similar across headform with low variance.

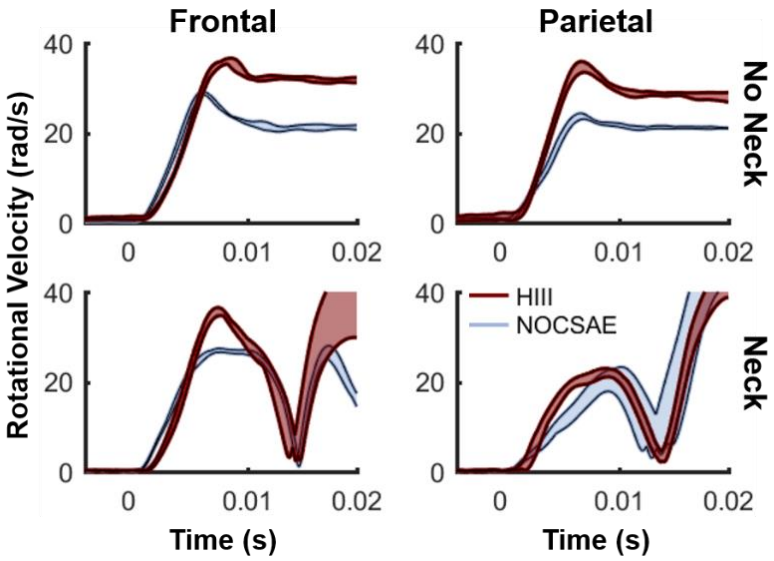

Figure 5.3. Rotational velocity corridors (min/max) across headform. HIII PRV was mostly larger.

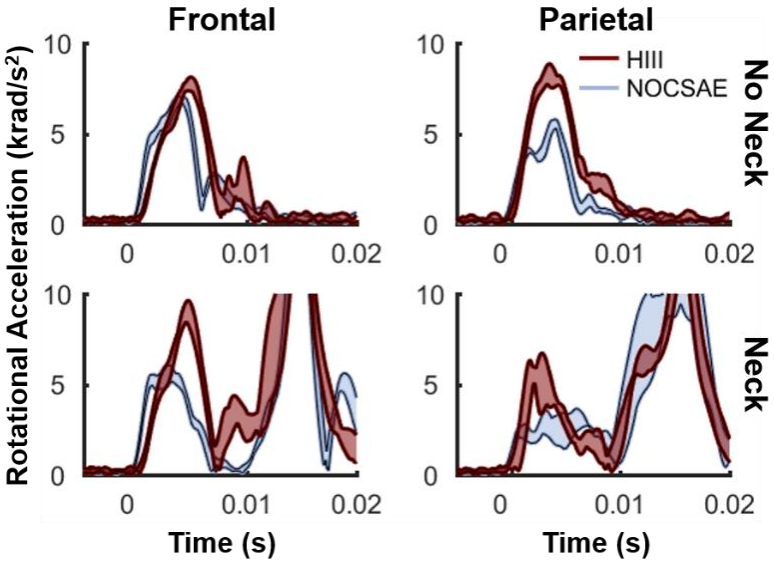

Figure 5.4. Rotational acceleration corridors (min/max) across headform. HIII PRA was greater.

The two neck conditions generated comparable time-based parameters (differences generally within 10%), although duration was shorter for No Neck ($p<0.01$). Differences in PLA, PRV, and PRA were larger (No Neck 17-35% greater, $p<0.01$), reflected in the time series of resultant linear acceleration and rotational velocity and acceleration (Fig. 5.5-5.7). All trends were again similar

across impact location. However, the rotational velocity curves appeared much more similar at the frontal location than at the parietal location (Fig. 5.6). Additionally, variance was greater for the Neck tests, producing an average CV of 8.0% compared to a CV of 3.6% for No Neck tests.

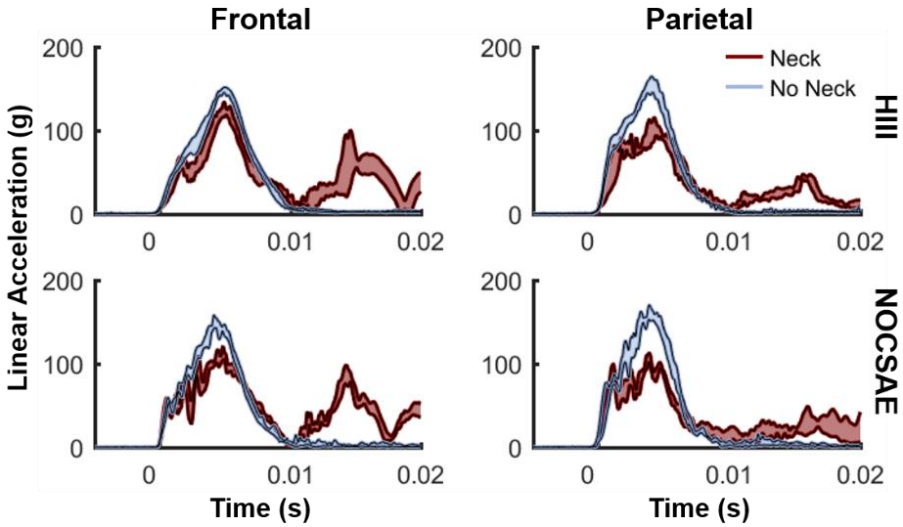

Figure 5.5. Linear acceleration corridors (min/max) across neck condition for the HIII (top) and NOCSAE (bottom). No neck produced greater PLA.

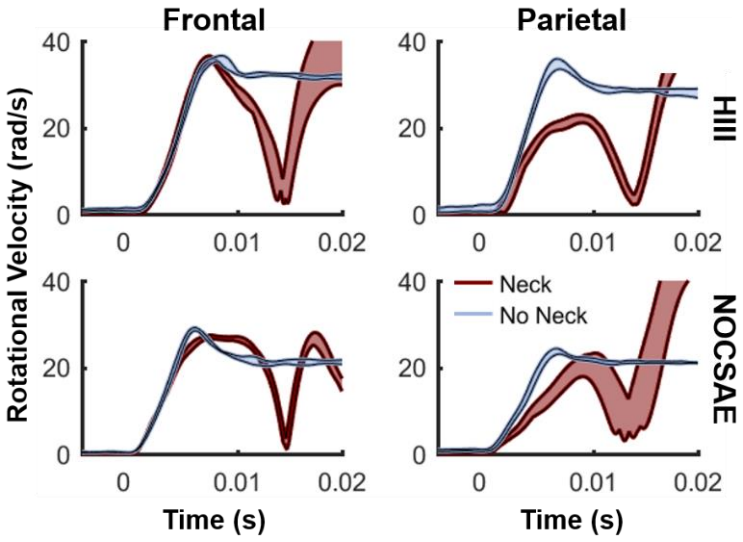

Figure 5.6. Rotational velocity corridors (min/max) across neck condition. No Neck PRV was

greater at the parietal location.

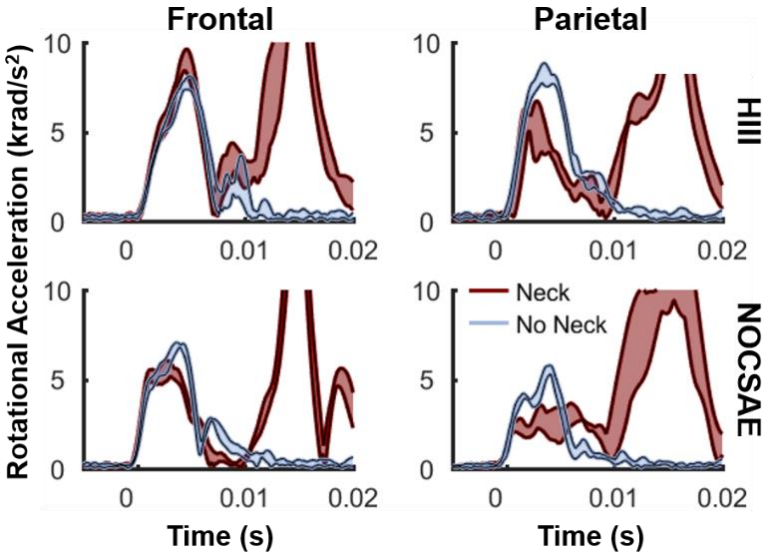

Figure. 5.7. Rotational acceleration corridors (min, max) across neck condition. PRA was generally greater for No Neck.

DISCUSSION

Each of the headform and neck conditions evaluated herein produced distinct kinematic profiles. Across all configurations, the greatest similarities in response curves were observed in linear acceleration between headforms (Fig. 5.2). This is likely attributable to both headforms being designed to reflect linear acceleration characteristics in PMHS head drop tests [54,56]. Conversely, rotational kinematic parameters varied considerably between the headforms, with the HIII averaging 22 and 31% greater PRV and PRA than the NOCSAE, respectively. This may due to the lower moments of inertia (MOI) about the x and y axes (SAE J211 convention) for the HIII relative to the NOCSAE [62]. Human head inertial properties vary considerably across the population [63], so the HIII and NOCSAE MOI values both fall within a biofidelic range. Additionally, differing frictional properties of the headforms may have also caused variation in

rotational responses. This is especially likely in the present impact scenario, where the high friction of the simulated road surface causes the helmet to stick initially and exacerbates effects at the helmet-headform interface. One recent study demonstrated that the HIII vinyl skin produces a much larger friction interface with helmet materials than human heads [64]. Future studies are needed to investigate dynamic friction properties of the NOCSAE headform. Importantly, both headforms produced little variance and thereby good repeatability, which is essential for comparative testing.

The present trends in headform results have varying levels of agreement with other studies comparing the two headforms. Cobb et al. used pendulum tests to impact football-helmeted headforms attached to a HIII neck [36]. The NOCSAE showed greater PLA and PRA than the HIII, although PLA differences were much lower and often not significant, similar to the results of this study. Kendall et al. also found greater PLA and PRA for the NOCSAE than the HIII in drop tests of both headforms onto a flat anvil through the CG [53]. However, both studies utilized different loading scenarios than the oblique, helmeted impacts assessed herein, and differences in the resultant force vectors and transfer of momentum involved complicate the generalizability of trends across studies. Nonetheless, Cobb et al. and Kendall et al. also demonstrated good repeatability of both headforms.

The use of a neck produced markedly different kinematics for both linear and rotational response curves. The No Neck tests generated significantly shorter durations than the Neck tests, likely owing to a delayed response of the neck and to the headform being constrained to the drop tower for the Neck tests. The No Neck tests also produced significantly greater PLA, PRV, and PRA. Linear acceleration differences suggest that the neck and effective torso mass play into the overall effective mass during impact, lowering PLA for the Neck tests. The increase in overall effective

mass would also contribute to inertial differences between the Neck and No Neck tests, affecting rotational characteristics as well. These results suggest that the neck and body do in fact affect the dynamic response of the head in ATD testing. Several simulation studies have predicted similar results for humans as well [50,51]. Lastly, it is also important to note that use of the neck produced considerably higher variance under these loading conditions.

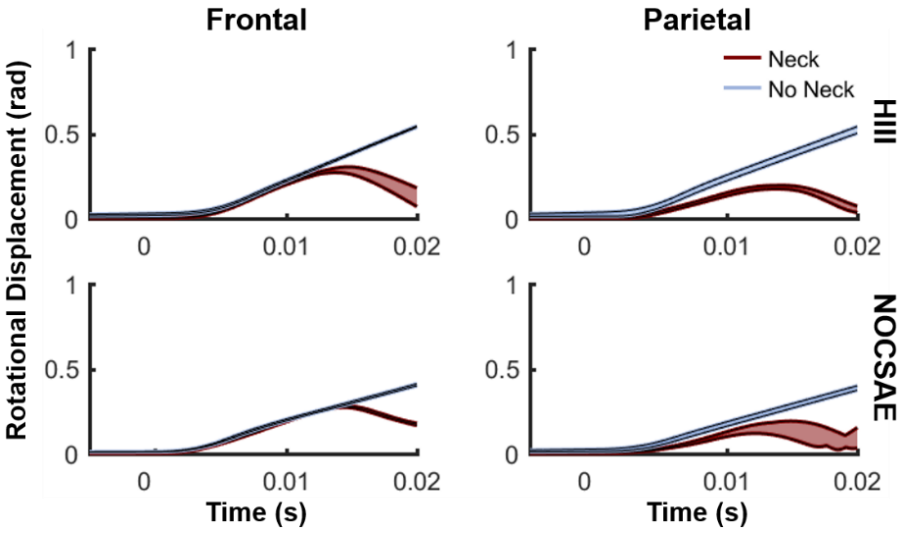

Figure 5.8. Rotational displacement corridors (min, max) across neck condition. The frontal location produced similar curves during the duration of the impact, while the parietal impacts differed more notably.

Trends in headform and neck condition differences were generally consistent across impact location. One notable exception was that PRV was significantly different between headform types for all configurations except the parietal, Neck configuration, as evidenced by the rotational velocity curves (Fig. 5.3). This may be attributable to the design of the HIII head-neck junction, which rotates in flexion-extension about a pin joint but is constrained (and therefore much stiffer) in the lateral direction. In lateral impacts, the motion of the head is thus translated to a point lower in the neck, and it is possible that this neck motion was a controlling factor in the dynamic

response. This is supported by the linear acceleration loading curves, which exhibit a plateaued region for parietal neck impacts. Further, when comparing across neck condition, rotational velocity curves at the frontal location are much more similar than those at the parietal location (Fig. 5.6), suggesting the neck plays a larger role in loading characteristics at the parietal location. This is also reflected in PRV values, which were significantly different between Neck and No Neck tests at the parietal location ($p<0.01$) but not at the frontal location ($p>0.13$). Differentiating these rotational velocity curves demonstrates the differences in rotational displacement paths (Fig. 5.8). At the frontal location, the Neck and No Neck curves are very similar up to ~12 ms, at which point the parietal curves are more distinctly different between neck conditions.

There are several limitations to the present study that the results should be interpreted in light of. First, only one helmet model, one velocity, one anvil angle, two locations, and one neck orientation relative to the anvil were tested. Results are specific to these prescribed impact conditions, although general trends may hold true in other conditions as well. However, varying orientations of the neck relative to the anvil likely has a large effect on neck condition trends, as this changes the contribution of the neck and effective torso mass to the overall effective mass. Another study with the body oriented horizontally in drop tests indeed shows different trends [48]. An additional consideration regarding relative neck orientation is the type of loading that results in the neck. In the present study, the HIII neck was likely subject to considerable axial loads, under which this neck is thought to behave much differently than a human neck [41,44]. Thus, the HIII neck in this orientation may not be representative of a human response, whereas it may be more realistic in other loading scenarios. Finally, effects of hair and a scalp were not considered in the present study, which likely affect the helmet-headform interface and resulting dynamics. Despite these limitations, the prescribed impact conditions reflect those common in published bicycle helmet oblique impact studies, and as such these results provide a basis upon which to evaluate

differences in results across other studies.

CONCLUSIONS

The present study demonstrates that choice of ATD headform and use of a neck have significant effects on dynamic response during bicycle-helmeted, oblique impacts. The NOCSAE headform produced similar PLA but lower PRV and PRA compared to the HIII, while the incorporation of the HIII neck generally decreased PLA, PRV, and PRA compared to headform-only tests. These trends provide a framework by which to interpret results across published bicycle helmet oblique impact studies and have important implications for injury risk assessment. Future research optimizing testing boundary conditions around replicating human responses can stimulate improved helmet design for cyclist safety.

REFERENCES

1. Association, Governors Highway Safety Association. A Right to the Road: Understanding and Addressing Bicyclist Safety. 2017.
2. Wen, L.M. and Rissel, C. Inverse associations between cycling to work, public transport, and overweight and obesity: findings from a population based study in Australia. *Preventive medicine*, 2008. 46(1): p. 29-32
3. Hamer, M. and Chida, Y. Active commuting and cardiovascular risk: a meta-analytic review. *Preventive medicine*, 2008. 46(1): p. 9-13
4. Sanford, T., McCulloch, C.E., and Callcut, R.A. Bicycle trauma injuries and hospital admissions in the United States, 1998-2013. *Jama*, 2015. 314(9): p. 947-949
5. Gaither, T.W., Sanford, T.A., et al. Estimated total costs from non-fatal and fatal bicycle crashes in the USA: 1997-2013. *Injury prevention : journal of the International Society for Child and Adolescent Injury Prevention*, 2017
6. Thompson, D.C., Rivara, F.P., and Thompson, R.S. Effectiveness of bicycle safety helmets in preventing head injuries. A case-control study. *The Journal of the American Medical Association*, 1996. 276(24): p. 1968-1973
7. Sacks, J.J., Holmgreen, P., Smith, S.M., and Sosin, D.M. Bicycle-associated head injuries and deaths in the United States from 1984 through 1988: How many are preventable? *The Journal of the American Medical Association*, 1991. 266: p. 3016-3018
8. Otte, D. Injury Mechanism and crash kinematics of cyclists in accidents. *Proceedings of 33rd Stapp Car Crash Conference*, 1989. Warrendale, PA
9. Olivier, J. and Creighton, P. Bicycle injuries and helmet use: a systematic review and meta-analysis. *International journal of epidemiology*, 2017. 46(1): p. 278-292
10. Amoros, E., Chiron, M., Martin, J.L., Thelot, B., and Laumon, B. Bicycle helmet wearing and the risk of head, face, and neck injury: a French case--control study based on a road trauma

registry. *Injury prevention : journal of the International Society for Child and Adolescent Injury Prevention*, 2012. 18(1): p. 27-32
11. Elvik, R. Corrigendum to: "Publication bias and time-trend bias in meta-analysis of bicycle helmet efficacy: a re-analysis of Attewell, Glase and McFadden, 2001" [Accid. Anal. Prev. 43 (2011) 1245-1251]. *Accident Analysis & Prevention*, 2013. 60: p. 245-53
12. McIntosh, A.S., Lai, A., and Schilter, E. Bicycle helmets: head impact dynamics in helmeted and unhelmeted oblique impact tests. *Traffic injury prevention*, 2013. 14(5): p. 501-8
13. Cripton, P.A., Dressler, D.M., Stuart, C.A., Dennison, C.R., and Richards, D. Bicycle helmets are highly effective at preventing head injury during head impact: head-form accelerations and injury criteria for helmeted and unhelmeted impacts. *Accident Analysis & Prevention*, 2014. 70: p. 1-7
14. Safety Standard for Bicycle Helmets Final Rule (16 CFR Part 1203). 1998, United States Consumer Product Safety Commission. p. 11711-11747.
15. European Committee for Standardization (CEN). EN 1078: Helmets for pedal cyclists and for users of skateboards and roller skates. 1997.
16. Verschueren, P. Biomechanical analysis of head injuries related to bicycle accidents and a new bicycle helmet concept, in *Faculteit Ingenieurswetenschappen Departement Werktuigkunde Afdeling Biomechanica en Grafisch Ontwerpen*. 2009, Katholieke Universiteit Leuven: Leuven.
17. Peng, Y., Chen, Y., Yang, J., Otte, D., and Willinger, R. A study of pedestrian and bicyclist exposure to head injury in passenger car collisions based on accident data and simulations. *Safety Science*, 2012. 50(9): p. 1749-1759
18. Fahlstedt, M., Baeck, K., et al. Influence of Impact Velocity and Angle in a Detailed Reconstruction of a Bicycle Accident. *IRCOBI Conference*, 2012. 12(84): p. 787-799
19. Bourdet, N., Deck, C., et al. In-depth real-world bicycle accident reconstructions. *International Journal of Crashworthiness*, 2014. 19(3): p. 222-232
20. Bourdet, N., Deck, C., Carreira, R.P., and Willinger, R. Head impact conditions in the case of cyclist falls. *Proceedings of the Institution of Mechanical Engineers, Part P: Journal of Sports Engineering and Technology*, 2012. 226(3-4): p. 282-289
21. Gennarelli, T., Ommaya, A., and Thibault, L. Comparison of translational and rotational head motions in experimental cerebral concussion. *Proceedings of 15th Stapp Car Crash Conference*, 1971.
22. Gennarelli, T.A., Thibault, L.E., and Ommaya, A.K. Pathophysiologic responses to rotational and translational accelerations of the head. *SAE Technical Paper Series*, 1972. 720970: p. 296-308
23. Ommaya, A.K., Hirsch, A.E., and Martinez, J.L. The role of whiplash in cerebral concussion. *Proceedings of Proc. 10th Stapp Car Crash Conference*, 1966.
24. Ommaya, A. and Hirsch, A. Tolerances for cerebral concussion from head impact and whiplash in primates. *Journal of biomechanics*, 1971. 4(1): p. 13-21
25. Takhounts, E.G., Hasija, V., Ridella, S.A., Rowson, S., and Duma, S.M. Kinematic rotational brain injury criterion (BRIC). *Enhanced Safety of Vehicles*, 2011. 11-0263-0
26. Rowson, S. and Duma, S.M. Brain injury prediction: assessing the combined probability of concussion using linear and rotational head acceleration. *Annals of Biomedical Engineering*, 2013. 41(5): p. 873-82
27. Unterharnscheidt, F.J. Translational versus rotational acceleration: animal experiements with measured inputs. *Proceedings of the 15th Stapp Car Crash Conference*, 1971. SAE 710880
28. King, A.I., Yang, K.H., Zhang, L., Hardy, W., and Viano, D.C. Is Head Injury Caused by Linear or Angular Acceleration? *Proceedings of Proceedings of the International Research Conference on the Biomechanics of Impact (IRCOBI)*, 2003. Lisbon, Portugal

29. Milne, G., Deck, C., et al. Bicycle helmet modelling and validation under linear and tangential impacts. *International Journal of Crashworthiness*, 2014. 19(4): p. 323-333
30. Aare, M. and Halldin, P. A new laboratory rig for evaluating helmets subject to oblique impacts. *Traffic injury prevention*, 2003. 4(3): p. 240-8
31. Mills, N.J. and Gilchrist, A. Oblique impact testing of bicycle helmets. *International Journal of Impact Engineering*, 2008. 35(9): p. 1075-1086
32. Pang, T.Y., Thai, K.T., et al. Head and neck responses in oblique motorcycle helmet impacts: a novel laboratory test method. *International Journal of Crashworthiness*, 2011. 16(3): p. 297-307
33. Hansen, K., Dau, N., et al. Angular Impact Mitigation system for bicycle helmets to reduce head acceleration and risk of traumatic brain injury. *Accident Analysis & Prevention*, 2013. 59: p. 109-17
34. Klug, C., Feist, F., and Tomasch, E. Testing of bicycle helmets for preadolescents. *Proceedings of IRCOBI Conference*, 2015. Lyon, France
35. Foster, J.K., Kortge, J.O., and Wolanin, M.J. Hybrid III~ A Biomechanically-Based Crash Test Dummy. *Proceedings of the 21st Stapp Car Crash Conference*, 1977. SAE 770938
36. Cobb, B.R., Zadnik, A.M., and Rowson, S. Comparative analysis of helmeted impact response of Hybrid III and National Operating Committee on Standards for Athletic Equipment headforms. *Proceedings of the Institution of Mechanical Engineers, Part P: Journal of Sports Engineering and Technology*, 2015. 230(1): p. 50-60
37. Pellman, E.J., Viano, D.C., et al. Concussion in professional football: helmet testing to assess impact performance--part 11. *Neurosurgery*, 2006. 58(1): p. 78-96; discussion 78-96
38. Viano, D.C., Withnall, C., and Wonnacott, M. Football Helmet Drop Tests on Different Fields Using an Instrumented Hybrid III Head. *Ann Biomed Eng*, 2012. 40(1): p. 97-105
39. Beckwith, J.G., Chu, J.J., and Greenwald, R.M. Validation of a noninvasive system for measuring head acceleration for use during boxing competition. *Journal of applied biomechanics*, 2007. 23: p. 238-244
40. Funk, J.R., Cormier, J.M., Bain, C.E., Guzman, H.M., and Bonugli, E. Validation and Application of a Methodology to Calculate Head Accelerations and Neck Loading, in *SAE World Congress*. 2009, Society of Automotive Engineers: Warrendale, PA.
41. Sances, A.J., Carlin, F., and Kumaresan, S. Biomechanical analysis of head-neck force in Hybrid III dummy during inverted vertical drops. *Biomedical sciences instrumentation*, 2002. 38: p. 459-464
42. Rousseau, P., Hoshizaki, T.B., and Gilchrist, M.D. Estimating the influence of neckform compliance on brain tissue strain during a helmeted impact. *Stapp car crash journal*, 2010. 54: p. 37-48
43. Nelson, T.S. and Cripton, P.A. A New Biofidelic Sagittal Plane Surrogate Neck for Head-First Impacts. *Traffic Inj Prev*, 2010. 11(3): p. 309-319
44. Yoganandan, N., Pintar, F.A., Zhang, J., Stemper, B.D., and Philippens, M. Upper neck forces and moments and cranial angular accelerations in lateral impact. *Ann Biomed Eng*, 2008. 36(3): p. 406-14
45. Herbst, B., Forrest, S., Chng, D., and Sances, A.J. Fidelity of anthropometric test dummy necks in rollover accidents. *Proceedings of 16th International Technical Conference on the Enhanced Safety of Vehicles*, 1998. Windsor, Canada
46. Yoganandan, N. and Sances, A.J. Biomechanical evaluation of the axial compressive responses of the human cadaveric and manikin necks. *Journal of biomechanical engineering*, 1989. 111: p. 250-255
47. Gilchrist, A. and Mills, N.J. Protection of the side of the head. *Accident; analysis and prevention*, 1996. 28(4): p. 525-35

48. Hering, A.M. and Derler, S. Motorcycle helmet drop tests using a Hybrid III dummy. *Proceedings of the International IRCOBI Conference on the Biomechanics of Impact*, 2000. Zurich, Switzerland
49. Bartsch, A., Benzel, E., Miele, V., Morr, D., and Prakash, V. Hybrid III anthropomorphic test device (ATD) response to head impacts and potential implications for athletic headgear testing. *Accid Anal Prev*, 2012. 48: p. 285-91
50. Ghajari, M., Peldschus, S., Galvanetto, U., and Iannucci, L. Effects of the presence of the body in helmet oblique impacts. *Accid Anal Prev*, 2013. 50: p. 263-71
51. Fahlstedt, M., Halldin, P., Alvarez, V.S., and Kleiven, S. Influence of the Body and Neck on Head Kinematics and Brain Injury Risk in Bicycle Accident Situations, in International Research Council on Biomechanics of Injury (IRCOBI) Conference. 2016: Malaga, Spain.
52. Rowson, S. and Duma, S.M. Development of the STAR evaluation system for football helmets: Integrating player head impact exposure and risk of concussion. *Annals of Biomedical Engineering*, 2011. 39(8): p. 2130-40
53. Kendall, M., Walsh, E.S., and Hoshizaki, T.B. Comparison between Hybrid III and Hodgson-WSU headforms by linear and angular dynamic impact response. *Proceedings of the Institution of Mechanical Engineers, Part P: Journal of Sports Engineering and Technology*, 2012. 226(3-4): p. 260-265
54. Hubbard, R.P. and McLeod, D.G. Definition and Development of A Crash Dummy Head. *Proceedings of the 18th Stapp Car Crash Conference*, 1974. SAE 741193
55. Padgaonkar, A.J., Kreiger, K.W., and King, A.I. Measurement of Angular Acceleration of a Rigid Body Using Linear Accelerometers. *J Appl Mech*, 1975. 42: p. 552-556
56. Hodgson, V.R. National Operating Committee on Standards for Athletic Equipment football helmet certification program. Medicine and science in sports, 1975. 7: p. 225-232
57. Cobb, B.R., MacAlister, A., et al. Quantitative comparison of Hybrid III and National Operating Committee on Standards for Athletic Equipment headform shape characteristics and implications on football helmet fit. *Proceedings of the Institution of Mechanical Engineers, Part P: Journal of Sports Engineering and Technology*, 2014. 229(1): p. 39-46
58. Rowson, B., Rowson, S., and Duma, S.M. Hockey STAR: A Methodology for Assessing the Biomechanical Performance of Hockey Helmets. *Annals of biomedical engineering*, 2015. 43(10): p. 2429-2443
59. ECE. R-22.05: Uniform Provisions Concerning the Approval of Protective Helmets for Drivers and Passengers of Motorcycles and Mopeds. 1999, United Nations Economic Commission for Europe.
60. Nightingale, R.W., McElhaney, J.H., Richardson, W.J., and Myers, B.S. Dynamic responses of the head and cervical spine to axial impact loading. *Journal of biomechanics*, 1996. 29(3): p. 307-318
61. Cobb, B.R., Tyson, A.M., and Rowson, S. Head acceleration measurement techniques: Reliability of angular rate sensor data in helmeted impact testing. *Proceedings of the Institution of Mechanical Engineers, Part P: Journal of Sports Engineering and Technology*, 2017: p. 1-6
62. Funk, J.R., Quesada, R.E., Miles, A.M., and Crandall, J.R. Inertial Properties of Football Helmets. Journal of biomechanical engineering, 2018. 140(6)
63. Yoganandan, N., Pintar, F.A., Zhang, J., and Baisden, J.L. Physical properties of the human head: mass, center of gravity and moment of inertia. *Journal of biomechanics*, 2009. 42(9): p. 1177-92
64. Trotta, A., Ni Annaidh, A., Burek, R.O., Pelgrims, B., and Ivens, J. Evaluation of the head-helmet sliding properties in an impact test. Journal of biomechanics, 2018. 75: p. 28-34

APPENDIX A

Table A.1. Parameter averages ± standard deviations across all impact configurations.

	HIII				NOCSAE			
	Neck		No Neck		Neck		No Neck	
	Frontal	Parietal	Frontal	Parietal	Frontal	Parietal	Frontal	Parietal
Duration (ms)	10.6 ± 0.3	9.7 ± 0.7	10.3 ± 0.6	9.4 ± 0.4	9.5 ± 0.5	11.4 ± 0.9	9.7 ± 0.2	8.7 ± 0.3
Time to PLA (ms)	4.9 ± 0.1	3.9 ± 0.8	5.0 ± 0.0	4.0 ± 0.2	4.8 ± 0.2	3.8 ± 0.1	4.4 ± 0.2	4.0 ± 0.3
Time to PRA (ms)	4.5 ± 0.1	2.1 ± 0.4	4.6 ± 0.2	3.7 ± 0.6	2.8 ± 1.0	5.1 ± 2.0	3.9 ± 0.3	4.0 ± 0.2
PLA (g)	128.6 ± 4.6	105.9 ± 8.5	148.7 ± 2.8	155.5 ± 7.0	115.4 ± 3.4	109.2 ± 3.5	152.7 ± 4.9	163.5 ± 5.4
PRV (rad/s)	35.5 ± 0.6	22.0 ± 0.9	35.9 ± 0.4	34.5 ± 1.1	27.0 ± 0.3	20.6 ± 2.4	28.9 ± 0.3	23.6 ± 0.5
PRA (rad/s^2)	8860 ± 509	6011 ± 602	7680 ± 284	6011 ± 602	5570 ± 293	3164 ± 432	6974 ± 60	5558 ± 246

Table A.2. Significant comparisons ($p<0.05$) per kinematic parameter, with H = HIII, N = NOCSAE, F = Frontal, P = Parietal. Only comparisons that differ by one factor are included (e.g. H-Neck-F not compared to H-NoNeck-P or N-Neck-P).

Duration (ms)	**Time to PLA (ms)**	**Time to PRA (ms)**	**PLA (g)**	**PRV (rad/s)**	**PRA (rad/s^2)**
H-Neck-F N-Neck-F	H-Neck-F H-Neck-P	H-Neck-F N-Neck-F	H-Neck-F N-Neck-F	H-Neck-F N-Neck-F	H-Neck-F N-Neck-F
H-Neck-P N-Neck-P	H-NoNeck-F H-NoNeck-P	H-Neck-P N-Neck-P	H-Neck-F H-Neck-P	H-NoNeck-F N-NoNeck-F	H-Neck-P N-Neck-P
N-Neck-F N-Neck-P	N-Neck-F N-Neck-P	H-Neck-F H-Neck-P	H-Neck-F H-NoNeck-F	H-NoNeck-P N-NoNeck-P	H-NoNeck-P N-NoNeck-P
N-Neck-P N-NoNeck-P		N-Neck-F N-Neck-P	H-Neck-P H-NoNeck-P	H-Neck-F H-Neck-P	H-Neck-F H-Neck-P
			N-Neck-F N-NoNeck-F	N-Neck-F N-Neck-P	N-Neck-F N-Neck-P
			N-Neck-P N-NoNeck-P	N-NoNeck-F N-NoNeck-P	N-NoNeck-F N-NoNeck-P
				H-Neck-P H-NoNeck-P	H-Neck-F H-NoNeck-F
				N-Neck-P N-NoNeck-P	H-Neck-P H-NoNeck-P
					N-Neck-F N-NoNeck-F
					N-Neck-P N-NoNeck-P

CHAPTER 6

DEVELOPMENT OF THE STAR EVALUATION SYSTEM FOR ASSESSING BICYCLE HELMET PROTECTIVE PERFORMANCE

ABSTRACT

Cycling is a leading cause of mild traumatic brain injury in the US. While bicycle helmets help protect cyclists who crash, limited biomechanical data exist differentiating helmet protective capabilities. This paper describes the development of a bicycle helmet evaluation scheme based in real-world cyclist accidents and brain injury mechanisms. Thirty helmet models were subjected to oblique impacts at six helmet locations and two impact velocities. The Summation of Tests for the Analysis of Risk (STAR) equation, which condenses helmet performance from a range of tests into a single value, was used to summarize measured linear and rotational head kinematics in the context of concussion risk. STAR values varied between helmets (10.9-25.3), with lower values representing superior protection. Road helmets produced lower STAR values than urban helmets. Helmets with slip planes produced lower STAR values than helmets without. This bicycle helmet evaluation protocol can educate consumers on the relative impact performance of various helmets and stimulate safer helmet design.

INTRODUCTION

Concussion, a mild traumatic brain injury (mTBI), has gained a national and international spotlight as long-term detrimental sequelae of repeated mTBI are brought to the public's eye [1,2]. Studies estimate that up to 3.8 million sport-related concussions occur each year in the United States [3]. While most of the research and public awareness surrounding concussive injury in sports focuses on football, injury surveillance systems indicate that cycling is among the leading causes of sport- or recreation-related concussions treated in the US [4]. Cycling has increased in popularity due to its many health and environmental benefits [5], with approximately 103.7 million Americans ages three and older having ridden a bicycle in 2015 [6]. Its increasing popularity is paralleled by increasing injury rates, accounting for an estimated $24.4 billion in US healthcare costs in 2013 [6-8]. Fortunately, helmet use has been demonstrated to reduce risk of head injury for cyclists involved in a crash [9-11].

Present safety standards related to head injury, including those for bicycle helmets, aim to reduce risk of catastrophic injury or death by placing a limit on headform linear acceleration (or other linear acceleration-derived metrics) during helmet impact testing. The Consumer Product Safety Commission (CPSC) standard is the mandatory standard for bicycle helmets in the US [12], and dictates that helmets must limit peak linear acceleration (PLA) to less than 300 g – a level associated with >50% risk of skull fracture or severe brain injury [13]. Linear acceleration-derived metrics used in standards are generally based on early human cadaver and animal testing. As brain injury was often observed in instances of skull fracture, it was deduced that brain injury could also be predicted by linear acceleration [14]. However, research has since suggested that the mechanisms of mTBI are more complex than can be described by linear acceleration alone, and that head rotation plays a large role in producing injury [15]. Linear acceleration has been correlated to transient intracranial pressure gradients resulting in focal injury, while rotational

velocity or acceleration has been correlated to shearing of the brain tissue resulting in diffuse injury [15-17]. Real-world head impacts involve both linear and rotational components, and metrics that include both have been shown to be good predictors of concussion [18,19].

The CPSC standard measures impact linear accelerations during drop tests using a single linear accelerometer at the center of gravity (CG) of a magnesium half-headform [12]. The test setup is constrained to linear motion during impact and does not reflect the nature of head impact rotations that a cyclist might experience. A cyclist's head typically approaches the impact surface at an angle between 30 and 60° during an accident, producing an oblique impact [20-22]. Standards specify drop tests in a direction normal to the impact surface. Use of an oblique impact test rig with a biofidelic headform capable of measuring of both linear and rotational kinematics would enhance assessment of a helmet's ability to reduce risk of concussion. Several such test rigs have already been developed for bicycle helmet testing [23-25].

Despite standards addressing risk of catastrophic head injury and the strides taken towards assessing helmet efficacy in reducing milder brain injury risk, limited comparative data are available to consumers indicating which bicycle helmets afford better protection. Existing objective impact data comparing helmets are either limited to standards testing or evaluate a relatively small subset of helmets on the US market [24-27]. While most helmets are designed with similar materials, including a traditional polycarbonate shell and expanded polystyrene (EPS) liner that permanently crushes and absorbs energy upon impact, previous research has demonstrated considerable differences in the ability of commercially-available helmets to reduce head injury risk [24-27]. To help reduce incidence of concussion in cycling and to stimulate improved helmet design for both mild and severe injury, consumers should have access to data differentiating helmet performance that is informed by real-world impact conditions and injury mechanisms.

The Summation of Tests for the Analysis of Risk (STAR) method is a biomechanical-based helmet evaluation protocol that quantifies the ability of individual helmet models to reduce concussion risk. This evaluation scheme has previously been employed for football and hockey helmets [28,29] and operates on two fundamental principles. First, a battery of laboratory tests informed by field-driven impact data are conducted, and test results are weighted based on how frequently the given impact may occur on the field. Second, measured linear and rotational kinematics are related to injury risk such that helmets that more effectively reduce kinematics produce lower concussion risks. These principles are supported by a retrospective study that found lower on-field concussion rates associated with a football helmet that better-reduced laboratory head impact kinematics in comparison to a helmet that produced higher kinematics [30]. The purposes of the present study are to describe the development of a similar STAR evaluation scheme for bicycle helmets, to explore the shape it takes when applied to a large array of bicycle helmets on the US market, and to assess how helmet design influences impact performance.

METHODS

Impact Testing

A custom oblique impact drop tower was used to conduct STAR testing (Fig. 6.1). A helmeted headform is dropped onto a 45° steel anvil to generate normal and tangential incident velocities. This angle falls central to a range of reported cyclist head impact angles [20-22]. Sandpaper was adhered to the anvil surface to simulate road friction (80 grit, in accordance with motorcycle helmet standards [31]), and was replaced after every fourth test. Prior to each test, a medium National Operating Committee on Standards for Athletic Equipment (NOCSAE) headform was fitted with a helmet so that the rim fell 6 cm above the basic plane (2.5 cm above the brow line) and tightened according to manufacturer recommendations. The helmeted headform was then positioned on a support ring constrained to the drop tower and secured in place using a lever arm, which released

just prior to impact. The support ring passed around the outside of the anvil upon impact, allowing the headform to separate from the ring as it contacted the anvil. No anthropomorphic test device (ATD) neck or effective torso mass was used in this testing, as previous work has suggested that oblique impacts may subject the neck to considerable axial loading, a scenario known to present limited biofidelity for common ATD necks [32-34]. It has been further suggested that human necks have minimal effect on initial head impact response during head-first impacts [34].

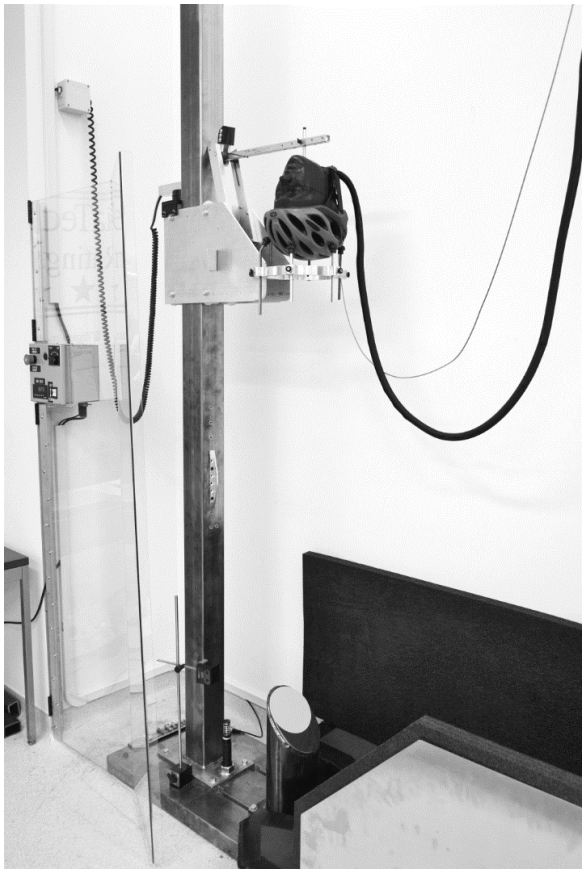

Figure 6.1. Custom impact rig used for STAR testing. A helmeted headform is dropped onto an angled anvil to generate an oblique impact.

Impact conditions were selected to reflect those common in cyclist head impact scenarios. Unlike football and hockey STAR, where volunteer data collected during the respective sports were used

to inform common head impact conditions, cyclist head impacts are not voluntary events, and thus impact conditions were instead determined retroactively through helmet damage replication studies and computational simulation studies [20-22,35,36]. Six impact locations dispersed around the helmet were selected to assess helmet performance over a range of impact scenarios (Fig. 6.2). Locations 2 and 5 fall at the helmet rim, a commonly impacted area that is not considered in standards testing [20-22,35-37]. Each location was set so that impact centers fell >120 mm apart, which the CPSC standard suggests is sufficient distance to prevent the damage profile from one test affecting other test locations [12]. To ensure precision and consistency in impacting each location, a dual-axis inclinometer was mounted to the base of the NOCSAE headform during positioning and was used to mark headform orientation for each location.

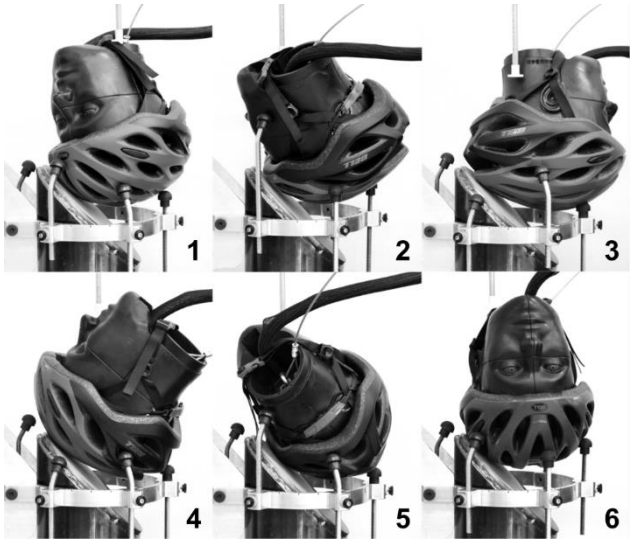

Figure 6.2. Impact locations 1-6. Locations 1, 2, and 6 represent body-driven impacts, in which the head leads the body, locations 3 and 5 represent skidding-type impacts, and location 4 represents an impact from flipping over the handlebars.

Impact velocities were assigned based on a digitization of data from helmet damage replication studies [35,36], which recreated damage to accident-involved helmets using standards test rigs,

then recorded normal velocities required to replicate the damage. The 50th and 90th percentile velocities of these data (3.4 and 5.3 m/s, respectively) were selected for testing in order to evaluate helmet performance at both average and more severe impact energies. It has been hypothesized that liner crush distance is a function of normal impact velocity [38], so resultant velocities of 4.8 and 7.4 m/s were selected in order to maintain the target normal velocities using the 45° anvil. Two trials of each of the 12 location-velocity configurations were conducted for every helmet model evaluated. As bicycle helmets crush permanently upon impact, a new helmet sample was used for subsequent impacts to the same location, necessitating four samples per helmet model. Each sample was tested in order of impact locations (location 1 tested first, 6 tested last), with three low-velocity and three high-velocity impacts tested per sample.

Linear and rotational kinematics were recorded at 20 kHz during each test using three linear accelerometers (Endevco 7264B-2000, Meggitt Sensing Systems, Irvine, CA) and a tri-axis angular rate sensor (ARS3 PRO-18K, DTS, Seal Beach, CA) at the headform CG. Linear acceleration was filtered according to SAE J211 using a channel frequency class (CFC) of 1000, while rotational velocity was filtered at a CFC of 175. The latter CFC has been used in previous studies and has been shown to optimize rotational response curves relative to those produced by the more conventional nine accelerometer array (9AA) in oblique impacts [33,39]. An ARS was selected over a 9AA because it is more readily compatible with the small instrumentation channel in the NOCSAE headform. Resultant peak linear acceleration (PLA) and peak rotational velocity (PRV) were then averaged across the two trials at each location-velocity configuration and used to estimate resulting risk of concussion, which was then implemented into the STAR equation.

Bicycle STAR Equation

The STAR equation summarizes helmet performance from a range of tests into a single value.

Bicycle STAR follows the general guidelines of the previously-published football and hockey STAR equations [28,29]. with slight modifications (Eq. 6.1). An exposure term, E, weights each impact configuration based on its likelihood of occurring in real-world accident scenarios. Each impact configuration is comprised of a location, *L*, and velocity, *V*. Impact locations were equally weighted to ensure helmets are not under-designed in any one location. Impact velocities were weighted using a cumulative distribution function (CDF) of the damage replication data used to select velocities (Fig. 6.3). Weightings were determined based on the number of impacts that might occur within ±0.5 m/s of the target velocities according to the CDF. Per 100 total head impacts, 38.0 impacts were found to lie in the 3.4±0.5 m/s range and 9.4 impacts in the 5.2±0.5 m/s range. The number of impacts were split evenly among the 6 locations to yield final weightings of 6.33 for each low-speed impact and 1.57 for each high-speed impact.

$$Bicycle\ STAR = \sum_{L=1}^{6} \sum_{V=1}^{2} E(L,V) * R(a,\omega) \quad (6.1)$$

The other major term in the STAR equation is concussion injury risk, R, which is a function of PLA, *a*, and PRV, *ω*. The PLA and peak rotational acceleration (PRA)-based bivariate risk function used in hockey STAR was generated using logistic regression analysis of head impact data collected from high school and collegiate football players, and accounts for underreporting of concussion [19]. To obtain the risk function for bicycle STAR, this function was modified using a linear relationship between PRV and PRA that was previously published based on six degree-of-freedom sensor data in football head impacts [40]. PRV is an attractive metric for use in the injury risk function as it involves less inherent measurement variability than PRA, allows for duration of loading to be accounted for, and has been shown to be among the best correlates to strain development in the brain leading to concussive injury [17,41]. Equation 6.2 shows the updated risk function with the linear relationship between PRV and PRA carried through.

$$R(a,\omega) = 1/(1 + e\text{^}(-(-10.2 + 0.0433a + 0.19686\omega - 0.0002075a\omega)) \quad (6.2)$$

For each impact configuration, risk was calculated using average PLA and PRV measurements and then multiplied by its respective exposure weighting, then weighted risks were summed to yield a total STAR value for each helmet model (Eq. 6.1). Each helmet's STAR value represents an estimated incidence of concussion from the given array of real-world impact conditions.

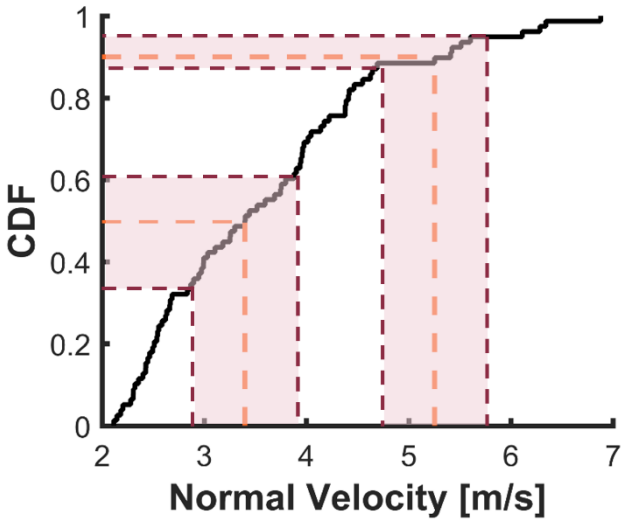

Figure 6.3. Cumulative distribution function (CDF) of data from helmet damage replication studies. STAR test velocities were chosen as the 50th and 90th percentiles (3.4 and 5.2 m/s normal velocities). A 0.5 m/s range from each velocity was mapped to the CDF (shaded region), and the number of impacts occurring within that range was used as weightings for the STAR equation.

Helmet Models

A set of 30 CPSC-certified bicycle helmet models were selected for STAR testing (Table 6.1). These helmets were determined to be among the most popular models in the US based on market trends and manufacturer feedback. Fourteen brands were represented. Manufacturer suggested retail price (MSRP) at the time of purchase ranged from $10-250, and styles were dichotomized into road and urban categories. Road helmets contain an elongated, aerodynamic shape and generally more vents, while urban helmets are characterized by a more rounded shape with less

venting and thicker shells. Many of the helmets contained Multi-directional Impact Protection System (MIPS) technology, a patented helmet insert designed to create a slip-plane layer between the wearer's head and the rest of the helmet during impact. The intended purpose of the slip plane is to reduce rotational forces experienced by the head and thereby the resulting brain injury risk. Visors and other extraneous attachments were removed prior to testing, and internal helmet features (i.e. retention system, MIPS) were re-secured between tests when necessary.

Statistical Analysis

Kinematics variance across trials one and two was assessed per impact configuration for each helmet as the range in PLA or PRV divided by the mean. The influence of impact location and velocity on overall kinematics and resulting injury risks were assessed using ANOVA with Tukey's HSD post hoc tests. Comparisons of STAR values based on helmet style and MIPS were assessed using unbalanced ANOVA (type III SS), while trends between STAR and helmet price were investigated using correlation analysis.

Possible variance in a helmet's STAR value was investigated by propagating the variance in kinematics through the STAR calculation. In determining a final STAR value, risk is calculated by first averaging PLA and PRV across the two trials per configuration, then plugging these average values into the risk function. To assess variance, risks were instead calculated for each individual trial using the PLA and PRV results specific to that trial, resulting in two different risk values per impact configuration. STAR was then recalculated using only one of the two risk values for each configuration, then calculated again using the other. Every possible permutation of first or second risk values for all twelve configurations was evaluated to yield possible STAR outcomes (2^{12} = 4096 possible permutations per helmet). Variance in STAR was assessed by evaluating the 95th percentile confidence intervals (95% CI) of these permutation sets.

Table 6.1. Helmet models selected for STAR testing. MSRP reflects the price provided by manufacturer websites at the time of purchase.

Make	Model	MSRP* [$]	Style	MIPS
Bell	Division	40	Urban	No
Bell	Draft MIPS	60	Road	Yes
Bell	Reflex	10	Road	No
Bell	Stratus MIPS	150	Road	Yes
Bern	Brentwood	70	Urban	No
Bern	Watts	60	Urban	No
Bontrager	Ballista MIPS	200	Road	Yes
Bontrager	Quantum MIPS	100	Road	Yes
Bontrager	Solstice	40	Road	No
Electra	Electra Helmet	70	Urban	No
Garneau	Le Tour II	50	Road	No
Garneau	Raid MIPS	120	Road	Yes
Giro	Foray MIPS	85	Road	Yes
Giro	Revel	45	Road	No
Giro	Savant	100	Road	No
Giro	Sutton MIPS	100	Urban	Yes
Giro	Synthe	250	Road	No
Kali	City	125	Urban	No
Lazer	Genesis	100	Road	No
Nutcase	Street	70	Urban	No
POC	Octal	200	Road	No
Schwinn	Flash	30	Road	No
Schwinn	Thrasher	14	Road	No
Scott	ARX Plus	100	Road	Yes
Smith	Overtake	163	Road	No
Specialized	Centro	60	Road	No
Specialized	Chamonix MIPS	75	Road	Yes
Specialized	Evade II	250	Road	No
Specialized	Prevail II	225	Road	No
Triple 8	Dual Certified MIPS	75	Urban	Yes

RESULTS

The 30 helmets evaluated produced a wide range in kinematic results across all impact configurations (Fig. 6.4). PLA averaged 114.0±22.8 g at 4.8 m/s and 183.4±33.5 g at 7.3 m/s, while PRV averaged 22.8±4.2 rad/s at 4.8 m/s and 33.9±5.9 rad/s at 7.3 m/s. Location 3 was associated with significantly lower PLA values and significantly higher PRV values than most other locations ($p<0.05$). Impact duration was comparable across velocities, averaging 9.7±1.3 ms and 9.4±1.7 ms at the low and high velocities, respectively. Kinematic measurements also varied considerably within single impact configurations, producing wide distributions of concussion risk (maximum range of 76% risk within a single configuration). Distributions of risk were greater at 4.8 m/s, where risk averaged 24.9±15.8% with an average range of 46% risk per location, compared to 7.3 m/s, where risk averaged 92.8±8.2% with an average range of 28% risk per location. Location 2 produced lower risk values than most other impact locations ($p<0.05$).

Variance in PLA between trials one and two averaged 4.6±4.1%, ranging 5.3±4.7 g and 8.0±6.9 g at 4.8 and 7.3 m/s, respectively. PRV variance averaged 3.9±4.1%, ranging 0.9±0.9 rad/s and 1.2±1.1 rad/s at 4.8 and 7.3 m/s. Variance in PLA and PRV were not significantly greater at either impact velocity (t-test, $p>0.18$), nor was PLA variance greater at later impact locations (correlation test, $R=0.03$, $p=0.55$). PRV variance increased significantly with later locations, although the correlation was not strong ($R=0.26$, $p<0.01$). Individual helmet model variance averaged 2.9-8.4% for PLA and 1.8-8.9% for PRV. The Ballista MIPS helmet produced the highest variance across all configurations for both PLA (8.4±6.3%) and PRV (8.9±7.6%).

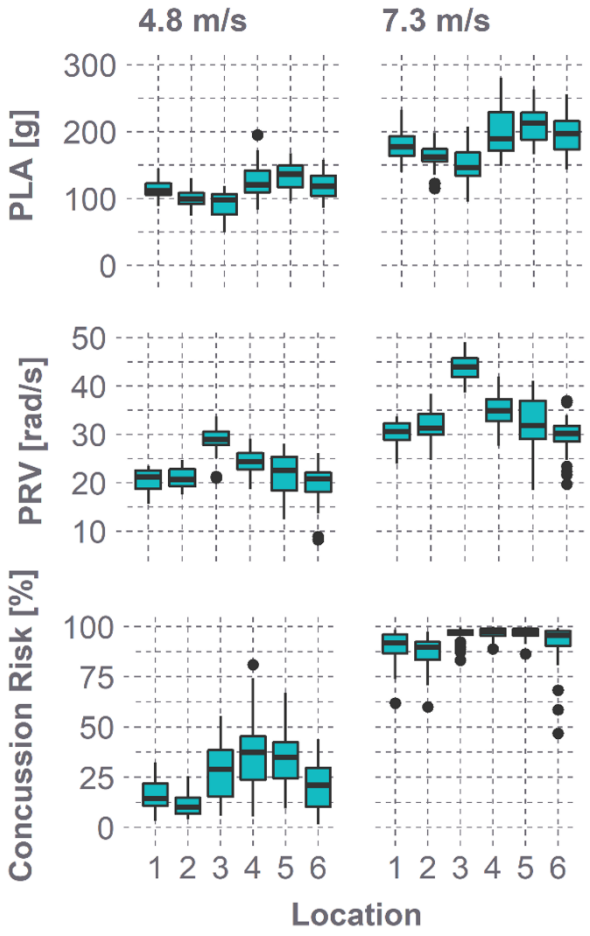

Figure 6.4. PLA, PRV, and concussion risk distributions for each impact configuration. Concussion risk was computed using a bivariate function including both PLA and PRV.

Helmets that better reduced impact kinematics generated lower risk estimates, which in turn produced lower STAR values (Fig. 6.5). STAR ranged from 10.9 (95% CI: [10.4, 11.5]) for the Ballista MIPS to 25.3 (95% CI: [24.1, 26.4]) for the Watts (Fig. 6.6). On average, the 95% CI range was 8.9±3.6% of a helmet's computed STAR value. Across all helmets, both impact velocities contributed evenly to the summed STAR value; weighted risks from 4.8 m/s impacts accounted for 50.3±8.9% of the STAR value, and weighted risks from 7.3 m/s impacts accounted for 49.7±8.9%. Impact locations contributed relatively evenly to STAR as well, with weighted risk contributions ranging from 11.6±2.4% at location 2 to 21.2±3.2% at location 4.

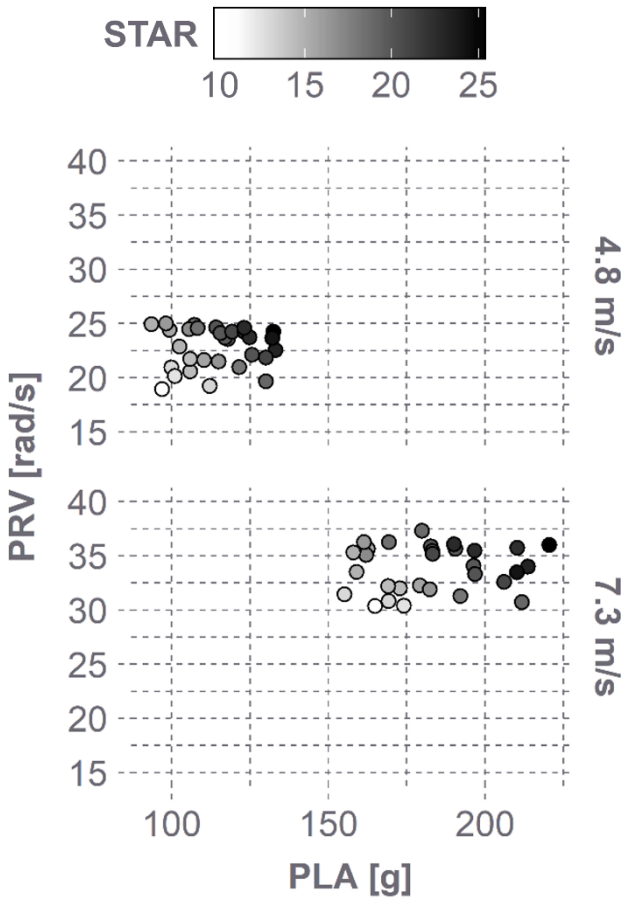

Figure 6.5. Effect of kinematic results on STAR values. Shown are PLA and PRV results averaged across impact locations for every helmet. Each helmet is represented by one circle per velocity, with its shade determined by its overall STAR value (e.g. the Ballista MIPS produced the lowest STAR value of 10.9 and is represented by a white circle near the lower left corner of each plot). STAR values increase with increasing kinematics.

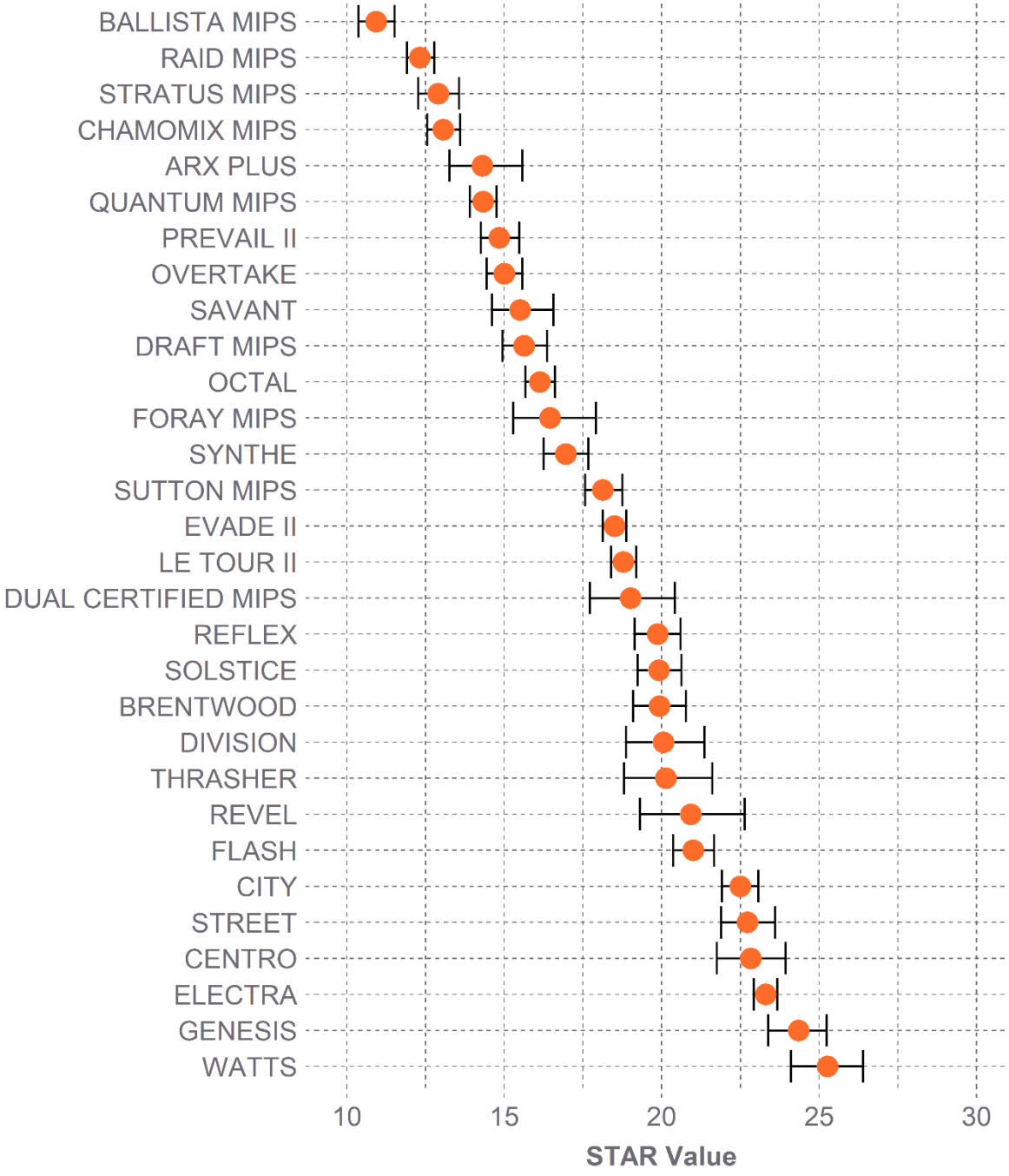

Figure 6.6. Range in STAR values across all helmet models. Lower STAR values indicate reduced incidence of concussion, and thereby enhanced protection. Error bars represent 95% CI ranges.

Of the 14 brands represented in this set of 30 helmets, no single brand dominated the higher or lower ends of the STAR results. Urban style helmets produced greater STAR values on average than road style helmets ($p<0.01$), with average STAR values of 21.4±2.4 and 17.0±3.6, respectively (Fig. 6.7). MIPS helmets produced lower STAR values than non-MIPS helmets ($p<0.01$), averaging 14.7±2.6 versus 19.9±3.1. There was no significant interaction between helmet style and MIPS ($p=0.53$). Road helmets with MIPS generated the lowest STAR values overall (13.7±1.8). Additionally, STAR values showed a slight negative correlation with MSRP, suggesting that more expensive helmets were associated with slightly greater protection. Although this trend was significant ($p=0.01$), considerable variance was observed ($R^2=0.22$), with several lower-priced helmets receiving low STAR values and vice versa.

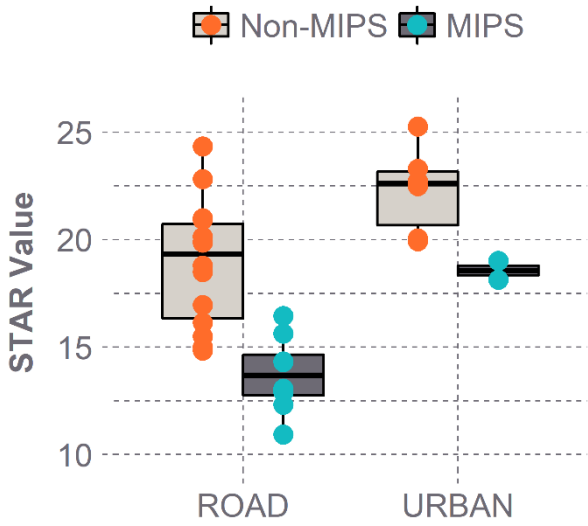

Figure 6.7. STAR value distributions based on style and MIPS. Road helmets with MIPS produced the lowest STAR values and thereby offer the greatest protection. MIPS helmets generated lower STAR values than non-MIPS helmets for both styles.

DISCUSSION

The present study details the development of an objective evaluation protocol for bicycle helmets and applies this protocol to 30 popular helmet models in the US. Impacts at the two velocities and six locations generated a wide range in kinematics. As expected, PLA and PRV were higher at 7.3 m/s than at 4.8 m/s, producing greater concussion risks as well. Location 3 was associated with notably lower PLA and higher PRV than other locations. This location is furthest offset from the CG of the head for many helmets due to aerodynamic elongation in this region, which suggests more EPS is present to mitigate normal forces and thereby PLA. Simultaneously, the greater distance from the CG may create a greater moment arm, increasing rotational kinematics. Because lower PLA and higher PRV values effectively offset in the bivariate concussion risk function, location 3 produced middle-ground risks compared to other locations. Conversely, although location 2 did not average the lowest kinematics of all locations, both PLA and PRV for this location were consistently low enough to produce significantly lower risks. Location 2 falls at the helmet rim and is below the testable region in standards. The present results suggest that this location offers suitable, if not superior, impact protection. However, previous work has shown that impacting this region at higher normal velocities (such as the CPSC test velocity) may cause some helmets to bottom out and produce extreme risk of injury [26].

Kinematic results varied considerably between helmets, producing large differences in concussion risk and STAR values spanning from 10.9 to 25.3. A helmet's STAR value estimates the number of concussions that might occur out of the total number of simulated impacts. Exposure was determined based on the percentage of impacts from helmet damage replication literature that fell within ±0.5 m/s of the target velocities. These ranges accounted for a combined 47.4% of impacts, suggesting that 47.4 out of 100 impacts were simulated. The helmet with the best STAR value (Ballista MIPS) might result in only 10.9 concussions out of these 47.4 impacts.

This low STAR value reflects lower overall kinematic results; the Ballista MIPS produced average PLAs of 97.0±23.5 g and 164.9±25.7 g at 4.8 and 7.3 m/s, respectively, and average PRVs of 18.9±5.4 rad/s and 30.4±9.5 rad/s at 4.8 and 7.3 m/s. Conversely, the Watts, which generated the highest STAR value of 25.2, produced PLAs of 132.4±19.5 g and 220.5±27.5 g at 4.8 and 7.3 m/s, respectively, and PRVs of 24.3±2.6 rad/s and 36.0±4.2 rad/s at 4.8 and 7.3 m/s.

On average, impact velocities and locations contributed relatively equal amounts to a helmet's STAR value. Location 2 contributed the least to STAR due to lower concussion risks associated with this location. Although each velocity generated similar weighted risks when averaged across helmets, of particular interest was whether a tradeoff in performance at the two velocities existed for individual helmets. Bicycle helmets are designed to protect against the severe conditions imposed by standards, and it is often questioned whether ensuring that a helmet offers superior protection at more severe energies necessitates a compromise of offering inferior protection at lower energies, or vice versa. To investigate this, each helmet's average PLA and PRV were determined at both 4.8 and 7.3 m/s, and Spearman correlations were assessed across velocities (Fig. 6.8). Strong correlations were observed ($\rho>0.93$, $p<0.01$), suggesting that helmets that reduced impact kinematics better at the high velocity also reduced kinematics better at the low velocity, and that no tradeoff in performance is evident at the energy levels assessed herein for these particular helmet models.

Trends between helmet design features and STAR were also assessed. More expensive helmets were associated with lower STAR values than less expensive ones. This trend could be attributed to the higher price often associated with MIPS helmets. However, removing MIPS helmets and repeating the correlation analysis between STAR and MSRP revealed a slightly stronger, equally significant trend (non-MIPS: $R=-0.56$, $p=0.01$, all helmets: $R=-0.47$, $p=0.01$). This suggests that

more expensive helmets may offer enhanced protection, although considerable scatter was observed in these data. Style and MIPS also had significant effects on STAR, with road MIPS helmets producing the lowest STAR values. Style mainly affected STAR via its influence on PLA. Urban helmets produced higher PLAs than road helmets across all locations, particularly at locations 3 and 4 (>25 g average difference). The large differences in PLA at these locations may relate to their distance from the helmet rim. For stiffer shells, higher energy is required to buckle the shell and compress the EPS at locations further from the rim or venting [42]. As most urban helmets contain thicker shells and less venting than road helmets, shell stiffness likely has more pronounced location effects for these helmets. Style had less of an effect on PRV. This was true at both velocities and all locations, with the exception of location 5, where urban helmets generated higher PRVs (~3 rad/s). Interactions between style and MIPS did not have significant effects on PLA or PRV ($p>0.13$).

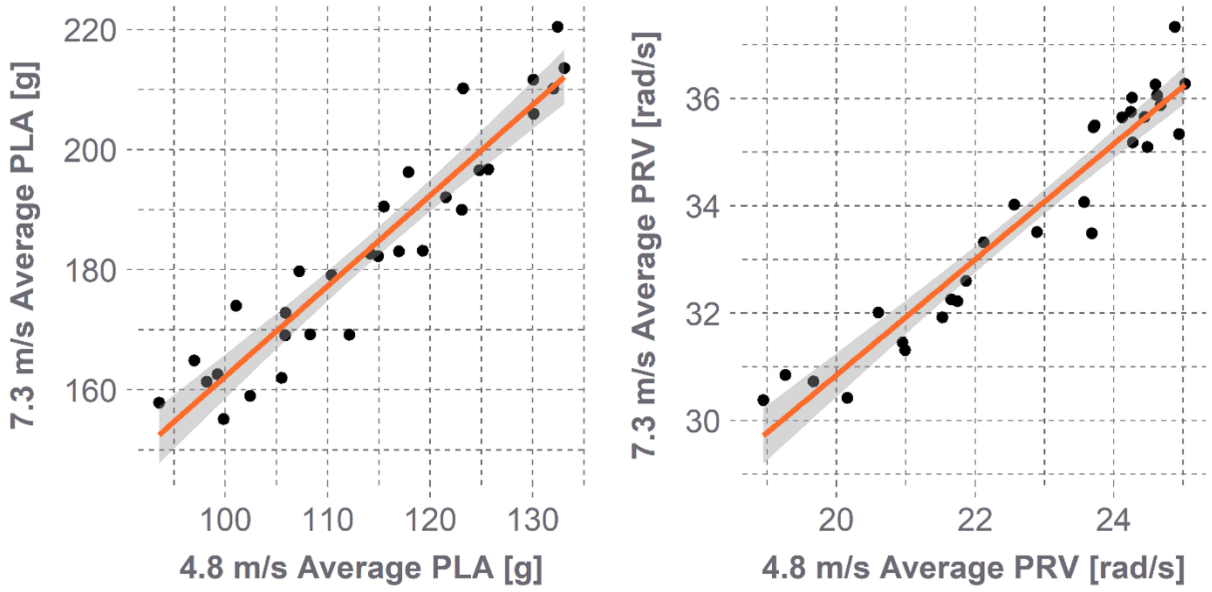

Figure 6.8. Average PLA (left) and PRV (right) values per helmet at 7.3 m/s versus 4.8 m/s. Each point represents one helmet's average values. Shaded regions represent the 95% prediction

interval. Strong correlations were observed, suggesting that a helmet's ability to reduce impact kinematics relative to other helmets is similar at both velocities.

The effects of MIPS on STAR were primarily related to differences in PRV across MIPS and non-MIPS helmets. PRV for MIPS helmets was ~14% lower across all locations at 4.8 m/s and ~11% lower at 7.3 m/s. MIPS-location interactions were not significant ($p = 0.08$), nor were MIPS-velocity interactions ($p=0.50$), suggesting MIPS reduced PRV similarly across all locations and at both velocities. MIPS helmets also produced significantly lower PLA than non-MIPS helmets ($p<0.01$), although differences were small. These results suggest that slip-planes can be an effective technology in helmets by reducing rotational impact kinematics. Another study comparing impact performance across bicycle helmet models using a similar test setup also found MIPS to be effective [27]. Conversely, an additional study demonstrated higher PRA for MIPS helmets compared to non-MIPS helmets [25]. The latter study used a different test setup incorporating a Hybrid III (HIII) neck. Only two MIPS helmets were included, and both produced greater PLA values as well, which may suggest that additional factors specific to those helmets contributed to reduced impact protection overall.

There are several limitations associated with the present study. First, although the impact configurations selected for STAR testing are comprehensive and based in real-world data, only a finite number of impact scenarios can be evaluated for practicality purposes. There likely exist other scenarios in which each helmet offers varying levels of protection that are not captured in the present testing. Second, the concussion risk function employed was derived from head impacts to football players, who may have differing characteristics than the general population [43]. The instrumentation used to collect this data also has associated limitations in measuring rotational kinematics [40]. and the function used herein is based on a transformation of this data

based on published trends between PRV and PRA, which may limit its accuracy. Nonetheless, the dataset used to generate this function is one of the largest comprehensive databases of concussive versus non-concussive impacts. It therefore provides a solid basis for conducting a comparative assessment by ultimately assigning helmets that produce lower head impact kinematics a better score than helmets that produce higher kinematics.

Additional limitations pertain to the testing boundary conditions and the limited sample size of helmets. Testing was conducted without a neck, as several studies have suggested that the commonly-used HIII neck is overly stiff in axial compressive loading [32], and the impact locations herein would involve varying degrees of this nature of loading. However, other similar oblique impact studies have utilized a HIII neck [11,33,34], which may offer additional insight into realistic helmet performance in certain scenarios despite the neck's limited biofidelity. Further, the sandpaper-coated steel anvil used for impacts is likely overly stiff compared to typical roadway surfaces [44], which may have inflated results. Helmets were also tested without extraneous attachments such as visors that could affect resulting kinematics [45]. Additionally, categorizing helmets by style resulted in small sample sizes for some categories, limiting the generalizability of results. For instance, there were only two urban helmets with MIPS. Although a few of the helmets were marketed as having a style meant for a particular type of cycling (i.e. mountain biking, aero), these helmets were also categorized into road or urban categories to avoid further reduction of sample sizes. Additional models should be tested to further assess trends between helmet design and impact protection.

CONCLUSIONS

Presently, consumers have limited access to objective biomechanical data differentiating bicycle helmet impact performance. As bicycle helmets are a safety feature, such information should be

made available to facilitate educated purchasing decisions. The bicycle STAR evaluation system provides a basis for disseminating helmet performance data that is founded in common cyclist head impact conditions and relevant injury mechanisms. A large range in STAR values across 30 popular helmets on the US market was found, enabling assessment of the influence of helmet design features on helmet performance. Evaluation protocols such as these can supplement standards, which ensure helmets reduce injury risk in severe accident scenarios, by indicating helmet protective capabilities in the most common impact conditions as well. This serves as a challenge to manufacturers to develop innovative helmet designs that push the boundaries of improved protective capabilities. In this way, the bicycle STAR evaluation system has the potential to provide knowledge to consumers regarding helmet safety and can continually encourage the design of safer helmets.

REFERENCES

1. Gavett, B.E., Stern, R.A., and McKee, A.C. Chronic traumatic encephalopathy: a potential late effect of sport-related concussive and subconcussive head trauma. *Clin. Sports Med.*, 2011. 30(1): p. 179-188
2. Omalu, B.I., DeKosky, S.T., et al. Chronic traumatic encephalopathy in a National Football League player. *Neurosurgery*, 2005. 57(1): p. 128-134
3. Daneshvar, D.H., Nowinski, C.J., McKee, A.C., and Cantu, R.C. The epidemiology of sport-related concussion. *Clin. Sports Med.*, 2011. 30(1): p. 1-17
4. Coronado, V.G., Haileyesus, T., et al. Trends in Sports- and Recreation-Related Traumatic Brain Injuries Treated in US Emergency Departments: The National Electronic Injury Surveillance System-All Injury Program (NEISS-AIP) 2001-2012. *J. Head Trauma Rehabil.*, 2015. 30(3): p. 185-197
5. Wen, L.M. and Rissel, C. Inverse associations between cycling to work, public transport, and overweight and obesity: findings from a population based study in Australia. *Prev. Med.*, 2008. 46(1): p. 29-32
6. Fischer, P. A Right to the Road: Understanding and Addressing Bicyclist Safety, G.H.S. Association, Editor. 2017, Governors Highway Safety Association.
7. Sanford, T., McCulloch, C.E., and Callcut, R.A. Bicycle trauma injuries and hospital admissions in the United States, 1998-2013. *Jama*, 2015. 314(9): p. 947-949
8. Gaither, T.W., Sanford, T.A., et al. Estimated total costs from non-fatal and fatal bicycle crashes in the USA: 1997-2013. *Inj. Prev.*, 2018. 24(2): p. 135-141
9. Olivier, J. and Creighton, P. Bicycle injuries and helmet use: a systematic review and meta-analysis. *Int. J. Epidemiol.*, 2017. 46(1): p. 278-292
10. Thompson, D.C., Rivara, F.P., and Thompson, R. Helmets for preventing head and facial injuries in bicyclists. *Cochrane Database Syst. Rev.*, 2010(2): p. CD001855

11. McIntosh, A.S., Lai, A., and Schilter, E. Bicycle helmets: head impact dynamics in helmeted and unhelmeted oblique impact tests. *Traffic Inj. Prev.*, 2013. 14(5): p. 501-8
12. CPSC. Safety Standard for Bicycle Helmets Final Rule (16 CFR Part 1203). 1998, United States Consumer Product Safety Commission. p. 11711-11747.
13. Mertz, H.J., Irwin, A.L., and Prasad, P. Biomechanical and scaling bases for frontal and side impact injury assessment reference values. *Stapp Car Crash J.*, 2003. 47: p. 155-88
14. Hardy, W.N., B., K.T., and King, A.I. Literature Review of Head Injury Biomechanics. *Int. J. Impact Eng.*, 1994. 15(4): p. 561-586
15. King, A.I., Yang, K.H., Zhang, L., Hardy, W., and Viano, D.C. Is Head Injury Caused by Linear or Angular Acceleration?, in *IRCOBI Conference*. 2003: Lisbon, Portugal. p. 1-12.
16. Gennarelli, T.A., Thibault, L.E., and Ommaya, A.K. Pathophysiologic responses to rotational and translational accelerations of the head. *SAE Technical Paper Series*, 1972. 720970: p. 296-308
17. Kleiven, S. Predictors for traumatic brain injuries evaluated through accident reconstructions. *Stapp Car Crash J.*, 2007. 51: p. 81-114
18. Zhang, L., Yang, K.H., and King, A.I. A proposed injury threshold for mild traumatic brain injury. *J. Biomech. Eng.*, 2004. 126(2): p. 226-236
19. Rowson, S. and Duma, S.M. Brain injury prediction: assessing the combined probability of concussion using linear and rotational head acceleration. *Ann. Biomed. Eng.*, 2013. 41(5): p. 873-82
20. Verschueren, P. Biomechanical analysis of head injuries related to bicycle accidents and a new bicycle helmet concept, in *Faculteit Ingenieurswetenschappen Departement Werktuigkunde Afdeling Biomechanica en Grafisch Ontwerpen*. 2009, Katholieke Universiteit Leuven: Leuven, Belgium.
21. Bourdet, N., Deck, C., et al. In-depth real-world bicycle accident reconstructions. *Int. J. Crashworthiness*, 2014. 19(3): p. 222-232
22. Bourdet, N., Deck, C., Carreira, R.P., and Willinger, R. Head impact conditions in the case of cyclist falls. *Proc. Inst. Mech. Eng. P*, 2012. 226(3-4): p. 282-289
23. Milne, G., Deck, C., et al. Bicycle helmet modelling and validation under linear and tangential impacts. *Int. J. Crashworthiness*, 2014. 19(4): p. 323-333
24. Mills, N.J. and Gilchrist, A. Oblique impact testing of bicycle helmets. *International Journal of Impact Engineering*, 2008. 35(9): p. 1075-1086
25. Bland, M.L., McNally, C., and Rowson, S. Differences in Impact Performance of Bicycle Helmets During Oblique Impacts. *J. Biomech. Eng.*, 2018. 140(9)
26. Bland, M.L., Zuby, D.S., Mueller, B.C., and Rowson, S. Differences in the protective capabilities of bicycle helmets in real-world and standard-specified impact scenarios. *Traffic Inj. Prev.*, 2018. 19(sup1): p. S158-S163
27. Stigson, H., Rizzi, M., Ydenius, A., Egnstrom, E., and Kullgren, A. Consumer Testing of Bicycle Helmets, in *IRCOBI Conference*. 2017, IRCOBI Conference: Antwerp, Belgium. p. 173-181.
28. Rowson, S. and Duma, S.M. Development of the STAR evaluation system for football helmets: Integrating player head impact exposure and risk of concussion. *Ann. Biomed. Eng.*, 2011. 39(8): p. 2130-40
29. Rowson, B., Rowson, S., and Duma, S.M. Hockey STAR: A Methodology for Assessing the Biomechanical Performance of Hockey Helmets. *Ann. Biomed. Eng.*, 2015. 43(10): p. 2429-2443
30. Rowson, S., Duma, S.M., et al. Can helmet design reduce the risk of concussion in football? Technical note. *J. Neurosurg.*, 2014. 120(4): p. 919-922

31. ECE. R-22.05: Uniform Provisions Concerning the Approval of Protective Helmets for Drivers and Passengers of Motorcycles and Mopeds. 1999, United Nations Economic Commission for Europe.
32. Sances, A.J., Carlin, F., and Kumaresan, S. Biomechanical analysis of head-neck force in Hybrid III dummy during inverted vertical drops. *Biomed. Sci. Instrum.*, 2002. 38: p. 459-464
33. Bland, M.L., McNally, C., and Rowson, S. Headform and Neck Effects on Dynamic Response in Bicycle Helmet Oblique Impact Testing, in *IRCOBI Conference*. 2018: Athens, Greece. p. 413-423.
34. Nelson, T.S. and Cripton, P.A. A New Biofidelic Sagittal Plane Surrogate Neck for Head-First Impacts. *Traffic Inj Prev*, 2010. 11(3): p. 309-319
35. Williams, M. The protective performance of bicyclists' helmets in accidents. *Accid. Anal. Prev.*, 1991. 23(2-3): p. 119-131
36. Smith, T.A., Tees, D., Thom, D.R., and Hurt, H.H. Evaluation and replication of impact damage to bicycle helmets. *Accid. Anal. Prev.*, 1994. 26(6): p. 795-802
37. Depreitere, B., Van Lierde, C., et al. Bicycle-related head injury: a study of 86 cases. *Accid. Anal. Prev.*, 2004. 36(4): p. 561-567
38. Mills, N.J. Critical evaluation of the SHARP motorcycle helmet rating. *Int. J. Crashworthiness*, 2010. 15(3): p. 331-342
39. Cobb, B.R., Tyson, A.M., and Rowson, S. Head acceleration measurement techniques: Reliability of angular rate sensor data in helmeted impact testing. *Proceedings of the Institution of Mechanical Engineers, Part P: Journal of Sports Engineering and Technology*, 2017. 232(2): p. 176-181
40. Rowson, S., Duma, S.M., et al. Rotational head kinematics in football impacts: an injury risk function for concussion. *Ann. Biomed. Eng.*, 2012. 40(1): p. 1-13
41. Hardy, W.N., Mason, M.J., et al. A study of the response of the human cadaver head to impact. *Stapp Car Crash J.*, 2007. 51: p. 17-80
42. Mills, N.J. Protective capability of bicycle helmets. *Br. J. Sports Med.*, 1990. 24(1): p. 55-60
43. Rowson, S., Bland, M.L., et al. Biomechanical Perspectives on Concussion in Sport. *Sports Med Arthrosc Rev*, 2016. 24(3): p. 100-7
44. Bonugli, E. The effects of dynamic friction in oblique motorcycle helmet impacts, in *Biomedical Engineering*. 2015, The University of Texas at San Antonio: Ann Arbor. p. 78.
45. Butz, R.C., Knowles, B.M., Newman, J.A., and Dennison, C.R. Effects of external helmet accessories on biomechanical measures of head injury risk: An ATD study using the HYBRIDIII headform. *J. Biomech.*, 2015. 48(14): p. 3816-3824

CHAPTER 7

A PRICE-PERFORMANCE ANALYSIS OF THE PROTECTIVE CAPABILITIES OF WHOLESALE BICYCLE HELMETS

ABSTRACT

Head injuries related to cycling are a common problem in the US and around the world. Although bicycle helmet use is an effective countermeasure against head injury, many cyclists choose not to wear one. One avenue for encouraging widespread helmet use is through community-driven helmet safety initiatives, which often offer helmet giveaways or subsidies. Wholesale bicycle helmet models are an attractive option for these programs given their low cost. However, the protective capabilities of these helmets during real-world accident conditions has previously been unexplored. The present study sought to investigate the impact performance of wholesale bicycle helmet models and to determine the relationship between helmet price and protective capabilities. Nine common wholesale helmet models were subject to the bicycle helmet Summation of Tests for the Analysis of Risk (STAR) methodology, which reflects realistic cyclist crash conditions and relevant injury mechanisms. Large differences in STAR values resulted across helmet models, ranging from 13.5 to 26.2. Lower STAR values indicate a lower predicted incidence of concussion. Price was not significantly associated with STAR value for the wholesale helmets, although incorporating these results into previous bicycle STAR results showed a slight negative trend between price and STAR value. Considerable scatter was associated with this trend, and the best-performing wholesale helmet produced one of the lowest overall STAR values for a price of $6.45. Helmet style was a superior predictor of STAR value, with multi-sport style helmets producing higher STAR values than bike style helmets. These results can guide helmet safety promotion organizers to distributing the safest wholesale bicycle helmet models.

INTRODUCTION

Cycling is a popular activity across all ages and around the world. In the US, 103.7 million persons over the age of 3 reported to have ridden a bicycle in 2015 [1]. However, cycling is not a risk-free activity. US hospital admissions due to cycling-related injuries have increased 120% from 1998 to 2013 [2], and there were 818 cyclist fatalities in 2015 alone [1]. These injuries are linked to considerable economic and societal burden, with costs for adults injured in a cycling-related accident estimated to total $24.4 billion in 2013 [3]. Among all cyclist injuries, the head represents one of the most commonly-injured body regions [4-6]. Concussion is among the most common diagnoses for patients presenting with cycling-related head injuries [4].

Bicycle helmet use has fortunately been shown to be an effective countermeasure for reducing head injury risk [5-11]. Nonetheless, helmet use is not universally adopted. While legislation related to helmet use is thought to be generally effective [12-14], only 21 states have enacted laws mandating helmet use for younger riders (often ages 15 and under), and no state laws require helmet use for adults [15]. Other efforts to promote helmet use include community-level helmet subsidy or give-away programs, which have shown increases in observed helmet wearing as a result [16,17]. Often, these community initiatives distribute helmets that were purchased from wholesale suppliers at a minimal expense. The price per individual helmet from these suppliers typically ranges anywhere from less than $5 to ~$15.

While wholesale helmet suppliers provide an excellent resource for community helmet promotion initiatives, no data are presently available on the impact performance of these helmets. Further, limited research efforts have been directed towards investigating the relationship between helmet price and impact performance. Helmet price can reflect a number of factors, including aerodynamics, aesthetics, ventilation, etc. Conventional bicycle helmets are comprised of an

expanded polystyrene (EPS) liner, which crushes upon impact to dissipate energy, and a plastic outer shell. More expensive helmets are often made with more complex manufacturing methods, such as in-molding of the EPS into the helmet shell or implementing a reinforcement cage into the EPS to allow for improved ventilation without compromising structural integrity. Given the low price of wholesale bicycle helmets, it is likely that these helmets are manufactured using lower-cost materials and construction methods. Whether or not these low costs are associated with a reduction in impact protection has yet to be evaluated.

All helmets sold in the US, regardless of price, must pass the Consumer Product Safety Commission (CPSC) standard [18], which mandates that helmets reduce impact peak linear acceleration (PLA) below a maximum acceptable level in prescribed testing. During testing, helmets are fitted onto a surrogate headform and subjected to guided drop tests onto an anvil such that the impact occurs at an angle normal to the anvil surface. One study used this standard setup to conduct a small-scale comparison of helmet price versus performance using three low price helmets and three high price helmets [19]. No considerable differences were found between groups. However, cyclist head impacts are thought to be more complex than the testing represented by standards, occurring oblique to the impact surface and resulting in rotational head kinematics as well as linear [20-25]. Rotational kinematics have been implicated as a key factor in producing diffuse brain injury such as concussion [26-29], so evaluation of both linear and rotational kinematics provides a more holistic assessment of helmet performance. A previous study compared oblique impact performance of 10 helmet models ranging in price from $23-250 [30]. Results showed a loose (although non-significant) correlation between price and performance, with more expensive helmets tending to provide greater reduction in concussion risks resulting from linear and rotational kinematics.

A more comprehensive comparison of bicycle helmet performance using oblique impacts has recently been conducted for 30 popular helmet models in the US ranging from $14-250 [31]. This study followed the Summation of Tests for the Analysis of Risk (STAR) evaluation protocol, in which helmet impact performance over a range of tests is summarized into a single metric. The bicycle STAR protocol subjects helmets to 12 impact conditions (six locations and two velocities) representative of real-world cyclist head impact conditions and interprets linear and rotational kinematic results in terms of concussion risk. Concussion risk from each impact condition is then weighted using an exposure term, which reflects the probability that the given impact would occur in the real world based on cyclist head impact data. Weighted risks from each condition are then summed into a final STAR value. This value represents an estimated incidence of concussion that might occur if the helmet model were subjected to all simulated impact scenarios. Helmets with a lower STAR value thereby are thought to provide superior head impact protection. The 30-helmet analysis revealed that higher-priced helmets were associated with significantly lower STAR values than lower-priced helmets, but considerable scatter was observed in this trend.

Although several studies have begun to shed light on potential correlations between helmet price and impact performance [19,30,31], this type of analysis has not been extended to include low-price wholesale helmet models. Evaluating the protective capabilities of these helmets could provide essential data to the organizations that support community helmet promotion initiatives. Of particular usefulness would be if recommendations could be made as to whether the more expensive ~$15 wholesale helmet models provide superior protection to the less expensive ~$5 models, or whether particular helmet features are associated with improved protective capabilities. The objective of this study was therefore to evaluate the impact performance of wholesale bicycle helmet models using the bicycle STAR methodology, and to investigate the association between helmet price and impact performance among these helmets and others.

METHODS

Helmet Models

Nine bicycle helmet models were purchased for testing from a wholesale helmet supplier (Table 7.1). Helmets were advertised under the categories of bike or multi-sport, and all were listed as being CPSC-certified. Only adult helmet sizes were purchased. The four helmets in the bike helmet category had construction similar to a conventional road helmet, with an elongated, aerodynamic shape, long, narrow vents throughout, and a thinner plastic outer shell. Conversely, the five helmets in the multi-sport category were comprised of a more rounded shape closer to the profile of the head, smaller, more circular vents, and a thicker plastic outer shell. Price ranged from $3.65-$12.95. The least expensive helmet was a bike helmet that did not contain an add-on visor or an occipital retention system for fit adjustment. Price was typically higher for helmets with enhanced graphics options, an add-on visor (only for bike), increased venting (only for bike), or an occipital retention system. Visors were not included in testing for the present study. Two of the multi-sport category helmets also were certified to meet US skate standards (ASTM F1492).

Table 7.1. Wholesale helmet models selected for testing. Several of the helmets contained notable features that appeared to be associated with an increase in helmet price.

Model	Price [$]	Category	Notable Features
Model 02 Supreme	7.95	Bike	Graphics, visor
Model 06	3.65	Bike	
Model 08 Premium	5.45	Bike	Occipital retention, visor
Model 09 Flash Graphics	6.45	Bike	Graphics, occipital retention, visor
Model 16	5.95	Multi-sport	
Model 18	8.95	Multi-sport	Skate certified
Model 36	6.95	Multi-sport	Occipital retention
Model 38	9.95	Multi-sport	Skate certified, occipital retention
Model 16 Brain Bucket	12.95	Multi-sport	Graphics

Impact Testing

Helmets were subject to oblique impacts according to the bicycle STAR protocol using a custom drop tower [31]. During STAR testing, a helmeted headform is dropped onto a 45° anvil, producing normal and tangential incident velocities characteristic of oblique impacts. This angle is central to a range of common cyclist head impact angles determined by cyclist accident simulation studies [20-23]. The surface of the steel anvil is coated with 80-grit sandpaper to simulate road conditions [32], which is replaced after every fourth test. A medium National Operating Committee on Standards for Athletic Equipment (NOCSAE) headform is used for all tests, with helmets fitted such that the rim sits ~1 inch above the brow line in accordance with typical manufacturer recommendations. The helmeted headform is then positioned in a support ring connected to the drop tower using a dual-axis inclinometer to define precise impact locations. Upon impact, the support ring passes around the outside of the anvil while the headform makes contact, allowing the headform to rotate off the anvil unhindered by any connection to the drop tower.

The STAR protocol dictates that helmets be tested under a range of impact configurations including six locations and two velocities. Impact locations reflect a range of accident scenarios and are dispersed around the surface area of the helmet to best encompass overall protective capabilities [20-22,33-35]. As bicycle helmets crush permanently upon impact, each sample per helmet model is impacted only once per location, with locations set sufficiently far apart to prevent overlap of damaged regions (as defined by the CPSC standard [18]). Helmets are impacted at 4.8 and 7.3 m/s, representing both average and severe cyclist head impact severities, respectively [33,34]. Two trials are conducted per location-velocity configuration. Four samples per helmet and 24 total tests are thus required to evaluate one helmet model. Individual helmet samples are subjected to three low-velocity impacts at locations evenly dispersed with three high-velocity impacts to further reduce the likelihood of overlapping damage profiles.

Each of the nine wholesale bicycle helmet models were subjected to the 24 required impacts. During all tests, impact kinematics were collected at 20 kHz using a tri-axis angular rate sensor (ARS3 PRO-18K, DTS, Seal Beach, CA) and three linear accelerometers (Endevco 7264B-2000, Meggitt Sensing Systems, Irvine, CA) at the center of gravity (CG) of the headform. Data traces were then filtered using a 4-pole, phaseless Butterworth low-pass filter at channel frequency classes (CFCs) of 1000 for linear accelerations (in accordance with automotive testing standard SAE J211) or 175 for rotational velocities. The rotational velocity CFC has been shown in previous studies of helmeted head impacts to optimize ARS data traces relative to the those produced by the more conventional nine-accelerometer array (9AA) setup [36,37]. The ARS is an attractive alternative to the 9AA for the NOCSAE headform, as its smaller size is better suited to the headform's narrow instrumentation channel. The resultant linear and rotational curves were them computed and used to determine peak linear acceleration (PLA) and peak rotational velocity (PRV) for all tests. Each helmet's average PLA and PRV were calculated per impact configuration and used as inputs into the bicycle STAR equation.

Bicycle STAR Equation

The bicycle STAR equation serves to consolidate results from a range of impact tests into a single performance value (Eq. 7.1). Its development has been outlined in full detail previously [31]. It is comprised of a concussion risk term, *R,* which translates impact kinematics from each configuration into an associated risk of concussive injury, and an exposure term, *E*, which weights risks from each impact configuration based on their likelihood of occurring in a real-world cycling accident.

$$Bicycle\ STAR = \sum_{L=1}^{6} \sum_{V=1}^{2} E(L,V) * R(a,\omega) \quad (7.1)$$

The concussion risk term is based on previously published bivariate risk functions relating PLA, *a*, and PRV, *ω*, to concussion diagnoses for high school and collegiate football players [38,39],

and is represented in Equation 7.2. The exposure term is comprised of both impact location, *L*, and velocity, *V*. Locations are weighted equally to ensure no region of the helmet is under-designed, while velocities are weighted to indicate their relative frequency in real-world impacts as determined by accident reconstruction data [33,34]. Final weightings come out to 6.33 for each low speed impact and 1.57 for each high speed impact. The low speed tests are weighted more heavily to reflect that they are more common in cyclist head impacts.

$$R(a,\omega) = 1/(1+e\text{^}(-(-10.2+0.0433a+0.19686\omega-0.0002075a\omega)) \quad (7.2)$$

For each helmet tested herein, PLA and PRV results were averaged across the two trials and used to compute risk for every impact configuration. Configuration-specific risks were then multiplied by their associated exposure weighting, then the 12 weighted risks were summed into a single STAR value per helmet. The STAR value represents a predicted incidence of concussive injury that might result out of the full range of impact configurations evaluated. It is estimated that 47.4% of cyclist head impacts are represented by the applied impact configurations, or 47.4 out of 100 impacts [31]. Thus, a helmet's STAR value approximates the number of concussions that would occur out of these 47.4 impacts.

Statistical Analysis

Across the two trials per impact configuration, kinematic variance was computed by dividing the range in PLA or PRV by the mean. Variance in STAR values was also assessed by propagating kinematic variance through the STAR calculation. Rather than averaging the PLA and PRV values across the two trials to compute concussion risk, risk was calculated independently for each trial using only the PLA and PRV results from that trial, in effect creating two risk values per impact configuration. Alternative STAR values were then recalculated using one of the two risk values for all 12 configurations. Every possible permutation of a helmet's STAR value using risk from the

first or second trial was computed (2^{12} = 4096 permutations) in order to identify a level of confidence surrounding the STAR value calculated from average kinematics. The 95th percentile confidence intervals (95% CI) of these permutation sets were identified for each helmet.

Relationships of impact locations and velocities with resulting kinematics and concussion risks were investigated using two-way ANOVA and Tukey's HSD post hoc tests. The trend between STAR and helmet price was assessed using the Pearson product-moment correlation coefficient. First, only the wholesale helmets were included in this assessment, then the analysis was expanded to include previously-determined STAR results from 30 popular bicycle helmets on the US market [31]. Finally, comparisons of wholesale helmet STAR values based on helmet style were also assessed using unbalanced ANOVA (type III SS).

RESULTS

A spectrum of kinematic results was produced across the nine wholesale helmets evaluated, with PLA averaging 116.6±25.7 g at 4.8 m/s and 195.5±35.7 g at 7.3 m/s, and PRV averaging 24.0±3.5 rad/s at 4.8 m/s and 35.9±5.6 rad/s at 7.3 m/s (Fig. 7.1). Each impact location showed distinct distributions of kinematics. Location 3 in particular generated the lowest PLA and highest PRV values compared to all other locations ($p<0.05$). The average kinematic variance between trials was 3.7±3.0% for PLA and 4.6±5.7% for PRV. Variance was not significantly different at either velocity or at any one location. Averaging PLA and PRV results across trials one and two and plugging them into the concussion risk function generated wide variations in concussion risk as well. Risk ranged from 6.5-99.9% across all tests, averaging 29.7±18.2% and 95.9±0.05% at 4.8 and 7.3 m/s, respectively. Within single impact locations, risk spanned 37.9% at 4.8 m/s and 11.0% at 7.3 m/s, reflecting considerable differences in the ability of these helmet models to reduce head impact kinematics.

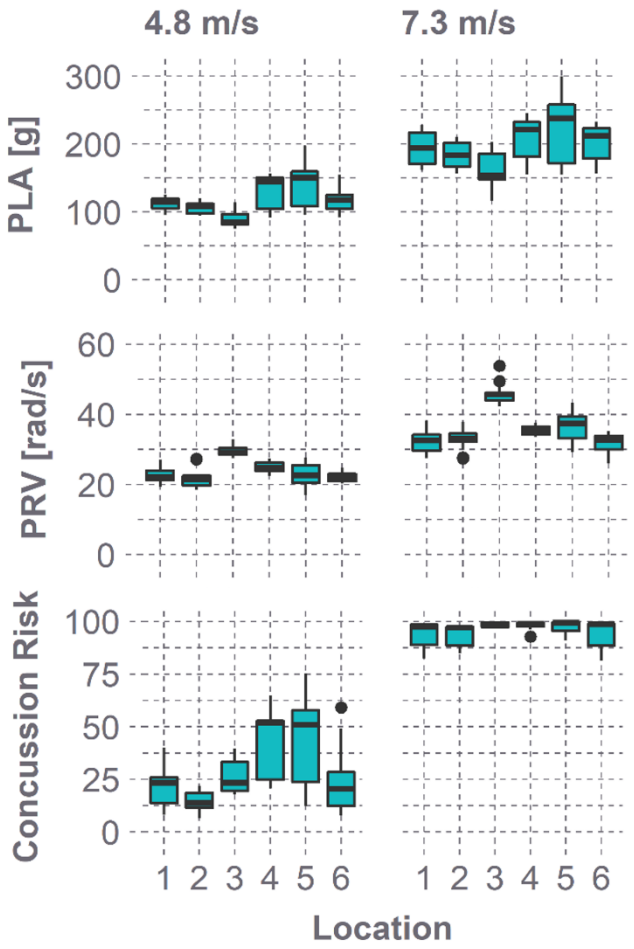

Figure 7.1. Distributions of measured impact kinematics and resulting concussion risks from STAR testing of the nine selected wholesale helmet models. Each impact configuration produced distinct distributions of kinematics and risks. Wide ranges in concussion risk were observed, reflecting varied protective capabilities across helmets.

The computed risks translated to a range in STAR values from 13.5 (95% CI: [12.9, 14.2]) for Model 9 to 26.2 [25.1, 27.4] for Model 38. The distribution of STAR values was fairly continuous, with no notable clustering of results (Fig. 7.2). On average, the 95% CI range represented 8.2±2.6% of the helmet's STAR value. The CI range did not increase significantly with increasing STAR value (p=0.60). Assessing the contributions of weighted risks from each impact

configuration to the overall STAR value revealed that each velocity was represented fairly evenly, with 4.8 m/s impacts contributing an average of 54.0±9.7% to the summed STAR value and 7.3 m/s impacts contributing an average of 46±9.7%. Locations were represented fairly evenly as well, with average contributions of each location to the summed STAR value ranging from 12.0±1.6% to 21.5±3.1%.

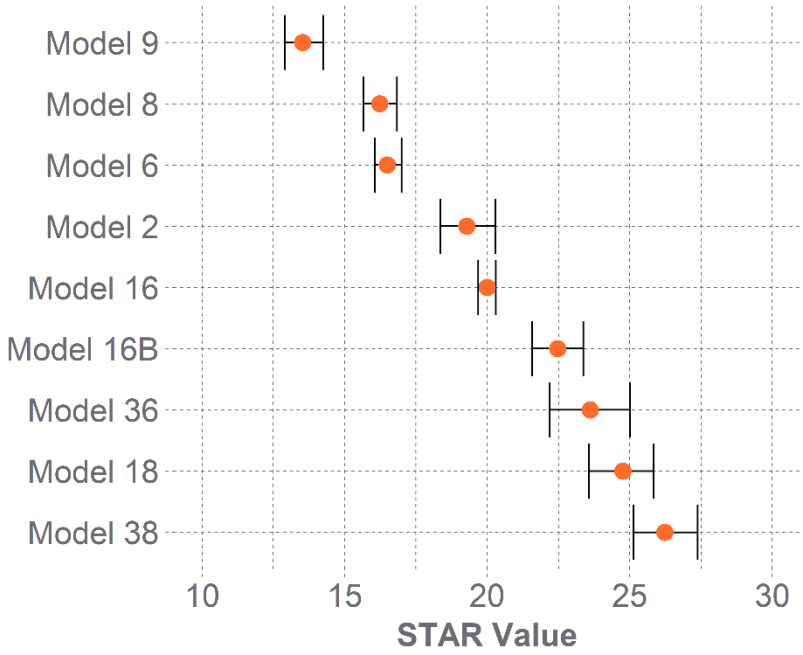

Figure 7.2. Computed STAR values for each helmet model evaluated. Error bars indicate the 95% CI. Lower STAR values represent a lower estimated incidence of concussion. The highest STAR value of 26.2 nearly doubled the lowest STAR value of 13.5.

A loose correlation between STAR values and helmet price was observed for the wholesale helmet models evaluated. Increasing price was associated with increasing STAR value (decreased protective capabilities), although this relationship was not significant (Fig. 7.3, R=0.64, p=0.06). Model 9, which generated the lowest STAR value, cost $6.45, while Model 38 generated the highest STAR value and cost $9.95. Additionally, the lowest price helmet outperformed

highest price helmet in this set of helmets, with STAR values of 16.5 and 22.5 for helmet prices of $3.65 and $12.95, respectively. Incorporating STAR results from the wholesale helmets into the STAR results from the previously-evaluated 30 popular helmet models [31] and reevaluating the relationship between STAR and price conversely revealed a slight negative relationship (Fig. 7.4). This trend was significant but characterized by considerable scatter (R=-0.44, p<0.01). The wholesale helmets made up the 9 lowest-price helmets of the entire set, while also populating nearly the entire spectrum of STAR values.

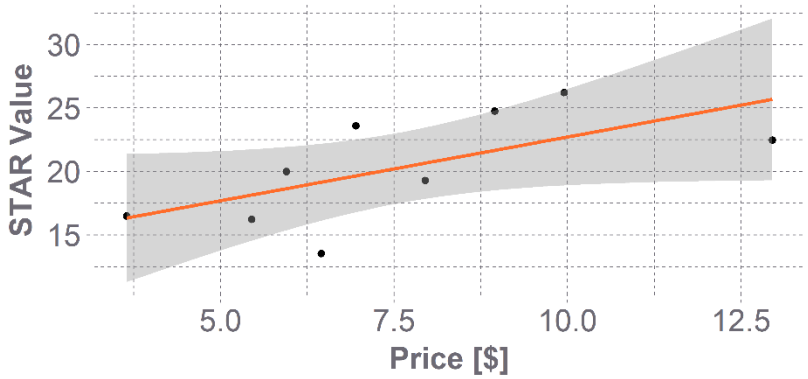

Figure 7.3. Relationship between wholesale helmet STAR values and individual helmet price. A slight positive, non-significant correlation was observed (R=0.64, p=0.06). The shaded region represents the 95% prediction interval.

Among the wholesale helmet models, trends between STAR values and helmet style were also assessed (Fig. 7.5). STAR was significantly lower for the helmets categorized as bike helmets (p<0.01), averaging 16.4±2.4 versus 23.4±2.4 for the multi-sport helmets. The associated PLA values were lower on average for bike helmets compared to multi-sport helmets, averaging 103.1±13.1 g at 4.8 m/s compared to 127.5±28.2 g for multi-sport, and 168.4±19.7 g at 7.3 m/s compared to 217.1±30.3 g for multi-sport. Conversely, PRV values were not notably lower for bike helmets, averaging 24.1±3.6 rad/s at 4.8 m/s compared to 23.9±3.3 rad/s for multi-sport and

35.2±6.3 rad/s at 7.3 m/s compared to 36.4±4.7 rad/s for multi-sport. The observed differences in STAR values across style were therefore driven by PLA differences.

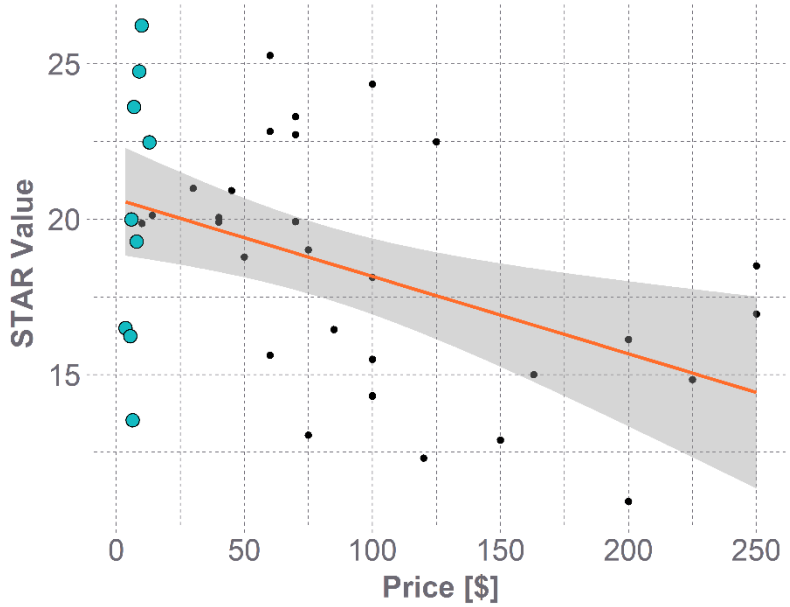

Figure 7.4. STAR value versus helmet price for the nine wholesale helmet models (larger, turquoise data points) in addition to 30 previously-evaluated helmet models (smaller, black data points). The shaded region represents the 95% prediction interval. A significant negative trend was observed overall (R=0.44, p<0.01). The wholesale models make up the nine lowest-price helmets while also spanning nearly the full distribution of STAR values.

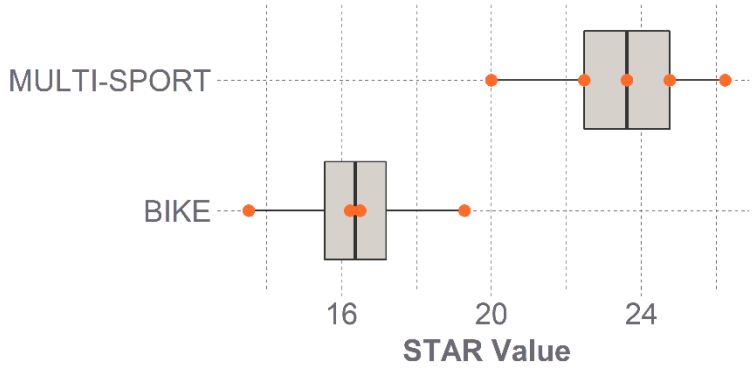

Figure 7.5. Distributions of STAR values based on wholesale helmet style. Lower STAR values

reflect enhanced protective capabilities. The bike helmet style far outperformed the multi-sport style.

DISCUSSION

Given the low costs of wholesale bicycle helmet models and their consequent appeal for community helmet promotion programs, the primary aims of this study were to investigate the impact performance of these helmets and to further evaluate the nature of the relationship between helmet price and protective capabilities. Using the bicycle STAR methodology, the wholesale helmets evaluated were found to offer a wide range in protective capabilities for a small range in helmet price ($3.65-12.95). Considerable variations in kinematics were observed, with each impact configuration characterized by distinct distributions. Notably, location 3 generated the lowest PLAs and highest PRVs compared to all other locations. This trend was also identified in the previous bicycle helmet STAR evaluation of 30 helmets [31], which attributed this to the impact location relative to the head CG; location 3 is furthest removed from the CG of the headform for most helmets, often falling on the elongated rear portion of the helmet. This suggests that there may be an associated increase in the moment arm from the contact point to the head CG, increasing rotational kinematics, and an increase in EPS thickness, decreasing linear kinematics. Location 3 produced relatively average concussion risks compared to other locations, as the decreased PLA and increased PRV offset each other to an extent when input in the bivariate concussion risk function.

The spectrum of kinematics produced across impact configurations produced a wide range in concussion risk values as well. Risks were fairly high even at the average-severity condition of 4.8 m/s, averaging ~30%, and were exceedingly high at the high-severity condition of 7.3 m/s, averaging ~96%. Since concussion is an exceptionally common injury for cyclists [4,40], these

results may simply suggest that the applied impact conditions are realistic, highlighting the need for helmet design to be improved to further mitigate risk of concussion while maintaining a high level of protection for severe impacts. Concussion risks at the high speed were nearly saturated at 100% for many helmets. As it pertains to the calculation of STAR, the high speed impacts are weighted lower since this condition is less likely to occur in the real world, resulting in STAR values that were generally evenly distributed between the high and low-speed results. This partial saturation of risks also served to make the helmets that managed risk well at this severity more distinct. In general, helmets that reduced risk better relative to other helmets at the high severity were likely to also reduce risk better at the low severity (Spearman ρ=0.82, p=0.01).

Exposure-weighted risks were summed across impact configurations to generate a STAR value for each helmet. STAR values ranged drastically across helmets, with the largest STAR value nearly doubling the lowest STAR value (26.2 versus 13.5, respectively). As STAR is a predictor of concussion incidence, the implication is that the helmet with the highest STAR value is liable to result in double the number of concussions than the helmet with the lowest STAR value from the given array of impact conditions. Such information provides essential aid for community helmet promotion organizers in purchasing top-safety helmet models. Establishing the relationships between helmet characteristics (e.g. price, style) and STAR values thus provides a useful tool for making purchasing decisions. In the present subset of wholesale helmets, helmet price was not found to be a significant predictor of STAR value. When considered within the framework of the additional grouping of 30 helmets, helmet price was significantly negatively correlated with STAR value. The scatter present in these data suggest that price is not a completely reliable predictor of performance, however. This is somewhat promising for helmet promotion initiatives using wholesale helmets, as it suggests that low-price helmets can still provide exceptional protection. The 30 helmets previously evaluated ranged from $14-$250, and

no helmet with a STAR value under 15 was less than $75. The present results showed that a helmet priced at $6.45 can afford the same level of protection.

The prices of the wholesale helmets evaluated herein likely reflect additional helmet features (i.e. graphics, add-on visor, occipital retention system) that do not necessarily affect impact performance. Helmets were tested without the add-on visor, but the occipital retention systems were tightened prior to testing for the models that had them. The Model 9 helmet, which generated the lowest STAR value, contained a turn-dial occipital retention system. Models 8 and 6 appeared to have very similar construction to Model 9, but with differing occipital retention systems (none at all for Model 6), which may suggest this dial influences impact performance. However, Models 36 and 38 also contained the turn-dial occipital retention system but performed worse than Models 16 and 18, which appeared to have very similar construction otherwise to 36 and 38, respectively. Additional evaluation using unbalanced ANOVA revealed that inclusion of an occipital turn-dial did not have a significant influence on resulting kinematics for the small sample size herein ($p>0.30$ for both PLA and PRV). Future studies could investigate this trend further.

Helmet style was found to be a key indicator of STAR value in this set of helmets, with bike helmets generating significantly lower STAR values than multi-sport helmets. Specifically, the bike style was associated with lower linear kinematics than the multi-sport style, while rotational kinematics were similar across style. Multi-sport helmets were characterized by a thicker shell, a more rounded profile, and smaller vents than bike helmets. It is likely that these features contribute to the helmet's overall stiffness. Thicker shells may distribute impact forces more than thinner shells, increasing the contact area and reducing the pressure at the point of impact, which may increase effective stiffness and decrease the amount of liner crush. The uniform shape and lack of large vents also likely contribute to increased contact area, potentially reducing liner crush by

the same mechanism [41]. The “multi-sport” classification of these helmets is similar to the “urban” classification from previous comparative studies of bicycle helmet impact performance, while the “bike” classification is similar to the “road” classification from these studies [30,31,42]. All studies, including the previous STAR evaluation of 30 helmet models, similarly showed greater impact kinematics for urban style helmets compared to road. One study using CPSC test equipment specifically demonstrated increased effective stiffness for urban helmets compared to road [42], corroborating the present trends. In their present form, helmet styles may thus be a reasonable indicator of impact performance, a trend which can be used to inform purchasing decisions.

Limitations to the present study pertain mainly to the STAR methodology and the limited sample size of helmets evaluated. The STAR methodology employs a comprehensive set of impact conditions reflective of real-world cyclist head impacts; however, it is impossible to evaluate all possible impact scenarios. The risk function used to determine concussion risk has inherent limitations associated with the sensors used to collect the underlying data and the all-male, football player population that the data are collected from [38,43]. Nonetheless, the underlying database represents one of the most comprehensive sources of concussive injury data. The test setup also has associated limitations. No surrogate neck was used in this testing, as several studies have indicated that commonly-used neck models have known biofidelity issues in the particular loading regimes involved in the present testing [36,44,45]. Incorporation of a neck may affect resulting kinematics, although it has been suggested that human necks exert minimal effects on the primary head impact response during head-first impacts [45]. Additionally, the sandpaper-coated steel anvil represents an approximation of a road surface that is likely overly stiff in reality [46], which may have inflated results slightly. Finally, the limited sample size of wholesale models evaluated limits inferences between helmet characteristics and STAR value, although supplementing this data with existing bicycle helmet STAR data enhances trends.

CONCLUSIONS

Wholesale bicycle helmet models are an attractive option for community helmet promotion initiatives that seek to give away helmets or subsidize costs. While encouraging widespread helmet use enhances cyclist safety, the extent to which these lower-priced helmets provide protection during head impacts has previously been unexplored. The present study evaluated the performance of such helmets using the bicycle STAR evaluation protocol and explored relationships between helmet price and impact performance. Wholesale helmets were found to provide a large range in protective capabilities across models, with STAR values ranging from 13.5 to 26.2. Price was not a significant indicator of performance among these helmets, although evaluating these results in the context of helmets that were previously subject to STAR testing revealed a slight negative correlation between helmet price and STAR, indicating that more expensive helmets may provide superior protection. However, considerable scatter was prevalent in this trend, especially among the wholesale helmet models. It is thus recommended that community programs make helmet purchasing decisions based on helmet style rather than price, which was more reflective of impact performance.

REFERENCES

1. Fischer, P. A Right to the Road: Understanding and Addressing Bicyclist Safety, G.H.S. Association, Editor. 2017, Governors Highway Safety Association.
2. Sanford, T., McCulloch, C.E., and Callcut, R.A. Bicycle trauma injuries and hospital admissions in the United States, 1998-2013. Jama, 2015. 314(9): p. 947-949
3. Gaither, T.W., Sanford, T.A., et al. Estimated total costs from non-fatal and fatal bicycle crashes in the USA: 1997-2013. Inj. Prev., 2018. 24(2): p. 135-141
4. Haileyesus, T., Annest, J.L., and Dellinger, A.M. Cyclists injured while sharing the road with motor vehicles. Injury prevention : journal of the International Society for Child and Adolescent Injury Prevention, 2007. 13(3): p. 202-6
5. Thompson, D.C., Rivara, F.P., and Thompson, R.S. Effectiveness of bicycle safety helmets in preventing head injuries. A case-control study. The Journal of the American Medical Association, 1996. 276(24): p. 1968-73
6. Sacks, J.J., Holmgreen, P., Smith, S.M., and Sosin, D.M. Bicycle-associated head injuries and deaths in the United States from 1984 through 1988: How many are preventable? The Journal of the American Medical Association, 1991. 266: p. 3016-3018

7. Olivier, J. and Creighton, P. Bicycle injuries and helmet use: a systematic review and meta-analysis. Int. J. Epidemiol., 2017. 46(1): p. 278-292
8. McIntosh, A.S., Lai, A., and Schilter, E. Bicycle helmets: head impact dynamics in helmeted and unhelmeted oblique impact tests. Traffic Inj. Prev., 2013. 14(5): p. 501-8
9. Olivier, J. and Radun, I. Bicycle helmet effectiveness is not overstated. Traffic injury prevention, 2017. 18(7): p. 755-760
10. Amoros, E., Chiron, M., Martin, J.L., Thelot, B., and Laumon, B. Bicycle helmet wearing and the risk of head, face, and neck injury: a French case--control study based on a road trauma registry. Injury prevention : journal of the International Society for Child and Adolescent Injury Prevention, 2012. 18(1): p. 27-32
11. Cripton, P.A., Dressler, D.M., Stuart, C.A., Dennison, C.R., and Richards, D. Bicycle helmets are highly effective at preventing head injury during head impact: head-form accelerations and injury criteria for helmeted and unhelmeted impacts. Accident Analysis & Prevention, 2014. 70: p. 1-7
12. Meehan, W.P., 3rd, Lee, L.K., Fischer, C.M., and Mannix, R.C. Bicycle helmet laws are associated with a lower fatality rate from bicycle-motor vehicle collisions. The Journal of pediatrics, 2013. 163(3): p. 726-9
13. Karkhaneh, M., Rowe, B.H., Saunders, L.D., Voaklander, D.C., and Hagel, B.E. Trends in head injuries associated with mandatory bicycle helmet legislation targeting children and adolescents. Accident; analysis and prevention, 2013. 59: p. 206-12
14. Macpherson, A. and Spinks, A. Bicycle helmet legislation for the uptake of helmet use and prevention of head injuries. The Cochrane database of systematic reviews, 2007(2): p. CD005401
15. Insurance Institute for Highway Safety, "Pedestrians and Bicyclists: State Laws" Internet https://www.iihs.org/iihs/topics/laws/bicycle-laws. [cited 2019 March 6].
16. Spinks, A., Turner, C., McClure, R., Acton, C., and Nixon, J. Community-based programmes to promote use of bicycle helmets in children aged 0-14 years: a systematic review. International journal of injury control and safety promotion, 2005. 12(3): p. 131-42
17. Royal, S., Kendrick, D., and Coleman, T. Promoting bicycle helmet wearing by children using non-legislative interventions: systematic review and meta-analysis. Injury prevention : journal of the International Society for Child and Adolescent Injury Prevention, 2007. 13(3): p. 162-7
18. CPSC. Safety Standard for Bicycle Helmets Final Rule (16 CFR Part 1203). 1998, United States Consumer Product Safety Commission. p. 11711-11747.
19. Bicycle Helmet Safety Institute. "Cheap or Expensive Bicycle Helmets" Internet https://helmets.org/testbycost.htm. [cited 2019 March 6].
20. Verschueren, P. Biomechanical analysis of head injuries related to bicycle accidents and a new bicycle helmet concept, in Faculteit Ingenieurswetenschappen Departement Werktuigkunde Afdeling Biomechanica en Grafisch Ontwerpen. 2009, Katholieke Universiteit Leuven: Leuven, Belgium.
21. Bourdet, N., Deck, C., et al. In-depth real-world bicycle accident reconstructions. Int. J. Crashworthiness, 2014. 19(3): p. 222-232
22. Bourdet, N., Deck, C., Carreira, R.P., and Willinger, R. Head impact conditions in the case of cyclist falls. Proc. Inst. Mech. Eng. P, 2012. 226(3-4): p. 282-289
23. Peng, Y., Chen, Y., Yang, J., Otte, D., and Willinger, R. A study of pedestrian and bicyclist exposure to head injury in passenger car collisions based on accident data and simulations. Safety Science, 2012. 50(9): p. 1749-1759
24. Fahlstedt, M., Baeck, K., et al. Influence of Impact Velocity and Angle in a Detailed Reconstruction of a Bicycle Accident. IRCOBI Conference, 2012. 12(84): p. 787-799
25. Otte, D. Injury Mechanism and crash kinematics of cyclists in accidents - An analysis of real accidents. Proceedings of 33rd Stapp Car Crash Conference, 1989. Warrendale, PA

26. Gennarelli, T., Ommaya, A., and Thibault, L. Comparison of translational and rotational head motions in experimental cerebral concussion. Proceedings of 15th Stapp Car Crash Conference, 1971.
27. Gennarelli, T.A., Thibault, L.E., and Ommaya, A.K. Pathophysiologic responses to rotational and translational accelerations of the head. SAE Technical Paper Series, 1972. 720970: p. 296-308
28. Ommaya, A.K., Hirsch, A.E., and Martinez, J.L. The role of whiplash in cerebral concussion. Proceedings of Proc. 10th Stapp Car Crash Conference, 1966.
29. Ommaya, A. and Hirsch, A. Tolerances for cerebral concussion from head impact and whiplash in primates. Journal of biomechanics, 1971. 4(1): p. 13-21
30. Bland, M.L., McNally, C., and Rowson, S. Differences in Impact Performance of Bicycle Helmets During Oblique Impacts. J. Biomech. Eng., 2018. 140(9)
31. *In review:* Bland, M.L. McNally, C., Zuby, D.S., Mueller, B.C., and Rowson, S. Development of the STAR evaluation system for assessing bicycle helmet protective performance. Ann. Biomed. Eng.
32. ECE. R-22.05: Uniform Provisions Concerning the Approval of Protective Helmets for Drivers and Passengers of Motorcycles and Mopeds. 1999, United Nations Economic Commission for Europe.
33. Williams, M. The protective performance of bicyclists' helmets in accidents. Accid. Anal. Prev., 1991. 23(2-3): p. 119-131
34. Smith, T.A., Tees, D., Thom, D.R., and Hurt, H.H. Evaluation and replication of impact damage to bicycle helmets. Accid. Anal. Prev., 1994. 26(6): p. 795-802
35. Depreitere, B., Van Lierde, C., et al. Bicycle-related head injury: a study of 86 cases. Accid. Anal. Prev., 2004. 36(4): p. 561-567
36. Bland, M.L., McNally, C., and Rowson, S. Headform and Neck Effects on Dynamic Response in Bicycle Helmet Oblique Impact Testing, in IRCOBI Conference. 2018: Athens, Greece. p. 413-423.
37. Cobb, B.R., Tyson, A.M., and Rowson, S. Head acceleration measurement techniques: Reliability of angular rate sensor data in helmeted impact testing. Proceedings of the Institution of Mechanical Engineers, Part P: Journal of Sports Engineering and Technology, 2017. 232(2): p. 176-181
38. Rowson, S., Duma, S.M., et al. Rotational head kinematics in football impacts: an injury risk function for concussion. Ann. Biomed. Eng., 2012. 40(1): p. 1-13
39. Rowson, S. and Duma, S.M. Brain injury prediction: assessing the combined probability of concussion using linear and rotational head acceleration. Ann. Biomed. Eng., 2013. 41(5): p. 873-82
40. Coronado, V.G., Haileyesus, T., et al. Trends in Sports- and Recreation-Related Traumatic Brain Injuries Treated in US Emergency Departments: The National Electronic Injury Surveillance System-All Injury Program (NEISS-AIP) 2001-2012. J. Head Trauma Rehabil., 2015. 30(3): p. 185-197
41. Mills, N.J. Protective capability of bicycle helmets. Br. J. Sports Med., 1990. 24(1): p. 55-60
42. Bland, M.L., Zuby, D.S., Mueller, B.C., and Rowson, S. Differences in the protective capabilities of bicycle helmets in real-world and standard-specified impact scenarios. Traffic Inj. Prev., 2018. 19(sup1): p. S158-S163
43. Rowson, S., Bland, M.L., et al. Biomechanical Perspectives on Concussion in Sport. Sports Med Arthrosc Rev, 2016. 24(3): p. 100-7
44. Sances, A.J., Carlin, F., and Kumaresan, S. Biomechanical analysis of head-neck force in Hybrid III dummy during inverted vertical drops. Biomed. Sci. Instrum., 2002. 38: p. 459-464
45. Nelson, T.S. and Cripton, P.A. A New Biofidelic Sagittal Plane Surrogate Neck for Head-First Impacts. Traffic Inj Prev, 2010. 11(3): p. 309-319

46. Bonugli, E. The effects of dynamic friction in oblique motorcycle helmet impacts, in Biomedical Engineering. 2015, The University of Texas at San Antonio: Ann Arbor. p. 78.

CHAPTER 8

METHODOLOGY FOR RECONSTRUCTING REAL-WORLD DAMAGE TO BICYCLE HELMETS USING OBLIQUE IMPACTS: A CASE STUDY

ABSTRACT

Cyclist head impact conditions and resulting kinematics are not well understood. One avenue for investigating these impacts is to reconstruct residual damage from helmets involved in real-world accidents using laboratory testing. To date, reconstruction studies have assessed normal-velocity impacts and linear accelerations. In reality, cyclist head impacts are oblique and involve both linear and rotational kinematics, an important combination in producing brain injury. The present study details a method for reconstructing bicycle helmet damage using oblique impacts and advanced damage quantification techniques. Damage to a helmet involved in a cyclist accident was quantified using computed tomography (CT). Scrape length and crush depth, area, volume, and centeredness were evaluated. Impact testing to identical, undamaged samples was then conducted, with impact angle and velocity successively updated based on visual observation of damage. Damage was then quantified using CT and compared to the original damage, and linear regression models were generated to relate each damage metric to applied normal and tangential velocities. Linear and rotational head impact kinematics were also recorded. These methods show promise for reconstructing real-world bicycle helmet damage, which can enhance understanding of cyclist head impact conditions and enable improved helmet design.

INTRODUCTION

Cycling is the leading cause of sport- and recreation-related head injuries in the US. [1]. Although helmet use reduces injury risk [2], safety standards evaluate bicycle helmet performance using tests that do not reflect typical cyclist head impacts. Standards instruct that a helmeted headform be dropped onto an anvil at an angle normal to its surface while headform linear acceleration is recorded [3]. Real-world cyclist head impacts involve normal and tangential velocities (termed “oblique”) and induce rotational impact kinematics as well as linear [4,5], an important interplay leading to brain injury [6,7]. Despite knowledge of the oblique nature of these impacts, exact cyclist head impact conditions and kinematics are relatively unknown. Better understanding of these impacts could aid in optimizing helmet design.

Cyclist head impact kinematics have traditionally been investigated via two means: computational simulation of cyclist crashes [4,5], or post-crash laboratory reconstructions of residual helmet damage [8-10]. Simulations are useful for gleaning trends pertaining to cyclist head impacts, but their accuracy relies on the computational model validity. As cyclists do not often wear instrumentation capable of measuring head impact kinematics, data from real-world cyclist head impacts are largely unavailable, limiting the validation of computational models for these scenarios.

Damage reconstructions provide an additional avenue for ascertaining cyclist head impact conditions. Bicycle helmet expanded polystyrene (EPS) liners dissipate energy by permanently crushing on impact. The damage can be matched on identical helmets through laboratory impact tests to deduce the nature of the impact. However, previous damage reconstruction studies are restricted by use of standards equipment and limited damage quantification [8-10]. The current study used an oblique impact rig with a biofidelic headform that measured linear and angular

kinematics combined with advanced damage quantification methods to better estimate the conditions of a cyclist head impact. The objective of this case study was to detail a methodology for quantifying and reconstructing damage to a bicycle helmet involved in a real-world accident using oblique impacts.

METHODS

A small, Zol Urban (ZU) helmet with considerable crush and scraping (3.5 cm, superior-inferior) to the left, temporal/parietal region was donated for the study by a cyclist who was hospitalized from a cycling-related accident. The patient claimed to have been riding at a high speed on bumpy pavement when they struck a pothole and fell off the bike, suffering slight memory impairment from the event. Records indicate the patient sustained a knee abrasion and was discharged. Related protocols were approved by the Virginia Tech Institutional Review Board (IRB 17-1036).

Five undamaged, small ZU helmets were purchased for reconstruction. To quantify the original damage, one new helmet and the original helmet were scanned using computed tomography (CT). CT has previously been shown to be a method for quantifying helmet damage [11,12]. Scans were taken at 120 kV and 200 mA with 0.625 x 0.625 mm pixel spacing and a slice thickness of 0.5 mm (Aquilion, Canon Medical Systems, Tustin, CA). Scans were imported into Mimics Research 21.0 (Materialise, Leuven, Belgium), where foam liners were segmented with a Hounsfield unit (HU) range of -960 to -850. Mimics semi-automated operations were used to separate liners from the surrounding environment, and manual editing of individual slices was used when necessary to correct slight image artifact. Liners were then auto-meshed to 3D triangular mesh models (>600,000 elements).

Models were imported into 3-matic Research 13.0 (Materialise, Leuven, Belgium), and the original

model was overlaid onto the undamaged model using a linear registration method that minimized the average distance error between models (0.7 mm). The crush region was visualized using a heat map showing distances from each node on the original model to the nearest node on the undamaged model (Fig. 8.1). The area of the model outer surface exceeding a 0.7 mm offset was recorded. Heat map bounds were then increased to locate the outer surface node with the largest offset. Damaged and undamaged liner radial thicknesses at this location were subtracted to compute maximum crush depth. The distance from this node to the superior and inferior bounds of the crush region in the direction of helmet scraping was measured, with the ratio of superior to inferior distances representing crush centeredness. Crush volume was calculated by subtracting the damaged liner volume from the undamaged liner volume within a cylindrical region that encompassed the crush area and ran radially through the liner.

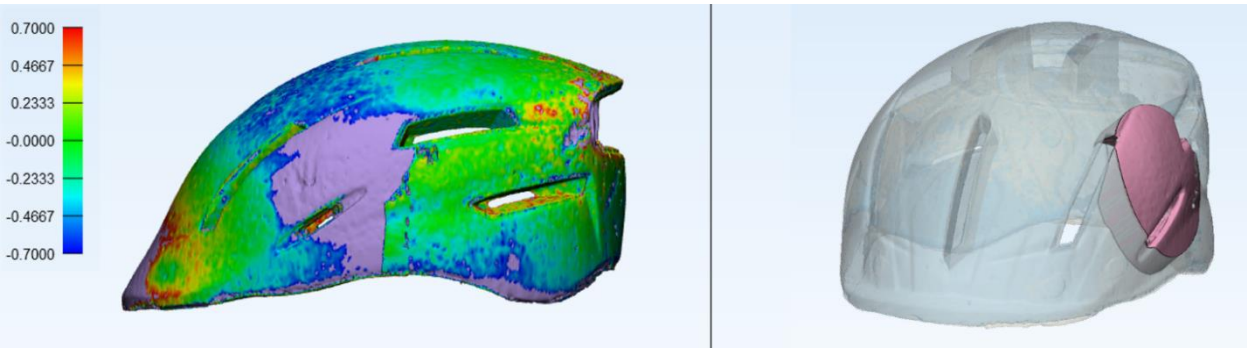

Figure 8.1. Heat map (left) showing distance offsets between the undamaged and original damaged helmet liners. The crush region was defined as the area exceeding -0.7 mm offset (purple) near the site of impact. The crush volume (right) was determined by isolating the crushed region using a cylindrical cross-section of both models and subtracting their volumes.

The five ZU helmets were tested on a custom drop tower containing an adjustable angled anvil to produce oblique impacts. The steel anvil was coated with 80-grit sandpaper (replaced per test) to simulate road friction [13]. Helmets were fitted to a medium National Operating Committee on

Standards for Athletic Equipment (NOCSAE) headform, which fell within the helmet's circumference range. The helmeted headform was positioned in a support ring such that the max crush location was the initial contact point and the direction of impact aligned with the original helmet scraping. The headform was then secured using a lever arm that released prior to impact. The support ring passed outside the anvil upon impact, separating from the headform. A light gate recorded impact velocity, while a tri-axis angular rate sensor (ARS) and three linear accelerometers at the head center of gravity measured kinematics at 20 kHz.

Initial impact boundary conditions (BCs, velocity and angle) were selected for the first test, after which damage was compared to the original damage by visual inspection of liner crush and surface scrapes. Iterative testing was employed using updated BCs, with one test per ZU sample. Normal and tangential velocities were calculated from resultant velocities and angles. CT scans were then taken of the tested helmets. Scans were segmented and damage quantified using the same process from the original helmet. Crush area, max crush depth, crush volume, crush centeredness, and scrape length were compared to the original, and were correlated with normal and tangential velocities via multiple linear regression (MLR).

Impact kinematics were filtered using a 4-pole, phaseless Butterworth low pass filter with a channel frequency class (CFC) of 1000 for accelerometer data (SAE J211) and a CFC of 175 for ARS data [14,15]. Resultant peak linear acceleration (PLA) and rotational velocity (PRV) values were extracted from each test, and were correlated with normal and tangential incident velocities.

RESULTS

The five ZU helmets were tested sequentially using visual observation to update BCs (effectively changing normal and tangential velocities). ZU1 was tested at a conservative velocity of 1.4 m/s

on a 45° anvil, producing minimal liner crush and surface scrapes that fell slightly too posterior compared to the original helmet damage. The velocity was thus increased and the position adjusted for ZU2, resulting in an improved contact area and location but limited crush and scrapes. Impact velocity was further increased, and the applied locations and anvil angles were adjusted slightly for helmets 3-5, which produced varied degrees of success in replicating the original damage visually (Table 8.1, scrape length).

CT scanning and segmentation was completed with relative ease, requiring minimal manual edits. The mean distance from nodes of the undamaged helmet to nodes of the original and tested helmets was <0.1 mm. Liner crush was more evident on the model exterior than the interior for all helmets. Samples 2-5 each matched the original damage best in at least one metric, although no one helmet appeared to be a clear best match to the original damage (Table 8.1). MLR models relating each metric to the applied normal and tangential incident velocities were also computed and used to predict the velocities necessary to produce the original helmet damage (Table 8.2).

Table 8.1. Original helmet damage metrics and tested helmet applied velocities and resulting damage metrics. Bolded values indicate the closest match to the original damage for each metric. Location error was calculated as the distance between the max crush depth location on the tested helmet and the max crush depth location on the original helmet.

Helmet	Normal/ tangential velocity [m/s]	Scrape length [cm]	Crush area [cm^2]	Crush depth [mm]	Location error [cm]	Crush volume [cm^3]	Crush centeredness
Original	--	3.5	40.71	4.58	--	5.53	1.32
ZU1	0.96 / 0.96	1.0	3.81	1.11	1.46	0.22	2.16
ZU2	2.60 / 2.60	2.2	27.02	3.79	**0.37**	**4.69**	1.80
ZU3	3.17 / 3.17	2.5	37.61	**4.48**	2.43	8.28	1.20
ZU4	3.06 / 4.37	5.0	35.02	4.25	1.10	8.48	**1.33**
ZU5	3.61 / 4.31	**4.0**	**40.88**	6.42	1.13	10.45	1.20

Table 8.2. MLR models for each damage metric as functions of normal and tangential velocities (norm, tan). All included factor coefficients were statistically significant (p<0.05). *Norm* and *tan* predictions were solved for using original damage values. **Tan* was computed using the average *norm* from all other metrics, then *norm* was computed using the average *tan*.

Scrape length*	Crush area	Crush depth	Crush volume*	Crush centeredness
$= -1.15norm + 2.28tan - 0.11norm \times tan$	$= -9.97 + 14.50norm$	$= 1.53norm$	$= 0.69norm \times tan$	$= 2.59 - 0.39norm$
norm = 2.42, *tan* = 3.75	*norm* = 3.50	*norm* = 3.00	*norm* = 2.58, *tan* = 2.47	*norm* = 3.25

Across all tests, PLA spanned ~50-175 g and PRV spanned ~5-25 rad/s (Fig. 8.2). PLA was highly correlated with normal velocity (R=0.99, p<0.01) and PRV with tangential velocity (R=0.99, p<0.01). Crush depth and scrape length also showed strong correlations with PLA and PRV, respectively (R>0.98, p<0.01), reflecting their relationships with normal and tangential velocities.

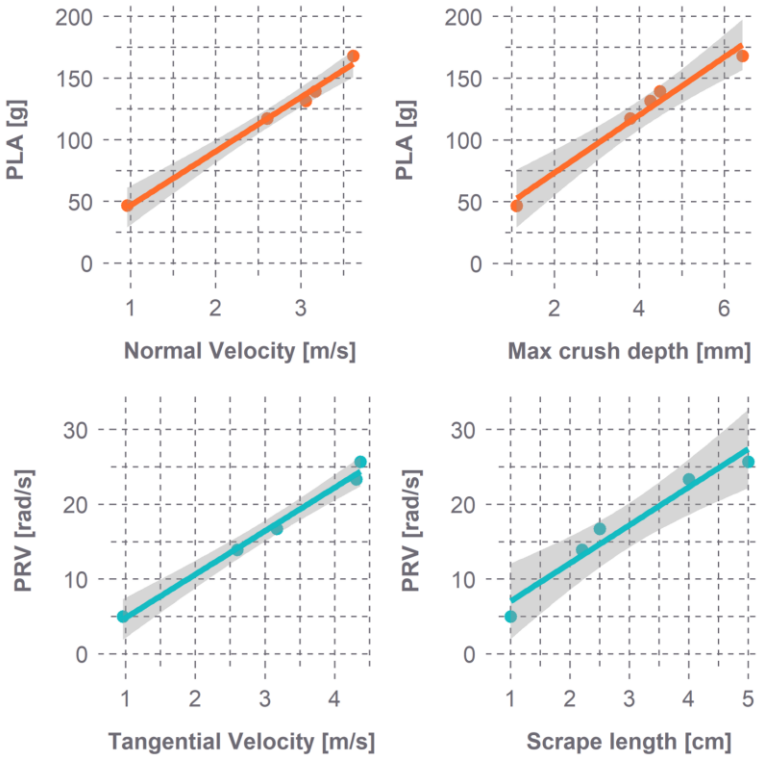

Figure 8.2. Kinematic correlations with applied velocities and select damage metrics. Crush depth

and scrape length were also well-correlated with normal and tangential velocities, respectively. Shaded regions indicate 95% prediction intervals.

DISCUSSION

The present study investigated CT-based quantification and oblique impact testing to reconstruct damage to a bicycle helmet involved in a cyclist accident. CT seemed to be reliable for rendering helmet volumes, as there was minimal offset between overlaid models outside of the damaged region. The offset variability outside of this region likely owes to manufacturing differences, scanner resolution-related noise, and artifact caused by higher-density plastics. Other studies have also shown the feasibility of CT for helmet damage quantification and have investigated issues surrounding scan artifact [11,12]. Artifact was minimal with the present helmet model, especially in the crush region.

Oblique impact testing with successively updated BCs resulted in damage similar to the original damage. Helmet shell scraping in the direction of impact was generated, representing an improvement over normal-impact studies [8-10]. Nonetheless, no single sample appeared to best match the damaged helmet across all metrics. Crush depth and area were within 8% of the target values for ZU3, while its crush volume was 50% greater. Volume was closest for ZU2, which produced crush depth and area values that were 17-34% low. This discrepancy between crush depth/area and volume may necessitate use of a rougher, more focal impact surface in future tests. The description of the pavement as “bumpy” and several small pockmarks on the original helmet’s surface corroborate this.

Damage metric MLR models provide insight into the influence of normal and tangential velocities on each metric and can be used to inform additional test BCs. Crush depth, area, and

centeredness were correlated to normal velocity alone, and predicted normal velocities of 3.0-3.5 m/s when solved with original damage values. Conversely, crush volume and scrape length were correlated to both velocities. Scrape length increased with normal velocity and appeared to be modulated by the normal-to-tangential velocity ratio. Although crush volume and scrape length models predicted lower normal velocities than other metrics, the volume model may be improved by using a more focal impact surface. All models were also limited by use of the same normal and tangential velocities for ZU1-3, clouding individual effects of each velocity. Additional tests informed by these models will refine BCs associated with the original helmet damage.

Kinematic results from reconstruction tests were highly correlated to incident velocities, with PLA best predicted by normal velocity and PRV by tangential velocity. Crush depth and scrape length were also well-correlated with PLA and PRV, respectively, reflecting how individual damage metrics can be indicative of resulting kinematics. As rotational kinematics are especially important in producing diffuse brain injury [6,7], and as cyclist head impacts typically involve a tangential component, there is room for innovation in helmet design to further reduce effects of these tangential forces. Interestingly, the observed kinematic ranges fell within a range often associated with concussive injury [16,17]. The patient was not reported to have sustained a head injury, despite slight memory loss. Once reconstruction is finalized and associated kinematics ascertained, data such as these may aid the development of injury risk curves.

There are several limitations associated with the present methodology. First, measuring scrape length is somewhat subjective, as scrape region boundaries are not always well-defined. Second, the high stiffness of the steel anvil may have influenced damage properties. Although real-world impact surfaces are often complex and difficult to reproduce exactly, testing various surfaces may lend additional insight. Further, a single, isolated impact was used to replicate the most severe

damage on the original helmet. In reality, cyclist accidents can involve secondary impacts, often of a lesser severity, which could become a source of error. Lastly, helmet damage and impact kinematics are likely influenced by specifics of the test setup, such as the NOCSAE headform or not using a neck, and results may vary slightly under other setups.

CONCLUSIONS

This case study outlines methods for quantifying bicycle helmet damage and using oblique impact testing to reconstruct that damage. CT scanning enabled an in-depth quantitative damage description to be formulated, while oblique testing produced damage profiles similar to the original. Regression models relating damage metrics to normal and tangential velocities were then generated to inform future testing. Reconstructing bicycle helmet damage using these methods can enhance knowledge of cyclist head impact conditions and kinematics, which is fundamental to designing helmets that better protect cyclists.

REFERENCES

1. Coronado, V.G., Haileyesus, T., et al. Trends in Sports- and Recreation-Related Traumatic Brain Injuries Treated in US Emergency Departments: The National Electronic Injury Surveillance System-All Injury Program (NEISS-AIP) 2001-2012. J. Head Trauma Rehabil., 2015. 30(3): p. 185-197
2. Olivier, J. and Creighton, P. Bicycle injuries and helmet use: a systematic review and meta-analysis. Int. J. Epidemiol., 2017. 46(1): p. 278-292
3. CPSC. Safety Standard for Bicycle Helmets Final Rule (16 CFR Part 1203). 1998, United States Consumer Product Safety Commission. p. 11711-11747.
4. Verschueren, P. Biomechanical analysis of head injuries related to bicycle accidents and a new bicycle helmet concept, in Faculteit Ingenieurswetenschappen Departement Werktuigkunde Afdeling Biomechanica en Grafisch Ontwerpen. 2009, Katholieke Universiteit Leuven: Leuven, Belgium.
5. Bourdet, N., Deck, C., et al. In-depth real-world bicycle accident reconstructions. Int. J. Crashworthiness, 2014. 19(3): p. 222-232
6. Gennarelli, T., Ommaya, A., and Thibault, L. Comparison of translational and rotational head motions in experimental cerebral concussion. Proceedings of 15th Stapp Car Crash Conference, 1971.
7. Gennarelli, T.A., Thibault, L.E., and Ommaya, A.K. Pathophysiologic responses to rotational and translational accelerations of the head. SAE Technical Paper Series, 1972. 720970: p. 296-308

8. Williams, M. The protective performance of bicyclists' helmets in accidents. Accid. Anal. Prev., 1991. 23(2-3): p. 119-131
9. Smith, T.A., Tees, D., Thom, D.R., and Hurt, H.H. Evaluation and replication of impact damage to bicycle helmets. Accid. Anal. Prev., 1994. 26(6): p. 795-802
10. McIntosh, A.S. and Patton, D.A. Impact reconstruction from damage to pedal and motorcycle helmets. Proceedings of the Institution of Mechanical Engineers, Part P: Journal of Sports Engineering and Technology, 2012. 226(3-4): p. 274-281
11. Bonin, S.J., Luck, J.F., et al. Dynamic Response and Residual Helmet Liner Crush Using Cadaver Heads and Standard Headforms. Ann Biomed Eng, 2017. 45(3): p. 656-667
12. Loftis, K.L., Moreno, D.P., Tan, J., Gabler, H.C., and Stitzel, J.D. Utilizing computed tomography scans for analysis of motorcycle helmets in real-world crashes. Proceedings of 48th Rocky Mountain Bioengineering Symposium & 48th International ISA Biomedical Sciences Instrumentation Symposium, 2011. Denver, Colorado
13. ECE. R-22.05: Uniform Provisions Concerning the Approval of Protective Helmets for Drivers and Passengers of Motorcycles and Mopeds. 1999, United Nations Economic Commission for Europe.
14. Bland, M.L., McNally, C., and Rowson, S. Headform and Neck Effects on Dynamic Response in Bicycle Helmet Oblique Impact Testing, in IRCOBI Conference. 2018: Athens, Greece. p. 413-423.
15. Cobb, B.R., Tyson, A.M., and Rowson, S. Head acceleration measurement techniques: Reliability of angular rate sensor data in helmeted impact testing. Proceedings of the Institution of Mechanical Engineers, Part P: Journal of Sports Engineering and Technology, 2017. 232(2): p. 176-181
16. Rowson, B., Rowson, S., and Duma, S.M. Hockey STAR: A Methodology for Assessing the Biomechanical Performance of Hockey Helmets. Ann. Biomed. Eng., 2015. 43(10): p. 2429-2443
17. Rowson, S. and Duma, S.M. Brain injury prediction: assessing the combined probability of concussion using linear and rotational head acceleration. Ann. Biomed. Eng., 2013. 41(5): p. 873-82

CHAPTER 9

EVALUATING THE SENSITIVITY OF BICYCLE HELMET DAMAGE RECONSTRUCTION METRICS USING OBLIQUE IMPACTS AND COMPUTED TOMOGRAPHY

ABSTRACT

Understanding common cyclist head impact conditions is fundamental to designing helmets that are best equipped to protect riders. These conditions can be investigated by reconstructing residual real-world helmet damage in a laboratory setting. However, previous reconstruction studies have employed limited methodologies, evaluating only head linear accelerations from normal impacts and measuring liner crush depth visually. Real-world cyclist head impacts are oblique and induce both linear and rotational head kinematics. Recent studies have also proposed computed tomography (CT) as a method for enhanced damage quantification. The present study explored use of oblique impacts and CT for bicycle helmet reconstruction by evaluating the sensitivity of damage metrics and impact kinematics to varied oblique impact conditions. A custom drop tower was used to impact helmeted headforms at velocities ranging from 1-7 m/s against anvil angles ranging from 0-60°. Peak linear acceleration (PLA) and rotational velocity (PRV) were recorded per test, while helmet damage metrics were measured using CT and visual observation. PLA and PRV were highly correlated with normal and tangential velocities, respectively. Normal velocity and PLA were best correlated with maximum liner crush. Associations with crush area and volume were also strong, although these metrics may be modulated slightly by tangential velocity as well. Tangential velocity and PRV were best correlated to shell scrape length, which was also influenced slightly by normal velocity. Use of oblique impacts and CT, supplemented with visual analysis, has the potential to enhance the accuracy of bicycle helmet damage reconstructions, expanding knowledge of common cyclist head impact conditions.

INTRODUCTION

Protective headgear are most effective when designed around the impact scenarios likely to be encountered during the activity they are marketed for. For bicycle helmets, this requires an understanding of common cyclist head impact conditions. While bicycle helmets have been demonstrated to reduce a cyclist's risk of head injury during a crash [1-5], head injuries from cyclist crashes remain a common problem in the US and around the world, and the precise head impact conditions associated with these crashes remain relatively unknown. It is estimated that cycling-related head injuries accounted for 81,000 emergency room visits in the US in 2015 alone [6], exceeding the number of head injuries related to other sports and recreational activities [6,7].

Bicycle helmets are presently designed around impact conditions required by mandatory safety standards. Standards assess helmet impact performance using guided drop tests of a helmeted headform at a normal angle to the impact anvil's surface [8,9]. Peak linear acceleration (PLA) of the headform is measured during each test. In the US standard, the metal half-headform is rigidly constrained to the drop mass, preventing rotation of the head upon impact [9]. In contrast, research has since suggested that real-world cyclist head impacts are in fact most often oblique to the impact surface, involving both normal and tangential velocity components and inducing rotational impact kinematics as well as linear [10-13]. Rotational kinematics are thought to be a causative agent in the development of shear strains in the brain, which lead to diffuse injuries such as concussion to more severe diffuse axonal injury (DAI), while linear kinematics are more closely correlated to focal injuries such as cerebral contusion or skull fracture [14-18]. Testing and designing helmets around evaluation of both linear and rotational kinematics is thus of critical importance. To this end, several research groups have designed oblique impact test rigs using more biofidelic headforms capable of evaluating linear and rotational responses [19-23].

Although it is widely accepted that cyclist head impacts are typically oblique in nature, identifying more specific impact characteristics, such as incident head impact velocities, impact locations, and resulting head impact kinematics, is challenging. Characterizing these impacts through direct instrumentation of cyclists' heads during crashes would provide optimal data. However, instrumenting enough cyclists to provide sufficient naturalistic data is impractical, as individual cyclists experience head impacts relatively infrequently, while instrumenting volunteers and instructing them to crash intentionally is unethical due to the high risks involved. Previous studies have instead taken alternative approaches to estimating cyclist head impact kinematics, including computational simulations of cyclist crash scenarios [10-13,24] or post-crash laboratory reconstruction of residual damage to bicycle helmets [25,26].

Computational studies of cyclist crash scenarios use combinations of multibody and finite element models to provide useful insight into common head impact configurations [10-13,24]. While results from these studies elucidate trends in cyclist head impacts, their absolute accuracy is limited by a lack of cyclist head impact data available for simulation validation. Damage reconstructions have the potential to provide more concrete head impact data by reverse engineering initial impact conditions [27]. Conventional bicycle helmets are comprised of a plastic outer shell and an inner expanded polystyrene (EPS) liner that crushes permanently upon impact, dissipating energy that would otherwise be transferred to the head. The residual helmet liner damage can be recreated through iterative laboratory testing to pristine samples of an identical helmet model until a suitable replicate is generated. Although a promising method, previous bicycle helmet reconstruction studies have been limited by simplified test setups and measurement techniques [25-28]. These studies have utilized standards test equipment with a flat anvil, which fails to address the oblique nature of many cyclist head impacts, and have evaluated liner damage by removing the shell and directly measuring liner thickness at several locations on the helmet. As present-day bicycle

helmet liners are typically in-molded into the shell, removal of the shell can be a particularly destructive process, complicating the assessment of liner damage.

Recent motorcycle helmet damage reconstruction studies have employed more advance testing and quantification techniques [28-30]. One study subjected motorcycle helmets to a variety of impact anvils, including anvils of differing shapes and angled anvils to simulate oblique impacts, and reported that visual observation-based measurements of shell and liner damage reflected the profile and angle of the anvil [28]. Others have explored the use of computed tomography (CT) as a more comprehensive method for assessing liner damage [29,30]. The use of CT for helmet damage assessment has been proposed as early as 1990 [31], and provides a non-destructive method for damage quantification that can account for spacing between the shell and liner that may result from impact. CT scans can be used to generate 3D models of helmets, and metrics such as maximum crush depth and volume can then be ascertained by overlaying the damaged helmet model with a model of an identical, undamaged helmet [29]. Paired with visual inspection and measurement of shell damage, this liner damage quantification technique enables an in-depth portfolio of damage characteristics to be formulated, which can ultimately enhance the damage reconstruction process.

Oblique impact bicycle helmet damage reconstructions have the potential to improve knowledge of common cyclist head impact conditions, which in turn can facilitate optimal design of helmets around these conditions. To the authors' knowledge, no bicycle helmet damage reconstruction studies using oblique impacts have been published to-date, nor have any that use CT to quantify damage to bicycle helmets for the reconstruction process. In order to establish oblique impact testing as a method for reconstructing bicycle helmet damage, it is important to understand how variations in applied laboratory impact conditions, such as impact angle and speed, affect both

visual and CT-derived helmet damage characteristics and resulting kinematics. Establishing relationships between impact conditions and damage metrics can also inform future damage testing, minimizing the number of tests required to complete reconstructions and reducing associated costs. The objective of the present study was thus to explore the utility of oblique impact testing and CT for reconstructing bicycle helmet damage by investigating the sensitivity of damage metrics and head impact kinematics to varied impact conditions.

METHODS

Oblique Impact Testing

Twenty-five Schwinn Intercept bicycle helmets were purchased for parametric, oblique impact testing. This helmet was chosen to represent a conventional road helmet, consisting of an EPS liner and a thin, polycarbonate shell, and having an elongated shape with several large vents. The permanent nature of impact damage to bicycle helmets necessitated that each helmet be tested only once. Prior to testing, helmets were fitted to a medium National Operating Committee on Standards for Athletic Equipment (NOCSAE) headform such that the helmet rim sat 1 inch above the brow line, then tightened according to manufacturer recommendation. The NOCSASE headform has enhanced biofidelity compared to headforms used in standards, is compatible with instrumentation capable of measuring linear and rotational impact kinematics, and is widely used in sports head impact testing [32-36]. The headform was not attached to any anthropomorphic test device (ATD) neck, as previous studies have suggested that oblique impacts may subject ATD necks to variable axial compressive forces, a loading regime in which common ATD necks are known to produce notably unrealistic impact responses compared to human necks [37-39]. Other studies have shown the human neck to play a minimal role in the initial head impact response during head-first impacts [39], so forgoing a neck was deemed reasonable herein.

The helmeted headform was positioned in a support ring connected to a custom oblique impact drop tower previously used in several bicycle helmet impact studies [37,40] (Fig. 9.1). Oblique impacts were created using an angled anvil, which generates normal and tangential incident velocities characteristic of cyclist head impacts. The anvil angle was adjustable from a range of 0 to 60° from the horizontal. Impact angles of 0, 15, 30, 45, and 60° were evaluated, representing a range of cyclist head impact angles predicted from computational simulation studies [10-12]. Testing was conducted at 1.0, 2.5, 4.0, 5.5, and 7.0 m/s at each angle, producing normal velocities ranging from 0.5 to 7.0 m/s and tangential velocities ranging from 0.0 to 6.1 m/s. For every test, the anvil surface was coated with sandpaper in order to simulate the road friction environment (80 grit, [41]). Helmets were set to impact the anvil at a parietal location for all tests, using a dual axis inclinometer (DMI600, Omni Instruments, Dundee, UK) mounted to the base of the headform to ensure precision in impacting this location. Once the helmeted headform was adjusted into position, it was secured in place from above using an additional support arm. During testing, the arm released just prior to impact while the support ring passed around the outside of the anvil upon impact, allowing the headform to move independently. Impact velocity was recorded for every test using a photogate (BeeSpi V, NaRiKa Corp., Tokyo, Japan).

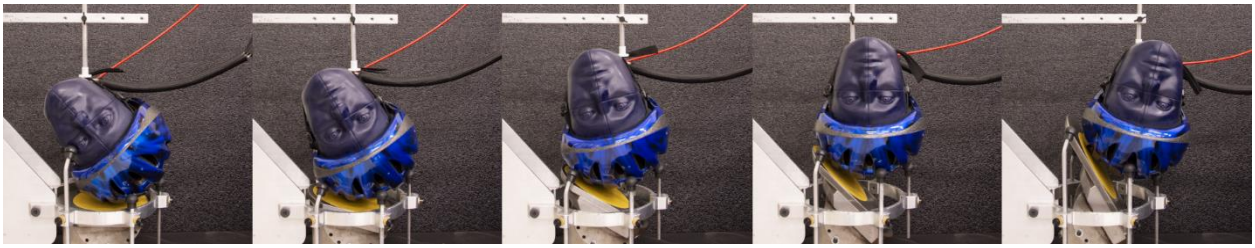

Figure 9.1. Positioning of the helmeted headform at each impact angle. Anvil angles range from 0° (left) to 60° (right) in 15° increments. Impacting the same parietal location for all tests required that the headform be rotated accordingly by 15° increments.

Kinematic data were collected at 20 kHz during all tests using three linear accelerometers (Endevco 7264B-2000, Meggitt Sensing Systems, Irvine, CA) and a tri-axis angular rate sensor (ARS3 PRO-18K, DTS, Seal Beach, CA) located at the head center of gravity (CG). Both linear acceleration and rotational velocity traces were filtered using 4-pole, phaseless Butterworth low-pass filters. A channel frequency class (CFC) of 1000 was employed for linear acceleration, in accordance with SAE J211, while a CFC of 175 was used for rotational velocities, which previous studies have shown to optimize rotational response curves relative to nine accelerometer array (9AA) responses [23,42]. An ARS was selected over the more conventional 9AA for its compact size, which is more compatible with the small instrumentation channel of the NOCSAE headform. Resultant traces were used to determine peak linear acceleration (PLA) and peak rotational velocity (PRV) for all tests.

Damage Quantification

After each test, visual observations of helmet damage were noted, and the length of the helmet shell scrape profile in the direction of scraping was recorded. Helmets were then CT scanned for further quantification at 120 kV and 200 mA with 0.625 x 0.625 mm pixel spacing and a slice thickness of 0.5 mm (Aquilion, Canon Medical Systems, Tustin, CA). Two undamaged helmets were also scanned prior to testing to provide an undamaged reference case and a control case. Digital Imaging and Communications in Medicine (DICOM) files of the scans were imported into Mimics Research 21.0 (Materialise, Leuven, Belgium). Helmet liners were segmented into masks using a Hounsfield unit (HU) density range of -960 to -850. As other features within the CT scanner environment also fell within this HU range, semi-automated operations within Mimics were used to split the liner mask from extraneous mask regions. Manual editing of individual slices was also employed as needed to correct for any image artifact arising from nearby high-density regions. Completed masks were then auto-meshed into 3D models comprised of a triangular surface mesh

(>600,000 elements per model), and models were smoothed to reduce pixilation effects.

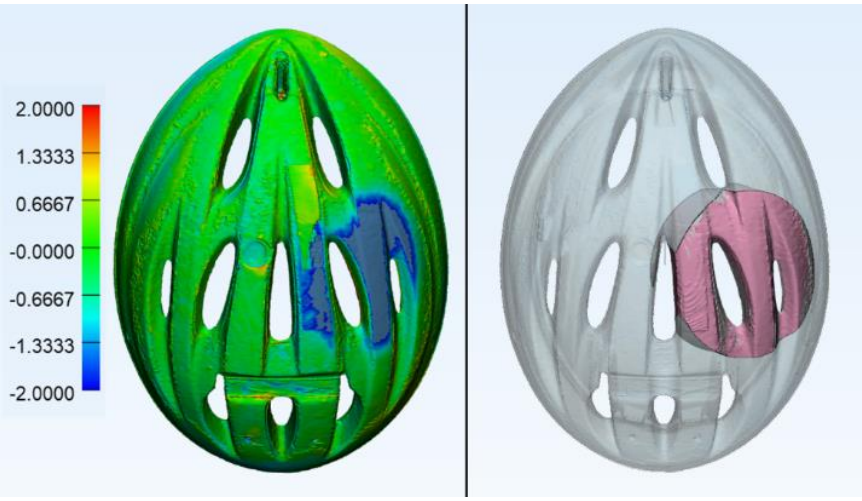

Figure 9.2. Crush region heat map (left) showing the distance offsets between undamaged and tested helmet models. A cylindrical volume encompassing the crushed region (right) was defined, wherein the damaged volume was subtracted from the undamaged volume to yield crush volume.

Models were imported into 3-matic Research 13.0 (Materialise, Leuven, Belgium) for damage assessment. The model of the helmet of interest was overlaid onto the undamaged helmet model using a linear registration operation that minimized the average distance error between a subset of similar model nodes. The two undamaged helmet models were overlaid to provide control measurements, with one undamaged model selected as a reference model. Liner crush regions on the tested helmets were visualized using a heat map reflecting approximate Hausdorff distances between every node on the reference undamaged model to the nearest node on the tested model (Fig. 9.2). Crush area was defined as the area of the damaged model's outer surface exceeding a 0.5 mm negative offset from the undamaged model. The thresholds of the heat map were then increased until the outer surface node with the greatest offset was located. Radial thicknesses of the undamaged and damaged liners at this location were subtracted to determine

the maximum crush depth, and the coordinates of the corresponding node on the outer surface of the undamaged model was recorded as the max crush location. The distance between the max crush depth node and the superior and inferior bounds of the crush area in the direction of scraping was measured. The ratio of the superior to inferior distances was taken to indicate the centeredness of the crush profile. Model volume was then measured within a cylindrical region encompassing the crush area and extending radially through the helmet liners (Fig. 9.2). The cylindrical volumes of the damaged and undamaged liners were subtracted to yield crush volume.

Statistical Analysis

Error associated with the testing and damage quantification process was assessed in multiple ways. Averages and standard deviations of the max crush location node coordinates were calculated to ascertain the precision with which the intended location was impacted across all tests. Overall volumes of the control undamaged helmets were subtracted to indicate error arising from manufacturing differences, scan resolution, and the segmentation process. Differences in control liner radial thicknesses were computed at the max crush location from every test, allowing an average depth error to be determined. Similarly, the cylindrical regions used to calculate crush volume for each test were superimposed onto the control samples, and control volume error specific to the cylindrical regions was calculated by subtracting the two control liner volumes within the region. This error was then normalized by the reference undamaged liner cylindrical volume to account for the varying sizes of the cylindrical volumes between tests. The average normalized cylindrical volume error across all tests was computed. The relationship between normalized volume error and cylinder size, which reflects the size of the crush area, was also assessed.

Pearson's correlations coefficients were used to investigate associations between PLA and PRV and anvil angle and velocity, as well as between PLA and PRV and component normal and

tangential velocities. Evaluating impact response trends using normal and tangential velocities, which are functions of resultant velocity and impact angle, may be more mechanistic than using resultant velocity and impact angle alone [43]. Correlations were also assessed between damage metrics (i.e. scrape length, crush area, max crush depth, crush centeredness, crush volume) and normal and tangential velocities, and between PLA and PRV and damage metrics. Specific relationships between damage metrics and normal and tangential velocities were further investigated using multiple linear regression (MLR) models. Model terms were successively removed in order of least statistical significance until a model comprised entirely of significant terms ($p<0.05$) was obtained.

RESULTS

A wide range in kinematics values was observed across all applied impact velocities and angles, with PLA spanning 19.2-247.7 g and PRV spanning 2.2-39.1 rad/s (Fig. 9.3). Both PLA and PRV increased with increasing velocity ($R>0.63$, $p<0.01$). Increasing anvil angle was associated with significant increases in PRV ($R=0.67$, $p<0.01$) and decreases, albeit not significant, in PLA ($R=-0.39$, $p=0.06$). The 15° degree anvil produced the highest average PLA (134.3±77.0 g) and the lowest average PRV (5.9±3.0 rad/s) compared to all other angles. Breaking down resultant velocities and impact angles into normal and tangential velocities allowed correlations between impact conditions and kinematics to be further investigated. PLA was strongly correlated with normal velocity ($R=0.99$, $p<0.01$), but not tangential ($R=0.16$, $p=0.45$). Conversely, PRV was strongly correlated with tangential velocity ($R=0.96$, $p<0.01$), but not normal ($R=0.24$, $p=0.25$).

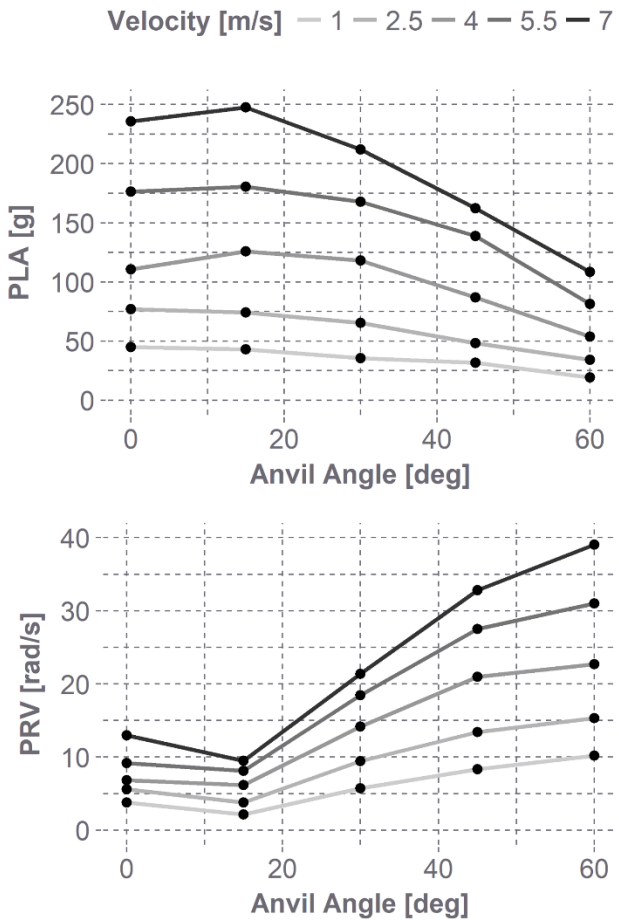

Figure 9.3. Kinematic results versus anvil angle across all velocities. PLA and PRV increased with velocity, while increasing anvil angles generally decreased PLA and increased PRV.

Minimal manual editing was required to segment helmet liners during CT scan processing, producing 3D liner models that reflected actual liner geometries with high fidelity. The mean approximated Hausdorff distance between all nodes of the two undamaged control helmet liners was -0.07 mm (first and third quartile values of -0.25 and 0.14 mm, respectively). The volumes of the two control liners differed by 17.1 cm^3, with the reference liner volume measuring 2352.9 cm^3 (volume error of 0.73%). Identifying max crush locations by overlaying tested helmet 3D liner models onto the undamaged reference liner revealed an average distance of 0.8±0.7 cm between the max crush location from each individual test to the overall mean max crush location. This

distance was not significantly affected by anvil angle ($R=-0.17$, $p=0.42$), but decreased significantly with increasing resultant velocity ($R=-0.56$, $p<0.01$). Projecting the max crush locations from each test onto the control liners and subtracting the two control liner radial thicknesses at these locations produced an average thickness error of 0.21±0.22 mm. In a similar fashion, superimposing the cylindrical regions used to compute crush volume for each test onto the control liners and subtracting the associated control liner volumes produced a volume error of 1.48±1.62 cm^3 (0.57±0.31% when normalized to the reference liner cylindrical volume). Volume error increased with increasing cylinder radius, even when normalized by the reference cylindrical volume ($R=0.84$, $p<0.01$).

Across all tests, scrape length ranged from 2.6-5.0 cm, crush area ranged from 3.1-112.0 cm^2, max crush depth ranged from -0.39-10.13 mm, crush centeredness ranged from 0.3-2.3, and crush volume ranged from -0.2-35.2 cm^3. The 1.0 m/s, 60° test helmet did not show detectable liner damage when overlaid onto the reference undamaged model, although scraping was evident on the shell surface. Crush area, max crush depth, and crush volume were accordingly assigned a value of 0 for this test, and the crush centeredness ratio was omitted. Correlations were then assessed between all damage metrics and normal and tangential velocities (Table 9.1). Crush area, max crush depth, and crush volume were highly correlated with normal velocity ($p<0.01$). Scrape length and crush centeredness were significantly correlated with tangential velocity, with scrape length yielding a greater correlation coefficient. No metric was significantly correlated with both velocities. Centeredness measurements were complicated by the presence of vents superior and inferior to the max crush location. For the lower velocity impacts (i.e. 1.0 and 2.5 m/s), the crush was often severe enough to extend into the vent regions but not severe enough to extend past them, obscuring the superior and inferior bounds of the crush area that were used to calculate centeredness. Correlations using centeredness were therefore assessed using only the tests

having impact velocities of 4.0, 5.5, and 7.0 m/s. All damage metrics were then also correlated with PLA and PRV. PLA was best correlated with max crush depth ($R=0.98$, $p<0.01$), while PRV was best correlated with scrape length ($R=0.95$, $p<0.01$) (Fig. 9.4).

Table 9.1. Significant correlations ($p<0.5$) between normal and tangential velocities and damage metrics. *Crush centeredness was only assessed for impact velocities 4.0-7.0 m/s.

Velocity	Damage Metric	R	p
Normal [m/s]	Area [cm^2]	0.973	<0.001
	Depth [mm]	0.974	<0.001
	Volume [cm^3]	0.916	<0.001
Tangential [m/s]	Scrape [cm]	0.901	<0.001
	Centeredness*	0.844	<0.001

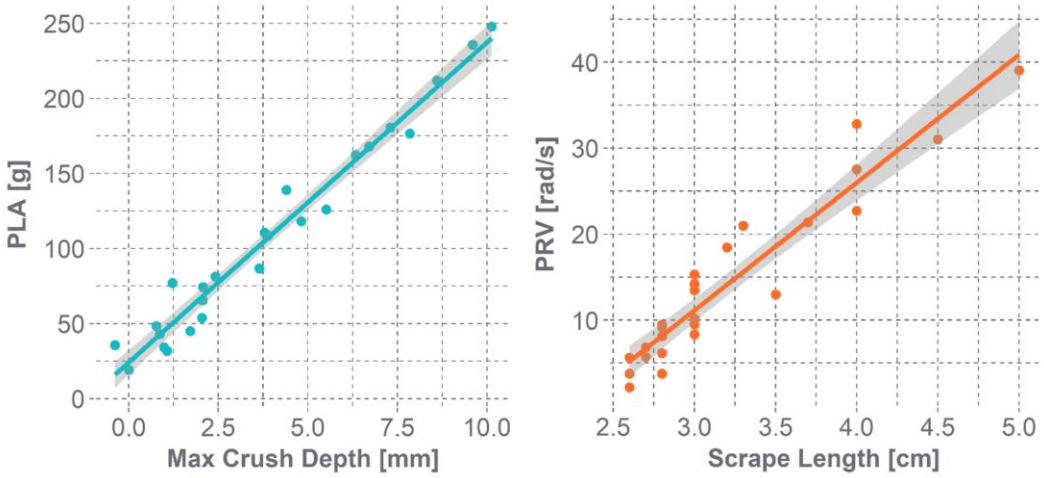

Figure 9.4. Correlations between kinematic measurements and damage metrics. PLA was best correlated with max crush depth (top), and PRV was best correlated with scrape length (bottom). Shaded regions represent 95% prediction intervals.

MLR models shed further light on the relationships between damage metrics and normal and tangential velocities (Table 9.2, Fig. 9.5). Max crush depth was the only damage metric that did

not contain both normal and tangential velocity factors in its model, depending significantly only on normal velocity. Crush area and volume both depended significantly on normal velocity, tangential velocity, and the interaction between the two. However, both of these metrics demonstrated an inflection point around a normal velocity of ~4 m/s, at which point the damage severity depended primarily on normal velocity. At normal velocities less than 4 m/s, damage severity decreased with increasing tangential velocity, and at normal velocities greater than 4 m/s, severity increased with increasing tangential velocity. Scrape length similarly showed an inflection point around a tangential velocity of ~2 m/s; at higher tangential velocities, increasing normal velocity caused decreases in scrape length, whereas at lower tangential velocities, increasing normal velocity caused increases in scrape length. The scrape length model also contained significant normal and tangential velocity terms as well as an interaction term.

Table 9.2. Damage metric MLR models as functions of normal and tangential velocities (norm and tan factors, respectively). Only significant terms ($p<0.05$) were included in each model. *The centeredness model was computed using only velocities ranging from 4.0-7.0 m/s.

Damage metric	Factor	Coefficient	p	Model
Scrape	*intercept*	2.31	<0.001	*Scrape* = 2.31 + 0.09 x *norm* + 0.52 x *tan* – 0.05 x *norm* x *tan*
	norm	0.09	0.030	
	tan	0.52	<0.001	
	norm x *tan*	-0.05	0.022	
Area	*intercept*	-9.49	0.033	*Area* = -9.49 + 16.21 x *norm* – 7.51 x *tan* + 1.87 x *norm* x *tan*
	norm	16.21	<0.001	
	tan	-7.51	0.007	
	norm x *tan*	1.87	0.008	
Depth	*intercept*	-1.13	0.001	*Depth* = -1.13 + 1.56 x *norm*
	norm	1.56	<0.001	
*Centeredness**	*norm*	0.12	<0.001	*Centeredness* = 0.12 x *norm* + 0.21 x *tan*
	tan	0.21	<0.001	
Volume	*norm*	3.05	<0.001	*Volume* = 3.05 x *norm* – 4.65 x *tan* + 1.13 x *norm* x *tan*
	tan	-4.65	<0.001	
	norm x *tan*	1.13	<0.001	

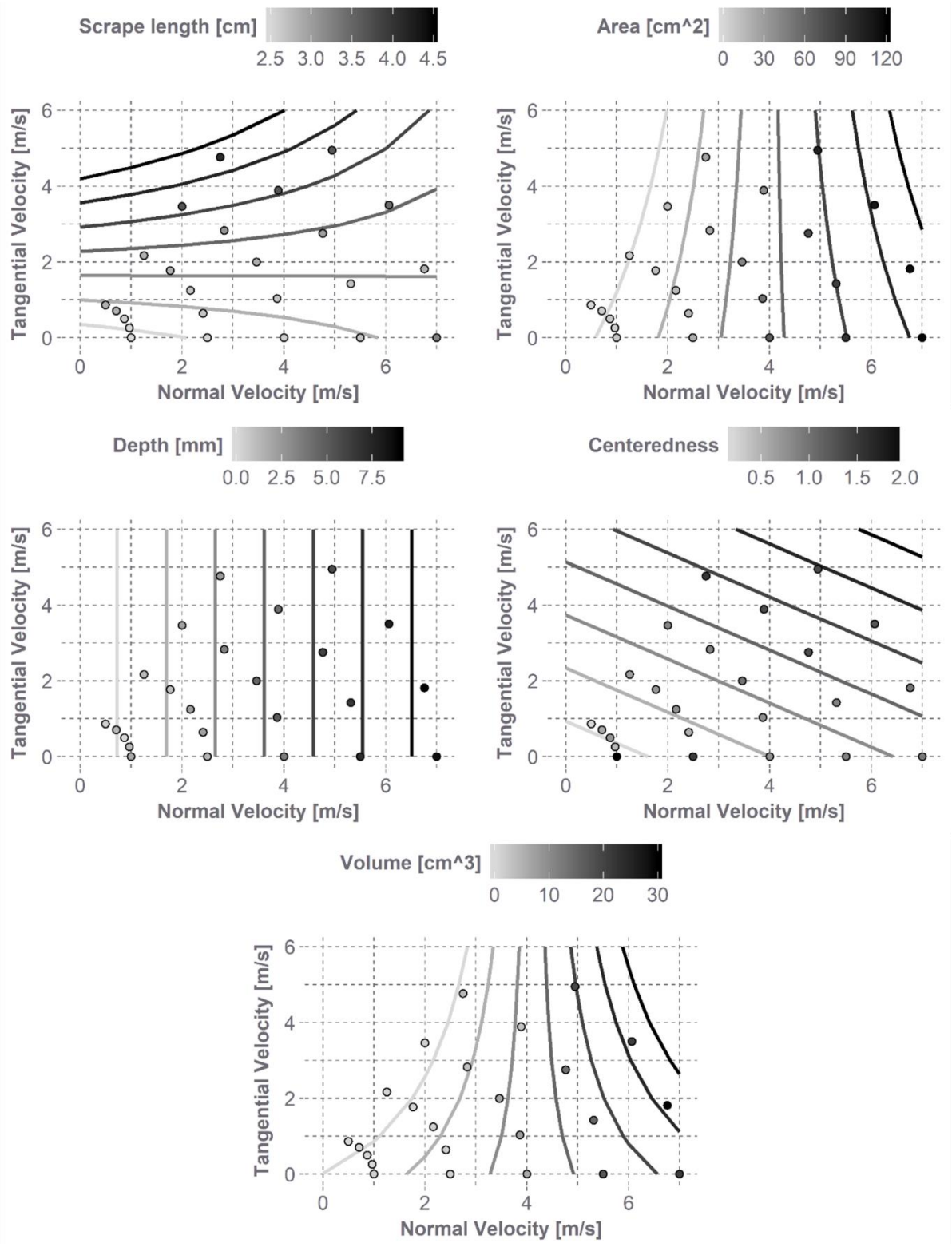

Figure 9.5. Damage metric results as functions of normal and tangential velocities. The points on each plot represent individual tests and are shaded to reflect damage metric severity. The

contours represent the predicted MLR model results for each damage metric and are also shaded to reflect damage metric severity. The centeredness MLR model was calculated based on velocities 4.0-7.0 m/s only, although its plot shows all data points.

DISCUSSION

To investigate the sensitivity of bicycle helmet damage reconstruction metrics to varied oblique impact conditions, helmets were tested under an array of impact angles and resultant velocities. A considerable range in measured impact kinematics was produced across all tests. Trends in PLA and PRV were generally well-correlated with impact angle and velocity. The increases in peak kinematics observed with increasing velocity are intuitive, as increasing impact velocity directly increases impact energy. Less intuitive were the highest average PLA and lowest average PRV produced at the 15° anvil. These results may relate to the orientation of the head relative to gravity (Fig. 1); at 15°, the reaction forces stemming from the contact point of the helmet on the anvil extended closest to the CG of the headform. For angles greater than 15°, the contact point fell further to the left of the head CG, and for the 0° anvil, the contact point fell to the right of the head CG. Increasing the distance between the contact point reaction force vector and the head CG increases the resulting moment arm and thereby the rotational kinematics. Additional analysis of the rotational velocities revealed that velocity about the X axis (SAE J211 coordinate system) indeed increased with increasing anvil angle from 15-60° and switched polarity at 0°. Further, when the reaction force vector is closer to direct alignment with the CG, most of the mass is directed through the contact point and resulting linear kinematics are increased.

Correlations between peak kinematics and impact conditions were stronger when evaluating impact conditions in terms of normal and tangential velocities. Specifically, PLA was highly correlated with normal velocity and PRV with tangential velocity. Previous studies have similarly

demonstrated strong relationships between PLA and applied normal velocity [43-45]. PLA has been shown to remain roughly constant in motorcycle helmet oblique impact simulations when tangential velocities are increased and normal velocities are held constant [45]. For a limited range of impact velocities, peak rotational acceleration (PRA) has also been shown to relate linearly to peak tangential force [44], factors that are directly related to PRV and applied tangential velocity, respectively. While the relationships between peak kinematics and normal and tangential velocities have been established, they are largely modulated by head orientation. Rotational kinematics are especially influenced by head orientation, as the changing distance between the contact point and the head CG cause the moments applied by the normal and tangential impact forces to counteract each other to varying degrees [44]. The present results suggest that the 15° anvil produced optimal alignment of the head for the normal and tangential forces to counteract each other; however, at the same anvil angle, moving the impact location closer to the helmet rim would require the head to be oriented more parallel to the anvil surface, which would increase the distance between the head CG and contact point and consequently increase the moment arm of the normal impact force. The sensitivity of rotational kinematics to changing impact angle should thus always be evaluated with regard to head orientation.

The sensitivity of various damage metrics to impact conditions was assessed using CT-based quantification supplemented with visual observation. The high fidelity with which CT scans rendered volumes of each liner highlights the suitability of CT as a technique for helmet damage quantification. Nonetheless, minor error exists in the quantification process. The 0.73% overall volume error between control liners likely points to manufacturing differences as well as noise associated with CT resolution. The error between control helmets translated to an average liner thickness error of 0.21±0.22 mm (0.66±0.77%) and an average cylindrical volume error of 1.48±1.62 cm^3 (0.57±0.31%) within the impacted region. Reconstruction of liner crush depth and

volume within these ranges of uncertainty is therefore less reliable. It should be noted that the measured crush volume did not exceed 1.48 cm^3 in any impacts below 4.0 m/s, while max crush depth exceeded 0.21 mm for all impacts but two at 1.0 m/s, suggesting crush depth may be more readily quantified at lower impact severities than crush volume. Interestingly, volume error increased with disproportionately with increasing size of the cylindrical volume region, averaging 0.37±0.20% error at 1.0 and 2.5 m/s, and 0.83±0.23% error at 5.5 and 7.0 m/s. In order to minimize measurement error in crush volume assessment, best practice is thus to minimize the measurement region size to only encompass the crush region. This is critical for lower severity impacts where the crush volume is minimal and more difficult to detect. Error in the max crush location was also higher at the lower impact velocities, likely resulting from greater noise-to-damage ratios and slight variability in positioning the helmet for impact.

Normal and tangential velocities had a strong influence on damage metrics, with normal velocity correlating best with max crush depth and area and tangential velocity correlating best with scrape length. Due to the high expense of CT, it is most practical for undamaged helmets to be iteratively tested in batches prior to scanning. During this process, successive impact conditions are informed by visual observation of damage from previous impacts. Understanding how normal and tangential velocities correlate with damage characteristics is thus very useful in minimizing the number of samples required to reconstruct the desired damage. However, there are also potential limitations to the reliability of quantifying certain metrics. Although crush area was well correlated with normal velocity in the present results, area quantification is highly dependent on the offset threshold used to determine crush bounds. Registering damaged liners onto the reference undamaged liner is subject to slight variability stemming from inherent volume differences, and the slight changes in surface offsets this could create may limit the accuracy of crush area from helmet to helmet. These effects are likely more pronounced with helmets damaged in real-world

crashes, which often present additional wear from general use. Further, vent location has large effects on damage quantification. Adjusting an impact location slightly relative to a vent can greatly influence crush area, volume, and centeredness measurements. Damage results should thus be assessed with location differences in mind. In the present study, centeredness measurement was very affected by nearby vents, although at higher velocities, centeredness increased with increasing tangential velocity, suggesting that the head rotated down the anvil more upon impact for steeper angles.

The present MLR models further elucidate specific relationships between damage metrics and normal and tangential velocities. Crush volume, area, and scrape length showed significant associations with both velocities and their interaction. Inflection points were observed in these metrics' models. Increasing normal velocity decreased scrape length at high tangential velocities, but had the opposite effect at low tangential velocities. While higher tangential velocities can cause the helmet to slide during impact, increasing normal velocity increases normal force and the resulting friction force. At high enough friction forces, the helmet will begin to roll rather than slide during impact [44], possibly reducing the appearance of scraping. At low tangential velocities, increases in scrape length with increasing normal velocities may merely reflect the growing size of the crush region. Crush volume and area similarly showed an inflection point, wherein increasing tangential velocity produced more severe damage in impacts at a high normal velocity, but less severe damage in impacts at a low normal velocity. At high normal velocities, increasing tangential velocity may increase the crush severity simply by increasing the energy of impact. At low normal velocities, the normal force may be too low to generate detectable liner crush, especially if the force is insufficient to buckle the helmet shell. Increasing the tangential velocity at these low normal velocities may further deflect the impact energy away from buckling the shell and crushing the liner. It is also possible that the observed MLR trends are influenced in

part by the nonuniform spacing of the normal and tangential velocities evaluated. In any case, generating similar helmet-specific damage MLR models during the reconstruction process can help fine-tune predictions of the necessary impact conditions for reproducing the original damage.

Damage metrics also showed significant associations with kinematic results, indicating that helmet characteristics influence or reflect the impact severity experienced by the head. PLA was best correlated to max crush depth. As standards mandate that bicycle helmets reduce linear accelerations during normal impacts, helmet design for decades has been centered around the EPS liner crushing effectively with normal force and limiting the PLA experienced by the head. This trend between PLA and liner crush has previously been demonstrated in other studies as well [29]. It has been suggested that liner crush also plays a minor role in mitigating the rotational forces experienced by the head [43,44]. While no significant correlation was found between crush metrics and PRV in the present results, only one helmet was evaluated herein. Previous work comparing the impact performance of a number of bicycle helmets during oblique impacts showed helmets that reduced linear kinematics more effectively to also reduce rotational kinematics more effectively [23], which may suggest that mechanisms reducing linear accelerations within helmet models are not fully independent from those that reduce rotational. The normal force of an oblique impact rarely passes through the CG of the headform [44], so liner crush may reduce rotational kinematics in part by reducing the moment exerted by the normal force. In the present study, PRV was best correlated with scrape length. As shell scraping is not an impact-reducing mechanism, there is room for innovation in helmet technology to further reduce rotational forces transferred to the head. The high number of brain injuries such as concussion associated with cycling further support this [7]. Fortunately, several such technologies are already emerging for bicycle helmets.

There are several limitations to the present study. Only one impact location and one helmet model

were evaluated with one trial per condition in order to limit the test matrix size and the number of CT scans, which are costly. Previous work has shown low variance associated with CT-derived damage metrics and kinematics from helmet impact testing [29]. Results are specific to this helmet and location, although general trends likely hold true across other conditions as well. Additionally, at high impact forces, EPS can fully densify and transfer force directly to the head, which causes extreme PLAs and would influence the trends identified herein. The tested velocities, reflecting a reasonable range for cyclists with normal velocities even exceeding those in standards, were not severe enough to create this phenomenon at the chosen impact location. CT scans also present the potential limitation of artifact resulting from nearby high density materials. No substantial artifact was apparent in scanning the selected helmet model, and the liner could be segmented reliably with relative ease. Damage quantification was limited by helmet venting for some metrics. Scrape length measurement is also somewhat subjective, as the bounds of the scrape region are not always clear. Other limitations pertain to the testing setup; the steel anvil used likely results in greater peak kinematics and helmet damage than a less-stiff road surface [46], testing without an ATD neck may produce greater kinematics and reduced liner crush than testing with [37,47], and the ATD headform may present slight variations in results than a human headform [29]. In reality, cyclist head impacts are often fairly complex events, and the present damage reconstruction methods can serve to approximate associated conditions and kinematics. These methods represent enhanced accuracy compared to previous damage reconstruction methods.

CONCLUSIONS

In order to explore the utility of oblique impact testing and CT for reconstructing bicycle helmet damage, the present study evaluated the sensitivity of various bicycle helmet damage metrics and head impact kinematics to varied oblique impact test conditions. Linear and rotational kinematics were highly correlated with applied normal and tangential velocities, respectively. CT

scanning produced highly accurate 3D models of the helmet liners, allowing a quantitative portfolio of damage metrics to be developed. Maximum liner crush was best correlated to normal velocity and resulting PLA across the range of applied velocities herein, although crush area and volume were also highly correlated with normal velocity. MLR models of liner crush metrics further revealed that crush volume and area may be influenced in part by tangential velocities as well. Length of shell scraping, which was measured visually, was best correlated to tangential velocity and resulting PRV, and was also influenced slightly by normal velocity. At sufficiently high velocities, the relative centeredness of the liner crush profile also reflected applied tangential velocities. Conducting bicycle helmet damage reconstructions using oblique impacts and CT, supplemented with visual analysis, has the potential to enhance the accuracy of reconstructions, further informing knowledge of common cyclist head impact conditions and allowing helmet design to reflect such conditions.

REFERENCES

1. Thompson, D.C., Rivara, F.P., and Thompson, R. Helmets for preventing head and facial injuries in bicyclists. *Cochrane Database Syst. Rev.*, 2010(2): p. CD001855
2. Olivier, J. and Creighton, P. Bicycle injuries and helmet use: a systematic review and meta-analysis. *Int. J. Epidemiol.*, 2017. 46(1): p. 278-292
3. McIntosh, A.S., Lai, A., and Schilter, E. Bicycle helmets: head impact dynamics in helmeted and unhelmeted oblique impact tests. *Traffic Inj. Prev.*, 2013. 14(5): p. 501-8
4. Amoros, E., Chiron, M., Martin, J.L., Thelot, B., and Laumon, B. Bicycle helmet wearing and the risk of head, face, and neck injury: a French case--control study based on a road trauma registry. *Injury prevention : journal of the International Society for Child and Adolescent Injury Prevention*, 2012. 18(1): p. 27-32
5. Cripton, P.A., Dressler, D.M., Stuart, C.A., Dennison, C.R., and Richards, D. Bicycle helmets are highly effective at preventing head injury during head impact: head-form accelerations and injury criteria for helmeted and unhelmeted impacts. *Accident Analysis & Prevention*, 2014. 70: p. 1-7
6. CPSC. "National Electronic Injury Surveillance System Database" Internet www.cpsc.gov/en/Research--Statistics/NEISS-Injury-Data/. July 26, 2016].
7. Coronado, V.G., Haileyesus, T., et al. Trends in Sports- and Recreation-Related Traumatic Brain Injuries Treated in US Emergency Departments: The National Electronic Injury Surveillance System-All Injury Program (NEISS-AIP) 2001-2012. *J. Head Trauma Rehabil.*, 2015. 30(3): p. 185-197
8. European Committee for Standardization (CEN) 1078: Helmets for pedal cyclists and for users of skateboards and roller skates. 1997.

9. CPSC. Safety Standard for Bicycle Helmets Final Rule (16 CFR Part 1203). 1998, United States Consumer Product Safety Commission. p. 11711-11747.
10. Verschueren, P. Biomechanical analysis of head injuries related to bicycle accidents and a new bicycle helmet concept, in *Faculteit Ingenieurswetenschappen Departement Werktuigkunde Afdeling Biomechanica en Grafisch Ontwerpen*. 2009, Katholieke Universiteit Leuven: Leuven, Belgium.
11. Bourdet, N., Deck, C., et al. In-depth real-world bicycle accident reconstructions. *Int. J. Crashworthiness*, 2014. 19(3): p. 222-232
12. Bourdet, N., Deck, C., Carreira, R.P., and Willinger, R. Head impact conditions in the case of cyclist falls. *Proc. Inst. Mech. Eng. P*, 2012. 226(3-4): p. 282-289
13. Peng, Y., Chen, Y., Yang, J., Otte, D., and Willinger, R. A study of pedestrian and bicyclist exposure to head injury in passenger car collisions based on accident data and simulations. *Safety Science*, 2012. 50(9): p. 1749-1759
14. Gennarelli, T., Ommaya, A., and Thibault, L. Comparison of translational and rotational head motions in experimental cerebral concussion. *Proceedings of 15th Stapp Car Crash Conference*, 1971.
15. Gennarelli, T.A., Thibault, L.E., and Ommaya, A.K. Pathophysiologic responses to rotational and translational accelerations of the head. *SAE Technical Paper Series*, 1972. 720970: p. 296-308
16. Gennarelli, T.A., Thibault, L.E., et al. Diffuse axonal injury and traumatic coma in the primate. *Ann Neurol*, 1982. 12(6): p. 564-74
17. King, A.I., Yang, K.H., Zhang, L., Hardy, W., and Viano, D.C. Is Head Injury Caused by Linear or Angular Acceleration?, in *IRCOBI Conference*. 2003: Lisbon, Portugal. p. 1-12.
18. Hardy, W.N., Mason, M.J., et al. A study of the response of the human cadaver head to impact. *Stapp Car Crash J.*, 2007. 51: p. 17-80
19. Milne, G., Deck, C., et al. Bicycle helmet modelling and validation under linear and tangential impacts. *Int. J. Crashworthiness*, 2014. 19(4): p. 323-333
20. Mills, N.J. and Gilchrist, A. Oblique impact testing of bicycle helmets. *Int. J. Impact Eng.*, 2008. 35(9): p. 1075-1086
21. Pang, T.Y., Thai, K.T., et al. Head and neck responses in oblique motorcycle helmet impacts: a novel laboratory test method. *International Journal of Crashworthiness*, 2011. 16(3): p. 297-307
22. Aare, M. and Halldin, P. A new laboratory rig for evaluating helmets subject to oblique impacts. *Traffic injury prevention*, 2003. 4(3): p. 240-8
23. Bland, M.L., McNally, C., and Rowson, S. Differences in Impact Performance of Bicycle Helmets During Oblique Impacts. *J. Biomech. Eng.*, 2018. 140(9)
24. Fahlstedt, M., Baeck, K., et al. Influence of Impact Velocity and Angle in a Detailed Reconstruction of a Bicycle Accident. *IRCOBI Conference*, 2012. 12(84): p. 787-799
25. Smith, T.A., Tees, D., Thom, D.R., and Hurt, H.H. Evaluation and replication of impact damage to bicycle helmets. *Accid. Anal. Prev.*, 1994. 26(6): p. 795-802
26. Williams, M. The protective performance of bicyclists' helmets in accidents. *Accid. Anal. Prev.*, 1991. 23(2-3): p. 119-131
27. McIntosh, A.S. and Patton, D.A. Impact reconstruction from damage to pedal and motorcycle helmets. *Proceedings of the Institution of Mechanical Engineers, Part P: Journal of Sports Engineering and Technology*, 2012. 226(3-4): p. 274-281
28. Chinn, B., Canaple, B., et al. COST 327: Motorcycle Safety Helmets, B. Chinn, Editor. 2001, European Commission, Directorate General for Energy and Transport: Belgium.
29. Bonin, S.J., Luck, J.F., et al. Dynamic Response and Residual Helmet Liner Crush Using Cadaver Heads and Standard Headforms. *Ann Biomed Eng*, 2017. 45(3): p. 656-667

30. Loftis, K.L., Moreno, D.P., Tan, J., Gabler, H.C., and Stitzel, J.D. Utilizing computed tomography scans for analysis of motorcycle helmets in real-world crashes. *Proceedings of 48th Rocky Mountain Bioengineering Symposium & 48th International ISA Biomedical Sciences Instrumentation Symposium*, 2011. Denver, Colorado
31. Cooter, R.D. Computed tomography in the assessment of protective helmet deformation. *The Journal of trauma*, 1990. 30(1): p. 55-68
32. Cobb, B.R., Zadnik, A.M., and Rowson, S. Comparative analysis of helmeted impact response of Hybrid III and National Operating Committee on Standards for Athletic Equipment headforms. *Proceedings of the Institution of Mechanical Engineers, Part P: Journal of Sports Engineering and Technology*, 2015. 230(1): p. 50-60
33. Cobb, B.R., MacAlister, A., et al. Quantitative comparison of Hybrid III and National Operating Committee on Standards for Athletic Equipment headform shape characteristics and implications on football helmet fit. *Proceedings of the Institution of Mechanical Engineers, Part P: Journal of Sports Engineering and Technology*, 2014. 229(1): p. 39-46
34. Rowson, B., Rowson, S., and Duma, S.M. Hockey STAR: A Methodology for Assessing the Biomechanical Performance of Hockey Helmets. *Ann. Biomed. Eng.*, 2015. 43(10): p. 2429-2443
35. Bartsch, A., Benzel, E., Miele, V., and Prakash, V. Impact test comparisons of 20th and 21st century American football helmets. *J Neurosurg*, 2012. 116(1): p. 222-33
36. Hodgson, V.R. National Operating Committee on Standards for Athletic Equipment football helmet certification program. *Medicine and science in sports*, 1975. 7: p. 225-232
37. Bland, M.L., McNally, C., and Rowson, S. Headform and Neck Effects on Dynamic Response in Bicycle Helmet Oblique Impact Testing, in *IRCOBI Conference*. 2018: Athens, Greece. p. 413-423.
38. Sances, A.J., Carlin, F., and Kumaresan, S. Biomechanical analysis of head-neck force in Hybrid III dummy during inverted vertical drops. *Biomed. Sci. Instrum.*, 2002. 38: p. 459-464
39. Nelson, T.S. and Cripton, P.A. A New Biofidelic Sagittal Plane Surrogate Neck for Head-First Impacts. *Traffic Inj Prev*, 2010. 11(3): p. 309-319
40. *In review:* Bland, M.L. McNally, C., Zuby, D.S., Mueller, B.C., and Rowson, S. Development of the STAR evaluation system for assessing bicycle helmet protective performance. Ann. Biomed. Eng.
41. ECE. R-22.05: Uniform Provisions Concerning the Approval of Protective Helmets for Drivers and Passengers of Motorcycles and Mopeds. 1999, United Nations Economic Commission for Europe.
42. Cobb, B.R., Tyson, A.M., and Rowson, S. Head acceleration measurement techniques: Reliability of angular rate sensor data in helmeted impact testing. *Proceedings of the Institution of Mechanical Engineers, Part P: Journal of Sports Engineering and Technology*, 2017. 232(2): p. 176-181
43. Ghajari, M., Caserta, G.D., and Galvanetto, U. The Impact Attenuation Test of Motorcycle Helmet Standards. *Proceedings of 1st International Conference on Helmet Performance and Design*, 2013. London, UK
44. Mills, N.J. Critical evaluation of the SHARP motorcycle helmet rating. *Int. J. Crashworthiness*, 2010. 15(3): p. 331-342
45. Mills, N.J., Wilkes, S., Derler, S., and Flisch, A. FEA of oblique impact tests on a motorcycle helmet. *International Journal of Impact Engineering*, 2009. 36(7): p. 913-925
46. Bonugli, E. The effects of dynamic friction in oblique motorcycle helmet impacts, in *Biomedical Engineering*. 2015, The University of Texas at San Antonio: Ann Arbor. p. 78.
47. Ghajari, M., Peldschus, S., Galvanetto, U., and Iannucci, L. Effects of the presence of the body in helmet oblique impacts. *Accident; analysis and prevention*, 2013. 50: p. 263-71

CHAPTER 10

LABORATORY RECONSTRUCTIONS OF BICYCLE HELMET DAMAGE: INVESTIGATION OF CYCLIST HEAD IMPACT CONDITIONS AND ASSOCIATED KINEMATICS

ABSTRACT

Although head injuries are common in cycling, the exact conditions associated with cyclist head impacts are difficult to ascertain. A thorough understanding of these conditions and the kinematics that result can lead to improved helmet design. Past studies have attempted to reverse engineer cyclist head impact conditions by reconstructing residual helmet damage using laboratory tests, but have been limited by simplified impact testing and damage quantification. The objective of the present study was to enhance knowledge of cyclist head impact conditions and kinematics by reconstructing helmet damage using advanced impact testing and damage quantification techniques. Oblique impacts were used to reconstruct the damage associated with helmets from 18 hospitalized cyclists. Original and tested helmet damage was quantified using computed tomography (CT). Damage metrics were related to normal and tangential velocities as well as peak linear accelerations (PLA) and peak rotational velocities (PRV) using case-specific multiple linear regression models. Models were then used to estimate exact impact conditions and kinematics associated with the original damage. Across all cases, helmets were most frequently damaged at the front and sides, often at the rim, and concussion was among the most common injury diagnoses. Resulting normal velocities and PLAs were similar to past reconstruction study distributions, with median values of 3.4 m/s and 102.5 g. Associated tangential velocity and PRV medians were 3.8 m/s and 22.3 rad/s, respectively. These distributions can used to set boundary conditions for bicycle helmet oblique impact testing, enabling improved helmet evaluation and design. Kinematic results can also be related to injury outcome to enhance understanding of the injuries associated with cyclist head impacts.

INTRODUCTION

Many protective countermeasures exist to protect humans from injury due to impact, such as body padding and helmets in sports or airbags and seatbelts in vehicles. These countermeasures are most effective if designed based around the impact scenarios they may be subjected to. Knowledge regarding the spectrum of impact conditions likely to be experienced during a particular activity and the relative frequency of these conditions is thus of vital importance for optimizing countermeasure design. Countermeasures must be able to protect users in the event of infrequent but severe impact scenarios as well as in the most frequent but potentially less injurious impacts. Understanding the distribution of potential impact scenarios and their relationships to injury risk is thus fundamental to designing safety measures that are best equipped to protect individuals who engage in a given activity.

The exact nature and distribution of head impact conditions related to cycling are relatively unknown. Cycling-related injuries accounted for an estimated $24.4 billion in US healthcare costs in 2010 alone, with injuries to the head among the most common and serious injuries [1-3]. Cycling in fact accounts for more head injuries treated in emergency rooms than any other sport or recreational activity [4,5]. Bicycle helmets, which fortunately have been shown to reduce risk of head injury [3,6-8], are presently designed around impact test conditions prescribed in mandatory safety standards [9]. Standards testing requires that helmets be fitted to an anthropomorphic test device (ATD) headform and subject to guided drop tests onto an anvil surface, approaching the anvil from the perpendicular. Linear acceleration is measured during all impacts, and the peak linear acceleration (PLA) from each test must be limited to below a set threshold of 300 g (representing >50% risk of skull fracture or severe brain injury [10]) for the helmet to pass.

While standards ensure a minimal adequate level of protection for bicycle helmets, research

suggests that real-world cyclist head impacts are much more complex than the conditions reflected in these tests. Namely, cyclist head impacts are thought to most often occur oblique to the impact surface rather than perpendicular, comprising of both normal and tangential incident velocities and producing both linear and rotational head impact kinematics in response [11-16]. The involvement of linear and rotational kinematics have particularly important implications for injury risk. Rotational kinematics have been shown to be well-correlated to shear strain measured in the brain during impact testing, resulting in diffuse brain injury such as concussion or other forms of diffuse axonal injury, while linear kinematics have been linked to the development of pressure gradients leading to focal injury such as skull fracture or cerebral contusion [17-21]. In light of these effects, a more holistic assessment of helmet performance would involve evaluating helmets in realistic impact conditions and recording both linear and rotational kinematics.

A number of test rigs have been developed to simulate oblique impacts for bicycle or motorcycle helmet evaluation [22-26]. Although this marks an improvement in helmet testing, the exact impact conditions commonly experienced by cyclists are still relatively unclear. Defining specific head impact conditions related to cycling is challenging due to the unpredictability of cyclist crashes. Measuring associated head impact kinematics through direct instrumentation would provide optimal data for characterization of these impacts. Head impacts in other sports have previously been quantified by instrumenting athletes with head impact sensors during practices and games [27-30]. However, given that cyclist crashes are involuntary in nature, head impact events are generally infrequent per rider, rendering collection of naturalistic data through instrumentation of a population of cyclists impractical. Alternatively, instrumenting volunteers and instructing them to crash while cycling is unethical due to the considerable injury risks involved. Previous studies have thus approached the study of cyclist head impact scenarios through other means, primarily including computational simulations of possible crash configurations or laboratory reconstructions

of helmet damage from real-world accidents [12,14-16,31-34].

Computational simulations of cyclist accidents use multibody models, often in conjunction with finite element models, to estimate initial head impact conditions and resulting kinematics associated with cyclist head impact events [12,14-16,34]. Results from these studies provide invaluable insight into the nature of these impacts. However, given the lack of real-world data available quantifying cyclist impact conditions, these simulations are somewhat limited by a lack of direct validation for the conditions being modeled. Damage reconstruction studies, on the other hand, provide an additional promising avenue for estimating cyclist head impact conditions and kinematics. Conventional bicycle helmets dissipate energy upon impact via permanent crushing of the expanded polystyrene (EPS) foam liner. The residual helmet damage serves as detectable evidence that can be used to inform laboratory reconstruction testing to undamaged samples of an identical helmet until the original damage profile is acceptably reproduced. Although this approach has potential, past reconstruction studies have been limited by largely simplified test setups and damage quantification [31,32,35,36]. Several studies have utilized standards testing equipment, neglecting to simulate the oblique nature of cyclist head impacts. Several have also conducted visual observation of helmet liners in order to quantify damage. Aside from a general lack of accuracy associated with visual assessment, this approach generally requires removal of the helmet shell from the liner in order to take measurements. A majority of bicycle helmets are now made using a direct in-molding technique to couple the liner to the shell, complicating the process of removing the shell as considerable damage could be accrued in the process.

More advanced impact testing and damage quantification methods have been proposed for helmet damage studies in recent years, largely in the motorcycle helmet space [36-39]. Main advances include the use of computed tomography (CT) to quantify helmet liner damage less

destructively while also accounting for gapping that may present between the liner and shell [37,39,40]. CT scans can be compiled into three-dimensional (3D) models of the helmet liner, which can then be overlaid with a model of an identical, undamaged helmet to allow damage metrics such as crush depth or volume to be ascertained. Previous work has demonstrated that damage quantification metrics such as these can be recreated with high reliability and precision [37]. When paired with visual-based measurement of helmet shell damage, CT thus has the potential to provide an enhanced assessment of helmet damage for the reconstruction process.

The reconstruction process could also be enhanced through more advanced laboratory testing, such as conducting oblique impacts rather than normal. One previous study of motorcycle helmet damage employed a number of anvil surfaces for impact testing, including angled anvils to simulate an oblique head-to-ground angle [36]. The authors reported that visually-based measurements of the helmet shells and liners were indicative of the angle and shape of the impact surface. To-date, no study has fully explored the use of oblique impact testing for bicycle helmet damage reconstruction, and very few have applied CT-based damage quantification to bicycle helmets. Use of these advanced approaches to reverse engineer conditions of cyclist head impacts could greatly supplement the body of knowledge surrounding these impacts, which could in turn stimulate both improved understanding of cyclist head injuries and improved helmet design. The objective of this study was to ascertain characteristics associated with cyclist head impacts by reconstructing real-world bicycle helmet damage through oblique impact testing and CT-based damage quantification.

METHODS

Case Information and Exclusion Criteria

Bicycle helmets damaged during cyclist accidents were donated by cyclists who were hospitalized

in one of four urban hospitals across the United States from 2015-2017. Hospitalized cyclists were given the opportunity to donate their helmet as part of a large-scale study investigating roadway factors surrounding cyclist accidents conducted by the Insurance Institute for Highway Safety (IIHS). Cases involving fatalities or children were not included as part of the study. Donated helmets were also accompanied by associated medical reports, details of road characteristics where the accident took place, and a patient description of accident events. All identifiable information regarding the cyclist was redacted prior to being sent to the author. Related protocols were approved by the Virginia Tech Institutional Review Board (IRB 17-1036).

The collected sample of helmets and their associated accident information were analyzed to determine the candidacy of each case for reconstruction testing. A total of 58 helmets were received. Helmets were immediately excluded if the patient indicated that their helmet was not damaged at the time of the accident (5 cases). Cases where the patient sustained a facial fracture from the accident were excluded as well (6 cases), as this implies that a large proportion of the impact force was directed to the face rather than the helmet. Inclusion of these cases under the assumption that the helmet damage was fully reflective of the accident severity could accordingly inflate estimates of the relative frequency of low-severity crashes. Helmet damage for the remaining cases was then visually assessed, and helmets that showed no conclusive evidence of damage were excluded as well. Thirty-seven helmets were designated as candidates for reconstruction after this process.

A purchasing phase then commenced to determine if identical samples of each helmet model could be allocated for reconstruction testing. Bicycle helmet manufacturers tend to frequently revise models or replace them altogether, so many of the models, which were manufactured as early as 2004, were no longer in production. For these helmets, third party vendors were searched

or the manufacturer was contacted directly to inquire about their availability. Helmet models for which less than three samples could be obtained were also excluded from the remainder of the study. A final total of 18 cases were designated as candidates for reconstruction.

Damage Quantification

Visual observations of damage to all candidate helmets were recorded, including the length of surface scraping evident on the helmet shells (measured in the direction of primary scraping). Each damaged helmet and one identical, undamaged counterpart were CT scanned for initial damage quantification at 120 kV and 200 mA with 0.625 x 0.625 mm pixel spacing and a 0.5 mm slice thickness (Aquilion, Canon Medical Systems, Tustin, CA). The associated Digital Imaging and Communications in Medicine (DICOM) files were then imported into a segmentation interface software for processing (Mimics Research 21.0, Materialise, Leuven, Belgium). Helmet liners were separated from the surrounding air, the scanner table, and the helmet shell by applying a Hounsfield Unit (HU) range of -960 to -850 followed by semi-automated mask-splitting operations. If needed, manual editing of individual slices was employed to correct for any slight artifact in the segmentation masks. Final liner masks were then smoothed to reduce pixilation and converted into 3D surface mesh models comprised of >600,000 triangular elements.

To overlay the matched helmets and quantify damage, 3D models were imported into 3-matic Research 13.0 (Materialise, Leuven, Belgium). Automated linear registration techniques were employed to optimally align the models, wherein the distances between a subset of similar nodes on each model were minimized. A global registration error was output from this process. An origin of the overlaid models, located at the center of the model length and width, was defined at the base of the model to serve as a center for radial measurements. A heat map reflecting the approximate Hausdorff distances between each node on the undamaged model to the nearest

node on the damaged model was then generated (Fig. 10.1). Heat map bounds were set to just outside the reported global registration error in order to visualize the crush region in its entirety while minimizing noise.

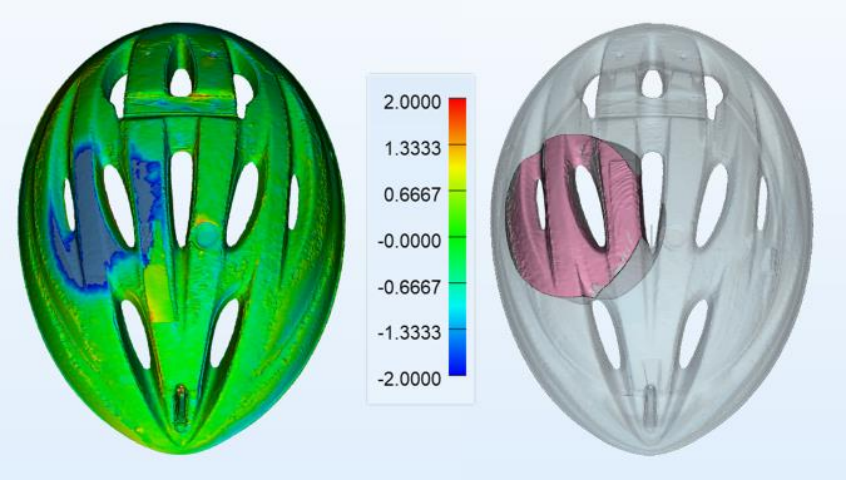

Figure 10.1. Damage quantification process for an exemplar helmet case. The crush area was defined as region of the model exceeding the negative heat map bound. Crush volume was defined by encompassing the crush area within a cylindrical volume and subtracting the volumes of the two models within this cylindrical region.

The area of the damaged liner's surface exceeding the heat map bounds was measured as the crush area. Bounds were then increased until a single node of the damaged liner was identified as being furthest offset from the undamaged liner. The radial thicknesses of the damaged and undamaged liners through this point were subtracted to yield max crush depth, while the corresponding point on the undamaged model outer surface was recorded as the max crush location. The distance from this point to the crush area boundaries along the direction of helmet shell scraping in either direction was then measured, and the ratio of superior/inferior or anterior/posterior measurements was computed to indicate the centeredness of the crush profile. Finally, a cylinder was defined with its circular face encompassing the crush area and its length

extending radially through the helmet models (Fig. 10.1). The volumes of the two models within this cylindrical region were subtracted to compute crush volume.

Impact Testing

Impact testing was carried out to the undamaged samples of each helmet using a custom, oblique impact rig. Oblique impacts were generated through guided drop tests of a helmeted headform onto an adjustable-angled anvil, creating normal and tangential incident velocities characteristic of cyclist head impacts (Fig. 10.2). National Operating Committee on Standards for Athletic Equipment (NOCSAE) headforms in small (53.4 cm circumference), medium (57.6 cm), and large (61.4 cm) sizes were used to reflect the range of helmet sizes among the reconstruction candidates. NOCSAE headforms are common in sports helmet testing and have enhanced biofidelity compared to other headforms [41,42]. Helmets were fitted to the headforms according to manufacturer fit recommendations, then the helmeted headform was positioned in a support ring connected to the drop tower. No ATD neck was used in this testing, as common ATD necks have been shown to possess limited biofidelity in axial loading scenarios [43,44]. Further, it has been suggested that the human neck plays a minimal role in head impact kinematics during the primary head impact phase of head-first impacts [44]. The exact positioning of the headform for each test was measured using a dual-axis inclinometer (DMI600, Omni Instruments, Dundee, UK). Once set, the headform was secured in place from above using an additional support arm.

Initial impact velocity was recorded by a photogate for each test (BeeSpi V, NaRiKa Corp., Tokyo, Japan). Impact kinematics of the headform were collected at 20 kHz using three linear accelerometers (Endevco 7264B-2000, Meggitt Sensing Systems, Irvine, CA) and a tri-axis angular rate sensor (ARS3 PRO-18K, DTS, Seal Beach, CA) located at the headform center of gravity (CG). Linear accelerations were filtered using a 4-pole, phaseless Butterworth low-pass

filter at a channel frequency class (CFC) of 1000 in accordance with standard practice for automotive impact testing (SAE J211). Rotational velocities were processed using the same filter type with a CFC of 175. This CFC has been optimized for sports head impact testing [41]. Resultant curves from the three directional traces were then computed and used to determine the peak linear acceleration (PLA) and peak rotational velocity (PRV) associated with each test.

Figure 10.2. Oblique impact drop tower containing angled anvils used for reconstruction testing. A variety of impact surfaces were employed as needed to simulate different accident conditions. A sandpaper-coated steel anvil simulates a smooth road condition (left), while a rough anvil

(aggregate of epoxy, sand, and stones) simulates a pockmarked road (top right), and a curbstone anvil coated with 80-grit sandpaper provides a more focal impact surface (bottom right).

An iterative process was employed for impact testing, with each test's boundary conditions updated based on visual assessment of damage from the previous test. Multiple tests were conducted prior to CT scanning tested helmets, as scanning larger batches at one time is more time and cost-efficient than scanning between each test. Initial impact velocity estimates were informed by the author's previous work evaluating the sensitivity of helmet liner damage metrics to varied normal and tangential velocity inputs. The orientation of the helmeted headform and the angle of the anvil were set to replicate the direction of surface scraping and the location of max crush for each helmet. It was generally assumed that all impacts were body driven, meaning the cyclist's head was leading the body and was traveling away from the bike during the crash (thought to be common in cyclist crashes), unless the accident description hinted otherwise. The anvil surface was selected to best reflect the characteristics of the helmet's surface damage and the patient's description of the riding surface (Fig. 10.2); a steel surface coated with 80-grit sandpaper was used to simulate smooth road conditions (based on motorcycle standards [45]); a "rough" surface made from a mixture of pebbles and sand in epoxy was used to simulate a pockmarked or bumpy road surface; and a curbstone was used to simulate more focal impact surfaces.

Prior to CT scanning the tested helmets, as many as three impacts were conducted per helmet model using a new, undamaged sample per test. A general goal of testing was to generate damage both more and less severe than the original helmet damage so that exact impact conditions could be interpolated based on linear models informed by damage metrics. After a round of testing was completed, additional CT scans were taken of the tested helmets and the

process of quantifying helmet damage was repeated using the same approach taken to quantify the original helmet damage. Damage metrics including crush area, max crush depth, max crush depth location, crush centeredness, and crush volume were recorded along with scrape length and were compared to the original damage. Additional testing with boundary conditions updated based on the damage metric results were conducted as needed, with as many as seven tests in total conducted per helmet model.

Model Development and Statistics

In order to generate as accurate an estimate of initial impact conditions and resulting head kinematics as possible for each case, multiple linear regression (MLR) models were developed for each helmet to relate damage metrics to impact characteristics. After testing was completed for a given helmet, damage metric results from the tested helmets (scrape length, crush area, max crush depth, crush centeredness, and crush volume) were first individually correlated with normal and tangential velocities and PLA and PRV using Pearson's correlation coefficient. Tests where the max crush location was located further than half of the approximate radius of the original damaged helmet crush area away from the target max crush location were excluded from this process, as the author's previous sensitivity evaluation determined that small variations in max crush location (especially near a vent) can have large effects on resulting damage metrics. Damage metrics were correlated to normal and tangential velocities rather than impact angle and resultant velocity, as the relationships between damage and normal and tangential velocities are generally stronger and thought to be more mechanistic in nature [46].

The two damage metrics that were most significantly correlated with normal velocity were selected for input into the normal velocity MLR model. In some cases, metrics were excluded from this process if it was deemed to be associated with high error for that particular case (e.g. seemingly

extreme crush area measurements in conjunction with high global registration error). Both damage metrics and their interaction were input as model terms given that there were enough trials to inform such a model; otherwise, models were built from various combinations of the two damage metrics and their interaction, then the model with the greatest overall significance was determined. The significance of individual terms in each model was evaluated, with least-significant terms successively removed until all remaining terms were significant ($p<0.05$) or a model based on only one term and an intercept remained. If multiple terms in a model produced similar effect sizes and neared significance (but not significant at the $p=0.05$ level), all terms were kept in the model if the overall model was significant at the $p=0.05$ level. This process was repeated to determine an MLR model for tangential velocity as well as for PLA and PRV. Resulting models were then solved at the damage metric values associated with the original helmet to generate estimates of the accompanying normal and tangential velocities and PLA and PRV for each case. The standard error of each model at these estimates was determined. Associated impact resultant velocities and angles were then also assessed, with the normal and tangential velocity errors propagated through in quadrature. Relationships between normal and tangential velocities and head kinematics were evaluated using Pearson's correlation coefficient.

RESULTS

The 18 cases of helmet damage reconstructed in the present study were associated with an array of injury types and severities (Table 10.1). Following upper extremity injuries, the head was the most commonly injured body regions from these accidents. Many of the head injuries were more superficial, including skin abrasions or lacerations and contusions. However, seven concussions were diagnosed among these 18 cyclists, with a loss of consciousness involved in four cases. Other more severe injuries include one case of subarachnoid hemorrhage and several serious lung injuries, the latter of which were all associated with a single patient. Helmet damage

quantification revealed that the locations of max crush for both concussed and non-concussed patients were fairly evenly interspersed. This may suggest that the two groups experienced impacts of similar directionality (Fig. 10.3). A majority of impacts were to the front and sides of the helmet, with very few to the top and rear regions. Five cases showed max crush locations very close to the helmet rim, and others showed evidence of surface scraping that extended down to the rim from max crush locations further superior. Relative to the defined origin at the base of each helmet, the average elevation of the max crush location was 32.1±16.2° and the average azimuth from the front of the helmet was 49.6±26.6°.

Table 10.1. Breakdown of all injuries sustained by patients with reconstruction candidate helmets. The head and the upper extremities were the most commonly injured body regions. Injuries are only reported once per patient here, although some patients sustained multiple of the same injury types (e.g. a patient having two separate recorded arm abrasions).

Body Region	Injury Type	Number of Cases
Head	Abrasion/ laceration/ contusion	9 (4 forehead/eye, 4 face – other, 1 scalp)
	Concussion	7 (4 with loss of consciousness)
	Subarachnoid hemorrhage	1
Neck	Fracture	1
	Sprain	1
Spine	Fracture	1
Hip/ Leg	Abrasion/ laceration/ contusion	9
Shoulder/ Arm/ Hand	Abrasion/ laceration/ contusion	11
	Fracture/ dislocation/ tear	8
Chest	Rib fracture	1
	Contusion	1
	Pneumothorax	1
	Hematoma	1

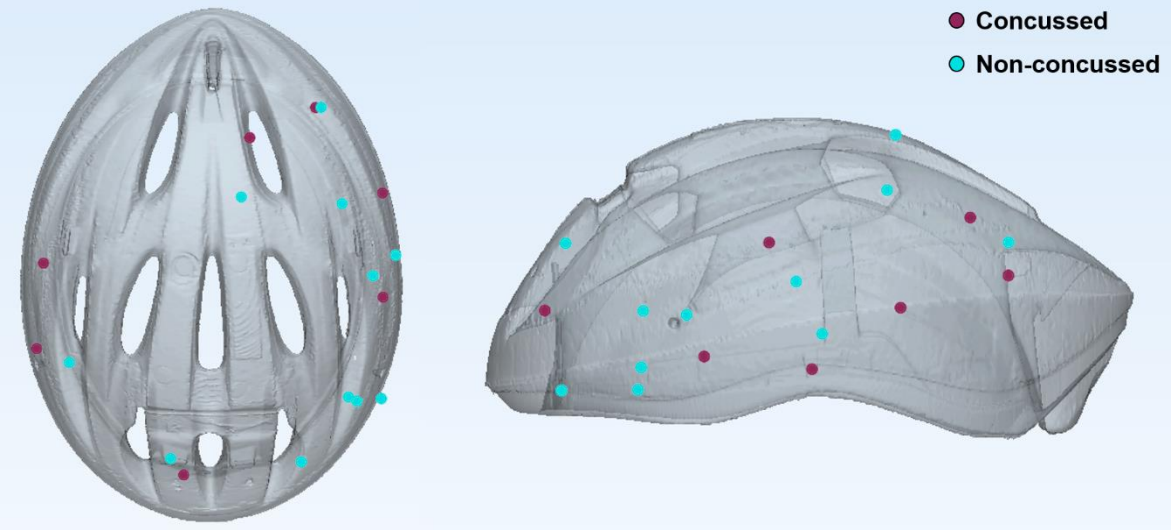

Figure 10.3. Locations of max crush for all cases, modeled on an exemplar helmet. Cases associated with a concussion are shown in maroon, while cases not associated with a concussion are shown in aqua. A majority of impacts were to the front and sides of the helmets, often at the helmet rim.

Impact testing to simulate damage associated with each case necessitated a variety of test conditions. Helmet sizing mostly fell in the range of the medium NOCSAE headform, although the small headform was used for two cases and the large headform used for one. Anvil surfaces were chosen per case to best reflect the nature of the damage to the helmet exterior. The smooth road surface anvil (steel anvil with sandpaper) was sufficient to generate close damage replicates for 10 of the cases. Four of the cases showed very pockmarked damage to the outer helmet surface, requiring use of the rough anvil surface, while four cases showed evidence of more focal loading, requiring use of the curbstone surface. Several cases indicated that the impact was caused by collision with a vehicle; however, the description did not specify what surface the helmet came in contact with. The decision of which anvil to use for these cases was thus informed primarily by surface damage, with the curbstone anvil selected for two cases. Three additional helmets did

not appear to be scraped while still presenting with liner crush damage. Normal impacts were carried out for these cases.

The average scrape length across all original helmets was 5.7 ± 4.1 cm, with several helmets showing considerable scrape lengths of up to 13.0 cm. Max crush depth ranged from 0.3-13.9 mm across all cases, while crush area ranged from 0.0-88.4 cm^2, centeredness ranged from 0.2-6.2, and volume ranged from -0.1-29.4 cm^3. Below certain thresholds of damage (~1% of the undamaged measurement), several of the damage metrics are not as reliable due to the presence of a noise floor associated with manufacturing differences across samples, CT scanner resolution, segmentation error, etc. Metrics that resulted in <1% damage relative to the undamaged helmet value of the same metric were generally excluded from the model development process.

Data from an average of ~4 tests were included in the MLR models for each case. The average distance of the max crush location from each test to the desired location was 1.3±0.7 cm. For two cases, data from only two tests could be included in the MLR models. Test data for these cases were interpolated to estimate normal and tangential velocities and PLA and PRV, and error was reported as the range between the estimate and the further of the two test values in order to reflect the larger uncertainty. Another case was associated with a unique damage pattern, in which liner peaks at the rear of the helmet were avulsed but the surrounding liner was minimally damaged. Normal velocity curbstone impacts were conducted for this case. It was observed that the liner peaks avulsed from the helmet once the applied normal velocity reached a particular severity, but not at lower velocities. Test results from the impact that first produced this liner avulsion were assigned as the associated velocity and kinematic estimates for this case. A wide error range was determined, reflecting the difference between these results and the results of the nearest test that did not produce liner avulsion. All other cases showed more typical damage profiles that could be

characterized by a number of damage metrics.

Across all cases, the normal velocity MLR models included a max crush depth term more frequently than all other damage metrics, indicating that crush depth and normal velocity are generally well-correlated. Crush volume was the most frequently included metric in in tangential velocity models, crush area and depth were most frequently included in PLA models, and crush area was most frequently included in PRV models followed closely by scrape length and crush volume. The average standard errors associated with normal and tangential velocity estimates were 0.15 and 0.22 m/s, respectively, while average standard errors associated with PLA and PRV were 5.4 g and 1.4 rad/s. The distribution of normal velocity estimates across all cases produced a median value of 3.4 m/s with 2.5 and 97.5 percentile values (95% range) of 0.24 m/s and 6.0 m/s (Fig. 10.4). The median tangential velocity estimate was 3.8 m/s with a 95% range of -0.02-7.5 m/s. The negative lower bound was influenced by a single case with a tangential velocity estimate of -0.04 m/s (essentially 0). This particular case had minimal damage, and the estimated results may have been subject to slightly greater noise ratios. Computing the associated impact angles and resultant velocities from the normal and tangential velocities of all cases produced a median impact angle of 40.3° between the head and the ground (95% range: 26.3-90°) and a median resultant velocity of 5.5 m/s (95% range: 0.4-8.5 m/s). The average propagated errors associated with impact angle and resultant velocity were 0.3° and 0.2 m/s, respectively.

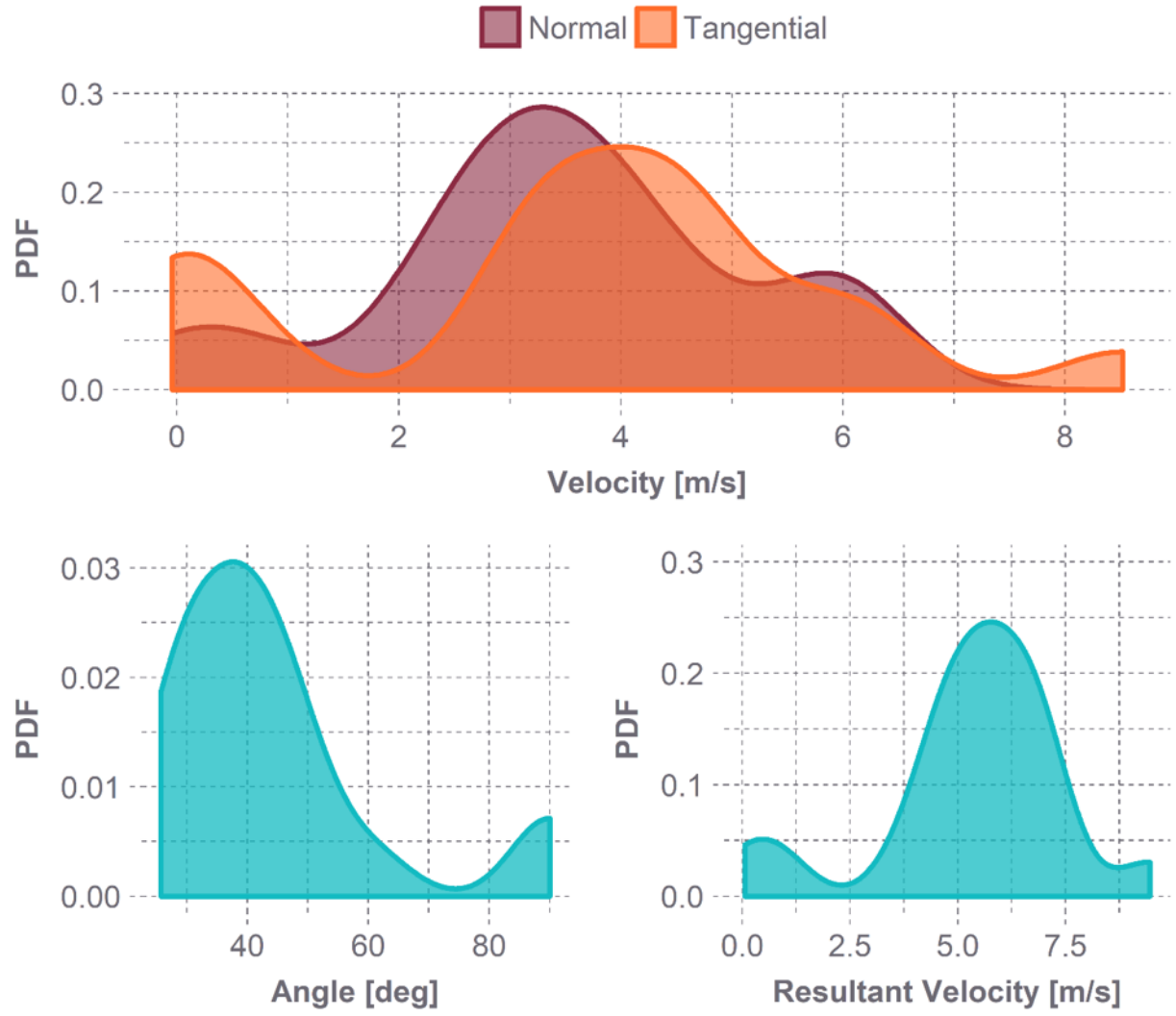

Figure 10.4. Probability density functions (PDFs) of normal and tangential velocity estimates across all cases and their associated impact angle and resultant velocity estimates. The impact angle is angle between the resultant velocity vector and the impact surface, such that 90 degrees represents a purely normal impact.

Head impact PLA associated with each case ranged from 11.1-218.8 g, with a median value across all cases of 102.5 g and a 95% range of 18.3-202.4 g. PRV ranged from 2.1-48.1 rad/s, with a median of 22.3 rad/s and a 95% range of 2.3-44.8 rad/s. PLA and PRV generally increased

with increasing normal and tangential velocities, respectively (Fig. 10.5). The correlation between PLA and normal velocity was significant (R=0.61, p=0.01), while the correlation between PRV and tangential velocity was not (R=0.35, p=0.16). The single case associated with subarachnoid hemorrhage produced the greatest PLA value of 218.8 g. Cases resulting in a concussion produced a greater average PLA of 109.8 ± 55.0 g compared to 98.1 ± 58.5 g for non-concussion cases, while PRV was slightly greater for non-concussion cases, averaging 24.2 ± 14.8 rad/s, while concussion cases averaged 19.3 ± 7.4 rad/s (Fig. 10.6). Neither difference was significant, however (p>0.37).

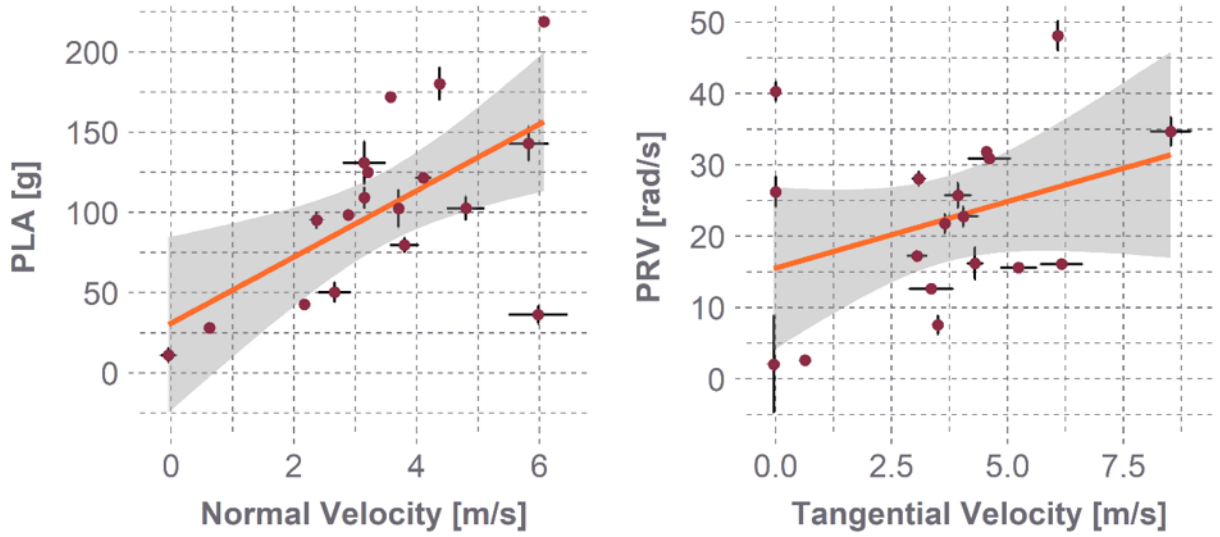

Figure 10.5. Trends between PLA and PRV estimates for all cases and their associated normal and tangential velocity estimates. PLA increased significantly with increasing normal velocity, while PRV increased, but not significantly, with increasing tangential velocity.

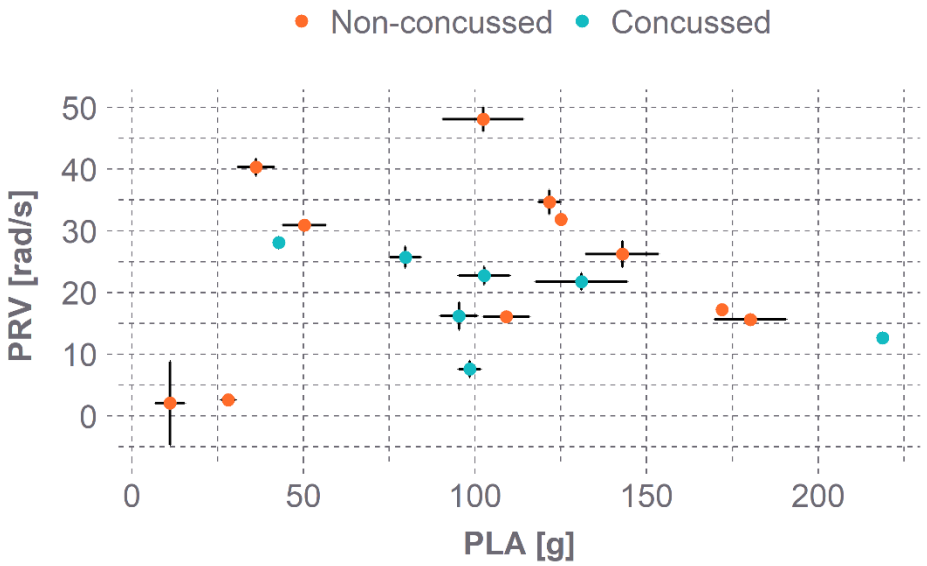

Figure 10.6. PLA and PRV estimates for each case and the associated concussive injury diagnosis. Concussive and non-concussive kinematics were largely interspersed, with average PLA and PRV not differing significantly across groups ($p>0.37$).

DISCUSSION

The goals of this helmet damage reconstruction study were to investigate common head impact conditions and kinematics involved in cyclist crashed using oblique impact testing and CT-based damage quantification. A first step in this process was to assess the residual damage associated with each donated helmet that had been involved in a real-world accident. Impact locations (defined as the location of maximal crush) most often fell at the front and sides of the helmets, frequently near the helmet rim. These impact locations are consistent with those previously reported in cyclist accident simulation studies, helmet damage reconstruction studies, and helmet damage field studies [12-15,31-33,47]. Impacts to the helmet rim are particularly important to note, as helmet standards specify a test line below which helmet impact performance is not evaluated during the certification process. This test line excludes the rim from testing. The results

of the present study supplement a growing body of evidence suggesting that the rim is in fact one of the most commonly-impacted regions of the helmet. Although not evident in these results, previous work has demonstrated a liner densification phenomenon for some standards-certified helmets during impact testing to the helmet rim, which in turn transfers very large and likely injurious forces to the head [48]. It is therefore recommended that standards be adapted so that helmet protective capabilities are regulated in this region.

The normal and tangential velocity estimates generated from the present reconstructions, along with associated impact angles and resultant velocities, were similar to ranges of values reported from previous cyclist simulation and damage reconstruction studies [12,14-16,31,32]. Specifically, the median normal velocity and PLA herein were near matches to median values of data from helmet damage reconstruction studies using standards test equipment [31,32]. Previous work has demonstrated that liner crush depth is strongly correlated with applied normal velocity, which in turn is generally well-correlated with PLA [37,46,49]. Given that the headform masses are comparable between the NOCSAE headforms and standards headforms, it is intuitive that normal velocity and PLA results are comparable across study type, reinforcing the level of certainty surrounding these estimates. Compiling cyclist simulation study results reveals slightly greater median head impact velocities and angles than those determined in the present work [12,14-16], although overall distributions are markedly similar. The reasonably low errors associated with the present estimates of impact conditions and kinematics further highlight the reliability of these results. Utilization of oblique impact testing to quantify damage has the added benefit of estimating associated cyclist head impact tangential velocities and PRV responses as well, which have meaningful implications for injury risk assessment.

Standards testing in United States assesses helmet impact performance during much more

severe impacts, conducting normal impacts against a flat anvil at 6.2 m/s and limiting PLA to less than 300 g [9]. While it is essential for standards to ensure risk of catastrophic injury is mitigated, the present results suggest that less severe impacts are much more common in cyclist crashes, but still have the potential to produce injuries such as concussion. Evaluating helmet performance at lower impact severities as well could present a challenge to manufacturers to design helmets around providing optimal protection in both the most common impact scenarios as well as more severe scenarios. Evaluating performance using oblique impact conditions informed by the present study offers further insight into helmet protective capabilities, as these impacts comprise the majority of cyclist head impact scenarios. Further, the oblique impacts herein produced considerable rotational head impact kinematics, which are known to be associated with diffuse brain injury such as concussion [20,21].

The process of generating MLR models to relate damage metrics to normal and tangential velocities and resulting PLA and PRV revealed that these relationships are somewhat case-specific. Max crush depth was commonly included in the normal velocity and PLA models, although other metrics were frequently included in these models in addition to or instead of crush depth. Similarly, crush volume was a frequent predictor of tangential velocity, while crush area and scrape length were frequent predictors of PRV, although models for both tangential velocity and PRV often incorporated other metrics in addition to or instead of these. The author's previous work investigating relationships between various damage metrics and associated velocities and kinematics (using a single helmet model and impact location) also showed PLA and normal velocities to be best correlated to max crush depth, while tangential velocity and PRV were best correlated to scrape length. It is likely that the relationships between damage and associated velocities and kinematics are modulated by the specific helmet model as well as the orientation of the head relative to the impact surface. For example, scrape length may not have reflected

tangential velocity or resulting PRV as closely if the impact location for a particular model was located close to a vent, which could obfuscate measurement of scrape length slightly. These case-specific relationships suggest that there is benefit to creating individualized models to predict impact conditions and kinematics from damage metrics.

Relative head orientation and impact location likely modulate relationships between impact normal and tangential velocities and resulting PLA and PRV as well. Changing the head orientation changes how the CG of the head is directed relative to the contact point on the anvil surface. Although normal velocity and PLA were significantly correlated in the present results, the amount of mass directed through the impact center affects resulting PLA, so that less directly-oriented impacts produce lower PLAs for a given normal velocity. The effect is potentially more substantial on resulting rotational kinematics, as the distance between the gravity vector extending from the headform CG to the contact point dictates the associated applied moment. These trends have been suggested previously [46], and provide explanation for the lack of significant correlation between tangential velocity and PRV and the considerable scatter present in the normal velocity-PLA relationship. A case that highlights this effect particularly well was the helmet that showed evidence of liner avulsion; these normal velocity, curbstone impacts were applied to the rear of the helmet, meaning very little of the headform mass was directed through the contact point. The result was very low PLAs and high PRVs for considerably high applied normal velocities and virtually zero applied tangential velocities, representing an outlier in the data. In light of this, estimates of associated normal and tangential velocities required for reconstruction cases should be made with consideration of potential head orientation in mind.

Grouping kinematic results by concussive injury diagnosis revealed surprising trends, or rather a lack thereof. The high proportion of concussions out of all injuries in this dataset supports

epidemiological studies showing that concussion is a common injury for cyclists [2,4]. However, risk of concussion generally increases with increasing impact kinematics [50], and rotational kinematics in particular have been implicated as key factor in producing concussive injury [19-21]. In the present study, average PLA was greater for the concussion cases while average PRV was lower (neither difference was significant). Although there are considerable subject-to-subject variations in susceptibility to concussion [51], it is also possible that differences in injury reporting across cases contributed to this trend. One indicator of this is that all diagnosed concussions among the reconstruction cases stemmed from the same hospital. Assigning PLA and PRV an overall rank for each case and summing these ranks to indicate relative head impact severity revealed that several of the most severe impacts did not result in a concussion diagnosis. Two of these patients were diagnosed with neck injuries, however, which can present similar symptoms to concussion and may have resulted in a missed diagnosis. Error in the reconstruction process may have also contributed to higher PRV estimates for non-concussion cases or vice versa, although the similarities between the present results and other studies bolster confidence in these estimates. Regardless, the high incidence of concussion out of these cases suggest there is room for improvement in helmet design to reduce risk of concussion while still protecting against severe injuries.

The lack of significant differences in average kinematics across concussed and non-concussed groups may also be indicative of the general nature of helmet damage reconstruction studies. Reconstructing damage to a helmet, by definition, requires that the helmet present with a definitive damage region. Many field-used helmets show dings and scrapes on the liner and shell that are evidence of everyday wear. Additionally, permanent crush of the EPS foam requires that the foam be subject to stresses exceeding its initial yield stress [52]. It is possible that in some instances, a head impact occurred of low enough severity to not induce a substantial, visually-observable

region of damage that was distinguishable from overall helmet wear. Supporting this theory, several non-concussed patients claimed their helmet was damaged at the time of injury, while visual assessment of the helmet (sometimes supplemented by CT scans) did not identify a definitive damage region. If a head impact did occur in these cases, it is likely that the associated kinematics were extremely low. Not including such cases in the reconstruction results likely over-weights estimated impact velocities and kinematics slightly. It also may blur the distinction between the concussed and non-concussed kinematic results to a limited extent.

There are a number of challenges and limitations associated with the present study that are important to weigh the results in light of. Any laboratory testing-based reconstruction study represents a simplification of real world events. As such, many assumptions were required in order to simulate test conditions, including assumptions regarding the direction of impact and the impact surface, which are made more complex if a motor vehicle is involved in the accident. Further, reconstruction testing represents a single, idealized head impact event. Secondary impacts likely occurred in a few cases, potentially introducing error into the damage quantification process. In cases where additional potential impact locations were identified, the primary impact location was assumed to be at the location of max crush. Additionally, one or two cases characterized by extensive damage showed longer scrape lengths than could be replicated using a single isolated impact, even when the max crush depth was matched for individual tests and the steepest angle anvil was employed. It is possible that these cases represented instances of extended, body-driven contact between the head and impact surface, which would likely be of lesser force than the initial impact event. While scrape length was intentionally excluded from the model development process for these cases, resulting tangential velocity and PRV estimates may still have been inflated as a result.

Other potential sources of error were evident during CT scan processing and model comparison. Although extraneous helmet attachments were removed prior to scanning, the presence of cage structures or riveting caused patches of artifact within the scans for several cases. These were manually corrected to the degree possible and fortunately did not frequently overlap with the crush region. Small differences existed in overall volume between identical helmet 3D models (typically less than 2%) that likely influenced registration error as well as crush volume and area measurements slightly. Crush volume measurement was constrained to the cylindrical region of interest to minimize this effect. Damage metrics were also limited at times by slight offsets of the max crush location relative to a nearby vent, rendering crush area or centeredness difficult to ascertain. MLR models were developed with consideration given to these issues. Despite these limitations, the present CT-based quantification methods represent a highly advanced approach to helmet damage assessment. Scrape length was the only metric not derived from CT, and its measurement was limited at times by obscure boundaries of the scrape region.

Additional limitations pertain to the source of helmets and characteristics of the impact test setup. As the present sample of helmets was provided from hospitalized patients in an urban setting, the cases may reflect higher-severity accident scenarios and may be specific to an urban cycling environment. However, no fatalities were included and there were a number of cases with no head injury, suggesting a range of head impact severities was represented. Additionally, estimates of normal and tangential velocities and resulting head impact kinematics related to the damage for each case were likely influenced by specific characteristics of the test equipment. The use of an ATD headform may produce slight differences in damage profiles compared to a human head [37], while testing without any simulated neck may represent an oversimplification of head impact kinematics that could affect damage results and associated kinematics [44]. Further, the anvil impact surfaces used have associated shortcomings in representing real-world road

surfaces, likely producing slightly more severe results due to exaggerated stiffness and frictional properties [53]. Despite these limitations, this study represents one of the most comprehensive bicycle helmet damage reconstructions to date. The similarities between results from this study and past studies, paired with the relatively low associated errors, instills confidence in the overall results.

CONCLUSIONS

The present study reconstructed helmet damage from 18 helmets involved in real-world cyclist accidents with the objective of further informing knowledge of cyclist head impact conditions and associated kinematics. Advanced reconstruction techniques were employed, involving CT-based damage quantification and oblique impact laboratory tests, representing a first study of its kind to apply these methods to bicycle helmet reconstructions. Damage metrics resulting from helmet-specific, controlled impact tests were used to develop regression models relating applied impact conditions and resulting kinematics to helmet damage for each case. A majority of impacts were to the helmet front and sides, including several at the helmet rim. The resulting estimates of associated normal velocities and PLAs produced general agreement with past damage reconstruction studies. These estimates and their associated tangential velocity and PRV estimates can be used to inform realistic boundary conditions for oblique impact testing of bicycle helmets. Results can also be related to injury outcome and can be combined with future advanced reconstruction data to develop injury risk functions, enhancing understanding of head injuries associated with cyclist crashes and enabling improved helmet design.

REFERENCES

1. Gaither, T.W., Sanford, T.A., et al. Estimated total costs from non-fatal and fatal bicycle crashes in the USA: 1997-2013. *Inj. Prev.*, 2018. 24(2): p. 135-141

2. Haileyesus, T., Annest, J.L., and Dellinger, A.M. Cyclists injured while sharing the road with motor vehicles. *Injury prevention : journal of the International Society for Child and Adolescent Injury Prevention*, 2007. 13(3): p. 202-6
3. Thompson, D.C., Rivara, F.P., and Thompson, R.S. Effectiveness of bicycle safety helmets in preventing head injuries. A case-control study. *The Journal of the American Medical Association*, 1996. 276(24): p. 1968-73
4. Coronado, V.G., Haileyesus, T., et al. Trends in Sports- and Recreation-Related Traumatic Brain Injuries Treated in US Emergency Departments: The National Electronic Injury Surveillance System-All Injury Program (NEISS-AIP) 2001-2012. *J. Head Trauma Rehabil.*, 2015. 30(3): p. 185-197
5. CPSC. "National Electronic Injury Surveillance System Database" Internet www.cpsc.gov/en/Research--Statistics/NEISS-Injury-Data/. July 26, 2016].
6. McIntosh, A.S., Lai, A., and Schilter, E. Bicycle helmets: head impact dynamics in helmeted and unhelmeted oblique impact tests. *Traffic Inj. Prev.*, 2013. 14(5): p. 501-8
7. Olivier, J. and Radun, I. Bicycle helmet effectiveness is not overstated. *Traffic injury prevention*, 2017. 18(7): p. 755-760
8. Cripton, P.A., Dressler, D.M., Stuart, C.A., Dennison, C.R., and Richards, D. Bicycle helmets are highly effective at preventing head injury during head impact: head-form accelerations and injury criteria for helmeted and unhelmeted impacts. *Accident Analysis & Prevention*, 2014. 70: p. 1-7
9. CPSC. Safety Standard for Bicycle Helmets Final Rule (16 CFR Part 1203). 1998, United States Consumer Product Safety Commission. p. 11711-11747.
10. Mertz, H.J., Irwin, A.L., and Prasad, P. Biomechanical and scaling bases for frontal and side impact injury assessment reference values. *Stapp Car Crash J.*, 2003. 47: p. 155-88
11. Otte, D. Injury Mechanism and crash kinematics of cyclists in accidents - An analysis of real accidents. *Proceedings of 33rd Stapp Car Crash Conference*, 1989. Warrendale, PA
12. Verschueren, P. Biomechanical analysis of head injuries related to bicycle accidents and a new bicycle helmet concept, in *Faculteit Ingenieurswetenschappen Departement Werktuigkunde Afdeling Biomechanica en Grafisch Ontwerpen*. 2009, Katholieke Universiteit Leuven: Leuven, Belgium.
13. Depreitere, B., Van Lierde, C., et al. Bicycle-related head injury: a study of 86 cases. *Accid. Anal. Prev.*, 2004. 36(4): p. 561-567
14. Bourdet, N., Deck, C., et al. In-depth real-world bicycle accident reconstructions. *Int. J. Crashworthiness*, 2014. 19(3): p. 222-232
15. Bourdet, N., Deck, C., Carreira, R.P., and Willinger, R. Head impact conditions in the case of cyclist falls. *Proc. Inst. Mech. Eng. P*, 2012. 226(3-4): p. 282-289
16. Peng, Y., Chen, Y., Yang, J., Otte, D., and Willinger, R. A study of pedestrian and bicyclist exposure to head injury in passenger car collisions based on accident data and simulations. *Safety Science*, 2012. 50(9): p. 1749-1759
17. Gennarelli, T.A., Thibault, L.E., et al. Diffuse axonal injury and traumatic coma in the primate. *Ann Neurol*, 1982. 12(6): p. 564-74
18. King, A.I., Yang, K.H., Zhang, L., Hardy, W., and Viano, D.C. Is Head Injury Caused by Linear or Angular Acceleration?, in *IRCOBI Conference*. 2003: Lisbon, Portugal. p. 1-12.
19. Hardy, W.N., Mason, M.J., et al. A study of the response of the human cadaver head to impact. *Stapp Car Crash J.*, 2007. 51: p. 17-80
20. Gennarelli, T., Ommaya, A., and Thibault, L. Comparison of translational and rotational head motions in experimental cerebral concussion. *Proceedings of 15th Stapp Car Crash Conference*, 1971.

21. Gennarelli, T.A., Thibault, L.E., and Ommaya, A.K. Pathophysiologic responses to rotational and translational accelerations of the head. *SAE Technical Paper Series*, 1972. 720970: p. 296-308
22. Mills, N.J. and Gilchrist, A. Oblique impact testing of bicycle helmets. *Int. J. Impact Eng.*, 2008. 35(9): p. 1075-1086
23. Milne, G., Deck, C., et al. Bicycle helmet modelling and validation under linear and tangential impacts. *Int. J. Crashworthiness*, 2014. 19(4): p. 323-333
24. Pang, T.Y., Thai, K.T., et al. Head and neck responses in oblique motorcycle helmet impacts: a novel laboratory test method. *International Journal of Crashworthiness*, 2011. 16(3): p. 297-307
25. Aare, M. and Halldin, P. A new laboratory rig for evaluating helmets subject to oblique impacts. *Traffic injury prevention*, 2003. 4(3): p. 240-8
26. Bland, M.L., McNally, C., and Rowson, S. Differences in Impact Performance of Bicycle Helmets During Oblique Impacts. *J. Biomech. Eng.*, 2018. 140(9)
27. Rowson, S., Brolinson, G., Goforth, M., Dietter, D., and Duma, S.M. Linear and angular head acceleration measurements in collegiate football. *Journal of biomechanical engineering*, 2009. 131(6): p. 061016
28. Mihalik, J.P., Guskiewicz, K.M., et al. Head impact biomechanics in youth hockey: comparisons across playing position, event types, and impact locations. *Ann Biomed Eng*, 2012. 40(1): p. 141-9
29. Press, J.N. and Rowson, S. Quantifying Head Impact Exposure in Collegiate Women's Soccer. *Clin J Sport Med*, 2017. 27(2): p. 104-110
30. Campolettano, E.T., Gellner, R.A., and Rowson, S. High-magnitude head impact exposure in youth football. *J Neurosurg Pediatr*, 2017. 20(6): p. 604-612
31. Williams, M. The protective performance of bicyclists' helmets in accidents. *Accid. Anal. Prev.*, 1991. 23(2-3): p. 119-131
32. Smith, T.A., Tees, D., Thom, D.R., and Hurt, H.H. Evaluation and replication of impact damage to bicycle helmets. *Accid. Anal. Prev.*, 1994. 26(6): p. 795-802
33. Ching, R.P., Thompson, D.C., et al. Damage to bicycle helmets involved with crashes. *Accident Analysis & Prevention*, 1997. 29(5): p. 555-62
34. Fahlstedt, M., Baeck, K., et al. Influence of Impact Velocity and Angle in a Detailed Reconstruction of a Bicycle Accident. *IRCOBI Conference*, 2012. 12(84): p. 787-799
35. McIntosh, A.S. and Patton, D.A. Impact reconstruction from damage to pedal and motorcycle helmets. *Proceedings of the Institution of Mechanical Engineers, Part P: Journal of Sports Engineering and Technology*, 2012. 226(3-4): p. 274-281
36. Chinn, B., Canaple, B., et al. COST 327: Motorcycle Safety Helmets, B. Chinn, Editor. 2001, European Commission, Directorate General for Energy and Transport: Belgium.
37. Bonin, S.J., Luck, J.F., et al. Dynamic Response and Residual Helmet Liner Crush Using Cadaver Heads and Standard Headforms. *Ann Biomed Eng*, 2017. 45(3): p. 656-667
38. Knox, E.H., Mathias, A.C., Stern, A.R., Van Bree, M.P., and Brickman, D.B. Methods of accident reconstruction: biomechanical and human factors consideration. *Proceedings of AMSE 2015 International Mechanical Engineering Conference and Exposition*, 2015. Houston, TX
39. Loftis, K.L., Moreno, D.P., Tan, J., Gabler, H.C., and Stitzel, J.D. Utilizing computed tomography scans for analysis of motorcycle helmets in real-world crashes. *Proceedings of 48th Rocky Mountain Bioengineering Symposium & 48th International ISA Biomedical Sciences Instrumentation Symposium*, 2011. Denver, Colorado
40. Cooter, R.D. Computed tomography in the assessment of protective helmet deformation. *The Journal of trauma*, 1990. 30(1): p. 55-68

41. Cobb, B.R., Tyson, A.M., and Rowson, S. Head acceleration measurement techniques: Reliability of angular rate sensor data in helmeted impact testing. *Proceedings of the Institution of Mechanical Engineers, Part P: Journal of Sports Engineering and Technology*, 2017. 232(2): p. 176-181
42. Cobb, B.R., MacAlister, A., et al. Quantitative comparison of Hybrid III and National Operating Committee on Standards for Athletic Equipment headform shape characteristics and implications on football helmet fit. *Proceedings of the Institution of Mechanical Engineers, Part P: Journal of Sports Engineering and Technology*, 2014. 229(1): p. 39-46
43. Sances, A.J., Carlin, F., and Kumaresan, S. Biomechanical analysis of head-neck force in Hybrid III dummy during inverted vertical drops. *Biomed. Sci. Instrum.*, 2002. 38: p. 459-464
44. Nelson, T.S. and Cripton, P.A. A New Biofidelic Sagittal Plane Surrogate Neck for Head-First Impacts. *Traffic Inj Prev*, 2010. 11(3): p. 309-319
45. ECE. R-22.05: Uniform Provisions Concerning the Approval of Protective Helmets for Drivers and Passengers of Motorcycles and Mopeds. 1999, United Nations Economic Commission for Europe.
46. Mills, N.J. Critical evaluation of the SHARP motorcycle helmet rating. *Int. J. Crashworthiness*, 2010. 15(3): p. 331-342
47. McIntosh, A., Dowdell, B., and Svensson, N. Pedal cycle helmet effectiveness: A field study of pedal cycle accidents. *Accident Analysis & Prevention*, 1998. 30(2): p. 161-168
48. Bland, M.L., Zuby, D.S., Mueller, B.C., and Rowson, S. Differences in the protective capabilities of bicycle helmets in real-world and standard-specified impact scenarios. *Traffic Inj. Prev.*, 2018. 19(sup1): p. S158-S163
49. Ghajari, M., Caserta, G.D., and Galvanetto, U. The Impact Attenuation Test of Motorcycle Helmet Standards. *Proceedings of 1st International Conference on Helmet Performance and Design*, 2013. London, UK
50. Rowson, S. and Duma, S.M. Brain injury prediction: assessing the combined probability of concussion using linear and rotational head acceleration. *Ann. Biomed. Eng.*, 2013. 41(5): p. 873-82
51. Rowson, S., Bland, M.L., et al. Biomechanical Perspectives on Concussion in Sport. Sports Med Arthrosc Rev, 2016. 24(3): p. 100-7
52. Mills, N.J. and Gilchrist, A. Finite-element analysis of bicycle helmet oblique impacts. International Journal of Impact Engineering, 2008. 25: p. 1087-1101
53. Bonugli, E. The effects of dynamic friction in oblique motorcycle helmet impacts, in Biomedical Engineering. 2015, The University of Texas at San Antonio: Ann Arbor. p. 78.

CHAPTER 11

CLOSING REMARKS

SUMMARY OF RESEARCH

The present work aims to enhance understanding of the efficacy of bicycle helmets in reducing head injury risk. A number of varied-design helmet models were evaluated on both standards and oblique impact drop towers, the former of which all bicycle helmets must presently be certified by in order to be sold in the US, and the latter of which is more representative of cyclist accident conditions. Significant differences in impact performance existed between helmet models on both drop towers, although the addition of rotation using an oblique setup augmented discrimination of performance and enabled realistic assessment of brain injury risk. Design correlations suggest that strategies aimed at optimizing helmet effective stiffness may be conducive to improved impact performance.

Varied boundary conditions associated with oblique impact drop towers were also assessed in order to better understand how test constraints may influence biofidelity and helmet performance. An optimized version of the oblique impact tower was implemented into an objective evaluation protocol informed by real-world cyclist accident conditions and relevant injury mechanisms. This protocol summarized concussion risks from a variety of tests into a single metric indicative of overall helmet performance. A set 30 popular bicycle helmet models in the US were directly and quantitatively compared using this method. The impact performance of low-price, wholesale bicycle helmets was then also compared to popular off-the-shelf models, allowing a price-performance analysis to be conducted. Wide ranges in protective capabilities were identified across all helmet models evaluated, highlighting the need for objective data to be made available for rider consumption.

To facilitate further understanding of common cyclist head impact conditions, an advanced method for reconstructing damage to bicycle helmets involved in real-world crashes was explored. The sensitivity of various CT-derived metrics using this method was investigated, and results were used to inform a larger scale bicycle helmet damage quantification effort. Damage to helmets from 18 real-world cyclist accidents were reconstructed, enabling identification of associated head impact conditions and kinematics. The results gleaned from this research provide consumers with objective impact data for making informed, safety-based helmet purchases, while simultaneously stimulating improved helmet evaluation and design and ultimately enhancing cyclist safety.

PUBLICATION PLAN

Each of the preceding chapters have or will be published in scientific, peer-reviewed journals or conference proceedings. Table 11.1 summarizes the publication plans for each chapter.

Table 11.1. Publication plan for research.

Chapter	Title	Journal (*Conference*)
2	Differences in the protective capabilities of bicycle helmets in real-world and standard-specified impact scenarios	Traffic Injury Prevention* *Association for the Advancement of Automotive Medicine (AAAM)*
3	Differences in impact performance of bicycle helmets during oblique impacts	Journal of Biomechanical Engineering*
4	Effect of anvil angle on impact kinematics in laboratory evaluation of bicycle helmets	Biomedical Science Instrumentation* *Rocky Mountain Bioengineering Symposium (RMBS)*
5	Headform and neck effects on dynamic response in bicycle helmet oblique impact testing	*International Research Council on Biomechanics of Injury (IRCOBI)**
6	Development of the STAR evaluation system for assessing bicycle helmet protective performance	Annals of Biomedical Engineering
7	A Price-Performance Analysis of the Protective Capabilities of Wholesale Bicycle Helmets	Proceedings of the Institution of Mechanical Engineers, Part P: Journal of Sports Engineering and Technology
8	Methodology for Reconstructing Real-world Damage to Bicycle Helmets Using Oblique Impacts: A Case Study	Biomedical Science Instrumentation* *Rocky Mountain Bioengineering Symposium (RMBS)*
9	Evaluating the Sensitivity of Bicycle Helmet Damage Reconstructions Metrics Using Oblique Impacts and Computed Tomography	Annals of Biomedical Engineering
10	Laboratory Reconstructions of Bicycle Helmet Damage: An Investigation of cyclist head impact conditions and associated kinematics	Accident Analysis and Prevention

*Published or accepted for publication